The role of the 20-hydroxyecdysone (20E) signaling pathway in modulating *Anopheles arabiensis* reproduction, gut microbiome and anti-bacterial immunity

Elodie Ekoka Etouman
(Professionally known as Elodie Ekoka)

A thesis submitted to the Faculty of Health Sciences, University of the Witwatersrand, in fulfilment of the requirements for the degree
Doctor of Philosophy

Supervisor: Prof Lizette Koekemoer

Co-supervisor: Dr Yael Dahan-Moss

30 May 2023

Plagiarism declaration

Thesis title

The role of the 20-hydroxyecdysone (20E) signaling pathway in modulating *Anopheles arabiensis* reproduction, gut microbiome and anti-bacterial immunity

Declaration

1. I understand what plagiarism entails and am aware of the University's policy in this regard.
2. I declare that this thesis is my own, original work. Where someone else's work was used (whether from a printed source, the internet or any other source) due acknowledgment was given and reference was made according to departmental requirements.
3. I did not make use of another student's previous work and submit it as my own.
4. I did not allow and will not allow anyone to copy my work with the intention of presenting it as his or her own work.

Signature:  **Date**:__30 May 2023___

Elodie Ekoka
(Student ID: 2069764)

Acknowledgments

While this PhD was certainly a turning point in my scientific career and an undeniable catalyst to my professional growth, I would not have been able to complete it without the continuous guidance and providence of **my Heavenly Father**. Thank you, Father, for giving me the opportunity to enroll for a PhD degree at Wits Medical School, and for ALWAYS providing what I needed (emotionally, spiritually, physically, academically, financially) every step of the way. Thank you for using this PhD to strengthen my character, faith, prayer life. Thank you for the new prayer partners I have acquired.

It is said that the product of one's PhD is not his/her thesis; it is rather the person he/she has become. It couldn't be truer. There is no comparison between the shy girl who started this PhD in 2018, and the confident, resilient, assertive, prayerful and bold lady who is writing this thesis. Because it took a village to transform me into this person, I ask my Lord Jesus to bless the following people who have invested their valuable time in my personal and/or professional growth:

- Ms **Marilyn Ekoka** (sister) — I couldn't have completed this PhD without your unending emotional, spiritual, and technical support. Thank you for always believing in me even when I doubted myself. Thank you for standing by my side through all the ups and downs of my PhD journey. Thank you for keeping me accountable and focused on my goals. Thank you for all the discussions we regularly share on mental toughness, resilience, and personal growth.
- The **Ekoka Etouman family** — Thank you for all the moral, financial, emotional, and technical support provided. Thank you for always being my cheerleaders, especially during the hard times I faced. Thank you, dad, for fully covering all the expenses related to my first few international conferences and for teaching me the art of mental toughness in the workplace.
- My **prayer partners** and all those who prayed with and for me — I don't want to put you on the spot, but I just want to let you know that your prayers were answered.
- **Vusi** (my gym trainer) — Thank you for always pushing me beyond what I thought I could accomplish, for reminding me that the pain is part of the growing process, for never letting me give up even when I was tired! You did not just train my body; you trained my mind to be mentally tough and to be able to endure pain. And of course, thank you for helping me put off this #LockdownWeight ☺️.

- Prof **Lizette Koekemoer** (supervisor) — Thank you for molding me into an independent, self-driven, resilient, and confident researcher. Thank you for teaching me the art of *excelling and staying focused under pressure*. All these soft skills will be valuable for the next phase(s) of my scientific career.
- Dr **Luisa Nardini** (external collaborator) — Thank you for all the scientific discussions we shared, they shaped my critical thinking. Thank you for all your valuable input in my experimental design, data analysis, manuscripts, and for all the laboratory techniques you have taught me. Thank you for always offering a hand to help in the lab when I needed it.
- Dr **Yael Dahan-Moss** (co-supervisor) — Thank you for co-supervising this project.
- Mr **Raoul Diffouo** (best friend) — Thank you for your valuable friendship! Thank you for never sugar-coating things for me. Thank you for being an attentive ear and "counselor" when I faced challenging times, and a great buddy to celebrate my wins. But most importantly, thank you for introducing me to *Starbucks*! this coffee shop is surely a productivity booster!
- Mrs **Clowey Stevenson** — Thank you for reminding me that nobody determines my value but GOD, for giving a hand when I needed it, but most importantly for just being there; sometimes your presence was all I needed to keep going.
- Dr **Betty Maepa**, Dr **Angela Botes**, and Prof **Patrick Arbuthnot** — Thank you for welcoming me into your laboratories, and/or providing me with the bacterial cultures and GFP clones, I needed for my experiments.
- My **funding sources** — Thank you to the National Research Foundation, the WITS Health Consortium, the Communities of Practice, the South African Medical Research Council, and the Faculty of Health Sciences (University of the Witwatersrand) for the bursaries, scholarships, and/or research grants provided.

"If you believe, God will take you from the pit to the palace"

(Genesis 37 – 50)

Dedication

To the *Ekoka Etouman* family, for all the sacrifices they made and the support they provided to ensure that I could pursue a decent education from Grade 1 to PhD. I will never be able to pay you back, but I hope to pursue a career reflecting that your support was not in vain. I love you all.

Table of contents

List of tables

List of figures

Supplementary figures

Abbreviations

20E	20-hydroxyecdysone	**GFP**	green fluorescent protein
AMP	Antimicrobial peptides	**GSK3**	Glycogen Synthase Kinase 3
ATSB	Attractive toxic sugar baits	**hPBM**	hours post-blood meal
BLAST	Basic local alignment search tool	**hpi**	hours post-injection
bp	base pair	**hr(s)**	hour(s)
ca.	*circa (Approximately)*	**i.e.**	id est (That is)
CAP	Catabolite activator protein	**IGR**	Insect growth regulator
cDNA	Complementary DNA	**ILP3**	Insulin-like Peptide 3
Cq	Quantification cycle	**Imd**	Immune deficiency protein
Da	Dalton	**IRS**	Indoor residual spraying
DBH	Dibenzoylhydrazine	**Jak-STAT**	Janus kinase – signal transducer and cac
DNA	Deoxyribonucleic acid	**JNK**	c-Jun N-terminal Kinase
DNase	Deoxyribonuclease	**kbp**	Kilobase pairs
dNTP	Deoxyribonucleotide triphosphate	**kDa**	Kilodalton
dPBM	Day Post-Blood meal	**L**	Litre
dpi	Day post-injection	**LLIN**	Long lasting insecticide-treated nets
dsDNA	Double-stranded DNA	**LMIC**	Low- and middle-income countries
dsEcR	Double-stranded RNA against EcR	**LSM**	Larval source management
dsGFP	Double-stranded RNA against GFP	**M**	Molar
dsRNA	Double-stranded RNA	**mg**	Milligram
EcR	Ecdysone Receptor	**MISO**	Mating Induced stimulator of oogenesis
EcRE	Ecdysone Receptor Elements	**ml**	Millilitre
EDT	Early diagnosis and treatment	**mM**	Millimolar

mRNA	Messenger ribonucleic acid	**RNE**	Relative normalized expression
MW	Molecular weight	**RNS**	Reactive nitrogen species
NaOAc	Sodium acetate	**ROS**	Reactive oxygen species
ng	Nanogram	**rRNA**	Ribosomal RNA
nt	Nucleotides	**RXR**	Retinoid X Receptor
NTC	No-template control	**TAE**	Tris-acetate EDTA
OEH	Ovary Ecdysteroid Hormone	**TEP1**	Thioester protein 1
PAMP	Pathogen-associated molecular pattern	**TOR**	Target of Rapamycin
PBS	Phosphate buffer saline	**USP**	Ultraspiracle Protein
PCR	Polymerase chain reaction	**YPP**	Yolk Protein Precursor
pg	Picogram		
PGRP	Peptidoglycan recognition protein		
pmol	Picomole		
PPO	Prophenol oxidase		
PRR	Pattern recognition receptors		
qPCR	Quantitative PCR		
RNA	Ribonucleic acid		
RNAi	RNA interference		
RNAse	Ribonuclease		

Research outputs from this thesis

i. Publications in international peer-reviewed journals

Role: For each of these manuscripts, I co-designed the study, performed the laboratory experiments, analyzed the data, wrote the original draft, contributed to all revisions, and contributed to the funding.

1. E Ekoka, S Maharaj, L Nardini, Y Dahan-Moss, and LLL Koekemoer. 20-hydroxyecdysone (20E) signaling as a promising target for the chemical control of malaria vectors. *Parasites and Vectors*. 2021; 14(1):86
   Impact Factor: 3.169

ii. International conferences

Role: For each of these presentations, I performed the experiments, analyzed the data, and prepared the slides or poster, with some editorial input from my thesis committee. I also delivered the presentations.

1. E Ekoka, L Nardini, Y Dahan-Moss, and LL Koekemoer**.** "The tripartite relationship between *Anopheles arabiensis*' 20E signaling, gut microbiome, and vectorial capacity". 70th ASTMH annual meeting, Gaylord National Resort and Convention Centre, National Harbor, MD, USA, 17 -21 November 2021. (Poster presentation)

2. E Ekoka, L Nardini, Y Dahan-Moss, and LL Koekemoer**. "**Ecdysone signaling regulates *Anopheles arabiensis*' reproductive output"*.* Inaugural Women in Malaria virtual conference, 22 -24 March 2021. (Poster presentation)

3. E Ekoka, L Nardini, A Aswat, Y Dahan-Moss, and LL Koekemoer**. "**Ecdysone signaling regulates vitellogenesis and the microbiome in *Anopheles arabiensis* mosquitoes"*.* 68th ASTMH annual meeting, Gaylord National Resort and Convention Centre, National Harbor, MD, USA, 20 -24 November 2019. (Poster presentation)

4. E Ekoka, L Nardini, A Aswat, Y Dahan-Moss, and LL Koekemoer**. "**The role of ecdysone receptor in the vitellogenesis of *Anopheles arabiensis* mosquitoes". The Future of Malaria Research Symposium, Johns Hopkins university, USA, 18 November 2019. (Poster presentation)

iii. Local conferences

Role: For each of these presentations (except presentation no. 3), I performed the experiments, analyzed the data, and prepared the slides or poster, with some editorial input from my thesis committee. I also delivered the presentations. For presentation no.3, I contributed to the data and data analysis.

1. E Ekoka, L Nardini, Y Dahan-Moss, and LL Koekemoer. "20E agonists are promising insecticides for the chemical control of *Anopheles arabiensis* in South Africa". The Inaugural South African Clinician Scientists Conference, Johannesburg, South Africa, 25 -26 February 2021. (Oral presentation)

2. E Ekoka**,** L Nardini, Y Dahan-Moss, and LL Koekemoer**. "**Hormonal regulation of fecundity and immunity in *Anopheles arabiensis*". 14th Early Career Scientists Conference, Johannesburg, South Africa, 26 -27 October 2020. (Oral presentation)
   Award: Most interactive scholar

3. A Aswat, E Ekoka**,** L Nardini, Y Dahan-Moss and LL Koekemoer**. "**The role of 20-hyroxyecdysone on the expression of *Anopheles arabiensis* antimicrobial peptides". Molecular Biosciences Research Thrust (MBRT) research day, Johannesburg, South Africa, 28 November 2019. (Poster presentation)

4. E Ekoka, L Nardini, A Aswat, Y Dahan-Moss, and LL Koekemoer**. "**Hormonal regulation of the microbiome in *Anopheles arabiensis*". Molecular Biosciences Research Thrust (MBRT) research day, Johannesburg, South Africa, 28 November, 2019. (Poster presentation)

Award: Best poster presentation in the PhD/Postdoc category

5. E Ekoka, L Nardini, A Aswat, Y Dahan-Moss, and LL Koekemoer**. "**Ecdysone signaling regulates vitellogenesis and the microbiome in *Anopheles arabiensis* mosquitoes"*.* Community of Practice initiative research day, Pretoria, South Africa, 18 November 2019. (Poster presentation).

6. E Ekoka & LL Koekemoer**.** "Cloning and *in silico* characterization of the Ecdysone Receptor in *Anopheles arabiensis* adult female mosquitoes"*.* Biennial Research Day & Postgraduate Expo, Faculty of Health Sciences, University of the Witwatersrand, Johannesburg, South Africa, 06 September 2018. (Poster presentation)

7. E Ekoka & LL Koekemoer. "Identification and *in silico* characterization of the Ecdysone Receptor in *Anopheles arabiensis* adult female mosquitoes". 04th Malaria Research Conference, Johannesburg, South Africa, 30 July – 01 August 2018. (Poster presentation)

Abstract

The 20-hydroxyecdysone (20E) signaling pathway, which is activated when 20E binds to its ecdysone receptor, EcR, is a promising target to reduce *Anopheles* mosquitoes' ability to transmit malaria. The function of this pathway is typically assessed by altering the pathway and assessing how this manipulation affects a phenotype of interest. Two ways to alter this pathway include injecting mosquitoes with 20E or reducing *EcR* transcript levels with RNA interference (RNAi). Whether the 20E signaling pathway regulates *An. arabiensis* fecundity, fertility, gut bacteria, and immunity has never been investigated. These questions were addressed in this study by using a South African *An. arabiensis* strain. First, RNAi was used to investigate whether *EcR* silencing affects *An. arabiensis* reproductive output. While *EcR* depletion did not affect the mosquito fecundity, both vitellogenesis and egg fertility were impaired, as indicated by a decrease in the expression of some yolk genes and the number of eggs that hatched into larvae. Next, a link between the gut bacteria and *EcR* expression was established, by showing that antibiotic-fed (i.e., with less gut bacteria) mosquitoes displayed fewer *EcR* transcripts. To investigate whether the relationship between *An. arabiensis* gut microbiome and *EcR* expression was mediated by the mosquito innate immune defenses, the expression of ten selected anti-bacterial immune genes was measured in the gut and the whole mosquito after disturbing the 20E signaling pathway. This experiment uncovered that the 20E signaling pathway down-regulates the mosquito anti-bacterial immune defenses, which may favour bacterial proliferation post feeding. Finally, the effect of Gram-negative and Gram-positive bacteria on *EcR* expression was assessed by injecting mosquitoes with each type of bacteria and quantifying *EcR* transcripts. The results suggested that only Gram-negative bacteria influenced *EcR* expression. Altogether, these results demonstrated that *An. arabiensis* reproduction, gut microbiome, and antimicrobial peptides are regulated by 20E.

CHAPTER 1

Literature Review

Sections of this chapter were included in the following published article:
Ekoka E, Maharaj S, Nardini L, Dahan-Moss Y, and Koekemoer LL. 20-hydroxyecdysone (20E) signaling as a promising target for the chemical control of malaria vectors. *Parasites and Vectors.* 2021; 14(1):86

1.1 Introduction

Malaria is a vector-borne disease which spreads when protozoan *Plasmodium* parasites are transmitted to humans through the bites of *Anopheles* female mosquitoes. Common symptoms include fever, headaches, and chills, but these can escalate to anaemia, kidney failure, seizures, or even death should the infected individuals not receive the appropriate treatment on time (WHO, 2020). The socio-economic burden of malaria remains the highest in sub-Saharan Africa where in 2019, 215 million cases and 384,000 deaths were reported, in addition to nearly 3 billion USD invested in control and elimination programmes (WHO, 2020). Besides, recent models predict that with the unprecedented COVID-19 pandemic, deaths due to malaria in low- and middle-income countries could increase by 36% over the next five years (Hogan et al., 2020). Therefore, African countries, which currently represent more than 90% of all malaria deaths worldwide (WHO, 2020), are the most at risk.

To date, five *Plasmodium* species are known to cause human malaria: *P. falciparum*, *P. vivax*, *P. ovale*, *P. malariae*, and *P. knowlesi* (Ahmed and Cox-Singh, 2015, Sinden and Gilles, 2002). Of these, not only is *P. falciparum* the most virulent, but also, it was responsible for 99.7% of malaria cases in Africa in 2019 (WHO, 2020). With respect to malaria vectors in Africa, three species from the *Anopheles gambiae* complex (*An. gambiae sensus stricto*, *An. coluzzii*, and *An. arabiensis*), and one

species from the *An. funestus* group (*An. funestus s.s.*) have been characterized as major vectors in the continent (Coetzee, 2020, Derua et al., 2015, Sinka et al., 2012). *Anopheles arabiensis*, the focus of this thesis, is wildly distributed. In sub-Saharan Africa, it has been detected in West Africa, East Africa, and Southern Africa (Drake and Beier, 2014, Sinka et al., 2012, Wiebe et al., 2017).

The burden of malaria is managed by a multi-disciplinary approach which combines targeting the parasite (artemisinin combination therapy) (Gutman and Chico, 2020, Sinclair et al., 2009), the vector (WHO-approved insecticides and long-lasting insecticide treated bed nets) (WHO, 2012, WHO, 2019) and to some extent the environment (habitat modification or larval source management) (Castro et al., 2009, Randell et al., 2010, Utzinger et al., 2001). Additionally, the pre-erythrocitic stage RTS,S/AS01 vaccine which targets the circumsporozoite surface protein of *P. falciparum* has been approved in 2021 by the WHO (Adepoju, 2019, Gumulira, 2021, Laurens, 2020, WHO, 2020). This vaccine will be administered in children under five years old in malaria endemic countries such as those in the African continent (Gumulira, 2021).

Of all the above-mentioned interventions, vector control plays a central role. In fact, the WHO has stated that "*vector control is a vital component of malaria prevention, control, and elimination strategies because it can be highly effective in providing personal protection and/or reducing disease transmission*" (WHO, 2019). Therefore, in the following paragraphs the biology of malaria vectors is discussed while highlighting the mosquitoes physiological processes that enhance its vectorial capacity. In addition, the 20-hydroxyecdysone (20E) signaling pathway is presented as a key target for malaria control, based on its ability to influence *Anopheles* vectorial capacity. As a result, this chapter ends by elaborating on the status and limitations of the current

Anopheles chemical control strategies and underlining that insect growth regulators which target 20E signaling could be an asset for *Anopheles* chemical control.

1.2 Factors influencing *Anopheles* females vectorial capacity

As reviewed recently (Cansado-Utrilla et al., 2021, Shaw and Catteruccia, 2018), the factors influencing anopheline females vectorial capacity —and thus malaria transmission— are excellent targets for vector control strategies. These factors range from those pertaining to the mosquitoes lifecycle to the myriad of pathogens they ingest while feeding (Figure 1.1). In the sections below, a brief description of these factors is provided, while highlighting those that affect mosquitoes number or abundance, and those that affect mosquitoes vector competence, i.e., their ability to become infectious with *Plasmodium* sporozoites.

1.2.1 *Anopheles* mosquitoes lifecycle

After emergence, *Anopheles* male and female mosquitoes mate within a few days (Clements and Stanley-Samuelson, 1999). It has been suggested that males become sexually mature before females, and once they do, their phototactic behaviour drive them to aggregate in mating swarms of approximately 5 to 5,000 males (Howell and Knols, 2009). In multiple *Anopheles* species (including *An. gambiae*, *An. funestus*, *An. arabiensis*, *An. coluzzii*, and *An. merus*), virgin females are subsequently attracted to these swarms via the male-secreted pheromones (Mozūraitis et al., 2020). During copulation, males transfer a mating plug (containing sperm, allohormones, and other

proteins) to the females atrium, and these females are now inseminated (Gabrieli et al., 2014, Koene and ter Maat, 2001, Pondeville et al., 2008).

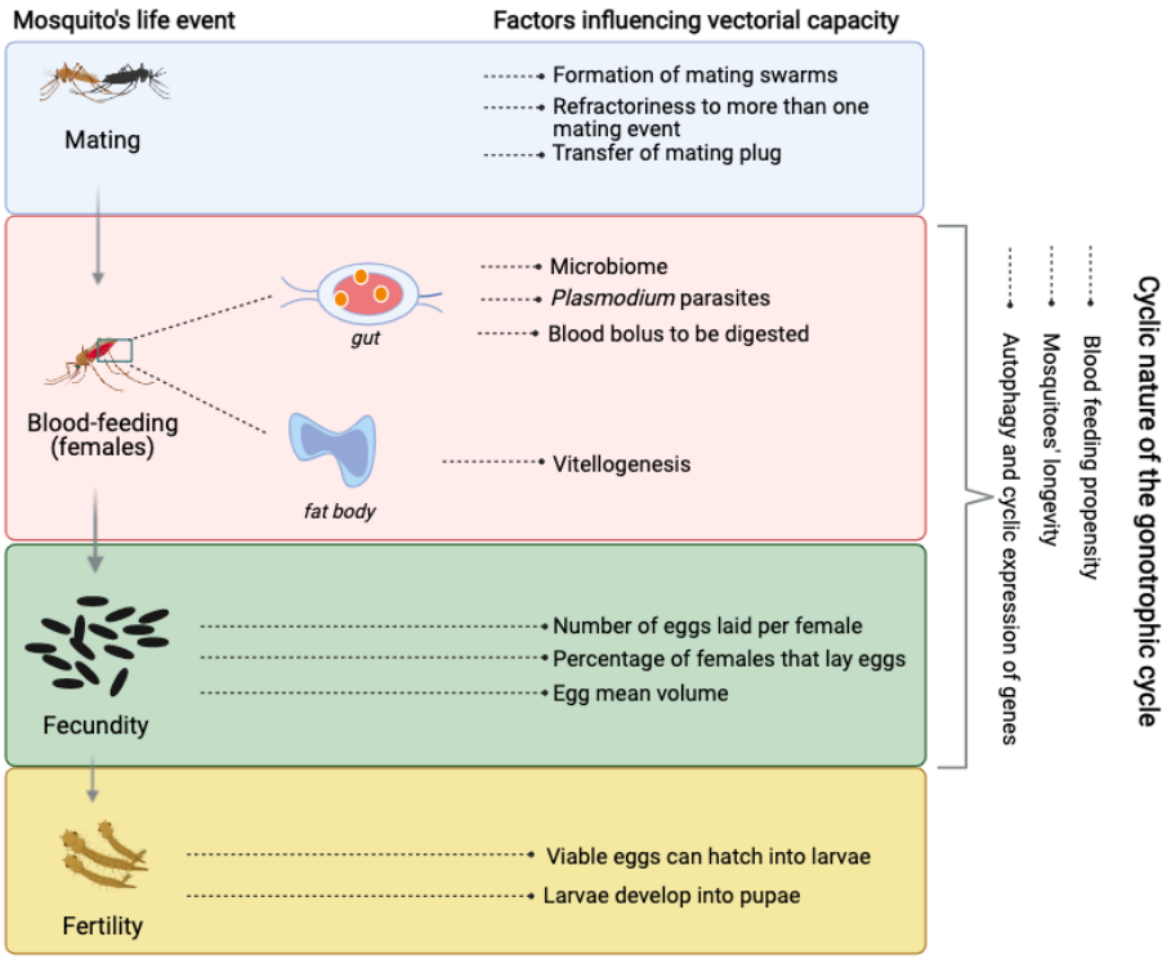

Figure 1.1: Factors influencing *Anopheles* females vectorial capacity [created with information from Bascuñán et al., 2020, Cansado-Utrilla et al., 2021, Mane-Padros et al., 2012, Romoli and Gendrin, 2018, Shaw and Catteruccia, 2018]. While this list is not exhaustive, it highlights the factors that are relevant to this thesis.

In the next phase, the proteases in the females atrium break down the plug to release its components (Bascuñán et al., 2020). One plug component in particular, the steroid hormone 20-hydroxyecdysone (20E), has been shown to regulate the processes that prevent inseminated females from copulating again (see later, section 1.3.2). Overall, because mating largely influences *Anopheles* abundance in a region,

vector control methods targeting males pheromones or the females atrial components involved in processing of the mating plug would help reduce malaria transmission.

Following mating, the inseminated *Anopheles* females enter a succession of gonotrophic cycles, each starting with blood feeding and ending with egg deposition (Figure 1.1). The exact number of gonotrophic cycles they can undergo is not clear, as sometimes they can take multiple blood meals —in the field— during a single gonotrophic cycle (Detinova et al., 1962, Silver, 2008). However, as described below, a successful completion of these gonotrophic cycles is essential to maintain *Anopheles* vector competence and abundance. First, it has been reported that blood-feeding propensity is regulated by the gut bacteria (see later, section 1.2.3) and possibly the steroid hormone 20E (Beach, 1979). This blood meal contains the nutrients needed for egg development (section 1.3.2), in addition to pathogens that form the insect microbiome (section 1.2.3), and putatively, if infected, also *Plasmodium* parasites (section 1.2.2). If the blood bolus is successfully digested in the gut lumen, the production of egg yolk proteins —that is, vitellogenesis— is initiated in the ovarian fat body. The gonotrophic cycle ends with the deposition of viable eggs. Because extensive details on vitellogenesis, fecundity, and fertility are provided elsewhere (sections 1.3.2, 2.1, and 3.1), these processes will not be described here. However, a brief discussion on how the cyclic nature of mosquitoes gonotrophic cycle is maintained, based on studies in *Ae. aegypti*, is provided below (Bryant and Raikhel, 2011, Wang et al., 2021).

There are at least two reasons why the number of gonotrophic cycles undergone by mosquitoes affect disease transmission. Firstly, the number of eggs deposited by females in their lifespan (and thus vector abundance) increases with the number of cycles. Secondly, females need at least two blood meals to transmit diseases: one meal to ingest the pathogen and the second one to transmit it to the next

vertebrate host. As a result, a higher number of gonotrophic cycles favours pathogen transmission. In 2011, a study identified autophagy —a mechanism by which damaged or used cells are destroyed— as a key event to occur in the fat body to regulate the cyclicity of the gonotrophic cycle (Bryant and Raikhel, 2011). They demonstrated that in autophagy-incompetent fat body tissues, the repression of *vitellogenin* expression which normally occurs at ~36 hours post- blood meal (hPBM) is delayed and as such, both the termination of vitellogenesis and the subsequent gonotrophic cycle are obstructed (Bryant and Raikhel, 2011). Notably, 20E was identified as a key hormone that regulates the fat body autophagic processes (Bryant and Raikhel, 2011). While little is known about the molecular mechanism whereby 20E regulates this autophagy, at least two proteins that mediate this regulation have been uncovered, namely E93 and HR3 (Mane-Padros et al., 2012, Wang et al., 2021).

1.2.2 *Plasmodium* extrinsic incubation period (EIP)

The sporogonic cycle of malaria parasites begins when *Anopheles* mosquitoes ingest *Plasmodium* gametocytes while blood-feeding on infected hosts (Figure 1.2). In the insect midgut, these gametocytes rapidly differentiate into male and female gametes, and these later fertilize to form a zygote within 1 day post- blood meal (dPBM). The zygote develops into motile ookinetes which, upon crossing the midgut epithelium and its basal membrane, transform into oocysts that remain fixed at the interface of the midgut and haemolymph (Singh et al., 2020, Vlachou et al., 2006). From 2 dPBM to 13 dPBM, the oocysts developed and once fully matured (~14 dPBM), they burst and release sporozoites into the haemolymph (Bennink et al., 2016, Singh et al., 2020). These navigate to the salivary glands, ready to be injected into the next host during a following blood meal (Figure 1.2). Finally, the duration of the sporogonic cycle is known as the extrinsic incubation period or EIP (Figure 1.2), which is a measure of the time

needed for a mosquito to become infectious (Ohm et al., 2018). The EIP can be affected by factors such as environmental temperature and underlying genetic features of both the vector and parasite (Ohm et al., 2018).

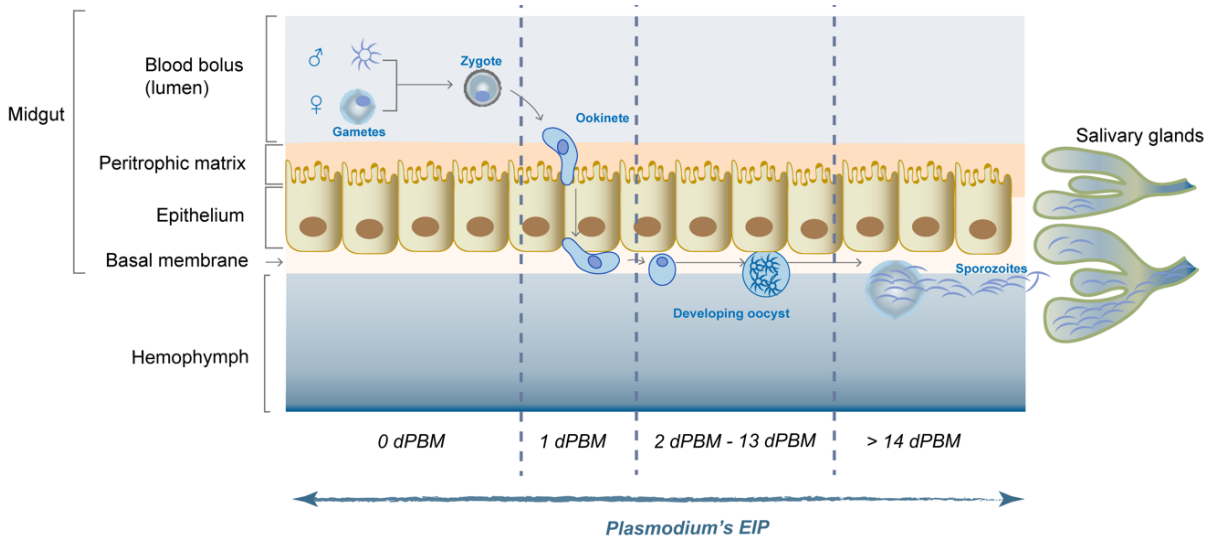

Figure 1.2: *Plasmodium* sporogonic cycle [created with information from Singh et al. ,2020]. Abbreviations: dPBM, days post- blood meal; EIP, extrinsic incubation period.

1.2.3 The gut microbiome

The midgut of mosquitoes is inhabited by bacteria, viruses, and fungi, which together form the midgut microbiome [reviewed in (Gao et al., 2019, Gao et al., 2020, Huang et al., 2020, Strand, 2018)]. This microbiome is primarily acquired from the aquatic breeding sites in which larvae grow, and subsequently carried through the adult mosquito stages (Bascuñán et al., 2018, Dickson et al., 2017, Gimonneau et al., 2014). In addition, other factors such as diet, blood meal source, mosquito species, developmental stage, seasonality (dry versus rainy season), bacterial transmission from adult females to their eggs, or pathogen infection can also alter the composition

of the gut microbiome (Akorli et al., 2016, Gonzales et al., 2018, Muturi et al., 2019, Saab et al., 2020, Surat et al., 2016). This section focuses on the bacterial microbiome. The midgut of adult female anophelines is dominated by Gram-negative bacteria, with members of the Enterobacteriaceae, Flavobacteriaceae, Acetobacteriaceace, Pseudomonadaceae, Moraxellaceae, Aeromonadaceae families being among the most common (Bascuñán et al., 2018, Gao et al., 2019, Gendrin and Christophides, 2013, Zoure et al., 2020). These bacteria regulate multiple physiological processes that are important for malaria transmission, such as blood digestion (de O Gaio et al., 2011, Dong et al., 2009), egg production (Coon et al., 2016, de O Gaio et al., 2011, Gnambani et al., 2020), larval development (Coon et al., 2017, Linenberg et al., 2016, Mitraka et al., 2013), adult longevity (Bahia et al., 2014, Gnambani et al., 2020, Tchioffo et al., 2016), insecticide resistance (Barnard et al., 2019), and refractoriness to *Plasmodium* infection (Dong et al., 2009, Kalappa et al., 2018, Song et al., 2018, Wang et al., 2019). In other words, the gut bacteria contribute widely to the vectorial capacity of *Anopheles* mosquitoes and their insecticide resistant/susceptible phenotype.

The role of gut bacteria in blood digestion and fecundity — In *An. gambiae*, *An. coluzzii,* and *Ae. aegypti*, blood-feeding induces an explosive (12-48 hPBM) proliferation of the midgut microbiome (Kirilly et al., 2011, Oliveira et al., 2011, Rodgers et al., 2017b, Xiao et al., 2017), especially Gram-negative bacteria of the Enterobacteriaceae family (Kirilly et al., 2011, Oliveira et al., 2011). Enterobacteria regulate blood digestion through lysis of red blood cells and among the midgut bacteria, they have the highest haemolytic activity (de O Gaio et al., 2011). Therefore, mosquitoes with reduced (or completely erased) microbiome have more undigested blood proteins than septic ones at 48 hPBM and they consequently have a lower egg clutch size (Correa et al., 2018, de O Gaio et al., 2011, Sharma et al., 2013, Xiao et al., 2017). In addition, Enterobacteria also play a role in the selection of oviposition

sites: *Culex pipiens* females prefer to lay eggs in aquatic environments enriched with *Klebsiella* spp. (Enterobacteriaceae) (Diaz-Nieto et al., 2016). Besides Enterobacteriaceae, other Gram-negative bacteria have also been implicated in blood digestion and fecundity. Gnambani et al. (2020) reported that infection of *An. coluzzii* with *Chromobacterium violaceum* decreases its blood-feeding propensity, fecundity and fertility. In another study, Flavobacteriaceae were associated with egg production in the facultative autogenous mosquito (i.e., does not need blood for the first egg batch, only for the subsequent ones) *Ae. atropalpus* (Coon et al., 2016). Finally, Benzon and colleagues reported that *Ae. aegypti* females oviposit preferentially in water containing *Acinetobacter* spp. (Moraxellaceae) (Benzon and Apperson, 1988).

The role of gut bacteria in *Plasmodium* susceptibility — There are at least three levels at which midgut bacteria regulate *Plasmodium* infection. Firstly, they create a peritrophic matrix around the ingested blood bolus (Rodgers et al., 2017a, Rodgers et al., 2017b), as a first barrier to *Plasmodium* ookinetes crossing the epithelium. It has been observed that antibiotic-treated mosquitoes have a fragmented (if any) peritrophic matrix. Secondly, they produce toxins that directly affect *Plasmodium* ookinetes such as reactive oxygen species (Cirimotich et al., 2011) and possibly Haemolysin F (Tchioffo et al., 2016). Thirdly, they induce a basal level of immunity by triggering the expression of antimicrobial peptides (Dong et al., 2009, Rodgers et al., 2017b, Tchioffo et al., 2016, Wang et al., 2019). Indeed, *Plasmodium*-infected *Anopheles* mosquitoes (*An. minimus*, *An. gambiae*, and *An*. *coluzzii*) have a higher load of Enterobacteriaceae in their guts compared to uninfected mosquitoes (Boissière et al., 2012, Dieme et al., 2020, Surat et al., 2016). Also, Tchioffo et al. (2016) showed that infection of *E. coli* (Enterobacteriaceae)-fed *An. gambiae* with *P. falciparum* decreases *P. falciparum* prevalence and infection intensity, while Wang et

al. (2019) showed that infection of *Serratia marcescens* (Enterobacteriaceae)-fed *An. stephensi* with *P. berghei* reduces the parasite prevalence and infection intensity.

1.3 The 20E signaling pathway is a key modulator of *Anopheles* mosquitoes vectorial capacity

1.3.1 The 20E signaling pathway in mosquitoes and its regulation

In mosquitoes, the 20E signaling pathway is initiated when 20E binds to its nuclear receptor, the ecdysone receptor complex (Figure 1.3a). The ecdysone receptor complex is a heterodimer consisting of the ultraspiracle protein (USP) and the ecdysone receptor protein (EcR) (Figure 1.3a). USP and EcR are orthologues of the mammalian retinoid-X receptor (RXR) and farnesoid X receptor (FXR), respectively (Koelle et al., 1991, Oro et al., 1990). Both EcR and USP are members of the steroid receptor superfamily, which is characterized by five domains (Figure 1.3b): A/B (transactivation), C (DNA-binding), D (hinge), E (ligand-binding), and F (transactivation) (Cho et al., 1995, Kapitskaya et al., 1996). Recently, the F-domain of *Ae. aegypti* EcR was shown to bind to the metal ions Cu^{2+} and Zn^{2+}, thereby inducing a helical structure in the protein and promoting ligand binding specificity (Rowinska-Zyrek et al., 2019).

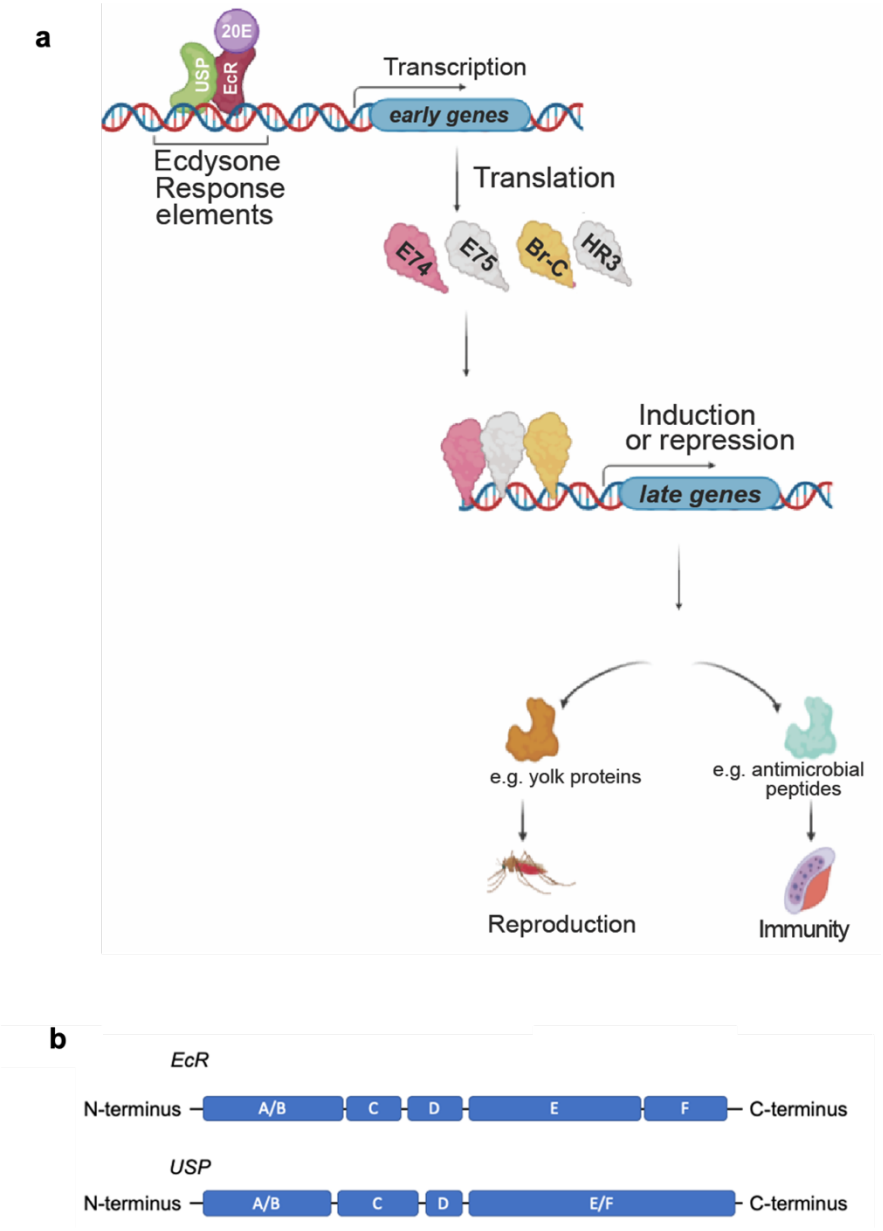

Figure 1.3: The 20E signaling pathway in mosquitoes [created with information from Chen et al., 2004, Cherbas et al., 1991, Kapitskaya et al., 2000, Mane-Padros et al., 2012, Margam et al., 2006, Sun et al., 2002, Sun et al., 2004, Yao et al., 1992, Zhu et al., 2007]. (**a**) Once 20E binds to its heterodimer EcR/USP receptor, this latter is activated and acts as a transcription factor, binding to an enhancer region known as the ecdysone response elements (EcRE). Binding of EcR/USP to EcRE activate the transcription of early genes (*E74* , *E75* , *Broad-Complex*, and *HR3*). These three early genes in turn act as transcription factors, inducing or repressing the expression of downstream genes involved in reproduction and immunity. Abbreviations: EcR, Ecdysone Receptor; USP, Ultraspiracle; 20E, 20-hydroxyecdysone; Br-C, Broad Complex; HR3, Hormone receptor 3. (**b**) Domain organization of the EcR and USP proteins, based on studies in *Ae. aegypti*.

Only EcR binds to 20E, but a study in *Drosophila* revealed that EcR requires heterodimerization with USP to successfully bind the hormone (Yao et al., 1992). It has also been reported that USP might be involved in the allosteric regulation of EcR, altering its conformation to favour the hormone- and DNA-binding properties of EcR (Hu et al., 2003, Kumar et al., 2002). The EcR-USP complex acts as a transcription factor, binding with high affinity to the ecdysone response elements (EcRE), an enhancer located in the upstream regulatory regions of ecdysone-responsive genes (Cherbas et al., 1991). In *Ae. aegypti*, EcRE are composed of DNA motifs that are either inverted or direct repeats (Wang et al., 1998). Binding of EcR-USP to EcRE activates the transcription of "early genes" such as *E75*, *E74*, *HR3*, and *Broad-Complex* (Chen et al., 2004, Kapitskaya et al., 2000, Mane-Padros et al., 2012, Margam et al., 2006, Sun et al., 2002, Zhu et al., 2007). These early genes in turn also act as transcription factors, inducing or repressing the expression of several downstream genes which control reproduction, immunity, and development (Figure 1.3a) (Johnson, 2018). However, the EcR-USP transcription factor sometimes directly binds to the EcRE regions of downstream genes, such as *vitellogenin* (Ekoka et al., 2021, Martín et al., 2001).

While only one EcR isoform has been identified to date in *Anopheles* species genomes (VectorBase), two EcR isoforms (A and B) have been identified in *Ae. aegypti* and they appear to vary in biological function as well as spatial and/or temporal expression (Cruz et al., 2009, Margam et al., 2006, Parthasarathy and Palli, 2007, Wang et al., 2002). For example, in the fat body*, EcR-A* expression increases during the vitellogenic period from 12 hPBM to 24 hPBM, and then decreases by 36 hPBM; while *EcR-B* is most abundant in the pre-vitellogenic and post--vitellogenic period (Wang et al., 2002). Similarly, two USP isoforms have been described in *Ae. aegypti* (Kapitskaya et al., 1996, Parthasarathy and Palli, 2007, Wang et al., 2000).

The abundance of *USP-A* in the fat body is highest in the pre-vitellogenic and late vitellogenic period, while *USP-B* is highly expressed during vitellogenesis (Wang et al., 2000). In the midgut of *Ae. aegypti* larvae, EcR-B and USP-A isoforms are more abundant than EcR-A and USP-B (Wu et al., 2006). Apart from *Ae. aegypti* fat body and midgut, isoforms of the ecdysone receptor subunits have also been detected in the ovaries and male accessory glands (Cruz et al., 2009, Pondeville et al., 2008). Also, while there is currently no experimental evidence in mosquitoes, EcR isoforms have also been detected in the central nervous system of the black cutworm *Agrotis ipsilon* (Abrieux et al., 2013), the honeybee *Apis mellifera* (Takeuchi et al., 2007), and the silkworm *Bombyx mori* (Hossain et al., 2006).

Several regulators coordinate the spatio-temporal expression and activation of EcR and USP. For example, before a blood meal, USP is bound to the nuclear factor HR38 in the fat body of *Ae. aegypti*, but HR38 is later displaced by EcR during the vitellogenesis period (12-24 hPBM) (Zhu et al., 2000). Another important regulator is the "early gene" *E75*. Three isoforms of E75 (E75A, E75B, and E75C) have been detected in the fat body of *Ae. aegypti* post--blood meal, and functional studies revealed that silencing either E75A or E75C shifts the peak expression of EcR-A (which normally occurs 12-24 hrs PBM) to 24-30 hrs PBM (Cruz et al., 2012). Two additional proteins, FISC and ßFTZ-F1, act as co-activators of EcR/USP in the fat body of blood-fed *Ae. aegypti* females, by recruiting and binding to the EcR/USP complex at the EcRE region of the *vitellogenin* promoter. This association was absent in the non-bloodfed cohorts (Zhu et al., 2006). Besides vitellogenesis, the timely regulation of metamorphosis also requires the presence cofactors to regulate EcR/USP. For example, in *Ae. aegypti* fourth instar larvae, the cAMP-response element binding protein (CREB)-binding protein or CBP —whose primary function is to loosen the chromatin structure to render the DNA regulatory regions accessible to transcription

factors— suppresses the expression of *EcR-A*, to prevent premature moulting. When *CBP* is silenced, *EcR-A* expression is elevated, and the larvae prematurely metamorphosed into pupae (Gaddelapati et al., 2020, Margam et al., 2006).

1.3.2 The 20E signaling pathway regulates *Anopheles* females vectorial capacity

Several *Anopheles* physiological processes that are essential to their vectorial capacity are regulated by the 20E signaling pathway. These include their susceptibility and tolerance to *Plasmodium* infection (Marcenac et al., 2020, Reynolds et al., 2020, Werling et al., 2019), longevity (Childs et al., 2016, Maharaj, 2021), mating (Bascuñán et al., 2020, Childs et al., 2016, Gabrieli et al., 2014), blood digestion and vitellogenesis (Chen et al., 2004, Cho et al., 1995, Maharaj, 2021, Raikhel et al., 2002) and the ability to lay viable/fertile eggs (Maharaj, 2021), amongst others.

***Plasmodium* infection** — Manipulating the titers, activity, or signaling of 20E affects parasites oocyst prevalence (*P. falciparum* and *P. berghei*), oocyst intensity (*P. falciparum* and *P. berghei*), and EIP (*P. falciparum*) (Reynolds et al., 2020, Werling et al., 2019). However, the molecular mechanisms by which these parasite parameters are regulated are poorly understood. From an immune response perspective, it is possible that 20E signaling regulates *P. berghei* development via several immune effectors, including antimicrobial peptides, prophenoloxidases, CLIP serine proteases, or lysozymes (Reynolds et al., 2020). In addition, given the increase in the number of phagocytic cells and activity reported after 20E injection (Reynolds et al., 2020), it is possible that the 20E pathway reduces susceptibility to *P. berghei* infection by increasing the phagocytic defence mechanism. Notably, while a male-to-female transfer of 20E has been reported in several species (Pondeville et al., 2008,

Robinson, 2013), it is still unclear whether the male-derived 20E contributes to *Anopheles* susceptibility to *P. falciparum* (NF54 strain) infection. Dahalan et al. (2019) showed that mating increased both *P. falciparum* oocyst prevalence and intensity in *An. coluzzii.* This effect was attributed to the male-to-female transfer of 20E, since 20E injection of virgin *An. coluzzii* produced similar results (Dahalan et al., 2019). On the other hand, Marcenac et al. (2020) reported no effect on parasite prevalence or intensity in mated *An. gambiae* and *An*. *stephensi*. Therefore, it is possible that the male-derived 20E is not solely responsible for the phenotypes observed, but rather, it acts in conjunction with other female genes that are affected by post--mating. Consistent with this idea, 13 genes (seven in the lower reproductive tract and six in the carcass) were found to be differentially expressed in females after mating in *An. coluzzii* versus *An. gambiae* (Thailayil et al., 2018). Further studies should investigate whether one of these genes is responsible for the discrepancy observed between Dahalan's and Marcenac's findings.

Longevity — To date, two studies have demonstrated that 20E regulates *Anopheles* longevity. First, Childs et al. (2016) have shown that boosting 20E signaling with the agonist methoxyfenozide (see section 1.4.2) reduced *An. gambiae* females longevity. These findings were corroborated when Maharaj (2021) demonstrated that silencing *EcR* reduces *An. funestus* female survival.

Mating — Since most *Anopheles* females mate only once in their lifetime (Clements and Stanley-Samuelson, 1999), identifying the factors that regulate the efficiency of this mating event and those that regulate the refractoriness to further mating is of utmost importance. Gabrieli et al. (2014) showed that 20E-injected virgin females lose their ability to become inseminated. Interestingly, they observed that two mating-regulated atrial proteases, namely MatRAP1 and MatRAP2, were significantly down-regulated in the atria of these 20E-injected females. In a recent study, the

functions of these two MatRAP proteins were elucidated, showing that they prevent *Anopheles* females to be re-inseminated (Bascuñán et al., 2020), according to a model described below (Figure 1.4).

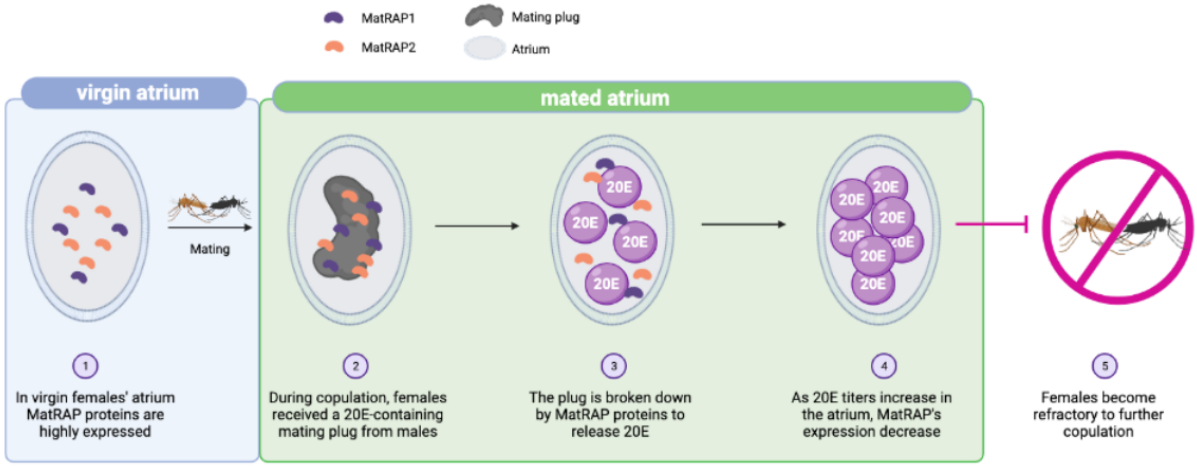

Figure 1.4: Male-secreted 20E induces the repression of two atrial proteases, thereby preventing the females to copulate more than once [created with information from Bascuñán et al., 2020 and Gabrieli et al., 2014].

Blood digestion — In anautogenous female mosquitoes, egg development requires nutrients obtained from a blood meal. After the ingested blood is digested to release cholesterol and proteins (Figure 1.5), the cholesterol is used for 20E production, while the midgut proteases hydrolyse the proteins into amino acids. These amino acids are incorporated into various metabolic pathways in the fat body such as lipid and carbohydrate metabolism, resulting in the production of lipids, yolk proteins, and energy (Figure 1.5). The carbohydrate metabolism pathways, including glycogen metabolism, gluconeogenesis, the citric acid cycle, and glycolysis were previously found to be up-regulated at 18-24 hPBM, which is also the peak of 20E synthesis in females (Hou et al., 2015). Further analysis revealed that silencing EcR down-

regulated the expression of several genes involved in glycolysis and glycogen metabolism, resulting in an increase in fat body glycogen, decreased ATP levels, and accumulation of sugars (glucose and fructose) (Hou et al., 2015). Dong et al. (2018) later reported that 20E regulates the carbohydrate metabolism via the HR38 nuclear transcription factor. Similarly, 20E signaling was also shown to regulate lipid metabolism in the fat body (Figure 1.5), as silencing of EcR resulted in increased levels of triacylglycerols (TAGs) and decreased ß-oxidation (Wang et al., 2017). This allows the insect to store lipids as either energy source for egg maturation, or to incorporate these lipids in the developing oocytes (Ziegler and Ibrahim, 2001).

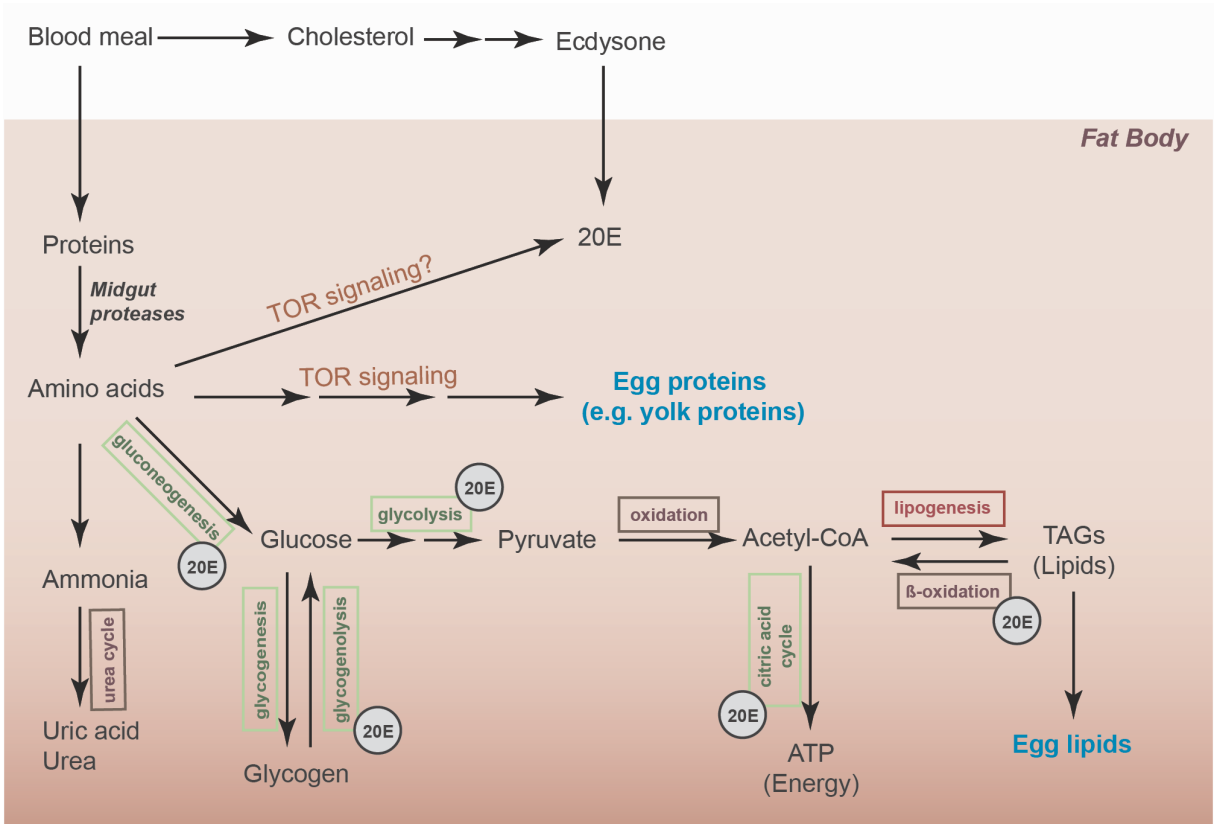

Figure 1.5: 20E regulates blood digestion in mosquitoes [created with information from Dong et al., 2018, Hou et al., 2015, Scaraffia, 2016, and Wang et al., 2017]. Anautogenous mosquitoes use the blood nutrients to produce egg components in the fat body. In *Aedes* aegypti, blood meal digestion involves several metabolic processes (indicated in boxes), many of which are regulated by 20E signaling, as indicated by the 20E sign. The carbohydrate-related metabolic pathways are indicated in green boxes,

while the lipid-metabolic pathways are indicated in red boxes. Abbreviations: TAGs, triacylglycerols; TOR, Target of Rapamycin; ATP, Adenosine Triphosphate.

Vitellogenesis — In *Ae. aegypti*, the ingestion of a blood meal triggers the brain to release two neurohormones —ovary ecdysteroidogenic hormone (OEH) and insulin-like peptide 3 (ILP3) — into the haemolymph (Brown et al., 2008, Brown et al., 1998) (Figure 1.6). ILP3 and OEH bind to their receptors (the insulin and OEH receptors, respectively), located on the follicle cells of the ovarioles (Riehle and Brown, 2002, Vogel et al., 2015). This binding triggers a phosphorylation cascade, which in turn activates the target of rapamycin (TOR) and insulin pathways, and ultimately blocks the activity of the glycogen synthase kinase 3 (GSK3) protein (Valzania et al., 2019). Blocking of GSK3 results in the proliferation of follicle cells, an indication that the ovarioles are ready to produce ecdysone (Valzania et al., 2019). Hence, the blood-derived cholesterol (transported by lipophorin, a fat body synthesized carrier protein), and amino acids (via amino acid-transporters) enter the follicle cells where they serve as building blocks for ecdysone synthesis (Attardo et al., 2006, Boudko et al., 2015, Capurro et al., 1994, Carpenter et al., 2012, Van Heusden et al., 1997). Ecdysone is then released from the ovaries and enters the fat body where it is converted into 20E (Figure 1.6). In the fat body, 20E triggers the synthesis of yolk protein precursors (YPPs) such as vitellogenin, vitellogenin carboxypeptidase, or cathepsin b-like protease (Roy et al., 2015). These YPPs are released into the haemolymph and transported to the growing oocytes in the ovaries where they are taken up by receptor-mediated endocytosis (Figure 1.6). Although the regulation of YPPs transport has not been investigated in mosquitoes, Carney et al. (2000) reported that *Drosophila* females with EcR mutations displayed decreased transport of YPPs to the ovaries compared to untreated controls (Carney and Bender, 2000).

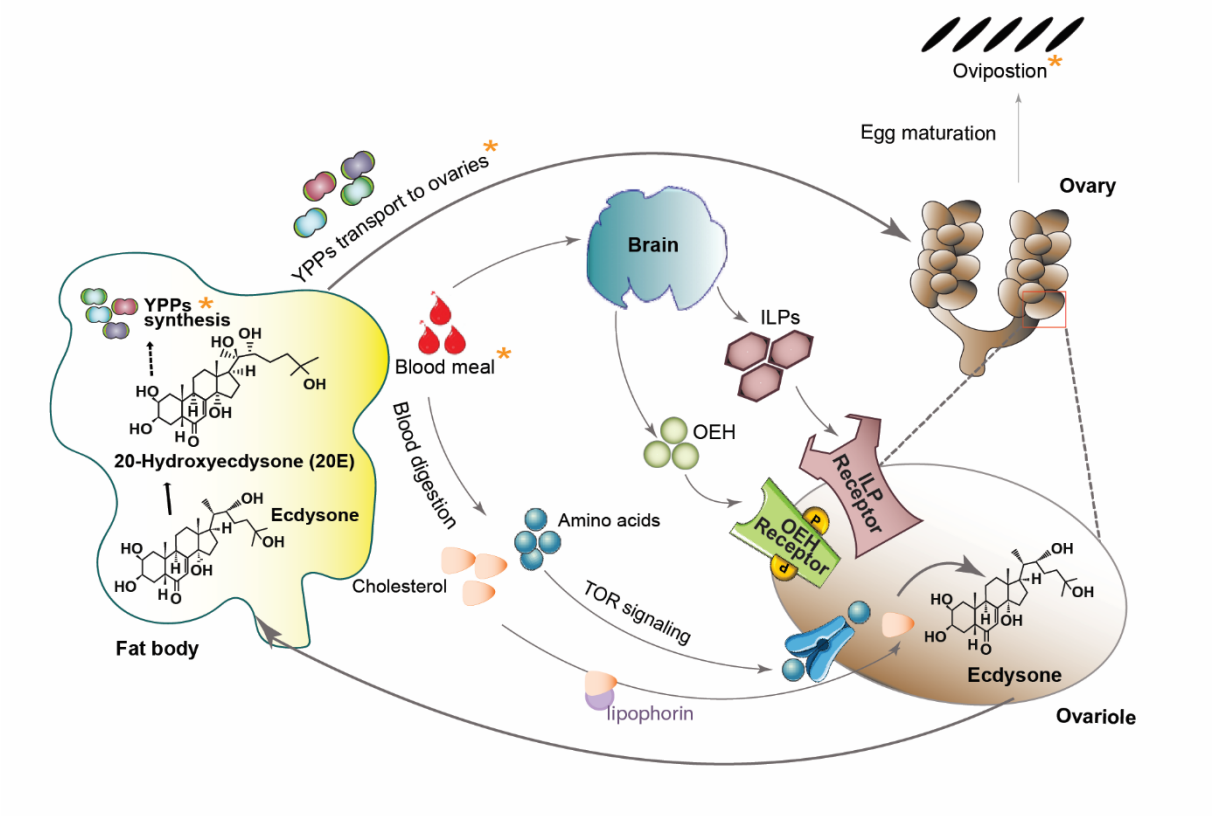

Figure 1.6: 20E signaling regulates vitellogenesis [created with information from Attardo et al., 2006, Brown et al., 2008, Carpenter et al., 2012, Riehle and Brown, 2002, and Vogel et al., 2015]. Refer to text for details. The steps regulated by 20E signaling in mosquitoes are indicated in orange asterisks (*). Abbreviations: P, phosphate group; TOR, Target of rapamycin; OEH, ovary ecdysteroidogenic hormone; ILP, insulin-like peptide; YPP, yolk protein precursor.

Ability of females to lay viable eggs — Laying viable or fertile eggs suggests that the mosquitoes successfully digest their blood meal, complete their vitellogenesis, in addition to a proper maturation of their ovaries. Because females 20E regulates these processes, it is no surprise that it also affects the production and deposition of fertile eggs. Hence, a previous report demonstrated that silencing *EcR* in *An. gambiae* adult females decreased the size of their ovarian follicles and their egg clutch size (Bryant and Raikhel, 2011). Similarly, Gabrieli et al. (2014) demonstrated that 20E-injected virgin *An. gambiae* females laid eggs that were sterile. Interestingly, the ability

to lay viable eggs is also regulated by the male-secreted 20E once it is transferred to the female atrium during copulation (Baldini et al., 2013, Dahalan et al., 2019, Gabrieli et al., 2014, Shaw et al., 2014). Although the mechanisms whereby the male-derived 20E regulates these processes are yet to be uncovered, it has been reported that the female atrium-specific MISO (mating-induced stimulator of oogenesis) protein interacts with the male-derived 20E to regulate egg production (Baldini et al., 2013). Besides, the male-to-female transfer of 20E activates the c-Jun N-terminal kinase (JNK) pathway in *An. gambiae* females head, a step that was proven essential for successful oviposition (Peirce et al., 2020). Yet another aspect of mosquitoes biology which is essential to their ability to lay viable eggs is the cyclic nature of their gonotrophic cycle (section 1.2.1). To date, two 20E-induced mosquitoes proteins (HR3 and E93) are known to regulate the cell deaths events that are essential for the cyclic expression of vitellogenin and thus the cyclic nature of the gonotrophic cycle (Mane-Padros et al., 2012, Wang et al., 2021).

1.4 Strengthening *Anopheles* chemical control by targeting the 20E signaling pathway

The existing WHO-approved chemical control strategies can be divided into two categories: core interventions and supplementary interventions (WHO, 2019). Core interventions comprise incorporating insecticides on bed nets (long lasting insecticide-treated nets, LLINs) or spraying them on the walls of houses (indoor residual spraying, IRS). At present, five WHO-approved classes of insecticides are used in IRS interventions (pyrethroids, carbamates, organophosphates, nicotinoids, and

organochlorines), as opposed to LLINs where only pyrethroids have been approved owing to their relative safety (WHO, 2019). Collectively, LLINs and IRS have led to an 18% global reduction in malaria cases over the past eight years (WHO, 2018). The second category, also called “supplementary interventions”, includes larval source management (LSM) via biological or chemical larvicides, as well as disruption of breeding sites (WHO, 2019). Although there are reports of highly successful LSM programs (Fillinger and Lindsay, 2011), in reality most malaria-endemic countries have so many breeding sites that LSM becomes both expensive and impractical.

Unfortunately, field resistance to insecticides is common and widespread and as a result, the efficacy of the core interventions has been drastically impaired. In particular, pyrethroid resistance has been detected in all the major African malaria vectors, including *An. gambiae*, *An. coluzzii*, *An*. *arabiensis*, and *An*. *funestus* (Knox et al., 2014, WHO, 2018). This has created an urgent need for enhanced insecticides, such as those carrying synergists (e.g., piperonyl butoxide) (Dadzie et al., 2017, Gleave et al., 2018) antimalarials (e.g. atovaquone) (Paton et al., 2019), or chemicals with novel targets. The latter would ideally target a mosquito pathway that is essential for vectorial capacity, such as 20E signaling. The paragraphs below thus describe our current knowledge on the efficacy of compounds that target 20E signaling.

1.4.1 Insect growth regulators that boost 20E signaling

20E agonists are insect growth regulators (IGRs) that compete with 20E to bind to its EcR receptor complex, thereby over-activating the 20E signaling pathway. Interestingly, both EcR and USP subunits of the receptor complex are needed for successful 20E agonist activity (Dhadialla et al., 1998, Reynolds and Smith, 2020). The most studied class of 20E agonists are the dibenzoylhydrazine (DBH) compounds (Dhadialla et al., 1998, Smagghe et al., 2019). Currently, many IGRs based on DBH

compounds are commercially available, such as tebufenozide (RH-5992), methoxyfenozide (RH-2485), halofenozide (RH-0345), fufenozide, chromafenozide (ANS-118), or RH-5849 (Carlson et al., 2001, Nakagawa, 2005, Wing et al., 1988). These compounds were initially formulated against lepidopteran and coleopteran crop pests, however there is increasing evidence that they could also be used to control mosquito populations at different developmental stages, including eggs, larvae, and adults (Beckage et al., 2004, Childs et al., 2016, Hamaidia and Soltani, 2016, Morou et al., 2013).

Water treatment with methoxyfenozide has been shown to reduce the egg hatch rate in *Cx. pipiens* (Hamaidia and Soltani, 2016), as well as larval mortality in *An. gambiae*, *Ae. aegypti*, and *Cx. quinquefasciatus* (Beckage et al., 2004, Morou et al., 2013). The effect of 20E agonists on pupae is yet to be tested in mosquitoes, but treating *Spodoptera litura* (cotton leafworm) pupae with RH-5849 resulted in pupal development abnormalities and a subsequent decrease in adult emergence (Tateishi et al., 1993). In *An. gambiae* adults, it has been demonstrated that methoxyfenozide and halofenozide reduced *P. falciparum* and *P. berghei* transmission, respectively (Childs et al., 2016, Reynolds and Smith, 2020). In addition, fecundity, fertility, mating success, and adult longevity were all significantly decreased after DBH exposure (Childs et al., 2016). As such, DBH compounds affects both vector abundance and vector competence, and have the additional benefit of showing minimal effect on non-target species, as opposed to conventional insecticides which may be toxic to humans and other arthropods (Table 1.1).

Table 1.1: Insecticidal properties of the DBH compounds. Only those which have shown promising results against mosquitoes (*An. gambiae*, *Culex pipiens*, *Cx. quinquefasciatus*, *Ae. aegypti*, Ae. *albopictus*) are mentioned. Compiled with information from Cao and Han, 2006, Dunley et al., 2006, Rehan and Freed, 2014, Shah et al., 2017, and Smirle et al., 2002.

DBH compounds	Cross-resistance	Absence of cross-resistance	Toxicity	Off/targets
Methoxyfenozide	Organophosphate - chlorpyriphos (low) - azinphosmethyl Pyrethroids - deltamethrin Others - cyromazine (low) - fipronil (low) - abamectin - Teflubenzuron (low)	Pyrethroid - bifenthrin Organochlorine - Indoxacarb Others - spinosad	Mammals, birds, and fish (very low)	Organisms Earthworms Birds (low) Fish (low) Honey bees Agricultural pests
Tebufenozide	DBHs - methoxyfenozide Pyrethroids - deltamethrin (low) Organophosphate - azinphosmethyl Others - abamectin - JS118	Pyrethroid - Cypermethrin Organophosphate - Trichlorfon - phoxim - acephate Others Fipronil Chlorfenapyr	Mammals, birds, and fish (very low)	Agricultural lepidopteran pests
Halofenozide	n/d	n/d	Mammals, birds, and fish (very low)	None against fish *G. affinis*
RH-5849	n/d	n/d	DNA damage of human blood lymphocytes	*D. magna*

n/d = no data available

Resistance to DBH compounds has been studied in the lepidopterans *Plutella xylostella*, *Cydia pomonella*, and *Spodoptera exigua* (Cao and Han, 2006, Jia et al., 2009, Qian et al., 2008, Sun et al., 2012, Tang et al., 2011), and two mechanisms have been identified. As with classic insecticides, the first mechanism involves an increase in the activity of detoxification enzymes such as carboxylesterase, aryl-acylamidase, cytochrome P450s, or glutathione-S-transferase (Mosallanejad et al., 2010, Mosallanejad and Smagghe, 2009, Tang et al., 2011, Yin et al., 2019). While an increased expression of cytochrome P450s also constitutes the resistance mechanism of some carbamates, pyrethroids, organochlorines (reviewed in (Adedeji et al., 2020), it is interesting to note that cross-resistance between DBH compounds and these classic insecticides is not always guaranteed (see next paragraph). The second resistance mechanism, identified in *P. xylostella*, involves the microRNA *miR-189942*, which decreases the expression of EcR-B isoform, thereby reducing the susceptibility to fufenozide (because fewer binding sites are available for the 20E agonist) (Li et al., 2020). However, resistance to DBH compounds is unstable, due to fitness cost such as higher mortality rate, decrease reproductive capacity, associated with the DBH-resistant phenotype (Rehan and Freed, 2015, Shah et al., 2017, Sun et al., 2012, Tang et al., 2011). As such, most insects revert back to the susceptible phenotype when the 20E agonist is removed (Sun et al., 2012, Tang et al., 2011). This is a significant advantage over classical insecticides where long-term use has resulted in fixed population-wide genetic changes that confer resistance. Alternatively, the emergence and spread of DBH resistance could be delayed by including available synergists to the DBH formulations (Smagghe, 2004), such as metyrapone and diethylmaleate, which inhibit the activities of oxidative and glutathione-s-transferase enzymes, respectively (Smagghe, 2004).

Another important consideration before implementing a chemical control strategy based on 20E agonists is the phenomenon of cross-resistance. This occurs when insects are resistant to multiple insecticides because these latter target similar detoxification mechanisms or have the same modes of action (Rogier et al., 2009). Studies in lepidopterans with methoxyfenozide and tebufenozide suggest that cross-resistance between DBH compounds is highly likely (Table 1.1), while cross-resistance between a DBH compound and the currently WHO-approved classes of insecticides (pyrethroids, organophosphates, carbamates, and organochlorines) is insecticide-dependent. For example, while a cross-resistance is observed between methoxyfenozide and deltamethrin (Type II pyrethroid), no such link is observed between methoxyfenozide and bifenthrin (Type I pyrethroid) (Table 1.1). In mosquitoes, cross-resistance between methoxyfenozide, pyrethroids, organochlorines (DDT), and carbamates has been characterized (Brown et al., 2020). The authors found that *Anopheles* populations (*An. gambiae s.s.*, *An. funestus s.s.*, and *An. coluzzii*) which were resistant to DDT, carbamates, and pyrethroids —regardless of the mechanism of pyrethroid-resistance— are still susceptible to methoxyfenozide (Brown et al., 2020). Collectively, these findings suggest that malaria vectors could be effectively controlled by a rotational strategy between DBHs and conventional insecticides, as part of an insecticide resistance management plan. Such a plan could for example involve (i) a rotation between pyrethroids and DBHs (with or without synergists/antimalarials) on LLINs, or (ii) a rotation between DBHs (with or without synergists/antimalarials), pyrethroids, DDT, and carbamates for IRS and larvicides.

Another limitation of LLINs and IRS interventions is the fact that they are designed to target mosquitoes indoors. Therefore, exophilic and exophagic vectors such as *An. arabiensis* are poorly controlled by these approaches (Sougoufara et al., 2020). To overcome this challenge, attractive toxic sugar baits (ATSB) have been

proposed. The components of ATSB include a floral scent, a sugar solution, and an oral insecticide, to attract, feed, and kill mosquitoes, respectively (Fiorenzano et al., 2017, Kline et al., 2018). This technique has already been proven successful against *An. gambiae* and *An. arabiensis* populations in experimental trials (Müller et al., 2010, Tenywa et al., 2017), and it would thus be worth investigating if the addition of DBH compounds to ATSB could enhance their efficacy. Additionally, one could also target exophilic/exophagic mosquitoes at the immature aquatic stages, using DBH compounds (with or without synergists) as larvicides and ovicides.

1.4.2 Insect growth regulators that weaken 20E signaling

The 20E signaling pathway is also targeted by IGRs that interfere with its activity or reduce 20E titers. These include cucurbitacins (class: triterpenoids) (DINAN et al., 1997, Zou et al., 2018), chlorantraniliprole or CAP (class: ryanoid) (Chen et al., 2020, Meng et al., 2020), and clothianidin (class: neonicotinoid) (Ullah et al., 2019). With respect to 20E biosynthesis and 20E signaling, a study in *Drosophila* showed that cucurbitacins can either displace a steroid hormone bound to EcR or prevent the formation of the EcR/USP heterodimer complex (DINAN et al., 1997). Application of CAP on *Chilo suppressalis* was shown to reduce vitellogenin expression, 20E titers, and increase the expression of three 20E biosynthetic enzymes (phantom, spook, and shade), likely in response to the decrease in 20E levels (Huang et al., 2016, Meng et al., 2020). Finally, a study of the effect of clothianidin on *Aphis gossypii* revealed that a sub-lethal dose of this insecticide reduced *vitellogenin* and *EcR* mRNA expression (Ullah et al., 2019). As expected for insecticides that target 20E signaling, the phenotypes induced by these chemicals include impaired development (*P. xylostella*, *B. mori, C. suppressalis*), reduced fecundity (*P. xylostella, C. suppressalis, Aphis gossypii*), and increased mortality (*P. xylostella, C. suppressalis, Aphis gossypii*) (Chen

et al., 2020, Han et al., 2012, Huang et al., 2016, Meng et al., 2020, Ullah et al., 2019). Although Werling et al. (2019) reported that *P. falciparum* EIP is reduced in *EcR*-depleted *An*. *gambiae*, the ability of *Plasmodium* parasites to complete their EIP also depends on the mosquito longevity. In other words, if the *EcR*-depleted mosquitoes die before the accelerated EIP, they lose their chance to become infectious. As a result, the risk to produce more infectious mosquitoes —by depleting EcR levels— is reduced. Overall, this section (section 1.4) demonstrates that both 20E agonists and IGRs weakening 20E signaling could be used in chemical control interventions, and perhaps be rotated to manage insecticide resistance.

1.5 Outstanding questions regarding how the 20E signaling pathway regulates mosquito reproduction and immunity

In mosquitoes, the role of the 20E signaling pathway in reproduction and immunity is typically studied by manipulating the pathway and assess how it affects a phenotype of interest. These manipulations include (i) depleting the enzymes necessary to produce 20E, i.e., reducing 20E titers, (ii) increasing 20E titers by injecting mosquitoes with 20E, (iii) compromising 20E activity by injecting mosquitoes with the ecdysone-22-oxidase (E22O), an enzyme that alters the molecular structure of 20E or (iv) reducing EcR levels with RNA interference or RNAi (Table 1.2).

Table 1.2: Manipulating 20E titers, activity, or EcR levels in mosquitoes affect their reproductive output (and thus mosquito abundance) and immunity.

Method	Species	Phenotype	References
The 20E signaling pathway and mosquitoes reproductive output			
20E injection (engorged females)	*An. freeborni*	-Longer retention of blood meal	(Rosenberg, 1980)
20E injection (virgin females)	*An. arabiensis*	- 47% increase in the number of females that oviposited - 86% reduction in the females that mated after 20E injection	(Mitchell et al., 2015)
	An. gambiae	- 32% increase in the number of females that oviposited - 100% reduction in the females that mated after 20E injection	(Mitchell et al., 2015)
	An. gambiae	-Lifetime refractoriness to mating in females -Eggs laid were sterile	(Gabrieli et al., 2014)
Reducing 20E titers and activity (adult males)	*An. gambiae*	-Females mating with those 20E-impaired males fail to oviposit after blood feeding	(Gabrieli et al., 2014)
Reducing 20E activity (adult females)	*An. gambiae*	-Reduced egg clutch size	(Werling et al., 2019)
EcR depletion (adult females)	*Ae. aegypti*	-Reduced egg production -Inhibition genes involved in autophagy -Decreased size of ovarian follicles -Egg developmental defects (Failure of eggs to develop after first oviposition)	(Bryant and Raikhel, 2011)
EcR depletion (adult females)	*An. gambiae*	- ~74.4% decreased expression of *MISO* (gene regulating oogenesis and oviposition) - ~54% decreased expression of *Vg* (Gene regulating vitellogenesis)	(Baldini et al., 2013)

Method	Species	Phenotype	References
EcR depletion (adult females)	*An. gambiae*	-Reduced egg clutch size	(Werling et al., 2019)
EcR depletion (adult females)	*An. funestus*	-Reduced number of eggs developed -No effect on number of eggs oviposited -Reduced egg fertility	(Maharaj, 2021)
The 20E signaling pathway and mosquitoes immunity			
Reducing 20E activity (adult females)	*An. gambiae*	-Reduced *P. falciparum* oocyst intensity -Reduced *P. falciparum* EIP, as indicated by earlier invasion of salivary glands with sporozoites	(Werling et al., 2019)
20E injection 24 hrs before infection (adult females)	*An. gambiae*	-Reduced *P. berghei* oocyst prevalence and intensity -Reduced *E. coli* infection	(Reynolds et al., 2020)
20E injection 2 hrs after infection (adult females)	*An. gambiae*	-No effect on *P. berghei* oocyst prevalence and intensity	(Yang et al., 2020)
20E injection (adult females)	*An. coluzzii*	-*P. falciparum* oocyst prevalence increased by ~93% -*P. falciparum* oocyst intensity increased by >100%	(Dahalan et al., 2019)
EcR depletion (adult females)	*An. gambiae*	-Reduced *P. falciparum* oocyst prevalence by 11-24% -Reduced *P. falciparum* EIP, as indicated by earlier invasion of salivary glands with sporozoites -Higher infectious sporozoite prevalence and intensity in EcR-silenced females at 10 dpi and 12 dpi, respectively	(Werling et al., 2019)

1.5.1 Outstanding questions pertaining to mosquitoes reproduction

While the above studies (Table 1.2) already show a range of reproduction phenotypes affected by manipulating the 20E signaling pathway, several questions remain unanswered. Firstly, most studies were performed in *An. gambiae*, with only one study conducted in *An. arabiensis* (Dongola strain, from Sudan). This study assessed how 20E injection affects the number of females that oviposit and the number of females that can mate post- 20E injection (Table 1.2). Therefore, the role of the 20E signaling pathway in the number of eggs oviposited by *An. arabiensis*, their sizes, their fertility, as well as *An. arabiensis* ovary development, expression of YPPS, and immunity has never been investigated. Secondly, all the studies investigating how the 20E signaling pathway regulates mosquitoes reproduction used septic mosquitoes, i.e., mosquitoes with intact bacterial microbiome. It would thus be interesting to investigate whether the presence of these bacteria is necessary for this 20E-mediated regulation. Next, the role of the 20E signaling pathway in reproduction also needs to be investigated in additional mosquito vectors, such as *Culex* spp., *Anopheles coluzzii*, and *An. stephensi*, to determine if it is conserved across these species. While Carney et al. (2000) reported that *EcR* mutations in *Drosophila* prevent the transport of YPPs from the fat body to the ovaries (Figure 1.6), this observation has never been investigated in mosquitoes. Another key factor which regulates mosquito reproduction is their blood-feeding propensity. A study in the cotton bollworm *Helicoverpa armigera* demonstrated that 20E binds to the brain dopamine receptor —when the insect has fed— to stop the desire to seek for food (Kang et al., 2019). It would be interesting to determine whether 20E also binds to mosquitoes brain dopamine receptor to regulate blood-feeding. In *An. gambiae* females, the atrium-specific MISO protein binds to the male-derived 20E to induce egg production (Baldini et al., 2013). Is this finding true for other *Anopheles* vectors? Mitchell et al. (2015) reported that a MISO sequence is present in the genome

of *An. arabiensis*, *An. funestus*, *An. stephensi*, *An. dirus*, *An. farauti*, *An. albimanus*, *An. sinensis*, and *An. atroparvus*. Furthermore, they show that these MISO sequences are evolutionary related to *An. gambiae* MISO sequence. However, there is no experimental evidence to confirm that MISO function is conserved among these species. Similarly, the role of the 20E-regulated MatRAP proteins which prevent *An. gambiae* females to be re-inseminated should be investigated in other mosquito vectors (Bascuñán et al., 2020).

1.5.2 Outstanding questions pertaining to mosquitoes immunity

With respect to mosquitoes immunity, Reynolds et al. (2020) reported that 20E injection reduced *E. coli* infection in *An. gambiae*. Thus, the 20E signaling pathway may play a role in the anti-bacterial immunity of mosquitoes. Following this idea, the 20E signaling pathway may also regulate the internal bacterial microbiome of mosquitoes. To date, these hypotheses remain unexplored. While it has been established that disturbing the 20E signaling pathway affects *Plasmodium* development (Table 1.2), the mechanisms whereby this phenomenon occurs are still unclear. It also appears that the timing of the 20E injection determines whether *P. berghei* development will be affected (Table 1.2). The mechanisms behind these findings should also be elucidated. Besides, the role of the male-derived 20E in female vector competence is still controversial. While Dahalan et al. (2019) reported that mating —and thus 20E transfer— increased *P. falciparum* development in *An. coluzzii*, Marcenac et al. (2020) did not find any change in *P. falciparum* development in mated *An. gambiae* and *An. stephensi*. Finally, like section 1.5.1, all the immunity-related phenotypes described in Table 1.2 should be investigated in other mosquito vector species.

1.6 Aim and research objectives

The list of outstanding questions mentioned above (section 1.5) is surely incomplete. However, it sets the stage for the purpose of this project. Hence, the aim of this study was to fill-in the gaps in our understanding of how the 20E signaling pathway regulates mosquitoes reproductive output and immunity, using *An. arabiensis* (KwaZulu-Natal strain, South Africa) as the model species.

In Chapter 2, I investigated whether EcR modulates *An. arabiensis* reproductive processes. The main research questions included: Does depleting *An. arabiensis* EcR levels affect its vitellogenesis, fecundity and fertility? And how does EcR sequence from *An. arabiensis* compare to that of other malaria vectors? Based on Table 1.2, it was hypothesized that depleting *EcR* levels by RNA interference (RNAi) would impair *An. arabiensis* reproductive processes. Also, because *An. gambiae* and *An. arabiensis* both belong to the *An. gambiae* complex, it was hypothesized that EcR sequences from these two species would be highly similar.

The focus of chapter 3 was to address the following questions: Are the 20E signaling pathway and the gut bacterial microbiome linked? And if so, what is the contribution (if any) of the gut microbiome to how EcR modulates *An. arabiensis* reproductive output? To assess the link between the gut bacterial microbiome and the 20E signaling pathway, the effect of silencing *EcR* on the gut bacterial load was determined; in addition, *EcR* transcripts were quantified in antibiotic-fed mosquitoes. It was hypothesized that *EcR* depletion would result in a reduced gut bacterial microbiome and conversely, antibiotic-fed mosquitoes would have less *EcR* transcripts. Therefore, silencing *EcR* in antibiotic-fed mosquitoes could result in a much

higher impact on the reproductive processes than when *EcR* was silenced in sugar-fed mosquitoes.

Finally, Chapter 4 explored this question: Are there any immune mechanism(s) by which the 20E signaling pathway regulates bacterial infection? Based on the role the Imd pathway plays in mosquitoes antibacterial immunity, and 20E signaling plays on bacterial infection, a relationship between 20E signaling and the Imd pathway was hypothesized. Furthermore, it was hypothesized that 20E regulates the proliferation of bacteria by controlling the expression of genes of the Imd pathway.

1.7 References

ABRIEUX, A., DEBERNARD, S., MARIA, A., GAERTNER, C., ANTON, S., GADENNE, C. & DUPORTETS, L. 2013. Involvement of the G-protein-coupled dopamine/ecdysteroid receptor DopEcR in the behavioral response to sex pheromone in an insect. *PLoS One,* 8**,** e72785.

ADEDEJI, E. O., OGUNLANA, O. O., FATUMO, S., BEDER, T., AJAMMA, Y., KOENIG, R. & ADEBIYI, E. 2020. *Anopheles* metabolic proteins in malaria transmission, prevention and control: a review. *Parasit. Vectors,* 13**,** 1-30.

ADEPOJU, P. 2019. RTS, S malaria vaccine pilots in three African countries. *The Lancet,* 393**,** 1685.

AHMED, M. A. & COX-SINGH, J. 2015. *Plasmodium knowlesi*–an emerging pathogen. *ISBT science series,* 10**,** 134-140.

AKORLI, J., GENDRIN, M., PELS, N. A. P., YEBOAH-MANU, D., CHRISTOPHIDES, G. K. & WILSON, M. D. 2016. Seasonality and locality affect the diversity of

Anopheles gambiae and *Anopheles coluzzii* midgut microbiota from Ghana. *PLoS One,* 11**,** e0157529.

ATTARDO, G. M., HANSEN, I. A., SHIAO, S.-H. & RAIKHEL, A. S. 2006. Identification of two cationic amino acid transporters required for nutritional signaling during mosquito reproduction. *J. Exp. Biol.,* 209**,** 3071.

BAHIA, A. C., DONG, Y., BLUMBERG, B. J., MLAMBO, G., TRIPATHI, A., BENMARZOUK-HIDALGO, O. J., CHANDRA, R. & DIMOPOULOS, G. 2014. Exploring *Anopheles* gut bacteria for *Plasmodium* blocking activity. *Environ. Microbiol.,* 16**,** 2980-2994.

BALDINI, F., GABRIELI, P., SOUTH, A., VALIM, C., MANCINI, F. & CATTERUCCIA, F. 2013. The interaction between a sexually transferred steroid hormone and a female protein regulates oogenesis in the malaria mosquito *Anopheles gambiae*. *PLoS Biol.,* 11**,** e1001695-e1001695.

BARNARD, K., JEANRENAUD, A. C., BROOKE, B. D. & OLIVER, S. V. 2019. The contribution of gut bacteria to insecticide resistance and the life histories of the major malaria vector *Anopheles arabiensis* (Diptera: Culicidae). *Sci. Rep.,* 9**,** 1-11.

BASCUÑÁN, P., GABRIELI, P., MAMELI, E. & CATTERUCCIA, F. 2020. Mating-regulated atrial proteases control reinsemination rates in *Anopheles gambiae* females. *Sci. Rep.,* 10**,** 1-10.

BASCUÑÁN, P., NIÑO-GARCIA, J. P., GALEANO-CASTAÑEDA, Y., SERRE, D. & CORREA, M. M. 2018. Factors shaping the gut bacterial community assembly in two main Colombian malaria vectors. *Microbiome,* 6**,** 1-12.

BEACH, R. 1979. Mosquitoes: biting behavior inhibited by ecdysone. *Science,* 205**,** 829-831.

BECKAGE, N. E., MARION, K. M., WALTON, W. E., WIRTH, M. C. & TAN, F. F. 2004. Comparative larvicidal toxicities of three ecdysone agonists on the mosquitoes *Aedes aegypti*, *Culex quinquefasciatus*, and *Anopheles gambiae*. *Arch. Insect Biochem. Physiol.,* 57**,** 111-122.

BENNINK, S., KIESOW, M. J. & PRADEL, G. 2016. The development of malaria parasites in the mosquito midgut. *Cell. Microbiol.,* 18**,** 905-918.

BENZON, G. L. & APPERSON, C. S. 1988. Reexamination of chemically mediated oviposition behavior in *Aedes aegypti* (L.)(Diptera: Culicidae). *J. Med. Entomol.,* 25**,** 158-164.

BOISSIÈRE, A., TCHIOFFO, M. T., BACHAR, D., ABATE, L., MARIE, A., NSANGO, S. E., SHAHBAZKIA, H. R., AWONO-AMBENE, P. H., LEVASHINA, E. A. & CHRISTEN, R. 2012. Midgut microbiota of the malaria mosquito vector *Anopheles gambiae* and interactions with *Plasmodium falciparum* infection. *PLoS Pathog.,* 8**,** e1002742.

BOUDKO, D. Y., TSUJIMOTO, H., RODRIGUEZ, S. D., MELESHKEVITCH, E. A., PRICE, D. P., DRAKE, L. L. & HANSEN, I. A. 2015. Substrate specificity and transport mechanism of amino-acid transceptor Slimfast from *Aedes aegypti*. *Nat. Commun.,* 6**,** 8546.

BROWN, F., PATON, D. G., CATTERUCCIA, F., RANSON, H. & INGHAM, V. A. 2020. A steroid hormone agonist reduces female fitness in insecticide-resistant *Anopheles* populations. *Insect Biochem. Mol. Biol.,* 121**,** 103372.

BROWN, M. R., CLARK, K. D., GULIA, M., ZHAO, Z., GARCZYNSKI, S. F., CRIM, J. W., SUDERMAN, R. J. & STRAND, M. R. 2008. An insulin-like peptide regulates egg maturation and metabolism in the mosquito *Aedes aegypti*. *Proc. Natl. Acad. Sci. U. S. A.,* 105**,** 5716-5721.

BROWN, M. R., GRAF, R., SWIDEREK, K. M., FENDLEY, D., STRACKER, T. H., CHAMPAGNE, D. E. & LEA, A. O. 1998. Identification of a steroidogenic neurohormone in female mosquitoes. *J. Biol. Chem.,* 273**,** 3967-3971.

BRYANT, B. & RAIKHEL, A. S. 2011. Programmed autophagy in the fat body of *Aedes aegypti* is required to maintain egg maturation cycles. *PLoS One,* 6**,** e25502-e25502.

CANSADO-UTRILLA, C., ZHAO, S. Y., MCCALL, P. J., COON, K. L. & HUGHES, G. L. 2021. The microbiome and mosquito vectorial capacity: rich potential for discovery and translation. *Microbiome,* 9**,** 1-11.

CAO, G. & HAN, Z. 2006. Tebufenozide resistance selected in *Plutella xylostella* and its cross-resistance and fitness cost. *Pest Manag. Sci.,* 62**,** 746-751.

CAPURRO, M. D. L., DE BIANCHI, A. & MARINOTTI, O. 1994. *Aedes aegypti* lipophorin. *Comp. Biochem. Physiol. B Biochem. Mol. Biol.,* 108**,** 35-39.

CARLSON, G. R., DHADIALLA, T. S., HUNTER, R., JANSSON, R. K., JANY, C. S., LIDERT, Z. & SLAWECKI, R. A. 2001. The chemical and biological properties of methoxyfenozide, a new insecticidal ecdysteroid agonist. *Pest Manag. Sci.,* 57**,** 115-119.

CARNEY, G. E. & BENDER, M. 2000. The *Drosophila* ecdysone receptor (EcR) gene is required maternally for normal oogenesis. *Genetics,* 154**,** 1203-1211.

CARPENTER, V. K., DRAKE, L. L., AGUIRRE, S. E., PRICE, D. P., RODRIGUEZ, S. D. & HANSEN, I. A. 2012. SLC7 amino acid transporters of the yellow fever mosquito *Aedes aegypti* and their role in fat body TOR signaling and reproduction. *J. Insect Physiol.,* 58**,** 513-522.

CASTRO, M. C., TSURUTA, A., KANAMORI, S., KANNADY, K. & MKUDE, S. 2009. Community-based environmental management for malaria control: evidence from a small-scale intervention in Dar es Salaam, Tanzania. *Malar. J.,* 8**,** 57.

CHEN, J., LU, Z., LI, M., MAO, T., WANG, H., LI, F., SUN, H., DAI, M., YE, W. & LI, B. 2020. The mechanism of sublethal chlorantraniliprole exposure causing silkworm pupation metamorphosis defects. *Pest Manag. Sci.,* 76**,** 2838-2845.

CHEN, L., ZHU, J., SUN, G. & RAIKHEL, A. 2004. The early gene Broad is involved in the ecdysteroid hierarchy governing vitellogenesis of the mosquito *Aedes aegypti*. *J. Mol. Endocrinol.,* 33**,** 743-761.

CHERBAS, L., LEE, K. & CHERBAS, P. 1991. Identification of ecdysone response elements by analysis of the *Drosophila* Eip28/29 gene. *Genes Dev.,* 5**,** 120-131.

CHILDS, L. M., CAI, F. Y., KAKANI, E. G., MITCHELL, S. N., PATON, D., GABRIELI, P., BUCKEE, C. O. & CATTERUCCIA, F. 2016. Disrupting mosquito reproduction and parasite development for malaria control. *PLoS Pathog.,* 12**,** e1006060-e1006060.

CHO, W.-L., KAPITSKAYA, M. Z. & RAIKHEL, A. S. 1995. Mosquito ecdysteroid receptor: analysis of the cDNA and expression during vitellogenesis. *Insect Biochem. Mol. Biol.,* 25**,** 19-27.

CIRIMOTICH, C. M., DONG, Y., CLAYTON, A. M., SANDIFORD, S. L., SOUZA-NETO, J. A., MULENGA, M. & DIMOPOULOS, G. 2011. Natural microbe-mediated refractoriness to *Plasmodium* infection in *Anopheles gambiae*. *Science,* 332**,** 855-858.

CLEMENTS, A. & STANLEY-SAMUELSON, D. W. 1999. *The Biology of Mosquitoes: Development, Nutrition and Reproduction,* Great Britain, CABI.

COETZEE, M. 2020. Key to the females of Afrotropical *Anopheles* mosquitoes (Diptera: Culicidae). *Malar. J.,* 19**,** 1-20.

COON, K. L., BROWN, M. R. & STRAND, M. R. 2016. Gut bacteria differentially affect egg production in the anautogenous mosquito *Aedes aegypti* and facultatively

autogenous mosquito *Aedes atropalpus* (Diptera: Culicidae). *Parasit. Vectors,* 9**,** 375.

COON, K. L., VALZANIA, L., MCKINNEY, D. A., VOGEL, K. J., BROWN, M. R. & STRAND, M. R. 2017. Bacteria-mediated hypoxia functions as a signal for mosquito development. *Proc. Natl. Acad. Sci. U. S. A.,* 114**,** e5362-e5369.

CORREA, M. A., MATUSOVSKY, B., BRACKNEY, D. E. & STEVEN, B. 2018. Generation of axenic *Aedes aegypti* demonstrate live bacteria are not required for mosquito development. *Nat. Commun.,* 9**,** 1-10.

CRUZ, J., MANE-PADROS, D., ZOU, Z. & RAIKHEL, A. S. 2012. Distinct roles of isoforms of the heme-liganded nuclear receptor E75, an insect ortholog of the vertebrate Rev-erb, in mosquito reproduction. *Mol. Cell. Endocrinol.,* 349**,** 262-271.

CRUZ, J., SIEGLAFF, D. H., ARENSBURGER, P., ATKINSON, P. W. & RAIKHEL, A. S. 2009. Nuclear receptors in the mosquito *Aedes aegypti*. *FEBS J.,* 276**,** 1233-1254.

DADZIE, S. K., CHABI, J., ASAFU-ADJAYE, A., OWUSU-AKROFI, O., BAFFOE-WILMOT, A., MALM, K., BART-PLANGE, C., COLEMAN, S., APPAWU, M. A. & BOAKYE, D. A. 2017. Evaluation of piperonyl butoxide in enhancing the efficacy of pyrethroid insecticides against resistant *Anopheles gambiae* sl in Ghana. *Malar. J.,* 16**,** 342.

DAHALAN, F. A., CHURCHER, T. S., WINDBICHLER, N. & LAWNICZAK, M. K. N. 2019. The male mosquito contribution towards malaria transmission: Mating influences the *Anopheles* female midgut transcriptome and increases female susceptibility to human malaria parasites. *PLoS Pathog.,* 15**,** e1008063.

DE O GAIO, A., GUSMÃO, D. S., SANTOS, A. V., BERBERT-MOLINA, M. A., PIMENTA, P. F. & LEMOS, F. J. 2011. Contribution of midgut bacteria to blood

digestion and egg production in *Aedes aegypti* (Diptera: Culicidae)(L.). *Parasit. Vectors,* 4**,** 105.

DERUA, Y. A., ALIFRANGIS, M., MAGESA, S. M., KISINZA, W. N. & SIMONSEN, P. E. 2015. Sibling species of the *Anopheles funestus* group, and their infection with malaria and lymphatic filarial parasites, in archived and newly collected specimens from northeastern Tanzania. *Malar. J.,* 14**,** 104.

DHADIALLA, T. S., CARLSON, G. R. & LE, D. P. 1998. New insecticides with ecdysteroidal and juvenile hormone activity. *Annu. Rev. Entomol.,* 43**,** 545-569.

DIAZ-NIETO, L. M., D´ ALESSIO, C., PEROTTI, M. A. & BERON, C. M. 2016. *Culex pipiens* development is greatly influenced by native bacteria and exogenous yeast. *PLoS One,* 11**,** e0153133.

DICKSON, L. B., JIOLLE, D., MINARD, G., MOLTINI-CONCLOIS, I., VOLANT, S., GHOZLANE, A., BOUCHIER, C., AYALA, D., PAUPY, C. & MORO, C. V. 2017. Carryover effects of larval exposure to different environmental bacteria drive adult trait variation in a mosquito vector. *Science advances,* 3**,** e1700585.

DIEME, C., ZMARLAK, N. M., BRITO-FRAVALLO, E., TRAVAILLÉ, C., PAIN, A., CHERRIER, F., GENÈVE, C., CALVO-ALVAREZ, E., RIEHLE, M. M. & VERNICK, K. D. 2020. Exposure of *Anopheles* mosquitoes to trypanosomes reduces reproductive fitness and enhances susceptibility to *Plasmodium*. *PLoS Negl. Trop. Dis.,* 14**,** e0008059.

DINAN, L., WHITING, P., GIRAULT, J.-P., LAFONT, R., DHADIALLA, S. T., CRESS, E. D., MUGAT, B., ANTONIEWSKI, C. & LEPESANT, J.-A. 1997. Cucurbitacins are insect steroid hormone antagonists acting at the ecdysteroid receptor. *Biochem. J.,* 327**,** 643-650.

DONG, D., ZHANG, Y., SMYKAL, V., LING, L. & RAIKHEL, A. S. 2018. HR38, an ortholog of NR4A family nuclear receptors, mediates 20-hydroxyecdysone

regulation of carbohydrate metabolism during mosquito reproduction. *Insect Biochem. Mol. Biol.,* 96**,** 19-26.

DONG, Y., MANFREDINI, F. & DIMOPOULOS, G. 2009. Implication of the mosquito midgut microbiota in the defense against malaria parasites. *PLoS Pathog.,* 5**,** e1000423-e1000423.

DRAKE, J. M. & BEIER, J. C. 2014. Ecological niche and potential distribution of *Anopheles arabiensis* in Africa in 2050. *Malar. J.,* 13**,** 213-213.

DUNLEY, J. E., BRUNNER, J. F., DOERR, M. D. & BEERS, E. 2006. Resistance and cross-resistance in populations of the leafrollers, *Choristoneura rosaceana* and *Pandemis pyrusana*, in Washington apples. *J. Insect Sci.,* 6**,** 14.

FILLINGER, U. & LINDSAY, S. W. 2011. Larval source management for malaria control in Africa: myths and reality. *Malar. J.,* 10**,** 353.

FIORENZANO, J. M., KOEHLER, P. G. & XUE, R.-D. 2017. Attractive toxic sugar bait (ATSB) for control of mosquitoes and its impact on non-target organisms: a review. *Int. J. Environ. Res. Public Health,* 14**,** 398.

GABRIELI, P., KAKANI, E. G., MITCHELL, S. N., MAMELI, E., WANT, E. J., ANTON, A. M., SERRAO, A., BALDINI, F. & CATTERUCCIA, F. 2014. Sexual transfer of the steroid hormone 20E induces the postmating switch in *Anopheles gambiae*. *Proc. Natl. Acad. Sci. U. S. A.,* 111**,** 16353-16358.

GADDELAPATI, S. C., DHANDAPANI, R. K. & PALLI, S. R. 2020. CREB-binding protein regulates metamorphosis and compound eye development in the yellow fever mosquito, *Aedes aegypti*. *Biochim. Biophys. Acta,* 1863**,** 194576.

GAO, H., CUI, C., WANG, L., JACOBS-LORENA, M. & WANG, S. 2019. Mosquito Microbiota and Implications for Disease Control. *Trends Parasitol.,* 36**,** 98-111.

GAO, L., SONG, X. & WANG, J. 2020. Gut microbiota is essential in PGRP-LA regulated immune protection against *Plasmodium berghei* infection. *Parasit. Vectors,* 13**,** 3.

GENDRIN, M. & CHRISTOPHIDES, G. K. 2013. The *Anopheles* mosquito microbiota and their impact on pathogen transmission. *Anopheles mosquitoes-New insights into malaria vectors.* IntechOpen.

GIMONNEAU, G., TCHIOFFO, M. T., ABATE, L., BOISSIÈRE, A., AWONO-AMBÉNÉ, P. H., NSANGO, S. E., CHRISTEN, R. & MORLAIS, I. 2014. Composition of *Anopheles coluzzii* and *Anopheles gambiae* microbiota from larval to adult stages. *Infect. Genet. Evol.,* 28**,** 715-724.

GLEAVE, K., LISSENDEN, N., RICHARDSON, M., CHOI, L. & RANSON, H. 2018. Piperonyl butoxide (PBO) combined with pyrethroids in insecticide-treated nets to prevent malaria in Africa. *Cochrane Database Syst. Rev.*

GNAMBANI, E., BILGO, E., SANOU, A., DABIRE, R. & DIABATE, A. 2020. Infection of highly insecticide-resistant malaria vector *Anopheles coluzzii* with an environment friendly entomopathogenic bacteria *Chromobacterium violaceum* reduces its survival, blood feeding propensity and fecundity. *Malar. J.,* 19**,** 1-10.

GONZALES, K. K., RODRIGUEZ, S. D., CHUNG, H.-N., KOWALSKI, M., VULCAN, J., MOORE, E. L., LI, Y., WILLETTE, S. M., KANDEL, Y. & VAN VOORHIES, W. A. 2018. The effect of SkitoSnack, an artificial blood meal replacement, on *Aedes aegypti* life history traits and gut microbiota. *Sci. Rep.,* 8**,** 1-14.

GUMULIRA, A. 2021. Malaria vaccine approval: a step change for global health. *N. Engl. J. Med.,* 385**,** 1005-1017.

GUTMAN, J. R. & CHICO, R. M. 2020. Evidence for treating malaria with artemisinin-based combination therapy in the first trimester of pregnancy. *Lancet Infect. Dis.,* 20**,** 880-881.

HAMAIDIA, K. & SOLTANI, N. 2016. Ovicidal activity of an insect growth disruptor (methoxyfenozide) against *Culex pipiens* L. and delayed effect on development. *J. Entomol. Zool.,* 4**,** 1202-1207.

HAN, W., ZHANG, S., SHEN, F., LIU, M., REN, C. & GAO, X. 2012. Residual toxicity and sublethal effects of chlorantraniliprole on *Plutella xylostella* (Lepidoptera: Plutellidae). *Pest Manag. Sci.,* 68**,** 1184-1190.

HOGAN, A. B., JEWELL, B. L., SHERRARD-SMITH, E., VESGA, J. F., WATSON, O. J., WHITTAKER, C., HAMLET, A., SMITH, J. A., WINSKILL, P. & VERITY, R. 2020. Potential impact of the COVID-19 pandemic on HIV, tuberculosis, and malaria in low-income and middle-income countries: a modelling study. *Lancet Glob. Health,* 8**,** e1132-e1141.

HOSSAIN, M., SHIMIZU, S., FUJIWARA, H., SAKURAI, S. & IWAMI, M. 2006. EcR expression in the prothoracicotropic hormone-producing neurosecretory cells of the *Bombyx mori* brain: An indication of the master cells of insect metamorphosis. *FEBS J.,* 273**,** 3861-3868.

HOU, Y., WANG, X.-L., SAHA, T. T., ROY, S., ZHAO, B., RAIKHEL, A. S. & ZOU, Z. 2015. Temporal coordination of carbohydrate metabolism during mosquito reproduction. *PLoS Genet.,* 11**,** e1005309-e1005309.

HOWELL, P. I. & KNOLS, B. G. J. 2009. Male mating biology. *Malar. J.,* 8**,** 1-10.

HU, X., CHERBAS, L. & CHERBAS, P. 2003. Transcription activation by the ecdysone receptor (EcR/USP): identification of activation functions. *Mol. Endocrinol.,* 17**,** 716-731.

HUANG, L., LU, M., HAN, G., DU, Y. & WANG, J. 2016. Sublethal effects of chlorantraniliprole on development, reproduction and vitellogenin gene (CsVg) expression in the rice stem borer, *Chilo suppressalis*. *Pest Manag. Sci.,* 72**,** 2280-2286.

HUANG, W., WANG, S. & JACOBS-LORENA, M. 2020. Use of Microbiota to Fight Mosquito-Borne Disease. *Front. Genet.,* 11**,** 196.

JIA, B., LIU, Y., ZHU, Y. C., LIU, X., GAO, C. & SHEN, J. 2009. Inheritance, fitness cost and mechanism of resistance to tebufenozide in *Spodoptera exigua* (Hübner)(Lepidoptera: Noctuidae). *Pest Manag. Sci.,* 65**,** 996-1002.

JOHNSON, L. K. 2018. *Regulation of Gene Expression Patterns During Reproduction in the Female Mosquito, Aedes aegypti.* UC Riverside.

KALAPPA, D. M., SUBRAMANI, P. A., BASAVANNA, S. K., GHOSH, S. K., SUNDARAMURTHY, V., URAGAYALA, S., TIWARI, S., ANVIKAR, A. R. & VALECHA, N. 2018. Influence of midgut microbiota in *Anopheles stephensi* on *Plasmodium berghei i*nfections. *Malar. J.,* 17**,** 385.

KANG, X.-L., ZHANG, J.-Y., DI WANG, Y.-M. Z., HAN, X.-L., WANG, J.-X. & ZHAO, X.-F. 2019. The steroid hormone 20-hydroxyecdysone binds to dopamine receptor to repress lepidopteran insect feeding and promote pupation. *PLoS Genet.,* 15**,** e1008331.

KAPITSKAYA, M., WANG, S., CRESS, D. E., DHADIALLA, T. S. & RAIKHEL, A. S. 1996. The mosquito ultraspiracle homologue, a partner of ecdysteroid receptor heterodimer: cloning and characterization of isoforms expressed during vitellogenesis. *Mol. Cell. Endocrinol.,* 121**,** 119-132.

KAPITSKAYA, M. Z., LI, C., MIURA, K., SEGRAVES, W. & RAIKHEL, A. S. 2000. Expression of the early-late gene encoding the nuclear receptor HR3 suggests its involvement in regulating the vitellogenic response to ecdysone in the adult mosquito. *Mol. Cell. Endocrinol.,* 160**,** 25-37.

KIRILLY, D., WONG, J. J. L., LIM, E. K. H., WANG, Y., ZHANG, H., WANG, C., LIAO, Q., WANG, H., LIOU, Y.-C. & WANG, H. 2011. Intrinsic epigenetic factors

cooperate with the steroid hormone ecdysone to govern dendrite pruning in *Drosophila*. *Neuron,* 72**,** 86-100.

KLINE, D. L., MULLER, G. C., JUNNILA, A. & XUE, R.-D. 2018. Attractive toxic sugar baits (ATSB): a novel vector management tool. *Advances in the Biorational Control of Medical and Veterinary Pests.* ACS Publications.

KNOX, T. B., JUMA, E. O., OCHOMO, E. O., JAMET, H. P., NDUNGO, L., CHEGE, P., BAYOH, N. M., N'GUESSAN, R., CHRISTIAN, R. N. & HUNT, R. H. 2014. An online tool for mapping insecticide resistance in major *Anopheles* vectors of human malaria parasites and review of resistance status for the Afrotropical region. *Parasit. Vectors,* 7**,** 76.

KOELLE, M. R., TALBOT, W. S., SEGRAVES, W. A., BENDER, M. T., CHERBAS, P. & HOGNESS, D. S. 1991. The *Drosophila* EcR gene encodes an ecdysone receptor, a new member of the steroid receptor superfamily. *Cell,* 67**,** 59-77.

KOENE, J. M. & TER MAAT, A. 2001. Allohormones: a class of bioactive substances favoured by sexual selection. *J. Comp. Physiol., A,* 187**,** 323-326.

KUMAR, M. B., FUJIMOTO, T., POTTER, D. W., DENG, Q. & PALLI, S. R. 2002. A single point mutation in ecdysone receptor leads to increased ligand specificity: implications for gene switch applications. *Proc. Natl. Acad. Sci. U. S. A.,* 99**,** 14710-14715.

LAURENS, M. B. 2020. RTS, S/AS01 vaccine (Mosquirix™): An overview. *Hum. Vaccin. Immunother.,* 16**,** 480-489.

LI, X., REN, X., LIU, Y., SMAGGHE, G., LIANG, P. & GAO, X. 2020. MiR-189942 regulates fufenozide susceptibility by modulating ecdysone receptor isoform B in *Plutella xylostella* (L.). *Pestic Biochem Physiol.,* 163**,** 235-240.

LINENBERG, I., CHRISTOPHIDES, G. K. & GENDRIN, M. 2016. Larval diet affects mosquito development and permissiveness to *Plasmodium* infection. *Sci. Rep.,* 6**,** 38230.

MAHARAJ, S. 2021. Impact of *Ecdysone receptor* knockdown on *Anopheles funestus* longevity, reproductive success and *Plasmodium falciparum* susceptibility (unpublished work). South Africa: University of the Witwatersrand.

MANE-PADROS, D., CRUZ, J., CHENG, A. & RAIKHEL, A. S. 2012. A critical role of the nuclear receptor HR3 in regulation of gonadotrophic cycles of the mosquito *Aedes aegypti*. *PLoS One,* 7**,** e45019-e45019.

MARCENAC, P., SHAW, W. R., KAKANI, E. G., MITCHELL, S. N., SOUTH, A., WERLING, K., MARROGI, E., ABERNATHY, D. G., YERBANGA, R. S. & DABIRE, R. K. 2020. A mating-induced reproductive gene promotes *Anopheles* tolerance to *Plasmodium falciparum* infection. *PLoS Pathog.,* 16**,** e1008908.

MARGAM, V. M., GELMAN, D. B. & PALLI, S. R. 2006. Ecdysteroid titers and developmental expression of ecdysteroid-regulated genes during metamorphosis of the yellow fever mosquito, *Aedes aegypti* (Diptera: Culicidae). *J. Insect Physiol.,* 52**,** 558-568.

MARTÍN, D., WANG, S.-F. & RAIKHEL, A. S. 2001. The vitellogenin gene of the mosquito *Aedes aegypti* is a direct target of ecdysteroid receptor. *Mol. Cell. Endocrinol.,* 173**,** 75-86.

MENG, X., ZHANG, N., YANG, X., MIAO, L., JIANG, H., JI, C., XU, B., QIAN, K. & WANG, J. 2020. Sublethal effects of chlorantraniliprole on molting hormone levels and mRNA expressions of three Halloween genes in the rice stem borer, *Chilo suppressalis*. *Chemosphere,* 238**,** 124676.

MITCHELL, S. N., KAKANI, E. G., SOUTH, A., HOWELL, P. I., WATERHOUSE, R. M. & CATTERUCCIA, F. 2015. Evolution of sexual traits influencing vectorial capacity in anopheline mosquitoes. *Science,* 347**,** 985-988.

MITRAKA, E., STATHOPOULOS, S., SIDEN-KIAMOS, I., CHRISTOPHIDES, G. K. & LOUIS, C. 2013. *Asaia* accelerates larval development of *Anopheles gambiae*. *Pathog. Glob. Health,* 107**,** 305-311.

MOROU, E., LIRAKIS, M., PAVLIDI, N., ZOTTI, M., NAKAGAWA, Y., SMAGGHE, G., VONTAS, J. & SWEVERS, L. 2013. A new dibenzoylhydrazine with insecticidal activity against *Anopheles* mosquito larvae. *Pest Manag. Sci.,* 69**,** 827-833.

MOSALLANEJAD, H., BADISCO, L., SWEVERS, L., SOIN, T., KNAPEN, D., BROECK, J. V. & SMAGGHE, G. 2010. Ecdysone signaling and transcript signature in *Drosophila* cells resistant against methoxyfenozide. *J. Insect Physiol.,* 56**,** 1973-1985.

MOSALLANEJAD, H. & SMAGGHE, G. 2009. Biochemical mechanisms of methoxyfenozide resistance in the cotton leafworm *Spodoptera littoralis*. *Pest Manag. Sci.,* 65**,** 732-736.

MOTA-SANCHEZ, D., WISE, J. C., POPPEN, R. V., GUT, L. J. & HOLLINGWORTH, R. M. 2008. Resistance of codling moth, *Cydia pomonella* (L.)(Lepidoptera: Tortricidae), larvae in Michigan to insecticides with different modes of action and the impact on field residual activity. *Pest Manag. Sci.,* 64**,** 881-890.

MOZŪRAITIS, R., HAJKAZEMIAN, M., ZAWADA, J. W., SZYMCZAK, J., PÅLSSON, K., SEKAR, V., BIRYUKOVA, I., FRIEDLÄNDER, M. R., KOEKEMOER, L. L. & BAIRD, J. K. 2020. Male swarming aggregation pheromones increase female attraction and mating success among multiple African malaria vector mosquito species. *Nat. Ecol. Evol.,* 4**,** 1395-1401.

MÜLLER, G. C., BEIER, J. C., TRAORE, S. F., TOURE, M. B., TRAORE, M. M., BAH, S., DOUMBIA, S. & SCHLEIN, Y. 2010. Successful field trial of attractive toxic sugar bait (ATSB) plant-spraying methods against malaria vectors in the *Anopheles gambiae* complex in Mali, West Africa. *Malar. J.,* 9**,** 210.

MUTURI, E. J., DUNLAP, C., RAMIREZ, J. L., ROONEY, A. P. & KIM, C.-H. 2019. Host blood-meal source has a strong impact on gut microbiota of *Aedes aegypti*. *FEMS Microbiol. Ecol.,* 95**,** fiy213.

NAKAGAWA, Y. 2005. Nonsteroidal ecdysone agonists. *Vitam. Horm.,* 73**,** 131-173.

OHM, J. R., BALDINI, F., BARREAUX, P., LEFEVRE, T., LYNCH, P. A., SUH, E., WHITEHEAD, S. A. & THOMAS, M. B. 2018. Rethinking the extrinsic incubation period of malaria parasites. *Parasit. Vectors,* 11**,** 1-9.

OLIVEIRA, J. H. M., GONÇALVES, R. L., LARA, F. A., DIAS, F. A., GANDARA, A. C. P., MENNA-BARRETO, R. F., EDWARDS, M. C., LAURINDO, F. R., SILVA-NETO, M. A. & SORGINE, M. H. 2011. Blood meal-derived heme decreases ROS levels in the midgut of *Aedes aegypti* and allows proliferation of intestinal microbiota. *PLoS Pathog.,* 7**,** e1001320.

ORO, A. E., MCKEOWN, M. & EVANS, R. M. 1990. Relationship between the product of the *Drosophila* ultraspiracle locus and the vertebrate retinoid X receptor. *Nature,* 347**,** 298-301.

PARTHASARATHY, R. & PALLI, S. R. 2007. Stage-and cell-specific expression of ecdysone receptors and ecdysone-induced transcription factors during midgut remodeling in the yellow fever mosquito, *Aedes aegypti*. *J. Insect Physiol.,* 53**,** 216-229.

PATON, D. G., CHILDS, L. M., ITOE, M. A., HOLMDAHL, I. E., BUCKEE, C. O. & CATTERUCCIA, F. 2019. Exposing *Anopheles* mosquitoes to antimalarials blocks *Plasmodium* parasite transmission. *Nature,* 567**,** 239-243.

PEIRCE, M. J., MITCHELL, S. N., KAKANI, E. G., SCARPELLI, P., SOUTH, A., SHAW, W. R., WERLING, K. L., GABRIELI, P., MARCENAC, P. & BORDONI, M. 2020. JNK signaling regulates oviposition in the malaria vector *Anopheles gambiae*. *Sci. Rep.,* 10**,** 1-12.

PONDEVILLE, E., MARIA, A., JACQUES, J.-C., BOURGOUIN, C. & DAUPHIN-VILLEMANT, C. 2008. *Anopheles gambiae* males produce and transfer the vitellogenic steroid hormone 20-hydroxyecdysone to females during mating. *Proc. Natl. Acad. Sci. U. S. A.,* 105**,** 19631-19636.

QIAN, L., CAO, G., SONG, J., YIN, Q. & HAN, Z. 2008. Biochemical mechanisms conferring cross-resistance between tebufenozide and abamectin in *Plutella xylostella*. *Pestic. Biochem. Physiol.,* 91**,** 175-179.

RAIKHEL, A. S., KOKOZA, V. A., ZHU, J., MARTIN, D., WANG, S.-F., LI, C., SUN, G., AHMED, A., DITTMER, N. & ATTARDO, G. 2002. Molecular biology of mosquito vitellogenesis: from basic studies to genetic engineering of antipathogen immunity. *Insect Biochem. Mol. Biol.,* 32**,** 1275-1286.

RANDELL, H. F., DICKINSON, K. L., SHAYO, E. H., MBOERA, L. E. & KRAMER, R. A. 2010. Environmental management for malaria control: knowledge and practices in Mvomero, Tanzania. *EcoHealth,* 7**,** 507-516.

REHAN, A. & FREED, S. 2014. Resistance selection, mechanism and stability of *Spodoptera litura* (Lepidoptera: Noctuidae) to methoxyfenozide. *Pestic. Biochem. Physiol.,* 110**,** 7-12.

REHAN, A. & FREED, S. 2015. Fitness cost of methoxyfenozide and the effects of its sublethal doses on development, reproduction, and survival of *Spodoptera litura* (Fabricius)(Lepidoptera: Noctuidae). *Neotrop. Entomol.,* 44**,** 513-520.

REYNOLDS, R. A., KWON, H. & SMITH, R. C. 2020. 20-hydroxyecdysone (20E) primes innate immune responses that limit bacteria and malaria parasite survival in *Anopheles gambiae*. *mSphere,* 5**,** e00983-00919.

REYNOLDS, R. A. & SMITH, R. C. 2020. The 20-hydroxyecdysone agonist, halofenozide, primes anti-*Plasmodium* immunity in *Anopheles gambiae* via the ecdysone receptor. *Sci. Rep.,* 10**,** 1-9.

RIEHLE, M. A. & BROWN, M. R. 2002. Insulin receptor expression during development and a reproductive cycle in the ovary of the mosquito *Aedes aegypti*. *Cell Tissue Res.,* 308**,** 409-420.

ROBINSON, R. 2013. His hormone, her oogenesis: how male malaria mosquitoes trigger female egg development. *PLoS Biol.,* 11**,** e1001694-e1001694.

RODGERS, F. H., GENDRIN, M. & CHRISTOPHIDES, G. K. 2017a. The mosquito immune system and its interactions with the microbiota: Implications for disease transmission. *Arthropod Vector: Controller of Disease Transmission.*

RODGERS, F. H., GENDRIN, M., WYER, C. A. & CHRISTOPHIDES, G. K. 2017b. Microbiota-induced peritrophic matrix regulates midgut homeostasis and prevents systemic infection of malaria vector mosquitoes. *PLoS Pathog.,* 13**,** e1006391.

ROGIER, C., HENRY, M., ROWLAND, M., CARNEVALE, P., CHANDRE, F., CORBEL, V., CURTIS, C. & HOUGARD, J. 2009. Guidelines for phase III evaluation of vector control methods against malaria. *Medecine Tropicale: Revue du Corps de Sante Colonial,* 69**,** 173-184.

ROMOLI, O. & GENDRIN, M. 2018. The tripartite interactions between the mosquito, its microbiota and *Plasmodium*. *Parasit. Vectors,* 11**,** 200.

ROSENBERG, R. 1980. Ovarian control of blood meal retention the the mosquito *Anopheles freeborni*. *J. Insect Physiol.,* 26**,** 477-480.

ROWINSKA-ZYREK, M., WIĘCH, A., WĄTŁY, J., WIECZOREK, R., WITKOWSKA, D., OŻYHAR, A. & ORŁOWSKI, M. 2019. Copper (II)-Binding Induces a Unique Polyproline Type II Helical Structure within the Ion-Binding Segment in the Intrinsically Disordered F-Domain of Ecdysteroid Receptor from *Aedes aegypti*. *Inorg. Chem.,* 58**,** 11782-11792.

ROY, S., SAHA, T. T., JOHNSON, L., ZHAO, B., HA, J., WHITE, K. P., GIRKE, T., ZOU, Z. & RAIKHEL, A. S. 2015. Regulation of gene expression patterns in mosquito reproduction. *PLoS Genet.,* 11**,** e1005450-e1005450.

SAAB, S. A., ZU DOHNA, H., NILSSON, L. K., ONORATI, P., NAKHLEH, J., TERENIUS, O. & OSTA, M. A. 2020. The environment and species affect gut bacteria composition in laboratory co-cultured *Anopheles gambiae* and *Aedes albopictus* mosquitoes. *Sci. Rep.,* 10**,** 1-13.

SCARAFFIA, P. Y. 2016. Disruption of mosquito blood meal protein metabolism. *In:* ADELMAN, Z. N. (ed.) *Genetic Control of Malaria and Dengue.* First ed.: Academic Press, Elsevier.

SHAH, R. M., SHAD, S. A. & ABBAS, N. 2017. Methoxyfenozide resistance of the housefly, *Musca domestica* L.(Diptera: Muscidae): cross-resistance patterns, stability and associated fitness costs. *Pest Manag. Sci.,* 73**,** 254-261.

SHARMA, A., DHAYAL, D., SINGH, O., ADAK, T. & BHATNAGAR, R. K. 2013. Gut microbes influence fitness and malaria transmission potential of Asian malaria vector *Anopheles stephensi*. *Acta tropica,* 128**,** 41-47.

SHAW, W. R. & CATTERUCCIA, F. 2018. Vector biology meets disease control: Using basic research to fight vector-borne diseases. *Nat. Microbiol.,* 4**,** 20-34.

SHAW, W. R., TEODORI, E., MITCHELL, S. N., BALDINI, F., GABRIELI, P., ROGERS, D. W. & CATTERUCCIA, F. 2014. Mating activates the heme

peroxidase HPX15 in the sperm storage organ to ensure fertility in *Anopheles gambiae*. *Proc. Natl. Acad. Sci. U. S. A.,* 111**,** 5854-5859.

SINCLAIR, D., ZANI, B., DONEGAN, S., OLLIARO, P. & GARNER, P. 2009. Artemisinin-based combination therapy for treating uncomplicated malaria. *Cochrane Database Syst. Rev.*

SINDEN, R. E. & GILLES, H. M. 2002. The malaria parasites. *Essential malariology,* 4**,** 8-34.

SINGH, M., TRIVEDI, S., BHUTANI, K., SINGH, G., DUBEY, A. & RAPALLI, C. K. 2020. *Plasmodium*'s journey through the *Anopheles* mosquito: A comprehensive review. *Biochimie,* 181**,** 176-190.

SINKA, M. E., BANGS, M. J., MANGUIN, S., RUBIO-PALIS, Y., CHAREONVIRIYAPHAP, T., COETZEE, M., MBOGO, C. M., HEMINGWAY, J., PATIL, A. P. & TEMPERLEY, W. H. 2012. A global map of dominant malaria vectors. *Parasit. Vectors,* 5**,** 69-69.

SMAGGHE, G. 2004. Synergism of diacylhydrazine insecticides with metyrapone and diethylmaleate. *J. Appl. Entomol.,* 128**,** 465-468.

SMAGGHE, G., ZOTTI, M. & RETNAKARAN, A. 2019. Targeting female reproduction in insects with biorational insecticides for pest management: a critical review with suggestions for future research. *Curr. Opin. Insect.,* 31**,** 65-69.

SMIRLE, M. J., THOMAS LOWERY, D. & ZUROWSKI, C. L. 2002. Resistance and cross-resistance to four insecticides in populations of obliquebanded leafroller (Lepidoptera: Tortricidae). *J. Econ. Entomol.,* 95**,** 820-825.

SONG, X., WANG, M., DONG, L., ZHU, H. & WANG, J. 2018. PGRP-LD mediates *A. stephensi* vector competency by regulating homeostasis of microbiota-induced peritrophic matrix synthesis. *PLoS Pathog.,* 14**,** e1006899.

SOUGOUFARA, S., OTTIH, E. C. & TRIPET, F. 2020. The need for new vector control approaches targeting outdoor biting Anopheline malaria vector communities. *Parasit. Vectors,* 13**,** 1-15.

STRAND, M. R. 2018. Composition and functional roles of the gut microbiota in mosquitoes. *Curr. Opin. Insect.,* 28**,** 59-65.

SUN, G., ZHU, J., LI, C., TU, Z. & RAIKHEL, A. S. 2002. Two isoforms of the early E74 gene, an Ets transcription factor homologue, are implicated in the ecdysteroid hierarchy governing vitellogenesis of the mosquito, *Aedes aegypti*. *Mol. Cell. Endocrinol.,* 190**,** 147-157.

SUN, G., ZHU, J. & RAIKHEL, A. S. 2004. The early gene E74B isoform is a transcriptional activator of the ecdysteroid regulatory hierarchy in mosquito vitellogenesis. *Mol. Cell. Endocrinol.,* 218**,** 95-105.

SUN, J., LIANG, P. & GAO, X. 2012. Cross-resistance patterns and fitness in fufenozide-resistant diamondback moth, *Plutella xylostella* (Lepidoptera: Plutellidae). *Pest Manag. Sci.,* 68**,** 285-289.

SURAT, W., MHUANTONG, W., SANGSRAKRU, D., CHAREONVIRIYAPHAP, T., ARUNYAWAT, U., KUBERA, A., SITTIVICHARPINYO, T., SIRIPAN, O. & POOTAKHAM, W. 2016. Gut Bacterial Diversity in *Plasmodium*-infected and Plasmodium-uninfected *Anopheles minimus*. *Chiang Mai J. Sci.,* 43**,** 427-440.

TAKEUCHI, H., PAUL, R. K., MATSUZAKA, E. & KUBO, T. 2007. EcR-A expression in the brain and ovary of the honeybee (*Apis mellifera* L.). *Zool. Sci.,* 24**,** 596-603.

TANG, B., SUN, J., ZHOU, X., GAO, X. & LIANG, P. 2011. The stability and biochemical basis of fufenozide resistance in a laboratory-selected strain of *Plutella xylostella*. *Pestic. Biochem. Physiol.,* 101**,** 80-85.

TATEISHI, K., KIUCHI, M. & TAKEDA, S. 1993. New cuticle formation and molt inhibition by RH-5849 in the common cutworm, *Spodoptera litura* (Lepidoptera: Noctuidae). *Appl. Entomol. Zool.,* 28**,** 177-184.

TCHIOFFO, M. T., BOISSIÈRE, A., ABATE, L., NSANGO, S. E., BAYIBÉKI, A. N., AWONO-AMBÉNÉ, P. H., CHRISTEN, R., GIMONNEAU, G. & MORLAIS, I. 2016. Dynamics of Bacterial Community Composition in the Malaria Mosquito's Epithelia. *Front. Microbiol.,* 6**,** 1500.

TENYWA, F. C., KAMBAGHA, A., SADDLER, A. & MAIA, M. F. 2017. The development of an ivermectin-based attractive toxic sugar bait (ATSB) to target *Anopheles arabiensis*. *Malar. J.,* 16**,** 1-10.

THAILAYIL, J., GABRIELI, P., CAPUTO, B., BASCUÑÁN, P., SOUTH, A., DIABATE, A., DABIRE, R., DELLA TORRE, A. & CATTERUCCIA, F. 2018. Analysis of natural female post-mating responses of *Anopheles gambiae* and *Anopheles coluzzii* unravels similarities and differences in their reproductive ecology. *Sci. Rep.,* 8**,** 1-10.

ULLAH, F., GUL, H., DESNEUX, N., TARIQ, K., ALI, A., GAO, X. & SONG, D. 2019. Clothianidin-induced sublethal effects and expression changes of vitellogenin and ecdysone receptors genes in the melon aphid, *Aphis gossypii*. *Entomol. Gen.,* 39**,** 137-149.

UTZINGER, J., TOZAN, Y. & SINGER, B. H. 2001. Efficacy and cost-effectiveness of environmental management for malaria control. *Trop. Med. Int. Health,* 6**,** 677-687.

VALZANIA, L., MATTEE, M. T., STRAND, M. R. & BROWN, M. R. 2019. Blood feeding activates the vitellogenic stage of oogenesis in the mosquito *Aedes aegypti* through inhibition of glycogen synthase kinase 3 by the insulin and TOR pathways. *Dev. Biol.,* 454**,** 85-95.

VAN HEUSDEN, M. C., ERICKSON, B. A. & PENNINGTON, J. E. 1997. Lipophorin levels in the yellow fever mosquito, *Aedes aegypti*, and the effect of feeding. *Arch. Insect Biochem. Physiol.,* 34**,** 301-312.

VLACHOU, D., SCHLEGELMILCH, T., RUNN, E., MENDES, A. & KAFATOS, F. C. 2006. The developmental migration of *Plasmodium* in mosquitoes. *Curr. Opin. Genet. Dev.,* 16**,** 384-391.

VOGEL, K. J., BROWN, M. R. & STRAND, M. R. 2015. Ovary ecdysteroidogenic hormone requires a receptor tyrosine kinase to activate egg formation in the mosquito *Aedes aegypti*. *Proc. Natl. Acad. Sci. U. S. A.,* 112**,** 5057-5062.

WANG, S., BAI, L., WANG, L., VEGA-RODRÍGUEZ, J. & WANG, G. 2019. A gut symbiotic bacterium *Serratia marcescens* renders mosquito resistance to *Plasmodium* infection through activation of mosquito immune responses. *Front. Microbiol.,* 10**,** 1580.

WANG, S.-F., LI, C., SUN, G., ZHU, J. & RAIKHEL, A. S. 2002. Differential expression and regulation by 20-hydroxyecdysone of mosquito ecdysteroid receptor isoforms A and B. *Mol. Cell. Endocrinol.,* 196**,** 29-42.

WANG, S.-F., LI, C., ZHU, J., MIURA, K., MIKSICEK, R. J. & RAIKHEL, A. S. 2000. Differential expression and regulation by 20-hydroxyecdysone of mosquito ultraspiracle isoforms. *Dev. Biol.,* 218**,** 99-113.

WANG, S.-F., MIURA, K., MIKSICEK, R. J., SEGRAVES, W. A. & RAIKHEL, A. S. 1998. DNA binding and transactivation characteristics of the mosquito ecdysone receptor-Ultraspiracle complex. *J. Biol. Chem.,* 273**,** 27531-27540.

WANG, X., DING, Y., LU, X., GENG, D., LI, S., RAIKHEL, A. S. & ZOU, Z. 2021. The ecdysone-induced protein 93 is a key factor regulating gonadotrophic cycles in the adult female mosquito *Aedes aegypti*. *Proc. Natl. Acad. Sci. U. S. A.,* 118**,** e2021910118.

WANG, X., HOU, Y., SAHA, T. T., PEI, G., RAIKHEL, A. S. & ZOU, Z. 2017. Hormone and receptor interplay in the regulation of mosquito lipid metabolism. *Proc. Natl. Acad. Sci. U. S. A.,* 114**,** e2709-e2718.

WERLING, K., SHAW, W. R., ITOE, M. A., WESTERVELT, K. A., MARCENAC, P., PATON, D. G., PENG, D., SINGH, N., SMIDLER, A. L., SOUTH, A., DEIK, A. A., MANCIO-SILVA, L., DEMAS, A. R., MARCH, S., CALVO, E., BHATIA, S. N., CLISH, C. B. & CATTERUCCIA, F. 2019. Steroid hormone function controls non-competitive *Plasmodium* development in *Anopheles*. *Cell,* 177**,** 315-325.

WHO 2012. Global plan for insecticide resistance management in malaria vectors. Geneva: World Health Organization.

WHO 2018. Global report on insecticide resistance in malaria vectors: 2010-2016. Geneva: World Health Organization.

WHO 2019. Guidelines for Malaria Vector Control. Geneva: World Health Organization.

WHO 2020. World Malaria Report. Geneva: World Health Organization.

WIEBE, A., LONGBOTTOM, J., GLEAVE, K., SHEARER, F. M., SINKA, M. E., MASSEY, N. C., CAMERON, E., BHATT, S., GETHING, P. W., HEMINGWAY, J., SMITH, D. L., COLEMAN, M. & MOYES, C. L. 2017. Geographical distributions of African malaria vector sibling species and evidence for insecticide resistance. *Malar. J.,* 16**,** 85-85.

WIĘCH, A., ROWIŃSKA-ŻYREK, M., WĄTŁY, J., CZARNOTA, A., HOŁUBOWICZ, R., SZEWCZUK, Z., OŻYHAR, A. & ORŁOWSKI, M. 2019. The intrinsically disordered C-terminal F domain of the ecdysteroid receptor from *Aedes aegypti* exhibits metal ion-binding ability. *J. Steroid Biochem. Mol. Biol.,* 186**,** 42-55.

WING, K. D., SLAWECKI, R. A. & CARLSON, G. R. 1988. RH 5849, a nonsteroidal ecdysone agonist: effects on larval Lepidoptera. *Science,* 241**,** 470-472.

WU, Y., PARTHASARATHY, R., BAI, H. & PALLI, S. R. 2006. Mechanisms of midgut remodeling: juvenile hormone analog methoprene blocks midgut metamorphosis by modulating ecdysone action. *Mech. Dev.,* 123**,** 530-547.

XIAO, X., YANG, L., PANG, X., ZHANG, R., ZHU, Y., WANG, P., GAO, G. & CHENG, G. 2017. A Mesh–Duox pathway regulates homeostasis in the insect gut. *Nat. Microbiol.,* 2**,** 17020.

YANG, J., SCHLEICHER, T. R., DONG, Y., PARK, H. B., LAN, J., CRESSWELL, P., CRAWFORD, J., DIMOPOULOS, G. & FIKRIG, E. 2020. Disruption of mosGILT in *Anopheles gambiae* impairs ovarian development and *Plasmodium* infection. *J. Exp. Med.,* 217**,** e20190682.

YAO, T.-P., SEGRAVES, W. A., ORO, A. E., MCKEOWN, M. & EVANS, R. M. 1992. *Drosophila* ultraspiracle modulates ecdysone receptor function via heterodimer formation. *Cell,* 71**,** 63-72.

YIN, Q., QIAN, L., SONG, P., JIAN, T. & HAN, Z. 2019. Molecular mechanisms conferring asymmetrical cross-resistance between tebufenozide and abamectin in *Plutella xylostella*. *J. Asia-Pacif. Entomol.,* 22**,** 189-193.

ZHU, J., CHEN, L. & RAIKHEL, A. S. 2007. Distinct roles of Broad isoforms in regulation of the 20-hydroxyecdysone effector gene, Vitellogenin, in the mosquito *Aedes aegypti*. *Mol. Cell. Endocrinol.,* 267**,** 97-105.

ZHU, J., CHEN, L., SUN, G. & RAIKHEL, A. S. 2006. The competence factor βFtz-F1 potentiates ecdysone receptor activity via recruiting a p160/SRC coactivator. *Mol. Cell. Biol.,* 26**,** 9402-9412.

ZHU, J., MIURA, K., CHEN, L. & RAIKHEL, A. S. 2000. AHR38, a homolog of NGFI-B, inhibits formation of the functional ecdysteroid receptor in the mosquito *Aedes aegypti*. *EMBO J.,* 19**,** 253-262.

ZIEGLER, R. & IBRAHIM, M. M. 2001. Formation of lipid reserves in fat body and eggs of the yellow fever mosquito, *Aedes aegypti*. *J. Insect Physiol.,* 47**,** 623-627.

ZOU, C., LIU, G., LIU, S., LIU, S., SONG, Q., WANG, J., FENG, Q., SU, Y. & LI, S. 2018. Cucurbitacin B acts a potential insect growth regulator by antagonizing 20-hydroxyecdysone activity. *Pest Manag. Sci.,* 74**,** 1394-1403.

ZOURE, A. A., SARE, A. R., YAMEOGO, F., SOMDA, Z., MASSART, S., BADOLO, A. & FRANCIS, F. 2020. Bacterial communities associated with the midgut microbiota of wild *Anopheles gambiae* complex in Burkina Faso. *Mol. Biol. Rep.,* 47**,** 211-224.

CHAPTER 2

The impact of silencing the ecdysone receptor (EcR) on *Anopheles arabiensis* reproduction and gut microbiome

2.1 Introduction

Anopheles arabiensis, one of the primary malaria vectors in sub-Saharan Africa, is currently poorly controlled due to its resistance to the four classes of insecticides used indoor (Brooke et al., 2015, Knox et al., 2014, WHO, 2014), as well as its ability to feed and rest outdoors, thereby escaping the indoor-based insecticide strategies (Mahande et al., 2007, Tirados et al., 2006). One attractive target for developing more effective vector control strategies is to harness the mosquitoes reproductive output, since it ultimately impacts vector abundance (Mitchell and Catteruccia, 2016, Shaw and Catteruccia, 2018). In anautogenous mosquitoes such as *An. arabiensis*, the reproductive output is influenced by mating, blood-feeding, the synthesis of egg yolk proteins (*i.e.*, vitellogenesis), egg development (*i.e.*, oogenesis), oviposition, and egg fertility (Figure 2.1). Indeed, an increase in each of these physiological processes ultimately results in a surge in the number of *Anopheles* vector species in a region and a higher malaria transmission rate. Therefore, developing vector control interventions that can effectively reduce mosquito abundance requires an understanding of the molecular mechanisms that regulate the physiological processes associated with reproduction.

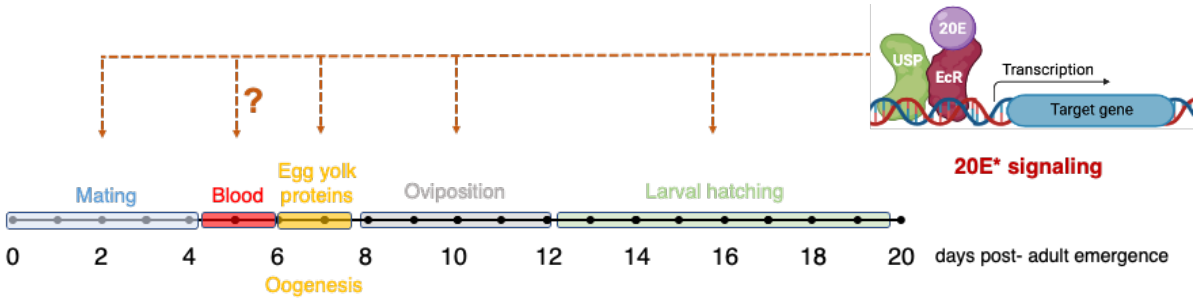

Figure 2.1: Six of the physiological processes that regulate mosquito abundance and their time of occurrence [created with information from Becker et al., 2010, Rodriguez et al., 1992]. The cycle from blood-feeding to egg-laying (oviposition) is known as the gonotrophic cycle. Mosquitoes typically undergo at least one cycle during their lifetime, and each female lays about 50-150 (0.5-2 mm long) eggs per gonotrophic cycle. *Abbreviation: 20E, 20-hydroxyecdysone.

To date, the 20E signaling pathway has been identified as a critical modulator of the physiological processes associated with mosquito reproductivity (section 1.3.2). Several studies have demonstrated that manipulating the mosquito 20E signaling pathway by altering 20E titers and activity, or by silencing the 20E receptor, impairs mating, vitellogenesis, oogenesis, fecundity, and fertility (Brown et al., 2020, Childs et al., 2016, Mitchell et al., 2015, Werling et al., 2019). For example, in terms of vitellogenesis, the expression of *EcR* and egg yolk genes such as *vitellogenin*, *vitellogenin carboxypeptidase*, and *cathepsin b-like protease* usually peaks at ~24 hours post-blood meal (24 hPBM) in the *Ae. aegypti* fat body (Raikhel et al., 2002, Roy et al., 2015). However, when the *EcR* transcript levels are depleted (i.e., silenced) by RNA interference, the abundance of these yolk genes in the fat body at 24 hPBM is also reduced, and this ultimately impairs egg development (Baldini et al., 2013, Roy et al., 2015, Wang et al., 2017, Werling et al., 2019). Another essential protein for *Aedes* and *Anopheles* egg development is lipophorin, which transports lipids to maturing eggs. Previous work suggests that *lipophorin* transcript abundance after *EcR*

silencing depends on the mosquito species and infection status. Werling et al. (2019) showed that *EcR* depletion increased *lipophorin* mRNA levels in the fat body of *Plasmodium*-infected and inseminated *An. gambiae*. In contrast, another study reported that *lipophorin* expression (after *EcR* silencing) is reduced in the fat body of uninfected yet inseminated *Ae. aegypti* females (Wang et al., 2017). With respect to reproduction, disturbing the 20E signaling pathway reportedly impairs egg fertility, oviposition, and ovary development in *An. gambiae* and *Ae. aegypti* (Table 1.2).

Besides the 20E signaling pathway, altering the gut microbiome also impairs a mosquito reproductive fitness (chapter 1, section 1.2.3). In *Anopheles arabiensis*, the gut microbiome consists of bacteria from different families including Enterobacteriaceae, Acetobacteriaceae, and Flavobacteriaceae (E Silva et al., 2021). These Gram-negative bacteria affect the mosquito reproductive output by preventing blood digestion, which in turn leads to a reduction in vitellogenesis and thus the number of eggs produced (chapter 1, section 1.2.3).

As described earlier (section 1.5), several phenotypes of *An. arabiensis* that result from manipulating the 20E signaling pathway have never been investigated. These include the number of eggs oviposited, their sizes, their fertility, as well as ovary development, the expression of YPPs and the gut microbiome. One way to study the role of the 20E signaling pathway in mosquitoes is to perform functional studies of the EcR protein. To date, no functional studies has been conducted on *An. arabiensis* EcR protein. Here, the expression profile of *An. arabiensis EcR* during vitellogenesis was assessed, to confirm that *EcR* is essential for this process. Next, several *in silico* analyses were conducted to compare how *An. arabiensis* EcR protein sequence relates to that of other mosquitoes. Finally, to increase our understanding of how the 20E signaling pathway affects *An. arabiensis* reproductive output, RNA interference

was used to deplete (i.e., silence) *EcR* transcripts in *An. arabiensis*; the following phenotypes were then assessed: the expression of YPPs, the mosquito fecundity, egg size, egg fertility, and the gut microbiome. The focus was on silencing *EcR* (and not *USP*, its binding protein) because although the complex is 20E:EcR:USP, 20E binds only to EcR (Figure 1.3). Nonetheless, silencing *USP* could have produced the same results based on findings showing that silencing USP also disrupts the positive correlation between egg production and pathogen development in *An. gambiae* (Werling et al., 2019).

2.2 Materials and Methods

2.2.1 Ethics statement

The procedures used in this study were approved by the animal research ethics committee (Ethics waiver: 20180723O) at the Faculty of Health Sciences, University of the Witwatersrand, South Africa (Appendix 1).

2.2.2 Mosquito rearing

All adult female mosquitoes used in this study were obtained from the Maureen Coetzee insectary (Wits Research Institute for Malaria, University of the Witwatersrand). They were maintained at 26-28°C, with ±70-90% relative humidity and 12:12 hours light: dark photoperiod. *Anopheles arabiensis* (KWAG strain, from KwaZ ulu-Natal) and *An. gambiae* (COGS strain, from Congo) served as experimental and positive control species, respectively (Koekemoer et al., 2011, Mouatcho et al., 2009). Adults were fed *ad libitum* on a cotton ball soaked in distilled

water containing 10% (w/v) sucrose. Unless indicated otherwise, only mated females were used.

2.2.3 Gene-specific primer design

Gene-specific primers were designed for use in PCR [*EcR*, *Green fluorescent protein* (*GFP*)], quantitative PCR (*EcR*, *lipophorin*, *vitellogenin carboxypeptidase*, *cathepsin b-like protease*, *ribosomal protein L19*, *ribosomal protein S7*, and *ß-actin*), and sequencing (same genes measured in qPCR) (Table 2.1). PrimerQuest (Integrated DNA Technologies) was used to ensure that all primers met the recommended criteria, such as 40-60% GC content, 18-25 nucleotide length, 55-65°C melting temperature, or primer-dimers with $\Delta G \geq -5$ Kj (Taylor et al., 2010).

Table 2.1: List of mosquito primers used in this study. The standard IUPAC nucleotide code was applied.

	Sequences (5' -> 3')	Amplicon size (bp)
qPCR primers		
EcR	Fwd: CCGAACACTTCCTCAATGG Rv: GGGTACGACTCCGTTACT	117
Lp	Fwd: GTGGCTGCCGATTTCTAC Rv: CACCTCCACCTTGTTCTTG	114
VCB	Fwd: GGCATCGAAAGCTCTATCTC Rv: CCTCGTTTAAGCCGGAATG	102
VCP	Fwd: CTGAAGCTGGACGTGATG Rv: CGGGTACGCCACAATAAT	108
Vg	Fwd: CCGTCAAGGGCTTCTATG Rv: GGTGAGGGTGTTGTTCTC	149
RpL19	Fwd: GGTGTGGTTGGATCCTAATG Rv: CAGACCATCCTTGATCAGTT	85
RpS7	Fwd: TCCTGGAGGATCTGGTATTC Rv: GTGGTCTGCTGGTTCTTATC	109
Actin	Fwd: CCCGATCTACGAAGGTTATG Rv: CTTCATCAGGTAGTCGGTAAG	85
Primers to amplify *EcR* coding region from *An. arabiensis* cDNA		
EcR-ORF	Fwd: CGCAAGATGATGAAAAGAAGG Rv: TGCCCTACGCTAGCTATACGA	2,218
Primers for *in vitro* transcription[a]		
EcR	Fwd: *taatacgactcactatagggaga*CATCAGTTCGTGGGCAATCT Rv: *taatacgactcactatagggaga*CTTCTTCTCCTTCCGCTTGATG	492
GFP	Fwd: *taatacgactcactatagggaga*ACGTAAACGGCCACAAGT Rv: *taatacgactcactatagggaga*GGGTGTTCTGCTGGTAGTG	498

[a]The sequences in lowercase italics are the T7 promoter sequences and the product length does not include these promoter sequences.
Abbreviations: Lp = Lipophorin; VCB = Cathepsin b-like protease; VCP = Vitellogenin carboxypeptidase; Vg = Vitellogenin; RpL19 = Ribosomal protein L19; RpS7 = Ribosomal protein S7; GFP = Green Fluorescent protein; Actin = ß-actin; Fwd = Forward primer; Rv = Reverse primer; ORF = Open Reading Frame

Primer-BLAST was used to test the specificity of the primers (Ye et al., 2012). The qPCR primers were designed to target a 75-150 bp region (Taylor et al., 2010), while the PCR primers would amplify the entire *An. arabiensis EcR* coding sequence (Table 2.1). All primers were synthesized by Inqaba Biotechnical industries (South Africa). For all the genes used in this study, the corresponding accession numbers are indicated in supplementary Table S1, while the qPCR efficiency and annealing temperatures of their primers are summarized in supplementary Table S2.

2.2.4 Total RNA extraction and DNase I treatment

Total RNA was isolated with the TRIzol™ Plus RNA purification kit (cat no: 12183555, Thermo Scientific). For this purpose, 13-15 mosquitoes were first placed in a tube containing 1 ml TRIzol™ reagent and stainless-steel beads. The tubes were then inserted in a Tissue Lyser II system (cat no: 85300, Qiagen), and the mosquito tissues were homogenized with high-speed shaking (25 shakes per second for 10 min). The grounded tissues were incubated for 5 min at room temperature for the nucleoproteins complex to dissociate completely. Then, 200 µl chloroform was added to the tubes, and the mixtures were subsequently incubated at room temperature for 3 min to allow for preliminary phase separation. Complete phase separation into three layers was achieved by centrifugation (12,000xg, 4°C, 15 min). The RNA-containing top layer was transferred to a spin cartridge, while the white interface and the bottom layer (containing denatured proteins/DNAs and proteins, respectively) were discarded. After binding the RNA to the membrane cartridge by centrifugation (12,000xg, 4°C, 15 secs), the RNA was washed once with Wash Buffer I and twice with Wash Buffer II via

centrifugation (12,000xg, 4°C, 15 secs). Lastly, 50 µl RNAse-free water was added to the column to elute the RNA (12,000xg, 4°C, 1 min).

DNase I digestion was performed with the TURBO DNA-free™ Kit (cat no: AM1907, Thermo Scientific) to remove any residual gDNA contaminants. The concentration and purity of DNA-free RNA samples were determined by spectrophotometry using the Nanodrop™ One Microvolume UV-Vis Spectrophotometer (cat no: ND-ONE, Thermo Scientific). The absorbance ratios $A_{260/280}$ and $A_{260/230}$ were recorded to assess the contamination with proteins and guanidine, respectively. In addition, a denaturing agarose gel electrophoresis assessed the size and integrity of RNA samples. For this purpose, RNA samples were mixed with a 2x RNA loading dye solution (cat no: R0641, Thermo Scientific), heated at 70°C for 10 min for denaturation, and then electrophoresed alongside an RNA ladder (cat no: SM1821, Thermo Scientific) on a 1% (w/v) agarose/TBE gel pre-stained with 0.2 µg/ml Ethidium Bromide (cat no: 17898, Thermo Scientific). All purified RNA samples were stored at -80°C until use.

2.2.5 cDNA synthesis

For *EcR* isolation, cDNA was synthesized with the Protoscript→ II first-strand cDNA synthesis kit (cat no: E6560S, New England Biolabs) and EcR-ORF reverse primer (Table 2.1). This kit allows the synthesis of cDNAs up to 10 kb in size. By priming cDNA synthesis with gene-specific primers, only *EcR* cDNAs were synthesized. Purified total RNA (1 µg) was mixed with 0.5 µM EcR-ORF reverse primer in UltraPure™ DNase/RNase-free distilled water (cat no: 10977035, Thermo Scientific), and a 5 min incubation at 65°C denatured these two nucleic acids. The Protoscript II reaction mix (C_{final} = 1x) and Protoscript II enzyme mix (C_{final} = 1x) were then added to

the tubes. The mixture was incubated in a thermocycler (42°C for 1 hour, 80°C for 5 min) to synthesize first-strand cDNAs.

For all qPCR experiments, cDNA was synthesized from 1 µg RNA with the iScript™ cDNA synthesis kit (cat no: 1708891, Bio-Rad), as described by the manufacturer's protocol. The reaction mixture included 1 µg total RNA, 1 µl iScript™ reverse transcriptase, 1x iScript™ reaction mix, and ultrapure water (cat no: 10977035, Thermo Scientific) to a final volume of 20 µl. First-strand cDNA synthesis took place in a thermal cycler set as follows: 25°C for 5 min, 42°C for 30 min, and 85°C for 5 min. All synthesized cDNAs were stored at -20°C until use.

2.2.6 Amplification of *An. arabiensis EcR* orthologue for cloning purposes

An. arabiensis Dongola strain *EcR* sequence available on VectorBase (Gene ID: AARA015604) was used as the template to design primers that would amplify the entire coding sequence of *An. arabiensis* KWAG strain from its cDNA (Table 2.1). Since the expected amplicon size was ~2.2 kb, the PCR reaction was performed with the Q5® High-fidelity DNA polymerase (cat no: M0491S, New England Biolabs). This enzyme can amplify products up to 20 kb.

For *EcR* amplification, the 50 µl reaction mixture contained 1x Q5® reaction buffer, 200 µM dNTPs, 0.5 µM each of the EcR-ORF sense and antisense primers (Table 2.1), 1 µl undiluted cDNA, 0.02 U/µl Q5® high-fidelity DNA polymerase, and ultrapure water. A positive control consisting of cDNA synthesized from *An. gambiae* total RNA was included, while a no-template reaction served as the negative control. The reaction mixtures were incubated in a thermal cycler set as follows: initial denaturation (98°C for 30 secs), 30 amplification cycles (98°C for 10 secs, 62°C for

20 secs, and 72°C for 75 secs), and a final elongation step (72°C for 2 min) to complete the synthesis of all strands.

All PCR products were electrophoresed on a 1% (w/v) agarose/TAE gel pre-stained with 0.2 µg/ml Ethidium Bromide (cat no: 17898, Thermo Scientific), alongside a 1 kb DNA molecular weight marker (cat no: SM0313, Thermo Scientific). Unincorporated dNTPs and excess primers were removed by column chromatography using the PureLink® PCR micro kit (cat no: K310050, Thermo Scientific). The purified amplicons concentration was determined with the Nanodrop™ One Microvolume UV-Vis Spectrophotometer (cat no: ND-ONE, Thermo Scientific), while their identity was confirmed by automated nucleotide sequencing at Inqaba Biotechnical Industries (South Africa).

2.2.7 Phylogenetic analyses

To further confirm that the sequence obtained encoded *An. arabiensis* EcR protein, a phylogenetic analysis was conducted to compare the above sequence (section 2.2.6) to functionally characterized insect EcR orthologues (Table 2.2). The phylogenetic tree was constructed with amino acid sequences because (i) an *in silico* analysis revealed that *An. gambiae* and *An. arabiensis* (KWAG strain) EcR sequences were 98% similar at both nucleotide and protein levels (supplementary figures S1, S2), and (ii) the amino acids alignment is more valuable to infer protein function.

As a first step towards constructing the phylogenetic tree, all EcR protein sequences were imported into MEGA v.10.2.4 and aligned with the MUSCLE algorithm (Edgar, 2004, Kumar et al., 2018). This algorithm was selected because it is more accurate and faster than ClustalW (Edgar, 2004). The second step was to determine the most suitable substitution model to account for multiple mutations at the

same residue. Based on MEGA analysis results (supplementary Table S3), the JTT+G model was selected. Also, pairwise deletions were computed to account for the gaps in the multiple sequence alignment. Finally, the phylogeny was constructed with the Maximum-likelihood method, and confidence in the nodes was assessed by performing a bootstrap analysis with 2,000 replicates. *Drosophila* EcR protein sequences were used as an outgroup.

Table 2.2: *EcR* protein sequences used to construct the phylogenetic tree. *An. arabiensis* (KWAG) sequence is the one obtained in this study; hence it does not have an accession number. All the other sequences have been confirmed by functional studies to be *EcR* orthologues.

Species	Database	Accession no.	EcR isoform
Aedes albopictus	VectorBase	LOC109414899-t1	A
	VectorBase	LOC109414899-t2	B
	VectorBase	LOC109414899-t3	C
	VectorBase	LOC109414899-t4	D
Aedes aegypti	VectorBase	AAEL019431-RA	A
	VectorBase	AAEL019431-RB	B
An. arabiensis (KWAG)	-	-	
Culex quinquefasciatus	NCBI	XM_001844529.1	
Drosophila melanogaster	NCBI	NP_001163061.1	G
	NCBI	NP_724456.1	A
	NCBI	NP_724459.1	B
An. gambiae	VectorBase	AGAP029539	

An. funestus	VectorBase	AFUN020231-RA	A
	VectorBase	AFUN020231-RB	B
Culex pipiens pallens	NCBI	XP_039432444.1	
An. stephensi	VectorBase	ASTE015863	

2.2.8 Gene expression analyses

qPCR reaction— All qPCR reactions in this study were performed in 10 µl volumes, containing 300 nM of each primer, 1 µl undiluted cDNA, and 1x iQ™ SYBR® Green Supermix (cat no: 1708882, Bio-Rad). Three technical repeats were performed for each biological replicate. The reactions were incubated in the CFX96™ Touch Deep Well Real-Time PCR Detection System (Bio-Rad), which was set as follows: an initial denaturation step (95˚C, 3 min) was followed by 40 cycles of denaturation (95˚C, 10 secs), annealing/extension (annealing temperature as indicated in supplementary Table S2, for 30 secs). The cycle ended with a melting curve analysis (55˚C to 95˚C, with an increment of 0.5˚C) for 5 secs. The Cq values and melting temperatures were automatically calculated by the CFX Maestro™ software (cat no: 12013758, Bio-Rad).

Standard curve— The efficiency of each qPCR primer pair (Table 2.1) was assessed using the standard curve method. For this purpose, cDNA (synthesized from *An*. *arabiensis* total RNA) was first diluted in ultrapure water in 1:1, 1:5, 1:10, 1:20, 1:40, 1:50, and 1:100 ratios. Then, 1 µl of each dilution was used as the template for a qPCR reaction with a specific primer pair. A negative no-template control (NTC) was included for each primer pair to test for the reagents contamination. To construct the standard curve, at least four dilutions that gave a PCR efficiency of 90-110% and an R^2-value of 0.98-1 were selected (Taylor et al., 2010).

2.2.9 RNA interference (RNAi)

dsRNA synthesis— PCR fragments flanked with T7 promoters were first synthesized by amplifying a ±490 bp region of EcR and GFP (negative control with no target within the mosquito genome, obtained from prof Arbuthnot's laboratory) from clones, using primers which included T7 sequences at their 5'end (Table 2.1, supplementary Figure S7). At least 10-15 reactions were prepared for each gene (and later pooled) to ensure that enough template was obtained for the *in vitro* transcription reaction. Each reaction contained 0.25 µl *Taq* DNA polymerase, 1x buffer, 0.2 mM dNTPs, 0.2 µM of each primer, 1.5 mM $MgCl_2$ (cat no: R011, Takara), a 1:10 dilution of the plasmid containing the target gene (*EcR* or *GFP*), and water was added to a final volume of 50 µl. The thermal cycler conditions were set as follows: an initial denaturation (94˚C, 30 secs), followed by five cycles of denaturation (94˚C, 30 secs), annealing (53˚C, 5 secs) and elongation (72˚C, 40 secs), then 15 cycles of denaturation (94˚C, 30 secs), annealing (72˚C, 5 secs), and elongation (72˚C, 40 secs). A final elongation (72˚C, 30 secs) completed the cycle. After purification with the PureLink™ PCR Micro kit (cat no: K310050, Thermo Scientific), these T7-containing DNA templates were used to produce EcR and GFP dsRNA (called dsEcR and dsGFP below) by *in vitro* transcription with the MEGAscript® RNAi kit (cat no: AM1626, Thermo Scientific). After removing contaminants (salts, ssRNAs, dsDNA), the quality and integrity of purified dsRNAs were assessed with electrophoresis and spectrophotometry, respectively. As in the literature for silencing *EcR* (Maharaj et al., 2022, Werling et al., 2019), the specificity of dsEcR and dsGFP was only assessed by qPCR, and no BLAST analysis was conducted to confirm that they only targets *EcR* and "no *An. arabiensis* gene", respectively.

dsRNA injection — Cold-anesthetized 4-6 days old, mated females were injected intrathoracically with 69 nl of a 10 ng/nl dsRNA solution using the Nanoject II (Drummond) as described previously (Kemp et al., 2018, Werling et al., 2019). Mosquitoes were randomly assigned to the two injection groups (dsEcR or dsGFP). *EcR* transcript levels in dsEcR- and dsGFP-injected groups were compared at 2 days post-injection (2 dpi) with qPCR to confirm mRNA knockdown.

2.2.10 Effect of *EcR* knockdown on vitellogenesis

Twenty-four hours after injecting mated *An. arabiensis* females with either dsEcR or dsGFP (60 females for each injecting group per biological replicate), a subset of the surviving mosquitoes (15 females per group per biological replicate) were blood-fed to induce vitellogenesis. One day later (i.e., 1-day post blood meal or 2 dpi), total RNA was extracted, and the expression of *EcR*, as well as that of four yolk transcripts — *lipophorin*, *vitellogenin*, *vitellogenin carboxypeptidase*, and *cathepsin b-like protease*— was quantified by qPCR.

2.2.11 Fecundity and fertility assays

Mated and dsRNA-injected *An. arabiensis* females (100 females per group per biological replicate) were blood-fed 24 hrs after the injection. One day post blood meal, each of the surviving mosquito female was placed in an oviposition vial (one mosquito per vial) containing moist filter paper for oviposition (Choi et al., 2014). Four days later, the number of eggs laid by each mosquito was counted manually under the microscope. The oviposited eggs were placed in a water-containing cup to allow the larvae to hatch for 7 days, with the hatched larvae counted and removed daily during this period. The reproductive outputs of dsEcR-injected and dsGFP-injected

mosquitoes were compared by measuring the following parameters: (i) Oviposition rate, i.e., the number of eggs laid per female; (ii) Percentage oviposition, i.e., the number of females that laid eggs relative to the total number of females in that group; (iii) Egg size, i.e., their length-to-width ratio. The egg dimensions were measured with the DinoXcope Imaging software v.2.0, connected to an SZX7 stereomicroscope (Olympus); and (iv) Percentage fertility, indicated by the number of larvae that hatched relative to the number of eggs laid.

2.2.12 Microbiome Quantification

To assess the role of *EcR* silencing on the gut microbiome, microbial genomic DNA was extracted from pooled guts of 15 mosquitoes in each group (dsEcR-injected or dsGFP-injected, per biological replicate) with the DNeasy® PowerSoil® Pro kit (cat no: 47016, Qiagen) and bacterial abundance was quantified by measuring the expression of selected regions of the V4 hypervariable segment of the16S rDNA gene, as previously described (Caporaso et al., 2011, Hermann-Bank et al., 2013, Rodgers et al., 2017, Smith et al., 2017). To ensure that no bacteria from the cuticle would contaminate the gut samples, mosquitoes were washed in 70% (v/v) EtOH/distilled water and rinsed twice in 1x sterile phosphate buffer saline (PBS) solution (cat no: 524650, Merck) prior to gut dissections (Coleman et al., 2007, Rodgers et al., 2017). In addition to measuring the load of three bacterial families — Enterobacteriaceae, Acetobacteriaceae, and Flavobacteriaceae— commonly found in anopheline guts (Table 2.3), the universal 515F/806R primer pair, which targets a ~250 bp fragment on the V4 variable domain of the 16S rDNA gene (Table 2.3), was also used to quantify the total eubacteria load (Bates et al., 2011, Hernández et al., 2015, Smith et al., 2017).

Table 2.3: Sequences of 16S rDNA primers used for bacterial quantification.
F = forward primer, R = reverse primer. The standard IUPAC nucleotide code was applied.

Target	Primers	Sequences (5' ->3')	References
Eubacteria	515_F 806_R	GTGCCAGCMGCCGCGGTAA GGACTACHVGGGTWTCTAAT	(Caporaso et al., 2011, Straub et al., 2020)
Enterobacteriaceae	Entero 16S_F Entero 16S_R	CGTCGCAAGMMCAAAGAG TTACCGCGGCTGCTGGCAC	(Hermann-Bank et al., 2013)
Acetobacteriaceae	Aceto 16S_F Aceto 16S_R	GTGCCGATCTCTAAAAGCCGTCTCA TTCGCTCACCGGCTTCGGGT	(Rodgers et al., 2017)
Flavobacteriaceae	Flavo 16S_F Flavo 16S_R	TAAGGTTGAAGTGGCTGGAATAA GTCCATCAGCGTCAGTTAAGACT	(Rodgers et al., 2017)

2.2.12 Data analysis

qPCR data analysis

The quantification cycles (Cq values) were automatically computed by the CFX Maestro software v.1.1 (cat no: 12013758, Bio-Rad). The Cq values of *EcR* and vitellogenesis-related genes were normalized to both *RpS7* and *RpL19* reference genes, unless indicated otherwise. In all cases, these relative normalized expression (RNE) values were calculated by the CFX Maestro software v.1.1, using an improved version of the $2^{-\Delta\Delta Cq}$ method, according to the formula below (Equation 2.1). The advantage of this formula is that it accounts for the use of multiple reference genes, and the fact that all genes used —in the formula— may have different qPCR

efficiencies. Unless indicated otherwise, the mean RNE of 3 independent biological replicates and standard error of the mean (SEM) were plotted on the graphs.

$$NRQ = \frac{E_{goi}^{\Delta Ct, goi}}{\sqrt[f]{\prod_{o}^{f} E_{ref_o}^{\Delta Ct, ref_o}}}$$

Equation 2.1: Determination of the Relative Normalized Expression (RNE) values. In this equation, RNE is indicated as NRQ, where NRQ stands for Normalized Relative Quantities. *E* represents the qPCR efficiency, *Ref* represents the reference genes, *f* is the number of reference genes, *Ct* represents the quantification cycles (i.e., Cq) *goi* is the gene of interest (i.e., either bacterial genes or vitellogenesis-related genes or *EcR*).

Statistical analyses

All experiments were performed with three independent biological replicates, and the means ± standard error of the mean (SEM) are shown. GraphPad Prism v.9.1.0 (GraphPad, Inc., USA) was used to compute all statistical analyses and plot the graphs. No data normalization test was performed, so a Gaussian distribution was assumed in all cases. For this reason, parametric statistical methods were selected. Whenever the means of two independent or unpaired groups were compared (e.g., comparing *EcR* expression or reproductive parameters between dsEcR-injected and dsGFP-injected mosquitoes), the unpaired Student's *t*-test was used. Exceptions include the difference in egg fertility and the percentage of females that oviposited between dsEcR-injected and dsGFP-injected mosquitoes. These were analysed with

a Fisher's exact test, as they are proportional data. The difference in *EcR* transcript levels at five-time points during vitellogenesis was assessed with a one-way ANOVA analysis. For all the above-mentioned statistical tests, significance was assessed by setting a *p*-value cutoff value of 0.05, unless indicated otherwise.

2.3 Results

Notes:

(1) The raw data associated with Figures 2.2, 2.8 and 2.9 can be found in Appendix 2.
(2) Each time the phrases "mRNA expression", "mRNA/transcript abundance", or "mRNA/transcript levels" are used, they refer to the relative normalized expression, i.e., the RNE values.

2.3.1 Validating all the primers used in this study

Since the primers were designed in this study (and thus not tested before), t he following three assays were conducted to ensure that the Minimum Information for publication of Quantitative real-time PCR Experiments (MIQE) guidelines were respected (Bustin et al., 2009). First, the primers specificity was assessed with a melting curve analysis (data not shown) to ensure that a single peak was obtained per primer pair. Second, all the qPCR amplicons were electrophoresed to confirm they were of the expected sizes (supplementary Figure S4). Finally, the qPCR products were cloned and sequenced to confirm that the primers amplified the right gene segment (supplementary Table S4).

2.3.2 *EcR* expression is induced during vitellogenesis

To determine whether EcR is induced during vitellogenesis, *EcR* transcript abundance was measured at five-time points after blood-feeding. The time points selected included 6, 12, 24, 36, and 48 hours post blood meal (hPBM), as described previously (Werling et al., 2019). *Lipophorin* expression was also measured as a positive control since this gene is reportedly induced during vitellogenesis in *An. gambiae* and *Ae. aegypti* (Marinotti et al., 2006, Sun et al., 2000). Both *EcR* and *lipophorin* expression were measured relative to *RpL19*, as this latter was stably expressed at all time points selected (supplementary Figure S3). The data revealed that *EcR* expression increased significantly (p = 0.0115) after blood-feeding from 12 hPBM to 24 hPBM where it reaches its peak, then it decreased significantly (p = 0.0213) from 24 to 36 hPBM (Figure 2.2). Similarly, *lipophorin* expression peaked at 24 hPBM, with an increase at 12-24 hPBM (p = 0.0005) and a decrease at 24-36 hPBM (p = 0.0028).

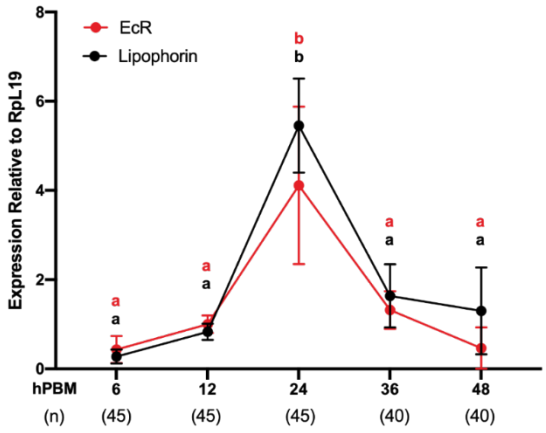

Figure 2.2: Expression of *EcR* at selected time points during vitellogenesis. *Lipophorin* was used as positive control. Statistical significance (one-way ANOVA, with

FDR *post hoc* analysis) in change in expression levels between time points is indicated by red and black lowercase letters, for *EcR* and *lipophorin*, respectively.

2.3.3 Generation of *EcR* and *GFP* double-stranded RNA (dsRNA) for RNA interference

While a *GFP*-containing plasmid was obtained from Prof Arbuthnot's laboratory (University of the Witwatersrand), no *EcR*-containing plasmid was readily available. The first step to generate EcR recombinant plasmids was to isolate *EcR* from *An. arabiensis* cDNA. For this purpose, *An. arabiensis* cDNA was used as a template in a PCR reaction that contained primers that could amplify *EcR* full-length coding sequence (2,218 bp). The choice for amplifying the entire coding sequence was to ensure that dsRNAs targeting different EcR regions could be synthesized if needed. A no-template control (NTC) was included to test if the reaction components were contaminated with foreign DNA. Also, *An. gambiae* cDNA served as a positive control. All the amplicons were visualized with agarose gel electrophoresis, and their sizes were estimated by comparison to a DNA molecular marker. The results (Figure 2.3) showed an amplicon of the expected size (2,218 bp) was obtained for each species. The lack of amplification in the NTC confirms that there was no DNA contamination in the reaction components.

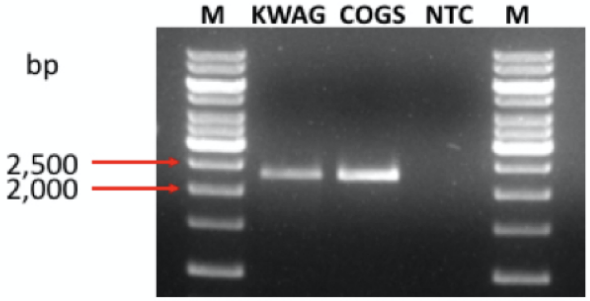

Figure 2.3: Amplification of full-length *An. arabiensis* (KWAG) *EcR* coding sequence from cDNA. *Anopheles gambiae* (COGS strain, from Congo) was used as positive control. NTC= No-template control. A 1% (w/v) agarose/TAE gel and a 1 kbp (or 10,000 bp) DNA ladder were used.

Anopheles arabiensis (KWAG) amplicon (Figure 2.3) was cloned and sequenced to confirm that it corresponds to *EcR*. The sequence obtained was used as a query in a BLAST search against the *An. arabiensis* genome (Dongola strain) available on VectorBase (data not shown). The hallmark features of EcR sequence have been published for *Ae. aegypti* and *Ae. albopictus* (Cho et al., 1995, Jayachandran and Fallon, 2000). These include nuclear localization signals, post-translational modifications (glycosylation and phosphorylation), helix-turn-helix motifs, as well as ligand-binding and DNA-binding domains, since EcR acts as a transcription factor. To test whether these features would be conserved in *An. arabiensis* (both Dongola and KWAG strains) EcR sequence, the four EcR sequences were aligned and screened for the published EcR hallmark features. As expected, all the features were conserved between the two *Aedes* species and the two *An. arabiensis* strains (Figure 2.4). Not only did this finding confirmed that the sequence isolated corresponded to *EcR*, but it also suggested that the *An. arabiensis* EcR orthologue could have the same function as that of *Aedes* species. Interestingly, this sequence alignment also revealed that for both the *An. arabiensis* strains, the EcR sequences are 99% similar at the protein level (Figure 2.4). These differences probably reflect the difference in environments (Sudan versus South Africa) where the two strains are localized. *Anopheles arabiensis* EcR sequence (KWAG strain) mutated to include some insertions [relative to *Aedes* spp. EcR sequences] at positions 610-613, 661-666, 668, 704-705, 725, 730 and 751.

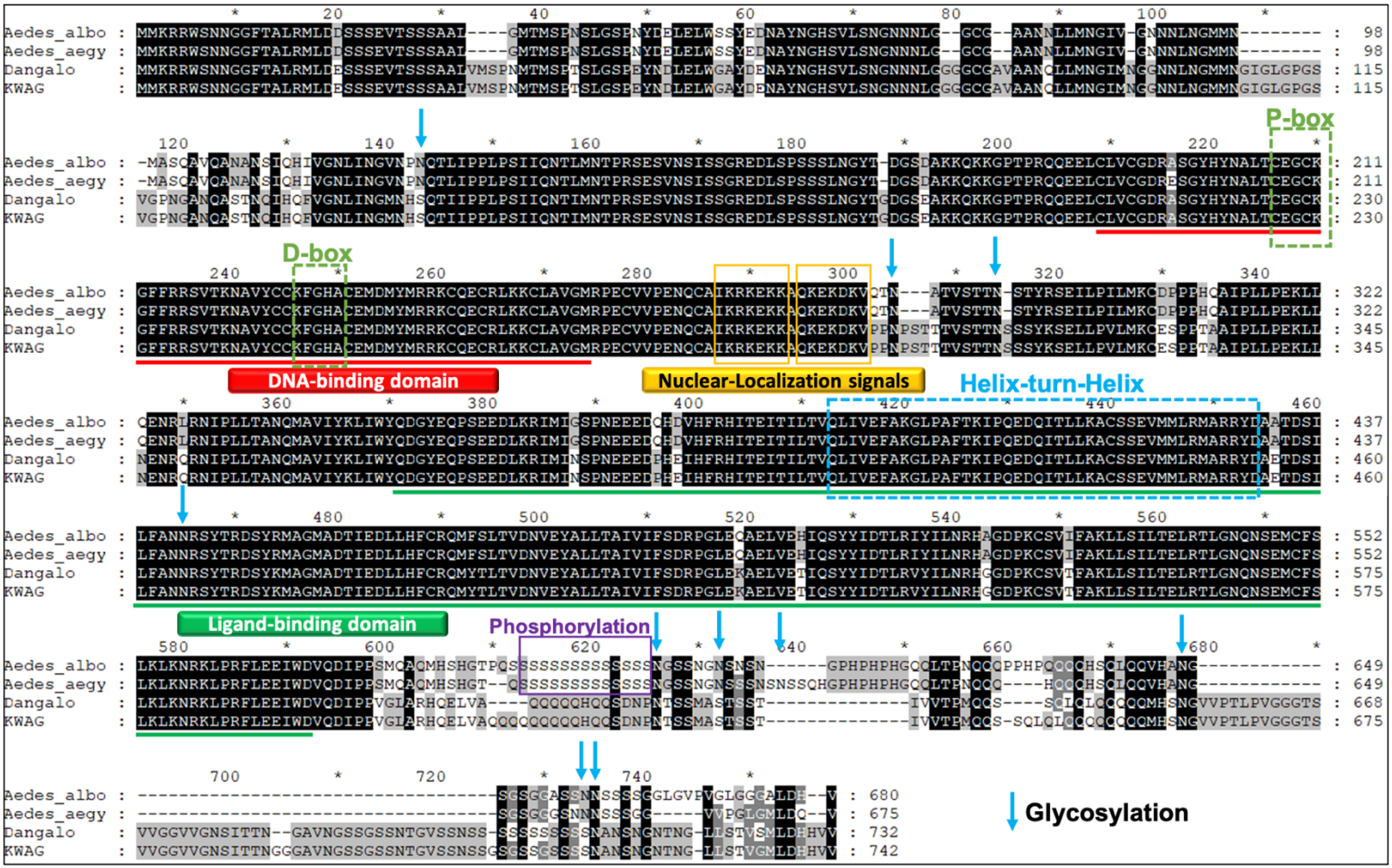

Figure 2.4: The hallmark features of *EcR* are conserved between *An. arabiensis* (KWAG, Dongola), *Ae. aegypti*, and *Ae. albopictus.*

The numbers at the top and side of the sequences indicate the amino acid position. Similarity is indicated by a grey scale, with black indicating 100% similarity, and grey indicating at least 50% similarity.

Next, a phylogenetic tree was constructed to evaluate *An. arabiensis* EcR evolutionary relationship to other mosquito species for which EcR protein sequences are available. A total of 16 EcR amino acid sequences from nine insect species were included in the maximum-likelihood phylogenetic analysis (Table 2.2). Notably, only one EcR isoform was detected in *Anopheles* genomes, but two isoforms (A and B) were detected in *An. funestus* genome, four isoforms in *Ae. albopictus*, two in *Aedes aegypti* and three in *D. melanogaster* (Figure 2.5). *An. arabiensis* EcR protein sequence fell within the *Anopheles* group (bootstrap = 100%) and was closely related to *An. gambiae* EcR sequence (bootstrap = 90%). Interestingly, this phylogeny also reveals that mosquito vectors EcR sequences have diverged from *Drosophila* EcR sequences (bootstrap = 100%), which agrees with the additional functions of EcR in vector-pathogen interactions (Figure 2.5). Finally, the genus-specific differences in EcR sequences between *Aedes* spp. (bootstrap = 81%), *Culex* spp. (bootstrap = 99%) and *Anopheles* species (bootstrap = 100%) could result from the different pathogens they transmit, or their different vector biology. Altogether the evolutionary relationship between *An. arabiensis* EcR sequence and that of functionally characterized EcR sequences (notably *An. gambiae*, *Ae. aegypti* and *Ae. albopictus*) suggest that EcR function is conserved between these species.

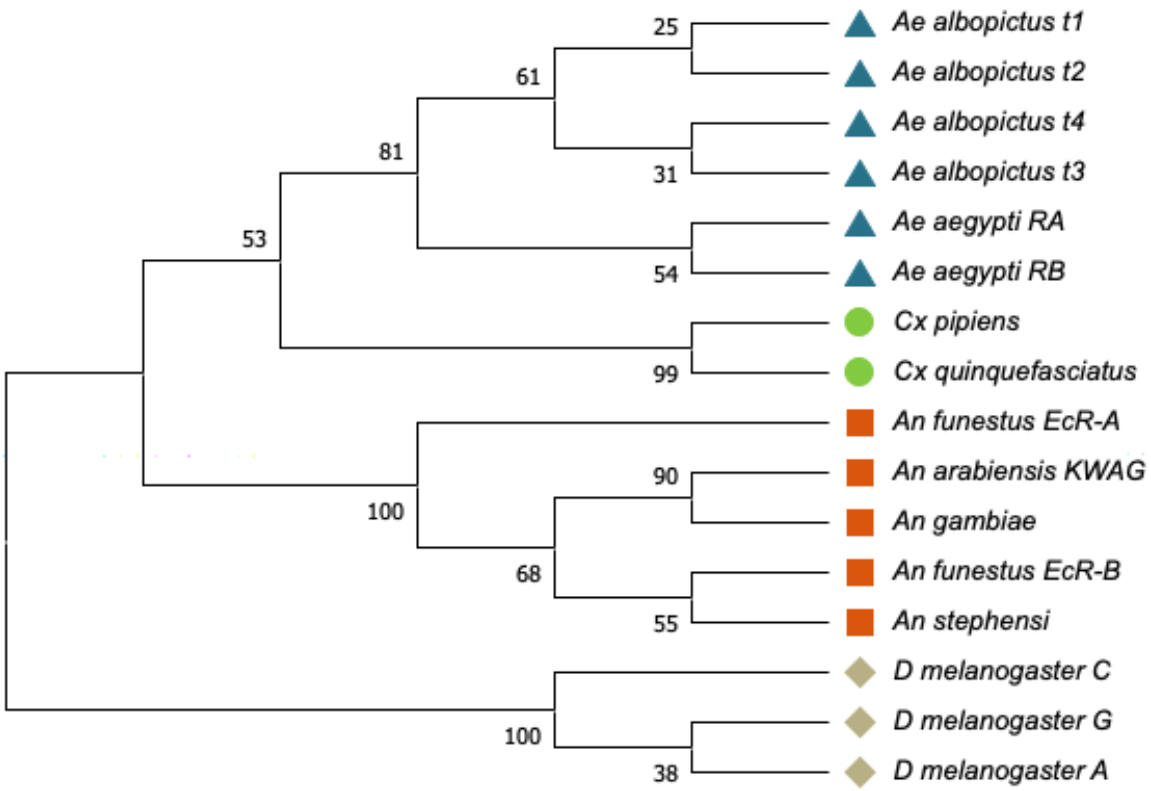

Figure 2.5: Maximum-likelihood phylogeny showing the evolution of EcR protein in selected insects. The tree was drawn to scale, with branch lengths reflecting the evolutionary distance between the sequences. Bootstrap values (%) on the nodes were based on 2,000 replicates. Similar genera are indicated by similar symbols. *Drosophila* EcR protein sequences were used as outgroups. Bootstrap values greater than 50% are considered significant.

Once the sequence identity and putative function of the EcR amplicon were confirmed (Figures 2.4, 2.5), the entire 2,218 bp fragment (Figure 2.3) was cloned at Inqaba Biotechnical Industries. The *EcR*-containing plasmid (received from Inqaba) and the *GFP*-containing plasmid were used as templates in a PCR reaction to produce DNA fragments flanked with T7 promoter sequences at their 5' end, i.e., T7 dsDNA templates (Figures 2.6a, supplementary figure S5). For this purpose, the *in vitro* transcription primers (Table 2.1) were used, and the expected amplicon sizes were 536 bp and 542 bp for *EcR* and *GFP* respectively, including the T7 promoter sequences. As indicated by the presence of a single amplicon at the expected size for

each gene, and the absence of amplification in the negative no-template control, the amplification was successful (Figure 2.6a). After purification, the T7 dsDNA templates were used as templates for *in vitro* transcription reactions. The integrity and quality of the purified dsRNAs (dsEcR and dsGFP for dsRNA synthesized from EcR and GFP T7 dsDNA templates, respectively) were assessed by agarose gel electrophoresis (Figures 2.6b, c). Both dsEcR and dsGFP were stored at -20˚C in 10 µg/µl aliquots until further use.

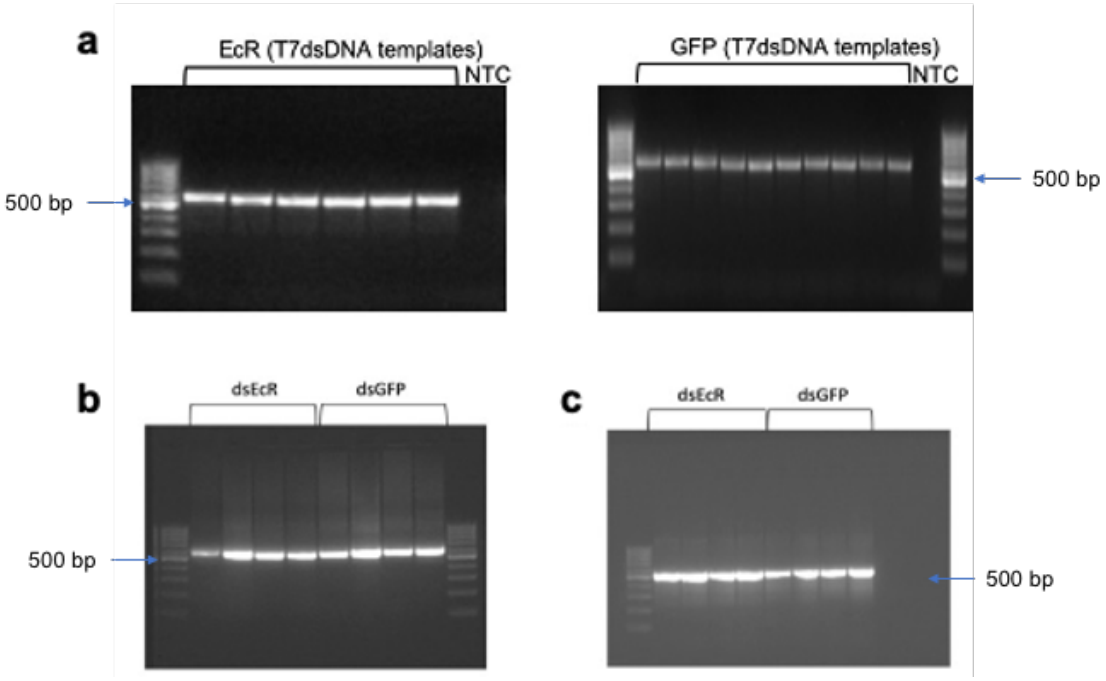

Figure 2.6: Synthesis of dsRNA targeting *EcR* and *GFP*. (**a**) DNA templates flanked with the T7 promoter sequences were first synthesized using primers that contained T7 sequences at their 5' end. These templates were then used to synthesize dsRNA by *in vitro* transcription. The dsRNA products before and after purification are shown in (**b**) and (**c**), respectively. All products in (**a-c**) were visualized on a 1% (w/v) agarose/TAE gel pre-strained with EtBr, and their sizes were estimated by comparison to a 100 bp DNA ladder, as no dsRNA ladder was available. NTC= No-template Control, dsEcR = dsRNA targeting EcR, dsGFP = dsRNA targeting GFP.

2.3.4 Effect of *EcR* knockdown on *An. arabiensis* fecundity and fertility

To determine whether the 20E signaling pathway affects *An. arabiensis* reproduction, *EcR* mRNA levels were depleted by RNAi (i.e., by injecting mosquitoes with either dsEcR or dsGFP, control) and the phenotypes described above (sections 2.1, 2.2.11) were compared between dsEcR-injected mosquitoes and dsGFP-injected mosquitoes (as described earlier, section 2.2.11).

Firstly, to determine whether *EcR* depletion affected oviposition, the number of eggs laid, the percentage of mosquitoes that laid eggs, and the egg length-to-width ratio between the two injected mosquito groups were compared. The average number of eggs laid per female was 58.63 ± 6.582 and 53.94 ± 6.361 eggs (means ± SEM) for the dsEcR-injected dsGFP-injected groups, respectively (Figure 2.7a). However, this difference was not significant (p = 0.6612). With respect to the percentage of mosquitoes that laid eggs, 33.6% and 40% of females oviposited in the dsEcR-injected and dsGFP-injected groups, respectively (Figure 2.7b, Table 2.4). Even though a decrease in oviposition rate (i.e., number of females that oviposited) was observed in the EcR-depleted group, this difference was not significant (p = 0.3433). Collectively, these data suggested that *EcR* silencing did not influence *An*. *arabiensis* fecundity in the first gonotrophic cycle. Although oviposition was seemingly unaffected by the treatments, the average egg length-to-width ratio between the two groups varied significantly (p < 0.01; Figure 2.7c). The average egg length-to-width ratio in dsEcR-injected and dsGFP-injected mosquitoes were 3.351 ± 0.1144 and 4.006 ± 0.1282 (mean ± SEM), respectively.

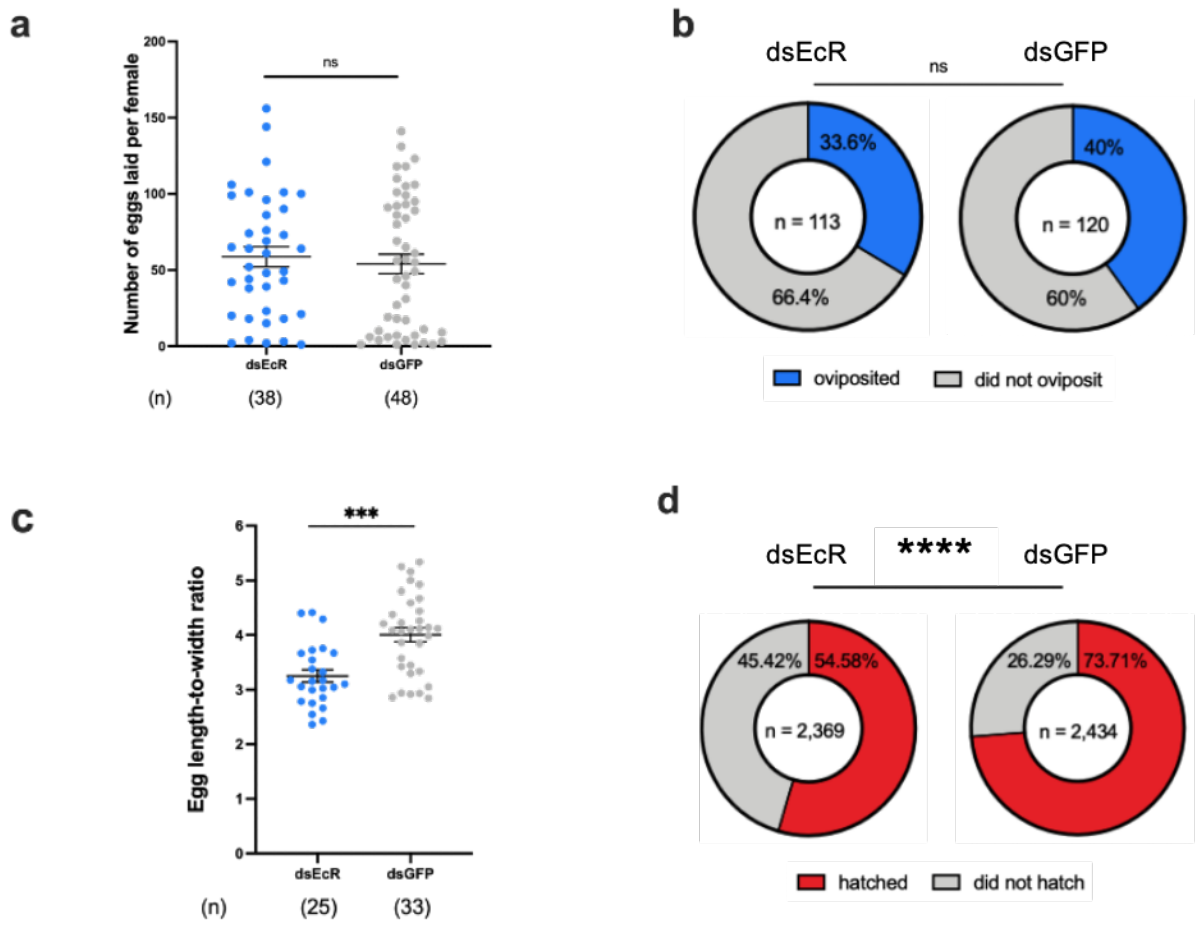

Figure 2.7: Effect of *EcR* silencing on *An. arabiensis* reproductive output. (**a**) *EcR* knockdown did not affect the number of eggs laid by mosquitoes (only those who laid eggs are represented, unpaired Student's *t*-test). (**b**) Likewise, the percentage of females that oviposited in each group was not affected by *EcR* silencing (Fisher's exact test, two-sided). (**c**) *EcR* silencing significantly decreased the eggs length-to-width ratio (unpaired Student's *t*-test). (**d**) Egg fertility was also decreased by *EcR* depletion (Fisher's exact test, two-sided). In (**a,b**) *n* represents the number of females, while in (**c,d**) *n* indicates the number of eggs. All experiments were performed in three independent biological replicates with error bars indicating SEM. ***$p<0.001$, ****$p<0.0001$, ^{ns} not significant.

Table 2.4: Data for the oviposition experiment. (**a**) Number of females that oviposited per biological replicate relative to the total number of females in that biological replicate. (**b**) Contingency table derived from these proportional data to perform the Fisher's Exact test. In both (**a,b**), dsEcR = mosquitoes injected with dsEcR, while dsGFP = mosquitoes injected with dsGFP.

a

	dsEcR		dsGFP	
	Oviposited	**total**	**Oviposited**	**Total**
Biological Replicate 1	12	36	18	40
Biological Replicate 2	12	40	13	40
Biological Replicate 3	14	37	17	40
Total	**38**	**113**	**48**	**120**

b

	oviposited	did not oviposit	**Total**
dsEcR	38	75	113
dsGFP	48	72	120
Total	86	147	233

Given the previous reports that EcR regulates fertility in mosquitoes (Bouaziz et al., 2017, Gabrieli et al., 2014), *EcR* silencing was expected to decrease *An*. *arabiensis* egg fertility. Hence, as a measure of fertility, the number of larvae that hatched from each group of mosquitoes —relative to the total number of eggs laid in that group— were recorded (Figure 2.7d, Table 2.5). The knockdown of *EcR* significantly decreased egg fertility from 73.71% (dsGFP-injected) to 54.58% (dsEcR-injected) ($p < 0.0001$).

Table 2.5: Data for the fertility experiment. (**a**) Number of eggs laid that hatched into larvae per biological replicate relative to the total number of eggs laid that biological replicate. (**b**) Contingency table derived from these proportional data to perform the Fisher's Exact test. In both (**a,b**), dsEcR = mosquitoes injected with dsEcR, while dsGFP = mosquitoes injected with dsGFP.

a

	dsEcR		dsGFP - sugar	
	Eggs laid	**larvae**	**Eggs laid**	**larvae**
Biological Replicate 1	886	523	736	516
Biological Replicate 2	776	366	785	564
Biological Replicate 3	707	404	913	714
Total	2369	1293	2434	1794

b

	hatched	did not hatch	**Total**
dsEcR	1293	1076	2369
dsGFP	1794	640	2434
Total	3087	1716	4803

2.3.5 Effect of *EcR* knockdown on the expression of yolk proteins

To determine whether an abnormal vitellogenesis rendered the eggs less fertile, the expression of four yolk genes (*vitellogenin*, *lipophorin*, *cathepsin b-like protease* [*VCB*], and *vitellogenin carboxypeptidase* [*VCP*]) was compared between the dsEcR-injected and dsGFP-injected groups (Figure 2.8). The results showed that *EcR* knockdown decreased the mRNA abundance of *vitellogenin* (76% reduction, $p = 0.0257$) and *VCP* (29.8% reduction, $p = 0.0461$), while it did not affect that of *VCB* ($p = 0.1008$) or *lipophorin* ($p = 0.3725$). Hence, the decrease in *vitellogenin* and *VCP* transcript levels could explain why the dsEcR-injected mosquitoes were less fertile than dsGFP-injected mosquitoes.

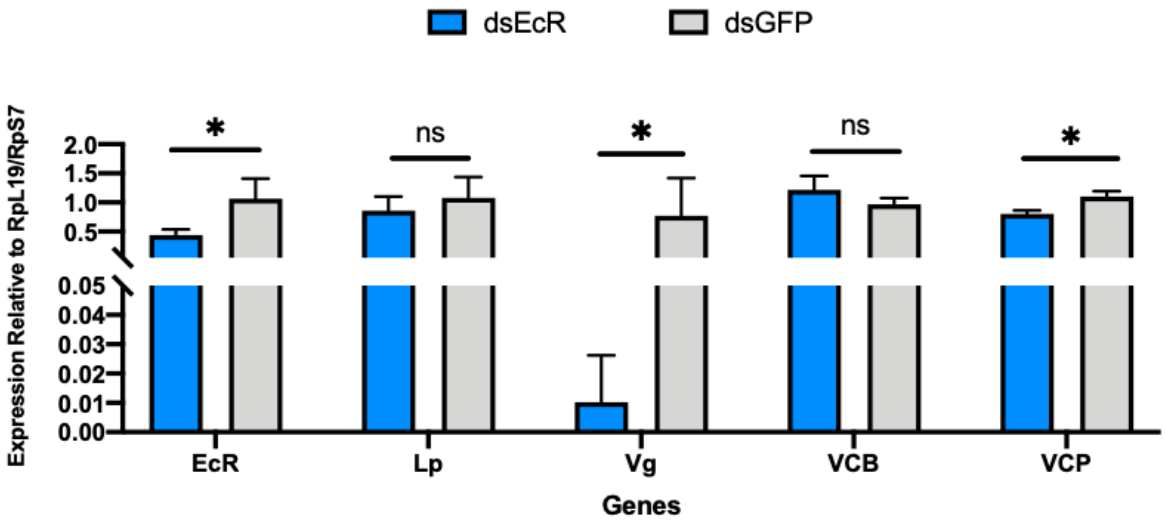

Figure 2.8: Effect of *EcR* depletion on the expression of selected yolk genes. An unpaired Student's *t*-test assessed statistical significance for each gene. Means ± SEM of three independent biological replicates is indicated. Expression levels are relative to that of *RpL19* and *RpS7*. **p*<0.05, ns not significant. *EcR = Ecdysone Receptor; Vg = Vitellogenin; Lp = lipophorin; VCB = cathepsin b-like protease; VCP = vitellogenin carboxypeptidase*.

2.3.6 Effect of *EcR* knockdown on the gut microbiome

To determine if EcR plays a role in the regulation of the microbiome, mosquitoes were injected with either dsEcR or dsGFP (negative control), and the gut bacterial load was quantified at three time points (1, 2, and 3 days post-injection [dpi]). Specifically, the bacterial load of three bacteria families commonly found in anopheline guts — Enterobacteriaceae, Acetobacteriaceae, Flavobacteriaceae— and the total or "eubacteria" were measured. Since both blood-feeding and mating can induce a proliferation of the gut bacterial microbiome of anopheline females (Dahalan, 2017, Oliveira et al., 2011, Wang et al., 2011), only virgin and non-blood fed females were used for this experiment. *EcR* expression was not significantly reduced between

dsEcR- and dsGFP-injected mosquitoes at any time point (unpaired *t*-test, $p = 0.3774$, $p = 0.4000$, and $p = 0.5386$, for 1 dpi, 2 dpi, and 3 dpi, respectively). Likewise, the load of Acetobacteriaceae, Flavobacteriaceae, Enterobacteriaceae, and Eubacteria was not statistically different between the dsEcR- and dsGFP-injected groups at any of the selected time points (see Table S6, for unpaired *t*-test results). Therefore, because of the high variation observed at each time point (Figure 2.9), the impact of *EcR* depletion on the gut bacterial load could not be measured.

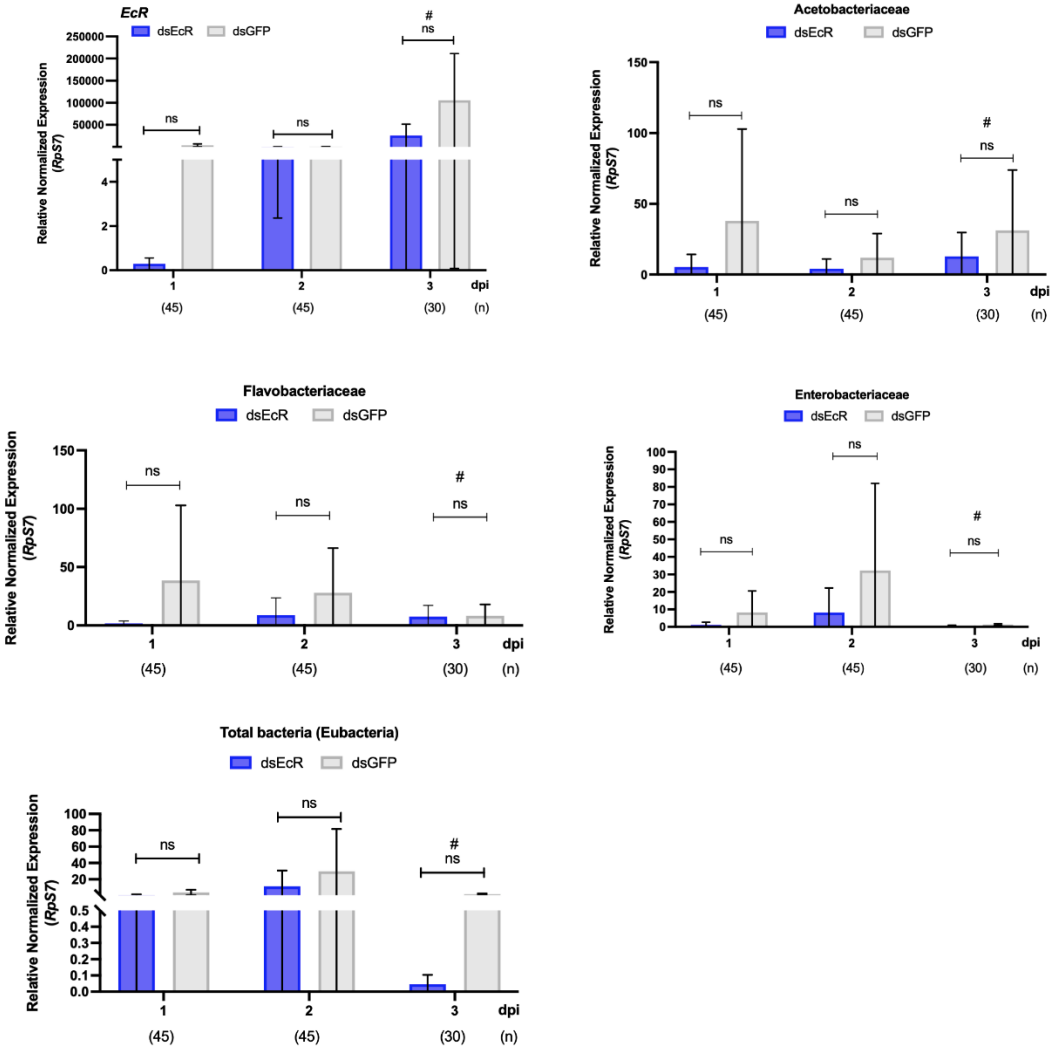

Figure 2.9: **Impact of dsEcR injection on bacterial gene expression at 1-3 days post injection (dpi).** Experiments were performed in 2-3 independent biological replicates. Those with 2 biological replicates are indicated with (#). Means RNE ± SEM are indicated. ^{ns} not significant, *(n)* number of mosquitoes or guts across the biological replicates.

2.4 Discussion

Understanding the molecular mechanisms that regulate *Anopheles* abundance is essential to develop malaria vector control interventions that decrease *Anopheles* reproductivity. In *An. gambiae*, several studies have identified the 20E signaling pathway as a critical modulator of the physiological processes that regulate vector abundance (Childs et al., 2016, Gabrieli et al., 2014, Werling et al., 2019). In contrast, this pathway is poorly studied in *An. arabiensis* (section 1.5), despite this mosquito species being a primary malaria vector in sub-Saharan Africa. In terms of EcR protein sequence, *An. arabiensis* (both the Dongola and KWAG strains) were 99% identical and 99% similar, probably because the sequences come from the same species, but different locations. The KWAG and the Dongola strain originated from South Africa and Sudan, respectively. Yet, the similarity might be caused by the fact that both species are vectors of *Plasmodium* parasites and have the same biology.

In contrast, there was a 92% identity and 75% similarity between the sequences from the *Aedes* species and *An*. *arabiensis* species (Figure 2.4). This was also highlighted in the phylogeny, where EcR sequences from *Anopheles* species group together (100% bootstrap value), and EcR sequences from *Aedes* species also group together (81% bootstrap) (Figure 2.5). The *Aedes* EcR sequences were shorter than their *Anopheles* counterpart with lengths of ~675 and ~730 bp, respectively. The

differences observed possibly result from the differences in the vector biology of these two genera as well as the fact that they are vectors of different pathogens: viruses and nematodes for *Aedes* species, as opposed to *Plasmodium* parasites for *Anopheles* species. The similarities in the EcR sequences between the two genera are probably because (i) both mosquitoes are vectors of pathogens, (ii) both genera have 4 stages in their lifecycle, (iii) EcR function is the same in both genera. The latter is exemplified by the fact that in both *Aedes* sp. and *Anopheles* sp., EcR is involved in egg production and larval development (Ekoka et al., 2021).

Strikingly, in all four species, the motifs/domains of EcR sequences were 100% conserved, suggesting that EcR function is the same in all these species. These domains include firstly a transcription activation domain —where RNA polymerase binds— indicated by a proximal and distant promoter regions (P-box and D-box, respectively). Secondly, a DNA-binding domain that is used by EcR to bind to its DNA region, the Ecdysone Receptor elements (EcREs). Thirdly, a nuclear localization signal that is used by the transcription factor to migrate to the nucleus where it performs its function to bind DNA and regulate transcription. Fourthly, a ligand-binding domain was also detected; this is possibly used by EcR to bind 20E or USP protein. Finally, a helix-turn-helix motif was detected. This motif is common in transcription factors, and its role is to help bind the ligand via the 3-helical bundle (Aravind et al., 2005).

Consistent with studies in *Ae. aegypti* (Raikhel et al., 2002), *EcR* expression was induced after blood-feeding with a peak expression detected at 24 hPBM (Figure 2.2), suggesting that *An. arabiensis* EcR protein also plays a crucial role in vitellogenesis and egg development. Although a high biological variation was observed at time point 24 hrs, the statistical significance between the expression at 24 hrs and that at other time points was still observed. It is unlikely that this variation was due to pipetting errors

because the same high variation was detected by Kristine et al. (2019), albeit at time point 36 hrs.

This study also hypothesized that in *An. arabiensis* females, the 20E signaling pathway would regulate vitellogenesis, fecundity, fertility, and the gut microbiome. To test this hypothesis, the expression profile of *EcR* during vitellogenesis was determined, and the effect of *EcR* depletion on vitellogenesis, fecundity, fertility, and the gut microbiome was examined. On this latter, *EcR* depletion was only measured at RNA levels —and not protein levels— to mimic what is done in the literature where EcR function is studied (Baldini et al., 2013, Werling et al., 2019).

EcR silencing did not influence the number of eggs laid or the percentage of females that oviposited in the first gonotrophic cycle (Figure 2.7). This finding agrees with Maharaj's data (Maharaj, 2021) where she demonstrates that *EcR* silencing in *An. funestus* only reduces the number of eggs developed, but not the number of eggs laid in the first gonotrophic cycle. Likewise, Werling et al. (2019) reported that *EcR* silencing in *An. gambiae* reduces the number of eggs developed. Yet, a study in *Ae. aegypti* suggests that *EcR* depletion affects the number of eggs oviposited in the second gonotrophic cycle (Bryant and Raikhel, 2011). Therefore, additional experiments should be conducted to determine whether *EcR* depletion would also decrease *An. arabiensis* fecundity in its second gonotrophic cycle. With respect to the percentage of females that oviposited, *EcR* depletion did not affect this percentage, like a finding in *An. funestus* (Maharaj, 2021). Yet, Mitchell et al. (2015) reported that the percentage of *An. arabiensis* females that oviposited was reduced after 20E injection. Could it be that the type of manipulation of the 20E signaling pathway (20E injection versus *EcR* silencing) influence whether the percentage of females that oviposit would be affected? This hypothesis should be investigated further. Consistent with previous studies which reported that the 20E signaling pathway regulates egg fertility (Gabrieli et al., 2014,

Hamaidia and Soltani, 2016), this study showed that manipulating the 20E signaling pathway (by reducing *EcR* expression) lowers the fertility of the eggs laid (Figure 2.7d). Therefore, in *An. arabiensis*, the 20E signaling pathway also regulates egg fertility. It is also noteworthy that mosquitoes fecundity is influenced by different pathways, such as the *akirin* pathway (da Costa et al., 2014), the *Juvenile hormone* pathway (Belles, 2005, Postlethwait and Handler, 1979, Raikhel et al., 2005) among others. Silencing key players of this pathway has been shown to impair mosquitoes reproductive output. While the 20E pathway controls egg fertility, the egg volume, and the total number of eggs developed, it is possible that oviposition itself could be controlled by akirin or the Juvenile Hormone.

Eggs length-to-width ratios —which influence their volumes — are important for at least two parameters. In *An. coluzzii*, the susceptibility to *P. falciparum* infection is correlated to the egg size. Indeed, a study reported that *An. coluzzii* mosquitoes laying small eggs typically displayed high levels of infection (Roux et al., 2015). On the other hand, a report in several insects (including the mosquito *An. quadrimaculatus*) suggested that the embryonic development time or EDT is positively correlated to the egg size, which means that EDT increases with egg size. Therefore, the fact that *EcR* silencing reduced *An. arabiensis* egg length-to-width ration (Figure 2.7c) may suggest that it increased their susceptibility to *Plasmodium* infection or increase their EDT. However, this hypothesis should be tested experimentally.

Consistent with studies in *Ae. aegypti* (Raikhel et al., 2002), *EcR* expression was induced after blood-feeding with a peak expression detected at 24 hPBM (Figure 2.2), suggesting that *An. arabiensis* EcR protein also plays a crucial role in vitellogenesis and egg development. Although a high biological variation was observed at time point 24 hrs, the statistical significance between the expression at 24 hrs and that at other time points was still observed. It is unlikely that this variation was due to

pipetting errors because the same high variation was detected by Kristine et al. (2019), albeit at time point 36 hrs. Nonetheless, the finding of the time point study (post blood feeding expression) was later confirmed when silencing *EcR* reduced vitellogenin and *VCP* expression in the whole mosquito (Figure 2.8), as previously reported (Roy et al., 2015, Wang et al., 2017). However, unlike these reports, *VCB* and *lipophorin* mRNA expression were not affected (Figure 2.8). There are three possible explanations for this discrepancy. First it is the fact that the studies mentioned measured the expression of yolk genes in the fat body (where they are synthesized) instead of the whole mosquito (Roy et al., 2015, Werling et al., 2019). Thus, it is likely that the tissue-specific effect of *EcR* silencing on *VCB* and *lipophorin* expression —i.e., reduction in expression— is not detected when RNA is extracted from the whole organism. Secondly, it is possible that these two proteins exist as isoforms and the primers were designed for the wrong isoform. This is unlikely, since in VectorBase, only one isoform was detected for each VCB and lipophorin proteins. The last explanation might have to do with the fact that different pathways regulate YPP expression (Hansen et al., 2014, Roy et al., 2015, Roy et al., 2017, Roy et al., 2016). These include the TOR pathway which indicates that the blood nutrients have entered the fat body and thus the activation of the YPPs is necessary. The insulin pathway which is needed in a synergistic manner to help 20E activate the expression of the YPPs; and finally the Juvenile hormone pathway which acts as a repressor of YPP expression until blood is ingested by the mosquitoes. This last explanation (i.e. that of the other pathways involved) is also unlikely because these different pathways would have affected the expression of the four YPPs similarly.

Finally, the effect of dsEcR injection on the proliferation of selected gut bacteria groups was investigated, since these bacteria also affect the mosquito reproductive output. However, no significant reduction in *EcR* transcript abundance was detected in

the dsEcR-injected mosquitoes —relative to that in the dsGFP-injected mosquitoes— probably because of the high variation between the biological replicates (Figure 2.9). A possible explanation for this high variation could be that some of the mosquitoes could have been mated by the time the experiment was conducted, resulting in an increase in their *EcR* expression (Baldini et al., 2013, Gabrieli et al., 2014, Pondeville et al., 2008). While the female adults were separated at 1 day post-emergence, their insemination status was not confirmed prior to dsEcR injection. To circumvent this problem in future, either (i) the females should be separated from the males at pupal stages, or (ii) the insemination status of adult females should be assessed before dsRNA injection (Carrasquilla and Lounibos, 2015). This will ensure that only virgin females are used for the experiment. Also, while repeating the experiment on the effect of dsEcR injection on the proliferation of commensal gut bacteria, it would be interesting to include *16S* rRNA sequencing to measure the bacterial diversity/abundance (D'Amore et al., 2016, Pichler et al., 2018), or metagenomics to measure bacteria, viruses, and fungi (Quince et al., 2017). Such studies will determine to what extent —if any— *EcR* regulates the gut microbiome of malaria vectors. An alternative explanation is that the collection of adults for these experiments need to be conducted at the same time as the pathway might be influenced by the mosquitoes circadian rhythm. The time of collections for adults in each biological replicate were not recorded and hence it is difficult to make any conclusions and future research should take this into consideration. A final explanation for this high variability may be due to the "unfed status" and "unmating status" of the mosquitoes used in this experiment. Indeed, as shown earlier (Figure 2.2), the level of EcR in mosquitoes is rather low — yet still detectable— before a blood meal. It is also known that mating increases EcR levels. It is thus possible that silencing EcR in unfed and unmated mosquitoes made

EcR levels in those mosquitoes reach a level that was beyond reliable detection by qPCR, hence the high variability.

Taken together, the results presented in this chapter demonstrate that disturbing the 20E signaling pathway by altering *EcR* expression affects *An. arabiensis* egg development. Therefore, like studies in *An. gambiae* and *Ae. aegypti* (Table 1.2), the 20E signaling pathway regulates *An. arabiensis* reproduction. With regards to the effect of *EcR* depletion on the microbiome, the experiment should be repeated with blood fed mosquitoes and at the same time (circadian rhythm) to minimize the high variation between the biological replicates. Conversely, antibiotics can be used to deplete the gut microbiome and see if there is an effect on *EcR* expression (see chapter 3).

2.5 References

BALDINI, F., GABRIELI, P., SOUTH, A., VALIM, C., MANCINI, F. & CATTERUCCIA, F. 2013. The interaction between a sexually transferred steroid hormone and a female protein regulates oogenesis in the malaria mosquito *Anopheles gambiae*. *PLoS Biol.,* 11**,** e1001695-e1001695.

BECKER, N., PETRIC, D., ZGOMBA, M., BOASE, C., MADON, M., DAHL, C. & KAISER, A. 2010. Biology of mosquitoes. *Mosquitoes and their control.* Second ed. Germany: Springer Science & Business Media.

BELLES, X. 2005. Vitellogenesis directed by juvenile hormone. *Reproductive biology of invertebrates,* 12**,** 157-197.

BROOKE, B. D., ROBERTSON, L., KAISER, M. L., RASWISWI, E., MUNHENGA, G., VENTER, N., WOOD, O. R. & KOEKEMOER, L. L. 2015. Insecticide resistance in the malaria vector *Anopheles arabiensis* in Mamfene, KwaZulu-Natal. *S. Afr. J. Sci.,* 111**,** 1-3.

BROWN, F., PATON, D. G., CATTERUCCIA, F., RANSON, H. & INGHAM, V. A. 2020. A steroid hormone agonist reduces female fitness in insecticide-resistant *Anopheles* populations. *Insect Biochem. Mol. Biol.,* 121**,** 103372.

BRYANT, B. & RAIKHEL, A. S. 2011. Programmed autophagy in the fat body of *Aedes aegypti* is required to maintain egg maturation cycles. *PLoS One,* 6**,** e25502-e25502.

BUSTIN, S. A., BENES, V., GARSON, J. A., HELLEMANS, J., HUGGETT, J., KUBISTA, M., MUELLER, R., NOLAN, T., PFAFFL, M. W. & SHIPLEY, G. L. 2009. The MIQE guidelines: minimum information for publication of quantitative real-time PCR experiments. *Clin. Chem.,* 55**,** 611-622.

CHILDS, L. M., CAI, F. Y., KAKANI, E. G., MITCHELL, S. N., PATON, D., GABRIELI, P., BUCKEE, C. O. & CATTERUCCIA, F. 2016. Disrupting mosquito reproduction and parasite development for malaria control. *PLoS Pathog.,* 12**,** e1006060-e1006060.

CHO, W.-L., KAPITSKAYA, M. Z. & RAIKHEL, A. S. 1995. Mosquito ecdysteroid receptor: analysis of the cDNA and expression during vitellogenesis. *Insect Biochem. Mol. Biol.,* 25**,** 19-27.

CHOI, K. S., CHRISTIAN, R., NARDINI, L., WOOD, O. R., AGUBUZO, E., MULEBA, M., MUNYATI, S., MAKUWAZA, A., KOEKEMOER, L. L. & BROOKE, B. D. 2014. Insecticide resistance and role in malaria transmission of *Anopheles funestus* populations from Zambia and Zimbabwe. *Parasit. Vectors,* 7**,** 1-8.

DA COSTA, M., PINHEIRO-SILVA, R., ANTUNES, S., MORENO-CID, J. A., CUSTÓDIO, A., VILLAR, M., SILVEIRA, H., DE LA FUENTE, J. & DOMINGOS, A. 2014. Mosquito Akirin as a potential antigen for malaria control. *Malar. J.,* 13**,** 470-470.

EDGAR, R. C. 2004. MUSCLE: multiple sequence alignment with high accuracy and high throughput. *Nucleic Acids Res.,* 32**,** 1792-1797.

GABRIELI, P., KAKANI, E. G., MITCHELL, S. N., MAMELI, E., WANT, E. J., ANTON, A. M., SERRAO, A., BALDINI, F. & CATTERUCCIA, F. 2014. Sexual transfer of the steroid hormone 20E induces the postmating switch in *Anopheles gambiae*. *Proc. Natl. Acad. Sci. U. S. A.,* 111**,** 16353-16358.

HAMAIDIA, K. & SOLTANI, N. 2016. Ovicidal activity of an insect growth disruptor (methoxyfenozide) against *Culex pipiens* L. and delayed effect on development. *J. Entomol. Zool.,* 4**,** 1202-1207.

JAYACHANDRAN, G. & FALLON, A. M. 2000. Evidence for expression of EcR and USP components of the 20-hydroxyecdysone receptor by a mosquito cell line. *Arch. Insect Biochem. Physiol.,* 43**,** 87-96.

KEMP, A., LETINIĆ, B. D., CHRISTIAN, R. N. & KOEKEMOER, L. L. 2018. Inoculation protocol for the African malaria vector, *Anopheles arabiensis*, by means of nano-injection. *Afr. Entomol.,* 26**,** 422-428.

KNOX, T. B., JUMA, E. O., OCHOMO, E. O., JAMET, H. P., NDUNGO, L., CHEGE, P., BAYOH, N. M., N'GUESSAN, R., CHRISTIAN, R. N. & HUNT, R. H. 2014. An online tool for mapping insecticide resistance in major *Anopheles* vectors of human malaria parasites and review of resistance status for the Afrotropical region. *Parasit. Vectors,* 7**,** 76.

KOEKEMOER, L. L., SPILLINGS, B. L., CHRISTIAN, R. N., LO, T.-C. M., KAISER, M. L., NORTON, R. A. I., OLIVER, S. V., CHOI, K. S., BROOKE, B. D. & HUNT, R.

H. 2011. Multiple insecticide resistance in anopheles gambiae (Diptera: Culicidae) from pointe Noire, Republic of the Congo. *Vector-Borne Zoonotic Dis,* 11**,** 1193-1200.

KUMAR, S., STECHER, G., LI, M., KNYAZ, C. & TAMURA, K. 2018. MEGA X: Molecular Evolutionary Genetics Analysis across Computing Platforms. *Mol. Biol. Evol.,* 35**,** 1547-1549.

MAHANDE, A., MOSHA, F., MAHANDE, J. & KWEKA, E. 2007. Feeding and resting behaviour of malaria vector, *Anopheles arabiensis* with reference to zooprophylaxis. *Malar. J.,* 6**,** 100.

MAHARAJ, S. 2021. Impact of *Ecdysone receptor* knockdown on *Anopheles funestus* longevity, reproductive success and *Plasmodium falciparum* susceptibility (unpublished work). South Africa: University of the Witwatersrand.

MARINOTTI, O., CAPURRO, M. D. L., NIRMALA, X., CALVO, E. & JAMES, A. A. 2006. Structure and expression of the lipophorin-encoding gene of the malaria vector, *Anopheles gambiae*. *Comp. Biochem. Physiol.,* 144**,** 101-109.

MITCHELL, S. N. & CATTERUCCIA, F. 2016. Anopheline reproductive biology: Impacts on vectorial capacity and potential avenues for malaria control. *Cold Spring Harb. Perspect. Med.,* 25593**,** 15-15.

MITCHELL, S. N., KAKANI, E. G., SOUTH, A., HOWELL, P. I., WATERHOUSE, R. M. & CATTERUCCIA, F. 2015. Evolution of sexual traits influencing vectorial capacity in anopheline mosquitoes. *Science,* 347**,** 985-988.

MOUATCHO, J. C., MUNHENGA, G., HARGREAVES, K., BROOKE, B. D., COETZEE, M. & KOEKEMOER, L. L. 2009. Pyrethroid resistance in a major African malaria vector Anopheles arabiensis from Mamfene, northern KwaZulu-Natal, South Africa. *S. Afr. J. Sci.,* 105**,** 127-131.

POSTLETHWAIT, J. & HANDLER, A. 1979. The roles of juvenile hormone and 20-hydroxy-ecdysone during vitellogenesis in isolated abdomens of Drosophila melanogaster. *J. Insect Physiol.,* 25**,** 455-460.

RAIKHEL, A., BROWN, M. & BELLES, X. 2005. 3.9 Hormonal control of reproductive processes. *Comprehensive molecular insect science,* 3**,** 433-491.

RAIKHEL, A. S., KOKOZA, V. A., ZHU, J., MARTIN, D., WANG, S.-F., LI, C., SUN, G., AHMED, A., DITTMER, N. & ATTARDO, G. 2002. Molecular biology of mosquito vitellogenesis: from basic studies to genetic engineering of antipathogen immunity. *Insect Biochem. Mol. Biol.,* 32**,** 1275-1286.

RODRIGUEZ, M. H., BOWN, D. N., ARREDONDO-JIMENEZ, J. I., VILLARREAL, C., LOYOLA, E. G. & FREDERICKSON, C. E. 1992. Gonotrophic cycle and survivorship of *Anopheles albimanus* (Diptera: Culicidae) in southern Mexico. *J. Med. Entomol.,* 29**,** 395-399.

ROUX, O., VANTAUX, A., ROCHE, B., YAMEOGO, K. B., DABIRÉ, K. R., DIABATÉ, A., SIMARD, F. & LEFÈVRE, T. 2015. Evidence for carry-over effects of predator exposure on pathogen transmission potential. *Proc. R. Soc. Biol. Sci. Ser. B,* 282**,** 20152430.

ROY, S., SAHA, T. T., JOHNSON, L., ZHAO, B., HA, J., WHITE, K. P., GIRKE, T., ZOU, Z. & RAIKHEL, A. S. 2015. Regulation of gene expression patterns in mosquito reproduction. *PLoS Genet.,* 11**,** e1005450-e1005450.

SHAW, W. R. & CATTERUCCIA, F. 2018. Vector biology meets disease control: Using basic research to fight vector-borne diseases. *Nat. Microbiol.,* 4**,** 20-34.

SUN, J., HIRAOKA, T., DITTMER, N. T., CHO, K.-H. & RAIKHEL, A. S. 2000. Lipophorin as a yolk protein precursor in the mosquito, *Aedes aegypti*. *Insect Biochem. Mol. Biol.,* 30**,** 1161-1171.

TAYLOR, S., WAKEM, M., DIJKMAN, G., ALSARRAJ, M. & NGUYEN, M. 2010. A practical approach to RT-qPCR—publishing data that conform to the MIQE guidelines. *Methods,* 50**,** S1-S5.

TIRADOS, I., COSTANTINI, C., GIBSON, G. & TORR, S. J. 2006. Blood-feeding behaviour of the malarial mosquito *Anopheles arabiensis*: implications for vector control. *Med. Vet. Entomol.,* 20**,** 425-437.

WANG, X., HOU, Y., SAHA, T. T., PEI, G., RAIKHEL, A. S. & ZOU, Z. 2017. Hormone and receptor interplay in the regulation of mosquito lipid metabolism. *Proc. Natl. Acad. Sci. U. S. A.,* 114**,** e2709-e2718.

WERLING, K., SHAW, W. R., ITOE, M. A., WESTERVELT, K. A., MARCENAC, P., PATON, D. G., PENG, D., SINGH, N., SMIDLER, A. L., SOUTH, A., DEIK, A. A., MANCIO-SILVA, L., DEMAS, A. R., MARCH, S., CALVO, E., BHATIA, S. N., CLISH, C. B. & CATTERUCCIA, F. 2019. Steroid hormone function controls non-competitive *Plasmodium* development in *Anopheles*. *Cell,* 177**,** 315-325.

WHO 2014. Malaria Threats Map.

YE, J., COULOURIS, G., ZARETSKAYA, I., CUTCUTACHE, I., ROZEN, S. & MADDEN, T. L. 2012. Primer-BLAST: a tool to design target-specific primers for polymerase chain reaction. *BMC Bioinformatics,* 13**,** 134-134.

ARAVIND, L., ANANTHARAMAN, V., BALAJI, S., BABU, M. M. & IYER, L. M. 2005. The many faces of the helix-turn-helix domain: transcription regulation and beyond. *FEMS Microbiol. Rev.,* 29**,** 231-262.

BALDINI, F., GABRIELI, P., SOUTH, A., VALIM, C., MANCINI, F. & CATTERUCCIA, F. 2013. The interaction between a sexually transferred steroid hormone and a female protein regulates oogenesis in the malaria mosquito *Anopheles gambiae*. *PLoS Biol.,* 11**,** e1001695-e1001695.

BATES, S. T., BERG-LYONS, D., CAPORASO, J. G., WALTERS, W. A., KNIGHT, R. & FIERER, N. 2011. Examining the global distribution of dominant archaeal populations in soil. *The ISME Journal,* 5**,** 908-917.

CAPORASO, J. G., LAUBER, C. L., WALTERS, W. A., BERG-LYONS, D., LOZUPONE, C. A., TURNBAUGH, P. J., FIERER, N. & KNIGHT, R. 2011. Global patterns of 16S rRNA diversity at a depth of millions of sequences per sample. *Proc. Natl. Acad. Sci. U. S. A.,* 108**,** 4516-4522.

CARRASQUILLA, M. C. & LOUNIBOS, L. P. 2015. Detection of insemination status in live *Aedes aegypti* females. *J. Insect Physiol.,* 75**,** 1-4.

COLEMAN, J., JUHN, J. & JAMES, A. A. 2007. Dissection of midgut and salivary glands from *Ae. aegypti* mosquitoes. *JoVE***,** e228.

D'AMORE, R., IJAZ, U. Z., SCHIRMER, M., KENNY, J. G., GREGORY, R., DARBY, A. C., SHAKYA, M., PODAR, M., QUINCE, C. & HALL, N. 2016. A comprehensive benchmarking study of protocols and sequencing platforms for 16S rRNA community profiling. *BMC Genomics,* 17**,** 55.

DAHALAN, F. A. B. 2017. *Impact of mating on Anopheles coluzzii in response to infection.* PhD, Imperial College London.

EKOKA, E., MAHARAJ, S., NARDINI, L., DAHAN-MOSS, Y. & KOEKEMOER, L. L. 2021. 20-Hydroxyecdysone (20E) signaling as a promising target for the chemical control of malaria vectors. *Parasit. Vectors,* 14**,** 86.

GABRIELI, P., KAKANI, E. G., MITCHELL, S. N., MAMELI, E., WANT, E. J., ANTON, A. M., SERRAO, A., BALDINI, F. & CATTERUCCIA, F. 2014. Sexual transfer of the steroid hormone 20E induces the postmating switch in *Anopheles gambiae*. *Proc. Natl. Acad. Sci. U. S. A.,* 111**,** 16353-16358.

HANSEN, I. A., ATTARDO, G. M., RODRIGUEZ, S. D. & DRAKE, L. L. 2014. Four-way regulation of mosquito yolk protein precursor genes by juvenile hormone-,

ecdysone-, nutrient-, and insulin-like peptide signaling pathways. *Front. Physiol.,* 5**,** 103-103.

HERMANN-BANK, M. L., SKOVGAARD, K., STOCKMARR, A., LARSEN, N. & MØLBAK, L. 2013. The Gut Microbiotassay: a high-throughput qPCR approach combinable with next generation sequencing to study gut microbial diversity. *BMC Genomics,* 14**,** 1-14.

HERNÁNDEZ, M., DUMONT, M. G., YUAN, Q. & CONRAD, R. 2015. Different bacterial populations associated with the roots and rhizosphere of rice incorporate plant-derived carbon. *Appl. Environ. Microbiol.,* 81**,** 2244-2253.

MAHARAJ, S., EKOKA, E., ERLANK, E., NARDINI, L., READER, J., BIRKHOLTZ, L.-M. & KOEKEMOER, L. L. 2022. The ecdysone receptor regulates several key physiological factors in Anopheles funestus. *Malar. J.,* 21**,** 1-13.

OLIVEIRA, J. H. M., GONÇALVES, R. L., LARA, F. A., DIAS, F. A., GANDARA, A. C. P., MENNA-BARRETO, R. F., EDWARDS, M. C., LAURINDO, F. R., SILVA-NETO, M. A. & SORGINE, M. H. 2011. Blood meal-derived heme decreases ROS levels in the midgut of *Aedes aegypti* and allows proliferation of intestinal microbiota. *PLoS Pathog.,* 7**,** e1001320.

PICHLER, M., COSKUN, Ö. K., ORTEGA-ARBULÚ, A.-S., CONCI, N., WÖRHEIDE, G., VARGAS, S. & ORSI, W. D. 2018. A 16S rRNA gene sequencing and analysis protocol for the Illumina MiniSeq platform. *MicrobiologyOpen,* 7**,** e00611.

PONDEVILLE, E., MARIA, A., JACQUES, J.-C., BOURGOUIN, C. & DAUPHIN-VILLEMANT, C. 2008. *Anopheles gambiae* males produce and transfer the vitellogenic steroid hormone 20-hydroxyecdysone to females during mating. *Proc. Natl. Acad. Sci. U. S. A.,* 105**,** 19631-19636.

QUINCE, C., WALKER, A. W., SIMPSON, J. T., LOMAN, N. J. & SEGATA, N. 2017. Shotgun metagenomics, from sampling to analysis. *Nat. Biotechnol.,* 35**,** 833-844.

RODGERS, F. H., GENDRIN, M., WYER, C. A. & CHRISTOPHIDES, G. K. 2017. Microbiota-induced peritrophic matrix regulates midgut homeostasis and prevents systemic infection of malaria vector mosquitoes. *PLoS Pathog.,* 13**,** e1006391.

ROY, S., SAHA, T. T., JOHNSON, L., ZHAO, B., HA, J., WHITE, K. P., GIRKE, T., ZOU, Z. & RAIKHEL, A. S. 2015. Regulation of gene expression patterns in mosquito reproduction. *PLoS Genet.,* 11**,** e1005450-e1005450.

ROY, S., SAHA, T. T., ZOU, Z. & RAIKHEL, A. S. 2017. Regulatory Pathways Controlling Female Insect Reproduction. *Annu. Rev. Entomol.,* 63**,** 489-511.

ROY, S., SMYKAL, V., JOHNSON, L., SAHA, T. T., ZOU, Z. & RAIKHEL, A. S. 2016. Regulation of reproductive processes in female mosquitoes. *Adv. Insect Physiol.,* 51**,** 115-144.

SMITH, A., SHIMADA, T. & RASKIN, L. 2017. A comparative evaluation of community structure in full-scale digesters indicates that two-phase digesters exhibit greater microbial diversity than single-phase digesters. *Environ. Sci. (Camb.),* 3**,** 304-311.

STRAUB, T. J., SHAW, W. R., MARCENAC, P., SAWADOGO, S. P., DABIRÉ, R. K., DIABATÉ, A., CATTERUCCIA, F. & NEAFSEY, D. E. 2020. The *Anopheles coluzzii* microbiome and its interaction with the intracellular parasite *Wolbachia*. *Sci. Rep.,* 10**,** 13847.

WANG, Y., GILBREATH III, T. M., KUKUTLA, P., YAN, G. & XU, J. 2011. Dynamic gut microbiome across life history of the malaria mosquito *Anopheles gambiae* in Kenya. *PLoS One,* 6**,** e24767-e24767.

WERLING, K., SHAW, W. R., ITOE, M. A., WESTERVELT, K. A., MARCENAC, P., PATON, D. G., PENG, D., SINGH, N., SMIDLER, A. L., SOUTH, A., DEIK, A. A., MANCIO-SILVA, L., DEMAS, A. R., MARCH, S., CALVO, E., BHATIA, S. N., CLISH, C. B. & CATTERUCCIA, F. 2019. Steroid hormone function controls non-competitive *Plasmodium* development in *Anopheles*. *Cell,* 177**,** 315-325.

CHAPTER 3

Ingested antibiotics do not influence how the ecdysone receptor (EcR) regulates *Anopheles arabiensis* reproductive output

3.1 Introduction

Upon emergence, *Anopheles* adult males and females typically mate within 1-4 days (Figure 3.1), after which the inseminated females seek out a host to blood-feed on (Becker et al., 2010, Clements and Stanley-Samuelson, 1994). During digestion in the mosquito gut, essential blood nutrients such as proteins and cholesterol are released and subsequently transported to the fat body and ovaries where they are used for the production of egg yolk proteins (in a process known as vitellogenesis), the maturation of ovaries, and egg development (Clements and Stanley-Samuelson, 1994, Raikhel et al., 2002, Scaraffia, 2016). Once vitellogenesis and egg development are completed, about 50-150 fully matured eggs (each 0.5-2 mm long) are released from the ovaries and oviposited in aquatic environments by each female (Becker et al., 2010). The females then wait for their next blood meal, to develop and lay their next batch of eggs (section 1.2.1). In water, the eggs hatch into larvae within 2-5 days (Becker et al., 2010, Clements and Stanley-Samuelson, 1994) (Figure 3.1), and the proportion of eggs laid that hatched into larvae is typically used as a measure of egg fertility (Baldini et al., 2013, Mekuriaw et al., 2019). Given that the number of *Anopheles* female mosquito vectors in a specific area greatly influences malaria transmission in that area (Shaw and Catteruccia, 2018), several studies have been conducted to identify which factors regulate mating, blood feeding and digestion, vitellogenesis, oviposition, and fertility, as they all contribute to vector abundance. Among the regulators identified to date are

the 20-hydroxyecdysone (20E) signaling pathway (Table 1.2, Figure 3.1) and the gut-associated bacteria (Figure 3.1).

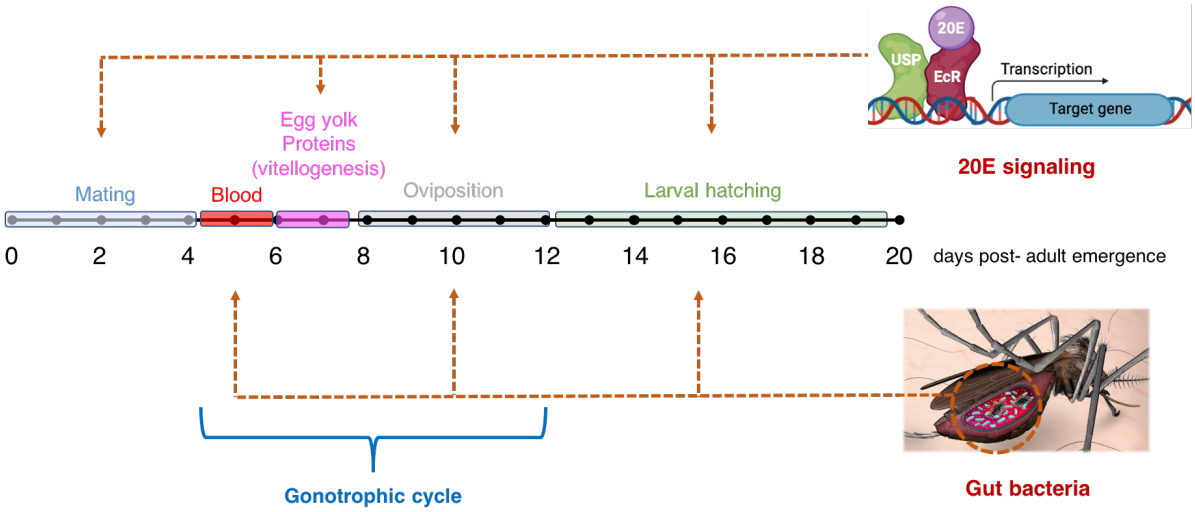

Figure 3.1: Physiological pathways regulating vector abundance in *Anopheles* mosquitoes [created with information from (Cansado-Utrilla et al., 2021, Ekoka et al., 2021, Strand, 2018)]. *Anopheles* abundance is regulated by physiological processes such as mating, blood-feeding, vitellogenesis, oviposition, and larval hatching. These processes are themselves regulated by at least two modulators, namely the mosquito's 20E signaling pathway, and its gut bacterial microbiome. The meaning of the gonotrophic cycle has been explained earlier (section 1.2.1). *Abbreviations*: 20E, 20-hydroxyecdysone; EcR, ecdysone receptor; USP, ultraspiracle.

As described earlier (section 1.5), the function of the 20E signaling pathway can be studied by disturbing the pathway and assessing how it affects a phenotype of interest. One of these manipulations include reducing —or silencing— *EcR* transcripts with RNAi. Depleting *EcR* levels impairs mating (Baldini et al., 2013), blood digestion (Bryant et al., 2010, Lucas et al., 2015, Zhang and Raikhel, 2020), vitellogenesis (Roy et al., 2015), as well as egg development and oviposition (Bryant and Raikhel, 2011, Werling et al., 2019), in *An. gambiae* and/or *Ae. aegypti*. In the *Ae. aegypti* fat body,

EcR silencing decreases the expression of yolk proteins (vitellogenin, vitellogenin carboxypeptidase [VCP], or cathepsin b-like protease [VCB]) (Baldini et al., 2013, Roy et al., 2015, Werling et al., 2019), extends vitellogenesis (Bryant and Raikhel, 2011), or reduces lipid and carbohydrate metabolisms (Hou et al., 2015, Wang et al., 2017), two metabolic processes required for the production of egg lipids and proteins. Finally, with respect to ovaries, *EcR* silencing has been associated with a lower fecundity and impaired development of ovarian follicles in *Ae. aegypti* and *An. gambiae* (Bryant and Raikhel, 2011, Werling et al., 2019). While there is no study linking *EcR* silencing to fertility, it has been reported that treating *Culiseta morsitans* mosquitoes with methoxyfenozide —an agonist of 20E which binds competitively to EcR (section 1.4.1)— reduced its egg fertility in a dose-dependent manner, with the highest dose of 0.072 mg/ml methoxyfenozide resulting in 100% inhibition of egg hatching (Haouari-Abderrahim and Rehimi, 2014).

Gendrin et al. (2015) found that *An. gambiae*'s fecundity is increased when they feed on human blood containing penicillin-streptomycin, due to their 92-fold reduction in Enterobacteriaceae. In other words, their work suggested that the level of human antibiotic consumption —especially those that can reduce the Enterobacteriaceae— in a region could influence *Anopheles* abundance. Therefore, the authors suggested that vector control interventions should be strengthened in areas where the human antibiotic consumption is elevated (Gendrin et al., 2015). This recommendation is particularly relevant to low- and middle-income countries (LMICs), where antibiotics are reportedly over-prescribed and/or inappropriately prescribed by health care providers (Sulis et al., 2020, Wilkinson et al., 2018). For example, a recent study estimated that between 2005 and 2017, the percentage of sick children (under the age of five) in LMICs receiving antibiotics increased from 36.8% to 43.1% (Allwell-Brown et al., 2020). Although this increase may reflect an improvement in access to

healthcare, it also comes at the cost of increasing the antibiotic consumption in the LMICs areas.

Can the interventions targeting the 20E signaling pathway equally reduce *Anopheles* abundance in aseptic (mosquitoes with reduced bacterial microbiome) and septic mosquitoes? In other words, is the role of the 20E signaling pathway in regulating *Anopheles*' reproductive output (Table 1.2, chapter 2) influenced by the gut bacteria? To answer this question, the objective of this chapter was to determine whether the gut bacteria affect how *EcR* silencing compromises *An. arabiensis*' reproduction. For this purpose, *An*. *arabiensis* females were used to (i) determine if a correlation existed between *EcR* transcript abundance and the gut bacterial load, and (ii) determine whether RNAi-mediated depletion of *EcR* differentially affects reproduction between aseptic (fed on sugar water supplemented with antibiotics) and septic (fed on sugar water) mosquitoes.

3.2 Materials and Methods

3.2.1 Ethics statement and mosquito rearing

The ethics statement and mosquito rearing protocol have been described earlier (section 2.2.2).

3.2.2 Antibiotics treatment and microbiome quantification

To generate aseptic mosquitoes, *An. arabiensis* were fed for four days from emergence with a 10% (w/v) sucrose/sterile water solution supplemented with 0.5% (v/v) gentamicin (cat no: G1397, concentration: 50 mg/ml, Sigma) and 1% (v/v) penicillin-streptomycin (cat no: 15070063, concentration: 5,000 U/mL, Thermo

Scientific) (Contreras-Garduno et al., 2015). The choice for these antibiotics is that they target Gram negative bacteria, including Enterobacteriaceae, Acetobacteriaceae, and Flavobacteriaceae which have been identified in *An. arabiensis* (E Silva et al., 2021)

The control cohort (*i.e.,* septic mosquitoes) were fed on a 10% (w/v) sucrose/sterile water solution. The solutions in each group were changed daily, to minimize bacterial contamination. To assess the effectiveness of the antibiotic treatment, microbial genomic DNA was extracted from pooled guts of 45 mosquitoes in each group (aseptic or septic, i.e. 15 mosquitoes per biological replicate) with the DNeasy® PowerSoil® Pro kit (cat no: 47016, Qiagen) and bacterial abundance was quantified by measuring the expression of selected regions of the V4 hypervariable segment of the16S rDNA gene, as previously described (Caporaso et al., 2011, Hermann-Bank et al., 2013, Rodgers et al., 2017, Smith et al., 2017). To ensure that no bacteria from the cuticle would contaminate the gut samples, mosquitoes were washed in 70% (v/v) EtOH/distilled water and rinsed twice in 1x sterile phosphate buffer saline (PBS) solution (cat no: 524650, Merck) prior to gut dissections (Coleman et al., 2007, Rodgers et al., 2017). The universal 515F/806R primer pair, which targets a ~250 bp fragment on the V4 variable domain of the 16S rDNA gene (Table 3.1), was used to quantify the total eubacteria load (Bates et al., 2011, Hernández et al., 2015, Smith et al., 2017).

Table 3.1: Sequences of 16S rDNA primers used for bacterial quantification.
F = forward primer, R = reverse primer. The standard IUPAC nucleotide code was applied.

Target	Primers	Sequences (5' ->3')	References
Eubacteria	515_F 806_R	GTGCCAGCMGCCGCGGTAA GGACTACHVGGGTWTCTAAT	(Caporaso et al., 2011, Straub et al., 2020)

3.2.3 RNA purifications, cDNA synthesis, and qPCR

Total RNA was purified as described in section 2.2.4, while gene expression analyses were carried out as outlined in section 2.2.8. All the qPCR primers optimized in Table 2.1 were also used here.

3.2.4 RNAi and measurement of RNAi phenotypes

RNAi was carried out as described earlier (section 2.2.9), and the phenotypes measured post-silencing included (i) the expression of four vitellogenic genes, namely *Lp*, *Vg*, *VCB*, *VCP*, (ii) mosquito fecundity, more specifically oviposition rates, percentage oviposition, egg length-to-width ratio, ovary length, and (iii) egg fertility (Figure 3.2). All the detailed protocols used for fecundity and fertility assays are described earlier (section 2.2.11), while the timeline for the experiments is described below (Figure 3.2a). Briefly, freshly emerged mosquitoes were first randomly divided into two groups, aseptic and septic (300 females per group). Within each group, mosquitoes were put in cages in a 1:1 male-to-female ratio and allowed to mate for 4 days. On day 5, a subset of females in each group (15 per biological replicate) was dissected to confirm the effectiveness of the antibiotic treatment (section 3.2.3), while the remaining females (150 females per group) were injected with dsRNA (either dsEcR or dsGFP) to induce RNAi. On day 6, the surviving mosquitoes (140 females

per group) were blood-fed and 24 hours later (i.e., on day 7), RNA was extracted from a subset of mosquitoes (60 females) in each of the four groups (dsEcR-injected aseptic, dsEcR-injected septic, dsGFP-injected aseptic, and dsGFP-injected septic) to measure the expression of *EcR* and the four above-mentioned vitellogenic genes. On the same day (day 7), the remaining 80 fully engorged mosquitoes were placed in glass vials (one mosquito per vial) containing a damp filter paper at the bottom to allow for oviposition (Figure 3.2b) (Choi et al., 2014).

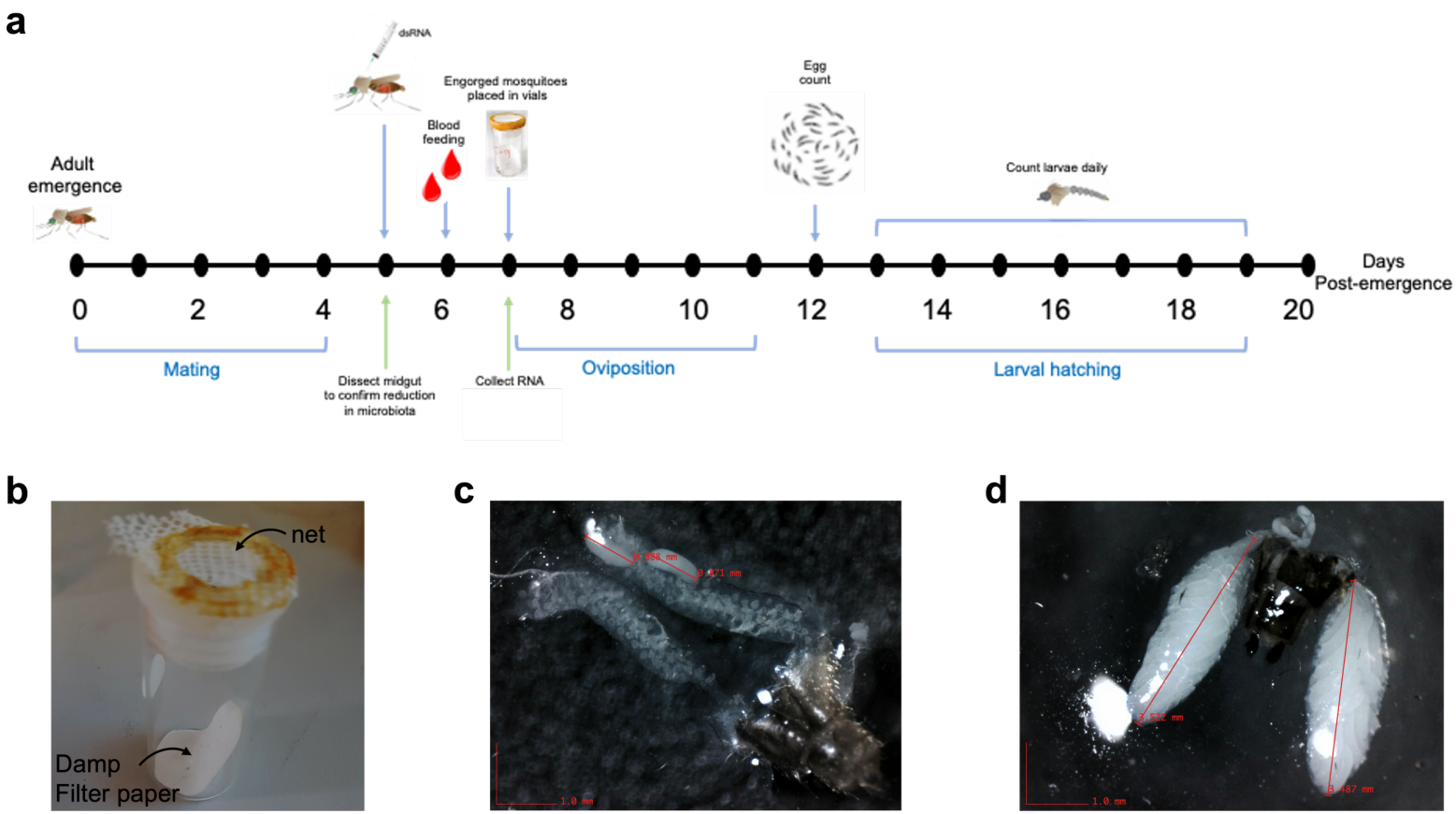

Figure 3.2: Experimental design for RNAi. (a) Timeline for the fecundity and fertility experiments**.** Aseptic (or septic) mosquitoes received antibiotics (or not) in their daily-changed sugar water throughout the first 12 days post-emergence. Although antibiotics were not included in the blood meal, the sugar water solutions (with or without antibiotics) were provided to the mosquitoes immediately after blood meal. Hence, aseptic mosquitoes were constantly exposed to antibiotics, except during blood-feeding. **(b)** Oviposition vial. **(c)** Example of egg length measurement with DinoXcope Imaging software. **(d)** Example of ovary length measurement with DinoXcope Imaging software. In (c) The measurements were made on eggs retained in the ovaries. All images were captured by me.

The mosquitoes in vials were left to lay eggs for 5 days (day 7 to day 11) and on day 12, the number of eggs laid in each vial was counted under the microscope (Figure 3.2a). The number of eggs deposited were used to compute the proportion of females that laid eggs relative to the total number of females in that group was calculated, as a measure of percentage fecundity, as well as oviposition rate, which is the average number of eggs per female. In addition, the ovaries of females in each group were dissected (Meadows, 1968), in order to measure egg length and width (Figure 3.2c), as well as ovary length (Figure 3.2d), all of these with the DinoXcope Imaging microscope software. The egg measurements were further used to compute the egg length-to-width ratio, as well as the egg mean volume (Equation 3.1).

$$\text{Egg mean volume} = \frac{\pi}{6} \times \text{mean length} \times [\text{mean width}]^2$$

Equation 3.1: Equation used to compute the egg mean volume [Taken from Faull et al., 2016, Sota and Mogi, 1992].

The eggs deposited were subsequently transferred from each filter paper to cups containing distilled water, and from day 13 to day 19, the eggs could hatch into larvae, and the number of first-instar larvae in each was counted and removed daily (Figure 3.2a), to prevent carnivorous larval behaviour and ensure accurate counting (Professor Koekemoer, *personal communication*). In each of the four groups mentioned earlier, the proportion of eggs that hatched into larvae relative to the total number of eggs laid in that group was calculated as a measure of percentage fertility.

3.2.5 Data analysis

qPCR data analysis

The quantification cycles (Cq values) were automatically computed by the CFX Maestro™ software v.1.1 (cat no: 12013758, Bio-Rad). For bacterial gene quantification, the Cq values of selected bacterial genes (Table 3.1) were normalized against that of the mosquito *RpS7* gene as previously described (Rodgers et al., 2017). On the other hand, the Cq values of *EcR* and vitellogenesis-related genes were normalized to both *RpS7* and *RpL19* reference genes, unless indicated otherwise. In all cases, these relative normalized expression (RNE) values were calculated by the CFX Maestro™ software v.1.1, as described previously (Equation 2.1). To determine the percentage change in RNE values between the experimental and control samples, the RNE of the control was subtracted from the RNE of the experimental (or vice-versa, depending on which RNE was the highest) and the result was multiplied by 100.

Statistical analysis

In this study, each experiment was performed in 2-3 independent biological replicates (see figure legends) and means ± SEM are shown. All statistical analyses were performed with GraphPad Prism v.9.1.0, with details presented in the text. No test for data normalization was performed and as such, Gaussian distribution was assumed in all cases, unless indicated otherwise. For this reason, parametric statistical methods were typically selected. Whenever the means of two independent or unpaired groups were compared (e.g., comparing *EcR* RNE between dsEcR-injected and dsGFP-injected insects or comparing bacterial gene RNE between aseptic and septic mosquitoes), the unpaired Student's *t*-test was used. To compare *EcR* RNE between two groups at different time points, a multiple unpaired *t*-test was used, meaning that at each time point, only two values were compared. To correct for the multiple

comparisons used in this test, a *post hoc* Holm Sidak analysis was conducted as it assumes that each comparison is independent to the next one (which was consistent with the fact that the mosquitoes used to measure *EcR* expression at a specific time point were not the same used for the following time point), as opposed to the Bonferroni-Dunn method which does not make this assumption. Next, to determine whether the differences observed in oviposition rates, egg length-to-width ratios, ovary length, and expression of yolk genes between the four groups (dsEcR-injected aseptic, dsGFP-injected aseptic, dsEcR-injected septic, and dsGFP-injected septic) were due to the antibiotics treatment, the dsRNA injections, or both simultaneously, a two-way ANOVA analysis was conducted. This was followed by a Tukey *post hoc* analysis to assess which specific group means were statistically different from one another. One advantage of the Tukey test is the fact that it accounts for the difference in sample sizes between the four groups. The statistical difference in the percentage fecundity and fertility —i.e., proportional data— were assessed with the Fisher's exact test, as described in chapter 2 (section 2.2.12). In all cases, statistical significance was assessed by setting a *p*-value cutoff of 0.05, so that all *p*-values below this cutoff would be considered statistically significant.

3.3 Results

Notes:

(1) All the raw data can be found in Appendix 4.
(2) Each time the phrases "mRNA expression", "mRNA/transcript abundance", or "mRNA/transcript levels" are used, they refer to the relative normalized expression, i.e., the RNE values.

3.3.1 *EcR* transcript abundance is influenced by antibiotics

To assess the role of the 20E signaling pathway in modulating the mosquito's gut bacterial microbiome, *EcR* transcript abundance was compared between aseptic (fed on antibiotic-treated sugar water solution) and septic (fed on sugar water without antibiotics) inseminated female mosquitoes. For this purpose, two groups of mosquitoes, septic and aseptic were prepared as described above (section 3.2.2). To first confirm the generation of aseptic mosquitoes, the guts of a subset of females from each group (n = 15 guts per group per biological replicate) were dissected after 4 days of antibiotic treatment, to compare the total bacterial load between the two groups, using the expression of the "total *16S* gene" (section 3.2.2). The results showed that the total *16S* gene expression in the guts of aseptic and septic mosquitoes were 0.0049 ± 0.0029 and 0.1599 ± 0.0132 (mean ± SEM), respectively, highlighting a significant 96% reduction in the bacterial load of aseptic mosquitoes (unpaired *t*-test, $p = 0.0075$) (Figure 3.3a). The mosquitoes that were not dissected were blood-fed, and *EcR* mRNA abundance was compared between adults from both groups at 24 hours post blood meal (hPBM). *EcR* expression was measured at 24 hPBM because it was previously established that at this time point, *EcR* expression reaches its peak (section 2.3.1). As hypothesized, *EcR* mRNA abundance was significantly lowered, from 0.1345 ± 0.0093 in septic mosquitoes to 0.0512 ± 0.0066 in aseptic mosquitoes, i.e., a 62% reduction in *EcR* expression (unpaired *t*-test, $p = 0.0182$) (Figure 3.3b).

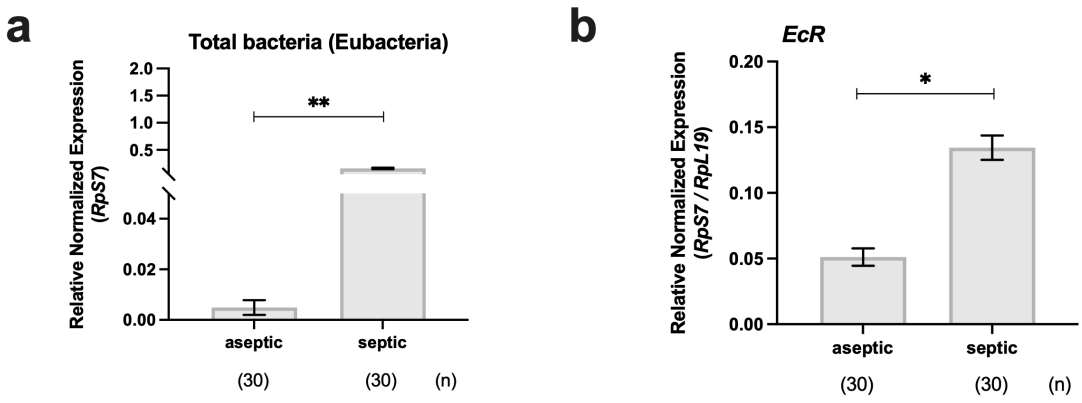

Figure 3.3: ***EcR* transcript abundance is related to the gut bacterial load.** RNE values are plotted for each gene. (**a**) Aseptic mosquitoes have fewer bacteria than septic mosquitoes. (**b**) Aseptic mosquitoes have less *EcR* transcripts at 24 hPBM relative to septic mosquitoes. (**a,b**) Two independent biological replicates were used. In all cases (**a,b**), means RNE ± SEM are indicated. **p*<0.05, ***p*<0.01, *(n)* number of mosquitoes or guts across the biological replicates.

3.3.2 *EcR*-mediated regulation of egg production is not influenced by the ingestion of antibiotics

Given the established relationship between *An. arabiensis EcR* transcript abundance and the gut bacterial microbiome (Figures 3.3a-b), and between *EcR* transcript abundance and the mosquito reproductive output (chapter 2), I wanted to know whether a reduction in gut bacterial load would impair EcR ability to induce fecundity and fertility. For this purpose, dsEcR- or control dsGFP-injected aseptic and septic mosquitoes were blood fed, and subsequently, multiple fecundity and fertility parameters were determined as described earlier (Figure 3.2).

To determine whether the oviposition rates were influenced by the antibiotics treatment and the dsRNA treatment, the number of eggs laid in each group was calculated. It was found that neither the antibiotics nor the dsRNA treatment affected the oviposition rates. Indeed, the oviposition rates of the dsEcR-antibiotic, dsGFP-

antibiotic, dsEcR-sugar, and dsGFP-sugar groups were 45.33 ± 4.173, 56.89 ± 4.872, 58.63 ± 6.582, and 53.94 ± 6.361 eggs (mean ± SEM) per female, respectively (Figure 3.4a). However, neither the antibiotics treatment (two-way ANOVA: F = 0.8576, df = 1, p = 0.3557), nor *EcR* depletion alone (two-way ANOVA: F = 0.3778, df = 1, p = 0.5395), nor both combined (two-way ANOVA: F = 2.114, df = 1, p = 0.1477) could account for these observed differences. As a result, the *post hoc* Tukey analysis did not detect any significant difference in the number of eggs laid per female in the dsEcR-injected versus dsGFP-injected antibiotic-treated mosquitoes (p = 0.4362), the dsEcR-injected versus dsGFP-injected non-antibiotic treated mosquitoes (p = 0.9387), the dsEcR-injected mosquitoes (antibiotic versus non-antibiotic; p = 0.3830) or the dsGFP-injected mosquitoes (antibiotic versus non-antibiotic; p = 0.9789).

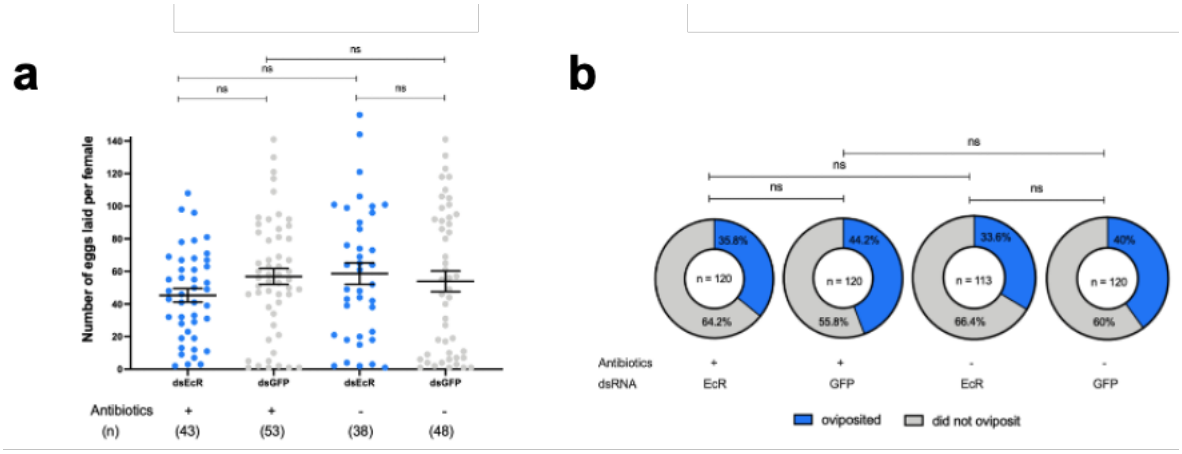

Figure 3.4: Influence of antibiotics on *EcR*-mediated regulation of fecundity. (**a**) Neither the antibiotics treatment alone, nor *EcR* knockdown alone, nor both treatments combined affected the oviposition rate (only mosquitoes who laid eggs are represented). (**d**) Likewise, the percentage of females that oviposited in each group was not affected by either of these two treatments. In (**a,b**) *n* represents the number of females or midguts in the experiment. All experiments were performed in 3 independent biological replicates. ^{ns} not significant.

Next, the proportion of females that laid eggs was calculated to determine whether it was influenced by these two factors. Again, neither the antibiotic treatment

nor the dsRNA treatment had an effect. Indeed, with respect to the proportion of females that laid eggs, 35.8%, 44.2%, 33.6%, and 40% of females oviposited in the dsEcR-antibiotic, dsGFP-antibiotic, dsEcR-sugar, and dsGFP-sugar groups, respectively (Figure 3.4b). Even though *EcR* silencing decreased the number of females that oviposited in both antibiotic-fed and non-antibiotic fed groups, this difference was not statistically significant (Fisher's exact test, two sided: $p = 0.2356$ and $p = 0.3433$, for the antibiotic and non-antibiotic groups, respectively). Similarly, while antibiotics augmented the number of females that oviposited in both dsEcR-injected and dsGFP-injected groups, this difference was not statistically significant (Fisher's exact test, two sided: $p = 0.7836$ and $p = 0.6011$, for the dsEcR- and dsGFP-injected groups, respectively). Altogether, these data suggested that neither antibiotics nor *EcR* silencing influenced fecundity in *An. arabiensis*, at least in the first gonotrophic cycle.

As described in Chapter 2, *Anopheles*' egg mean volume can influence the embryonic development time or its susceptibility to *Plasmodium* infection. Since the egg mean volume is largely influenced by the egg length-to-width ratio, the lengths and widths of eggs deposited in each *An*. *arabiensis* group were recorded and used to compute both the egg length-to-width ratios, and egg mean volumes. It was found that the egg length-to-width ratio was affected by the antibiotics treatment and EcR silencing separately, but neither of these treatments had an effect on the other. The average ratios for each group were 3.474 ± 0.1443, 4.433 ± 0.1230, 3.251 ± 0.1144, and 4.006 ± 0.1282 (mean ± SEM) for the dsEcR-antibiotic, dsGFP-antibiotic, dsEcR-sugar, and dsGFP-sugar groups, respectively (Table 3.2, Figure 3.5a). While the variation observed between these ratios was due to *EcR* silencing (two-way ANOVA: $F = 43.61$, df = 1, $p < 0.0001$), and antibiotics (two-way ANOVA: $F = 6.271$, df = 1, $p = 0.0138$), the interaction between these two factors was not statistically significant (two-

way ANOVA: F = 0.6177, df = 1, p = 0.4337), suggesting that antibiotics do not influence how *EcR* regulates the egg length-to-width ratio, and vice-versa. The Tukey *post hoc* analysis revealed that *EcR* silencing significantly reduced the egg length-to width ratio in both antibiotic and non-antibiotic treated groups (p < 0.0001 and p = 0.0002, respectively). In contrast, the ingestion of antibiotics did not affect this ratio in either the dsEcR-injected group (p = 0.6531) or the dsGFP-injected group (p = 0.0746), but only when comparing the dsEcR-antibiotic group to the dsGFP-sugar group (p = 0.0206), which however has no biological significance.

Table 3.2: Summary of egg measurements for each group. The average egg length-to-width ratio was calculated by measuring the average of the values in the columns “length/width”.

	dsEcR-aseptic			dsGFP-aseptic			dsEcR-septic			dsGFP-septic		
	Length (mm)	Width (mm)	length/width ratio	Length (mm)	Width (mm)	length/width ratio	Length (mm)	Width (mm)	length/width ratio	Length (mm)	Width (mm)	length/width ratio
1	0,904	0,286	3,1608	0,803	0,195	4,1179	0,605	0,141	4,2908	0,961	0,192	5,0052
2	0,692	0,318	2,1761	0,805	0,143	5,6294	0,514	0,14	3,6714	1,084	0,21	5,1619
3	0,898	0,289	3,1073	0,768	0,214	3,5888	0,489	0,154	3,1753	0,846	0,161	5,2547
4	0,779	0,253	3,0791	0,859	0,189	4,5450	0,414	0,113	3,6637	0,824	0,195	4,2256
5	0,823	0,249	3,3052	0,816	0,166	4,9157	0,426	0,16	2,6625	1,105	0,286	3,8636
6	0,73	0,208	3,5096	0,705	0,173	4,0751	0,522	0,221	2,3620	0,898	0,219	4,1005
7	0,589	0,273	2,1575	0,804	0,151	5,3245	0,624	0,176	3,5455	0,946	0,222	4,2613
8	0,978	0,224	4,3661	0,909	0,216	4,2083	0,563	0,221	2,5475	0,718	0,164	4,3780
9	0,823	0,157	5,2420	0,773	0,165	4,6848	0,605	0,195	3,1026	0,735	0,153	4,8039
10	0,894	0,251	3,5618	0,903	0,202	4,4703	0,561	0,231	2,4286	0,623	0,212	2,9387
11	0,859	0,234	3,6709	0,716	0,189	3,7884	0,551	0,184	2,9946	0,606	0,149	4,0671
12	0,888	0,259	3,4286	0,801	0,159	5,0377	0,549	0,173	3,1734	0,674	0,169	3,9882
13	0,871	0,299	2,9130	0,822	0,183	4,4918	0,541	0,144	3,7569	0,679	0,153	4,4379
14	1,114	0,241	4,6224	0,801	0,243	3,2963	0,547	0,179	3,0559	0,662	0,227	2,9163
15	1,022	0,286	3,5734	0,836	0,217	3,8525	0,472	0,156	3,0256	0,644	0,153	4,2092
16	0,919	0,317	2,8991	0,792	0,182	4,3516	0,662	0,196	3,3776	0,947	0,333	2,8438
17	1,231	0,327	3,7645	0,854	0,183	4,6667	0,443	0,161	2,7516	0,795	0,271	2,9336
18	0,876	0,262	3,3435	0,664	0,2	3,3200	0,54	0,145	3,7241	0,61	0,177	3,4463
19	0,919	0,268	3,4291	0,748	0,183	4,0874	0,479	0,172	2,7849	0,625	0,151	4,1391
20	0,98	0,262	3,7405	0,683	0,191	3,5759	0,508	0,178	2,8539	0,68	0,165	4,1212
21	1,047	0,325	3,2215	0,806	0,177	4,5537	0,572	0,13	4,4000	0,654	0,183	3,5738
22	0,944	0,225	4,1956	0,905	0,193	4,6891	0,546	0,173	3,1561	0,71	0,133	5,3383
23	0,98	0,286	3,4266	0,789	0,158	4,9937	0,496	0,163	3,0429	0,678	0,198	3,4242
24				0,77	0,14	5,5000	0,492	0,148	3,3243	0,677	0,145	4,6690
25				1,071	0,226	4,7389	0,578	0,131	4,4122	0,649	0,227	2,8590
26				0,89	0,187	4,7594				0,704	0,183	3,8470
27										0,771	0,168	4,5893
28										0,813	0,165	4,9273
29										0,723	0,177	4,0847
30										0,666	0,202	3,2970
31										0,629	0,206	3,0534
32										0,81	0,197	4,1117
33										0,727	0,218	3,3349
Mean length (mm)	0,9026			0,8113			0,5320			0,7537		
Mean width (mm)	0,2652			0,1856			0,1674			0,1928		
Mean volume (mm3)	0,0332			0,0146			0,0078			0,0147		

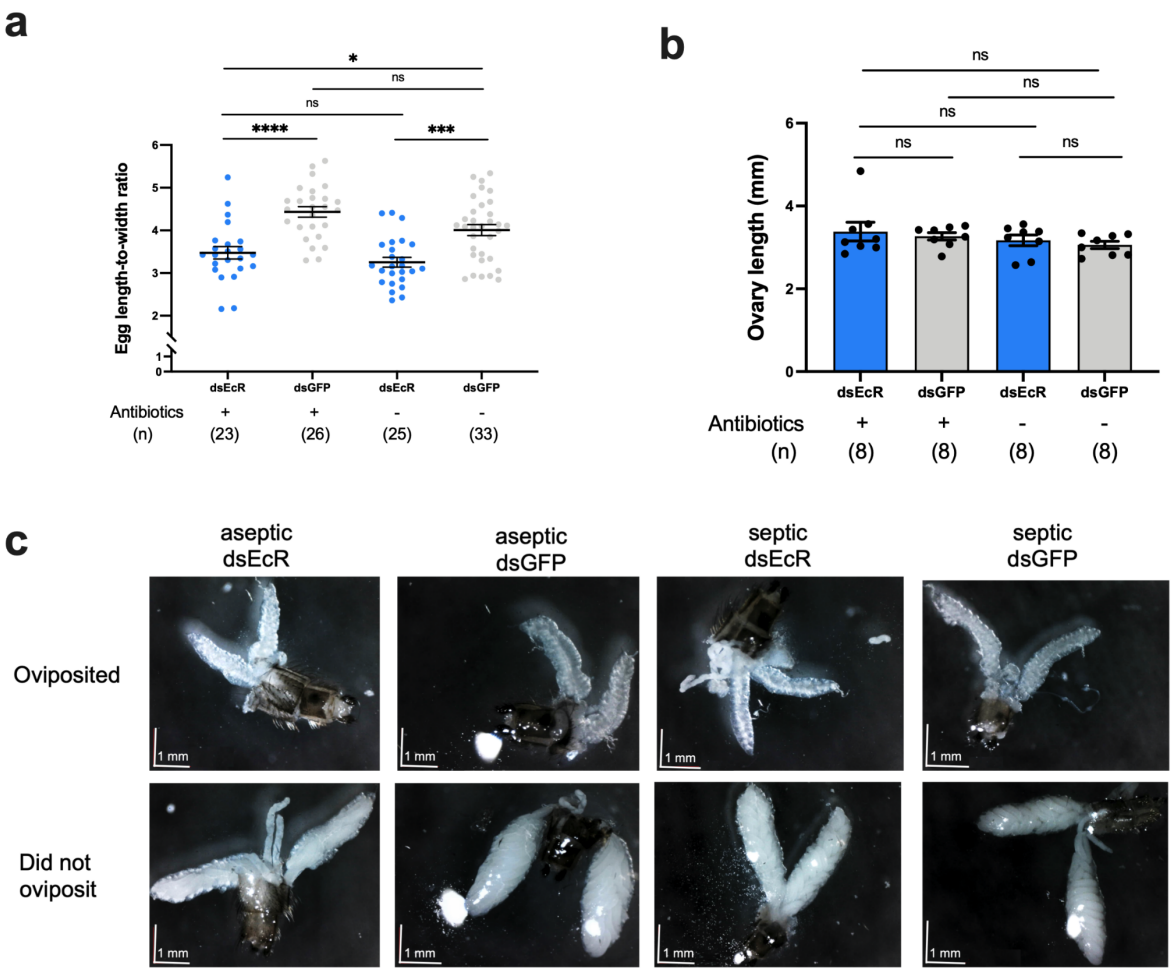

Figure 3.5: The effect of antibiotics and *EcR* silencing on egg size and ovaries. (**a)** egg length-to-width ratio was significantly affected by the antibiotic treatment and *EcR* expression. (**b**) Ovary length was neither affected by *EcR* silencing nor the antibiotics treatment. In (**a**) and (**b**), *n* represents the number of eggs and ovaries across three independent biological replicates, respectively. *p<0.05, ****p<0.0001, ^{ns} not significant. (**c**) No indication of abnormal ovaries was observed.

To explain the variation in egg length-to-width ratio, whether *EcR* silencing and/or antibiotics affected the development of ovaries was explored, based on a previous report that dsEcR-injected *Ae. aegypti* females displayed a reduced size of ovarian follicles (Bryant and Raikhel, 2011). In this study, the average ovary length in each group (mean ± SEM) were 3.381 ± 0.2248 mm (dsEcR-injected, antibiotic), 3.269 ± 0.08847 mm (dsGFP-injected, antibiotic), 3.172 ± 0.1308 mm (dsEcR-injected,

sugar), and 3.059 ± 0.08890 mm (dsGFP-injected, sugar) (Figure 3.5b). Nonetheless, the difference in ovary lengths between groups was neither affected by *EcR* silencing (two-way ANOVA: F = 0.6072, df = 1, p = 0.4424), antibiotics ingestion (two-way ANOVA: F = 2.106, df = 1, p = 0.1579), nor the interaction of these two factors (two-way ANOVA: F = 1.199×10^{-5}, df = 1, p = 0.9973). As a result, the Tukey *post hoc* analysis did not detect any statistically significant difference between the four groups: dsEcR antibiotic vs dsGFP antibiotic (p = 0.9462), dsEcR vs. dsGFP sugar (p = 0.9448), dsEcR antibiotic vs dsEcR sugar (p = 0.7372), dsGFP antibiotic vs dsGFP sugar (p = 0.7344), and dsEcR antibiotic versus dsGFP sugar (p = 0.4075). Likewise, no difference in ovary morphology or the presence of undeveloped eggs between the different groups were detected in the first gonotrophic cycle (Figure 3.5c).

Given the previous reports that the 20E signaling pathway and the gut bacterial microbiome regulate egg fertility in *Ae. aegypti* and/or *An. gambiae* (Figure 3.1), it was hypothesized that both *EcR* depletion and the antibiotics treatment could regulate *An. arabiensis*' egg fertility. Hence, as a measure of fertility, the number of larvae that hatched from each group of mosquitoes relative to the total number of eggs laid in that group was computed. Interestingly, both the antibiotic treatment and *EcR* depletion significantly affected fertility, albeit in opposite directions (Figure 3.6). *EcR* silencing significantly decreased egg fertility in both antibiotic-treated (from 81.49% to 60.18%, Fisher's exact test: p = 0.0002) and non-antibiotic treated (from 73.71% to 54.58%, Fisher's exact test: p = 0.0004) groups, suggesting that antibiotics do not affect how *EcR* silencing compromises egg fertility. In contrast, antibiotics feeding significantly increased egg fertility in dsGFP-injected mosquitoes (from 73.71% to 81.49%, Fisher's exact test: $p < 0.0001$), and dsEcR-injected mosquitoes (from 54.58% to 60.18%, Fisher's exact test: p = 0.0002) (Figure 3.6).

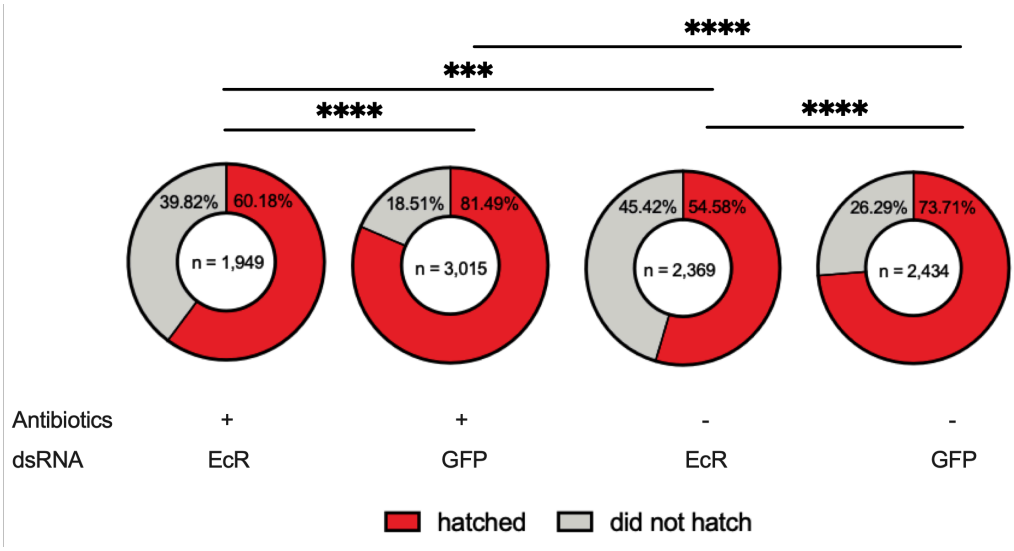

Figure 3.6: Both *EcR* silencing, and the antibiotic treatment affect egg fertility. Statistical significance was assessed with the Fisher's exact test. *n* represents the number of eggs across three independent biological replicates. ***$p<0.001$, ****$p<0.0001$.

Since the effects *EcR* knockdown and antibiotics ingestion had on egg mean volume and fertility could not be attributed to undeveloped ovaries, it was hypothesized that the phenotypes observed could result from a difference in mating (Beach, 1979, Mitchell et al., 2015), feeding (Beach, 1979, de O Gaio et al., 2011), or vitellogenesis (Roy et al., 2015, Roy et al., 2017, Roy et al., 2016). Because dsRNA injection occurred after mating (Figure 3.2a), and there is currently no experimental evidence —to my knowledge— supporting that antibiotics affect mating rates, the first hypothesis was discarded. Next, even though only fully engorged mosquitoes were selected for the oviposition experiments, more reliable methods such as measuring mosquito haemoglobin content (Briegel et al., 1979, Ogunrinade, 1980) would have perhaps

detected whether or not there was a difference in the volume of blood ingested between the different groups.

Lastly, to investigate whether a difference in vitellogenesis could explain the variation in fertility and egg size observed in the first gonotrophic cycle, the transcripts abundance of four egg yolk genes (*lipophorin, vitellogenin, VCB*, and *VCP*) at 24 hPBM in dsRNA-injected antibiotic and non-antibiotic mosquitoes were compared (Figure 3.7). This time point was selected because *An. arabiensis*' *lipophorin* expression peaked at 24 hPBM (chapter 2, Figure 2.2). Overall, only *EcR* silencing affected the expression of the yolk genes, but not the antibiotics treatment.

With respect to *vitellogenin* (Vg), the two-way ANOVA analysis demonstrated that *Vg* expression is neither affected by the antibiotic treatment (antibiotics: $F = 1.435$, $df = 1$, $p = 0.2652$), nor the interaction between the antibiotic and dsRNA treatments (interaction: $F = 1.328$, $df = 1$, $p = 0.2824$). However, *EcR* silencing did affect *Vg* expression (dsRNA: $F = 7.358$, $df = 1$, $p = 0.0266$). To determine which specific groups were affected by dsRNA treatment, a *post hoc* Tukey analysis was conducted. The results revealed that *EcR* depletion only significantly affected *Vg* expression in sugar-fed mosquitoes. Indeed, in the sugar-fed cohort, dsEcR injection reduced *Vg* expression by 76% ($p = 0.0257$), while it did not affect *Vg* expression in the antibiotic/sugar cohort ($p = 0.3020$) (Figure 3.7).

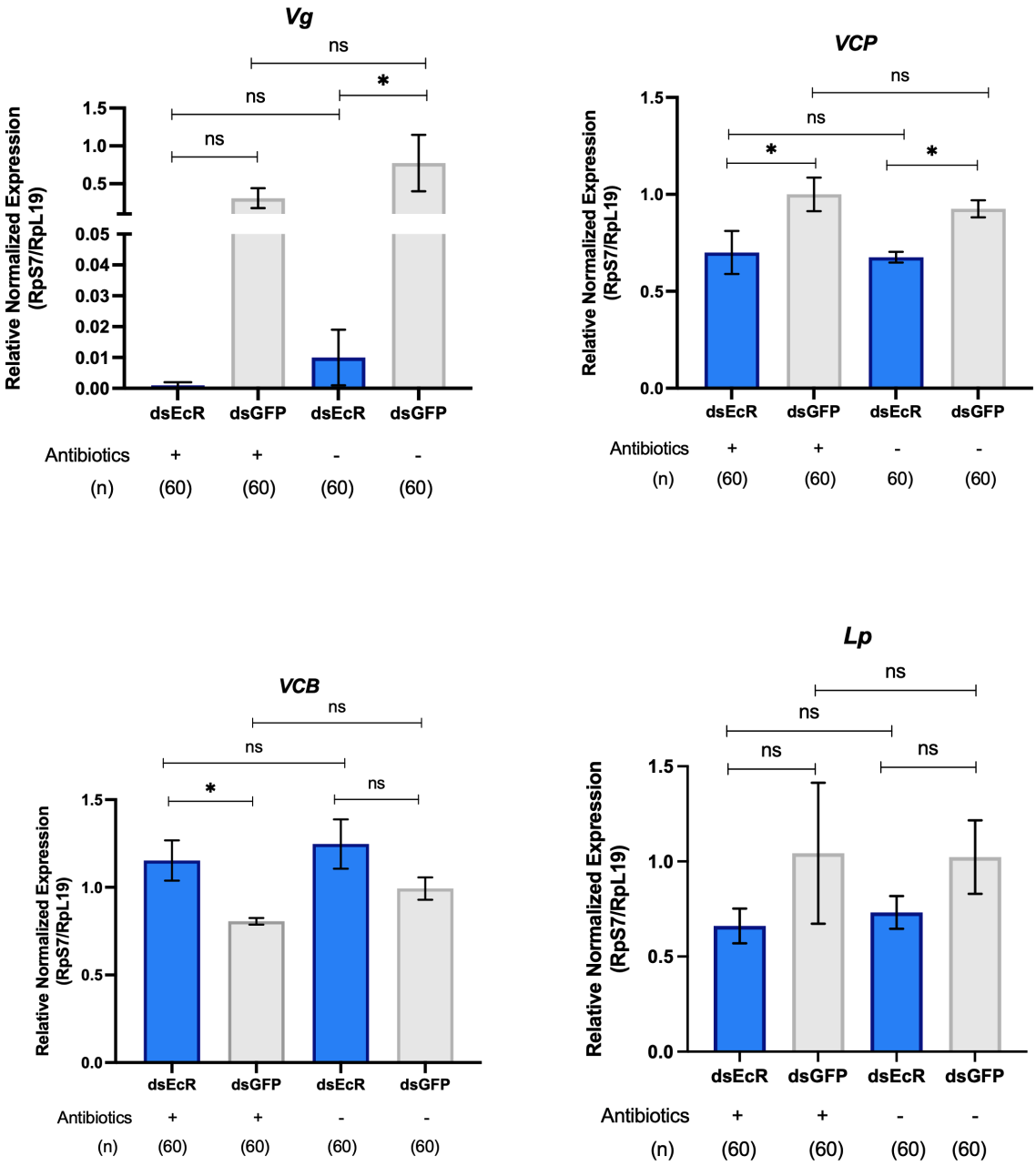

Figure 3.7: The ingestion of antibiotics does not influence how *EcR* regulates egg yolk genes expression. In this figure, the expression of four yolk genes after *EcR* silencing in aseptic and septic mosquitoes is presented. Each experiment was performed in three independent biological replicates. The RNE values of each gene were calculated with *RpL19* and *RpS7* as reference genes. Means RNE ± SEM are indicated on the y-axis. *p<0.05, ^{ns} not significant, *(n)* number of mosquitoes across all biological replicates.

The two-way ANOVA analysis of *VCP* also revealed that its expression is neither affected by the antibiotic treatment (antibiotics: F = 0.42485, df = 1, $p = 0.5328$), nor the interaction between the antibiotic and dsRNA treatments (interaction: F = 0.1106, df = 1, $p = 0.7480$). However, *EcR* silencing did affect *VCP* expression (dsRNA: F = 13.38, df = 1, $p = 0.0064$). To determine which specific groups were affected by dsRNA treatment, a *post hoc* Tukey analysis was conducted. The results showed that *EcR* depletion significantly affected *VCP* expression in both antibiotic-fed and sugar-fed mosquitoes. In the antibiotic cohort, dsEcR injection reduced *VCP* expression by 30% ($p = 0.0224$). In the non-antibiotic cohort, dsEcR injection reduced *VCP* expression by 25% ($p = 0.0466$) (Figure 3.7).

For *VCB*, the two-way ANOVA analysis demonstrated that its expression is neither affected by the antibiotic treatment (antibiotics: F = 2.102, df = 1, $p = 0.1851$), nor the interaction between the antibiotic and dsRNA treatments (interaction: F = 0.2303, df = 1, $p = 0.6442$). However, *EcR* silencing did affect *VCB* expression (dsRNA: F = 9.616, df = 1, $p = 0.0146$). To determine which specific groups were affected by dsRNA treatment, a *post hoc* Tukey analysis was conducted. The results revealed that *EcR* depletion only significantly affected *VCB* expression in antibiotic-fed mosquitoes. Indeed, in the sugar-fed cohort, dsEcR injection increased *VCB* expression by 35% ($p = 0.0351$), while it did not affect *VCB* expression in the septic cohort ($p = 0.1009$) (Figure 3.7).

Finally, *Lp* expression was neither affected by the antibiotic treatment (antibiotics: F = 0.01365, df = 1, $p = 0.9099$), *EcR* silencing (dsRNA: F = 2.377, df = 1, $p = 0.1617$), nor the interaction between these two treatments (interaction: F = 0.04345, df = 1, $p = 0.8401$). Consequently, the *post hoc* Tukey analysis was showed that *EcR* depletion did not affect *Lp* expression in both antibiotic-fed and sugar-fed mosquitoes ($p = 0.2510$ and $p = 0.3734$, respectively). Likewise, the antibiotic

treatment did not affect *Lp* expression in both dsEcR-injected and ds-GFP injected mosquitoes (p = 0.8239 and p = 0.9499, respectively) (Figure 3.7).

In order to further understand the link between the antibiotic, *EcR* signaling and the phenotypes analysed, the effectiveness of the antibiotics treatment and dsEcR injection were analysed using a subset (15 mosquitoes per biological replicate) of mosquitoes that were not used for phenotypic measurements. When the bacteria levels in aseptic and septic groups were compared after 4 days of antibiotic treatment, it was found that the Enterobacteria were reduced by 92% (on average) in the aseptic group relative to the septic group, while the total bacteria were reduced by 30% on average (Figure 3.8a). However, although the same dose and delivery method of antibiotics was used (as in section 3.3.1), the expression of the bacterial *16S* gene was not significantly reduced in this experiment ($p > 0.05$), due to the high variability between the biological replicates. This result suggested that the activity of the antibiotics had been reduced (Figure 3.8a). Indeed, the p-values for the statistical difference in *16S* RNE values between the antibiotic-fed and non-antibiotic groups for the Enterobacteriaceae and Eubacteria were 0.3360 and 0.3418 (unpaired t-test), respectively.

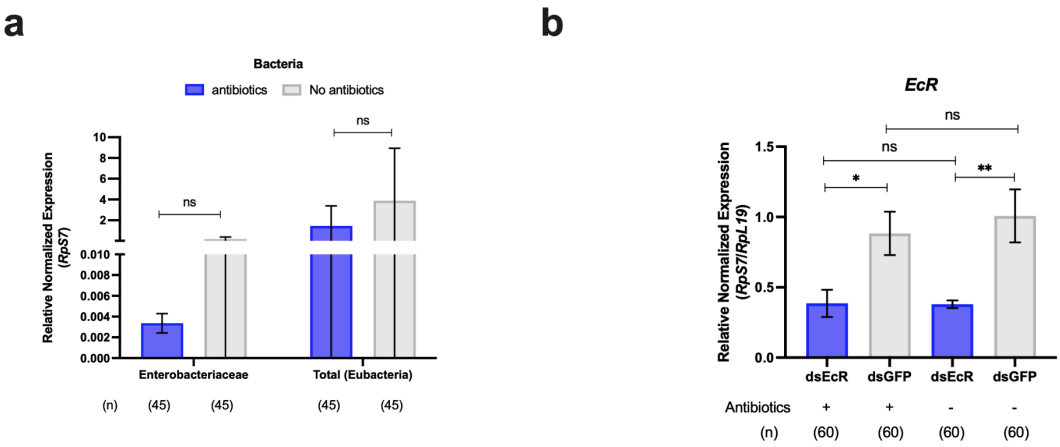

Figure 3.8: Influence of antibiotics on *EcR*-mediated regulation of fecundity. (**a**) Antibiotics treatment did not influence the gut bacteria number. (**b**) In both antibiotic-treated and untreated mosquitoes, *EcR* transcript abundance was significantly reduced. In (**a,b**) *n* represents the number of females or midguts in the experiment. All experiments were performed in 3 independent biological replicates. **p*<0.05, ***p*<0.01, ^{ns} not significant. Means RNE ± SEM are plotted.

EcR mRNA levels however were significantly affected by the dsRNA injection (Two-way ANOVA: F = 18.31, df =1, *p* = 0.0027), but not the antibiotic ingestion (Two-way ANOVA: F = 0.2011, df =1, *p* = 0.6658) (Figure 3.8b). Based on the results previously obtained showing that antibiotics ingestion decreases *EcR* expression (Figures 3.3a-b), this finding further suggests that the activity of the antibiotics could have been reduced. The *post hoc* analysis revealed that dsRNA injection significantly reduced *EcR* expression by 50% in the antibiotic-fed mosquitoes (*p* = 0.0283) and 63% in the non-antibiotic fed mosquitoes (*p* = 0.0096).

3.4 Discussion

In anautogenous mosquitoes, blood-feeding triggers several physiological changes, including a proliferation of the gut bacterial microbiome (Oliveira et al., 2011, Wang et

al., 2011, Xiao et al., 2017), and a boost in the 20E signaling pathway (Brown et al., 2020, Gabrieli et al., 2014, Mitchell et al., 2015, Raikhel et al., 2002, Roy et al., 2015), amongst others. Although both the gut bacterial microbiome and the 20E signaling pathway have previously been characterized as modulators of mosquito reproduction (Bryant and Raikhel, 2011, Coon et al., 2016, de O Gaio et al., 2011, Haouari-Abderrahim and Rehimi, 2014, Werling et al., 2019), whether these two modulators work in concert or independently has not been investigated, to my knowledge. Using RNAi to disturb the 20E signaling pathway by silencing *EcR*, in combination with oral administration of antibiotics (to reduce the gut bacterial load), it was demonstrated that in *An*. *arabiensis*, *EcR* transcript abundance and the gut bacterial abundance are linked. However, the *An. arabiensis* 20E signaling pathway that regulates fecundity and egg fertility is comparable in females that have or haven't ingested antibiotics.

This study presents the first experimental evidence that an antibiotic-fed anopheline species shows reduced *EcR* expression (Figure 3.3a-b). Though this is a novel finding in insects, previous studies in monkeys and humans had reported an association between steroid hormone levels and the gut microbiome (Colldén et al., 2019, Mallott et al., 2020). By using the DNeasy® PowerSoil® Pro kit (Qiagen) for microbial DNA extraction, the low DNA yield or reduced microbial diversity that is often associated with traditional extraction methods was mitigated (Gerasimidis et al., 2016, Henderson et al., 2013, Pollock et al., 2018).

Based on the link established between the gut bacterial abundance and *EcR* expression (Figures 3.3a-b), whether the gut bacteria and *EcR* work in concert to regulate *An. arabiensis* reproduction was investigated. In both antibiotic-fed and non-antibiotic fed mosquitoes, the impact of *EcR* silencing on oviposition and fertility was similar: no effect on fecundity, but a decrease in fertility (Figures 3.4-3.6). The effect of *EcR* silencing on fecundity and fertility have previously been discussed (section 2.4).

Thus, in the next paragraph, the focus will be on the effect of antibiotics on these phenotypes. Multiple factors can influence how antibiotics modulate mosquito fecundity and fertility in laboratory-based studies. One of these factors is the antibiotic cocktail used to generate aseptic mosquitoes. For example, *An. gambiae*'s egg production reportedly increases when the mosquitoes ingest a penicillin-streptomycin cocktail (Gendrin et al., 2015), but not when this cocktail is also supplemented with gentamicin (Ezemuoka et al., 2020). Consistent with the lack of effect on fecundity when *An. gambiae* ingested the gentamicin/penicillin-streptomycin cocktail (Ezemuoka et al., 2020), the results presented here showed that *An. arabiensis* fecundity is not affected by this antibiotic cocktail (Figures 3.4).

An increase in the egg fertility of both dsEcR-injected or dsGFP-injected antibiotic-fed mosquitoes was observed (Figure 3.6). Similarly, Ezemuoka et al. (2020) found that the same penicillin-streptomycin/gentamicin cocktail increased the fertility of eggs laid by *An. gambiae*. In the antibiotic-fed group, this increase in fertility could be linked with the *VCB* expression (Figure 3.7), but whether a change in YPP expression affects egg fertility should be further investigated.

In terms of the effect of the antibiotics/*EcR* silencing on YPP expression (Figure 3.7), the following observations can be made. *EcR* silencing decreased the expression of *Vg* in both the antibiotics and sugar-fed group, but this decrease was only significant in the sugar-fed group, suggesting that the gut microbiome is needed for *EcR* silencing to have an effect on *Vg* expression. Conversely, while *VCB* expression increased in both aseptic and septic groups, this increase was only significant in the aseptic group, suggesting that the effect of *EcR* knockdown on *VCB* expression requires a reduction of the gut bacteria. The remaining phenotypes measured (e.g., egg length, oviposition rate, ovary length) were not measured in *An. gambiae*, but based on the similarity between the two species, it is expected that the results would have been similar.

One limitation of this study however is that there is a possibility that antibiotics activity has been reduced (antibiotics shelf-life = 12 months), which may explain the high variability between biological replicates observed in Figures 3.8a. Indeed, although the experiment was performed before the antibiotic shelf life expired, the experiment in section 3.3.2 was conducted almost a year after that in section 3.3.1. This is in part due to COVID restrictions and therefore the antibiotics could have lost some of their activity by then. Hence in future, the results from this experiment (section 3.3.2) should be confirmed as soon as the antibiotics are received.

To conclude, *EcR* gene expression was significantly reduced in *An. arabiensis* females that were treated with antibiotics and had reduced gut bacteria. *EcR* silencing did not influence fecundity, but reduced eggs length-to-width ratio and fertility in antibiotic treated *An. arabiensis* females. Taken together with the results from chapter 2, these phenotypic changes occur after *EcR* silencing in the presence or "decreased presence" of gut bacteria. Finally, the gut bacteria are likely to be linked with *EcR* signaling and *Vg* and *VCB* gene expression in *An. arabiensis* females. However, this needs to be further confirmed with additional experiments

3.5 References

ALLWELL-BROWN, G., HUSSAIN-ALKHATEEB, L., KITUTU, F. E., STRÖMDAHL, S., MÅRTENSSON, A. & JOHANSSON, E. W. 2020. Trends in reported antibiotic use among children under 5 years of age with fever, diarrhoea, or

cough with fast or difficult breathing across low-income and middle-income countries in 2005–17: a systematic analysis of 132 national surveys from 73 countries. *Lancet Glob. Health,* 8**,** e799-e807.

BALDINI, F., GABRIELI, P., SOUTH, A., VALIM, C., MANCINI, F. & CATTERUCCIA, F. 2013. The interaction between a sexually transferred steroid hormone and a female protein regulates oogenesis in the malaria mosquito *Anopheles gambiae*. *PLoS Biol.,* 11**,** e1001695-e1001695.

BATES, S. T., BERG-LYONS, D., CAPORASO, J. G., WALTERS, W. A., KNIGHT, R. & FIERER, N. 2011. Examining the global distribution of dominant archaeal populations in soil. *The ISME Journal,* 5**,** 908-917.

BEACH, R. 1979. Mosquitoes: biting behavior inhibited by ecdysone. *Science,* 205**,** 829-831.

BECKER, N., PETRIC, D., ZGOMBA, M., BOASE, C., MADON, M., DAHL, C., et al. 2010. Biology of mosquitoes. *Mosquitoes and their control.* Second ed. Germany: Springer Science & Business Media.

BRIEGEL, H., LEA, A. O. & KLOWDEN, M. J. 1979. Hemoglobinometry as a method for measuring blood meal sizes of mosquitoes (Diptera: Culicidae). *J. Med. Entomol.,* 15**,** 235-238.

BROWN, F., PATON, D. G., CATTERUCCIA, F., RANSON, H. & INGHAM, V. A. 2020. A steroid hormone agonist reduces female fitness in insecticide-resistant *Anopheles* populations. *Insect Biochem. Mol. Biol.*

BRYANT, B., MACDONALD, W. & RAIKHEL, A. S. 2010. microRNA miR-275 is indispensable for blood digestion and egg development in the mosquito *Aedes aegypti*. *Proc. Natl. Acad. Sci. U. S. A.***,** 201016230-201016230.

BRYANT, B. & RAIKHEL, A. S. 2011. Programmed autophagy in the fat body of *Aedes aegypti* is required to maintain egg maturation cycles. *PLoS One,* 6**,** e25502-e25502.

CANSADO-UTRILLA, C., ZHAO, S. Y., MCCALL, P. J., COON, K. L. & HUGHES, G. L. 2021. The microbiome and mosquito vectorial capacity: rich potential for discovery and translation. *Microbiome,* 9**,** 1-11.

CAPORASO, J. G., LAUBER, C. L., WALTERS, W. A., BERG-LYONS, D., LOZUPONE, C. A., TURNBAUGH, P. J., et al. 2011. Global patterns of 16S rRNA diversity at a depth of millions of sequences per sample. *Proc. Natl. Acad. Sci. U. S. A.,* 108**,** 4516-4522.

CARRASQUILLA, M. C. & LOUNIBOS, L. P. 2015. Detection of insemination status in live *Aedes aegypti* females. *J. Insect Physiol.,* 75**,** 1-4.

CHOI, K. S., CHRISTIAN, R., NARDINI, L., WOOD, O. R., AGUBUZO, E., MULEBA, M., et al. 2014. Insecticide resistance and role in malaria transmission of *Anopheles funestus* populations from Zambia and Zimbabwe. *Parasit. Vectors,* 7**,** 1-8.

CLEMENTS, A. & STANLEY-SAMUELSON, D. W. 1994. The Biology of Mosquitoes, Volume 1: Development, Nutrition, and Reproduction. *J. Med. Entomol.,* 31**,** 181.

COLEMAN, J., JUHN, J. & JAMES, A. A. 2007. Dissection of midgut and salivary glands from *Ae. aegypti* mosquitoes. *JoVE (Journal of Visualized Experiments)***,** e228.

COLLDÉN, H., LANDIN, A., WALLENIUS, V., ELEBRING, E., FÄNDRIKS, L., NILSSON, M. E., et al. 2019. The gut microbiota is a major regulator of androgen metabolism in intestinal contents. *Am. J. Physiol. Endocrinol. Metab.,* 317**,** E1182-E1192.

-GARDUÑO J, RODRÍGUEZ MC, HERNÁNDEZ-MARTÍNEZ S, MARTÍNEZ-BARNETCHE J, ALVARADO-DELGADO A, IZQUIERDO J, et al.2015. *Plasmodium berghei i*nduced priming in *Anopheles albimanus* independently of bacterial co-infection. *Dev Comp Immunol*, 52(2):172-81.

COON, K. L., BROWN, M. R. & STRAND, M. R. 2016. Gut bacteria differentially affect egg production in the anautogenous mosquito *Aedes aegypti* and facultatively autogenous mosquito *Aedes atropalpus* (Diptera: Culicidae). *Parasit. Vectors,* 9**,** 375.

D'AMORE, R., IJAZ, U. Z., SCHIRMER, M., KENNY, J. G., GREGORY, R., DARBY, A. C., et al. 2016. A comprehensive benchmarking study of protocols and sequencing platforms for 16S rRNA community profiling. *BMC Genomics,* 17**,** 55.

DAHALAN, F. A. B. 2017. *Impact of mating on Anopheles coluzzii in response to infection.* PhD, Imperial College London.

DE O GAIO, A., GUSMÃO, D. S., SANTOS, A. V., BERBERT-MOLINA, M. A., PIMENTA, P. F. & LEMOS, F. J. 2011. Contribution of midgut bacteria to blood digestion and egg production in *Aedes aegypti* (Diptera: Culicidae)(L.). *Parasit. Vectors,* 4**,** 105.

EKOKA, E., MAHARAJ, S., NARDINI, L., DAHAN-MOSS, Y. & KOEKEMOER, L. L. 2021. 20-Hydroxyecdysone (20E) signaling as a promising target for the chemical control of malaria vectors. *Parasit. Vectors,* 14**,** 86.

E SILVA, B., MATSENA ZINGONI, Z., KOEKEMOER, L.L. AND DAHAN-MOSS, Y.L., 2021. Microbiota identified from preserved *Anopheles*. *Malar. J.l*, *20*(1), p.230

EZEMUOKA, L. C., AKORLI, E. A., ABOAGYE-ANTWI, F. & AKORLI, J. 2020. Mosquito midgut *Enterobacter cloacae* and *Serratia marcescens* affect the fitness of adult female *Anopheles gambiae* s.l. *PLoS One,* 15**,** e0238931.

FAULL, K. J., WEBB, C. & WILLIAMS, C. R. 2016. Desiccation survival time for eggs of a widespread and invasive Australian mosquito species, *Aedes* (Finlaya) *notoscriptus* (Skuse). *J. Vector Ecol.,* 41**,** 55-62.

GABRIELI, P., KAKANI, E. G., MITCHELL, S. N., MAMELI, E., WANT, E. J., ANTON, A. M., et al. 2014. Sexual transfer of the steroid hormone 20E induces the postmating switch in *Anopheles gambiae*. *Proc. Natl. Acad. Sci. U. S. A.,* 111**,** 16353-16358.

GENDRIN, M., RODGERS, F. H., YERBANGA, R. S., OUÉDRAOGO, J. B., BASÁÑEZ, M.-G., COHUET, A., et al. 2015. Antibiotics in ingested human blood affect the mosquito microbiota and capacity to transmit malaria. *Nat. Commun.,* 6**,** 1-7.

GERASIMIDIS, K., BERTZ, M., QUINCE, C., BRUNNER, K., BRUCE, A., COMBET, E., et al. 2016. The effect of DNA extraction methodology on gut microbiota research applications. *BMC Res. Notes,* 9**,** 365.

HAOUARI-ABDERRAHIM, J. & REHIMI, N. 2014. Biological and reproduction activities of mosquito larvae of *Culiseta morsitans* (Theobald) after treatment by Ecdysone agonist Methoxyfenozide. *Ann. Res. Rev. Biol***,** 4152-4165.

HENDERSON, G., COX, F., KITTELMANN, S., MIRI, V. H., ZETHOF, M., NOEL, S. J., et al. 2013. Effect of DNA extraction methods and sampling techniques on the apparent structure of cow and sheep rumen microbial communities. *PLoS One,* 8.

HERMANN-BANK, M. L., SKOVGAARD, K., STOCKMARR, A., LARSEN, N. & MØLBAK, L. 2013. The Gut Microbiotassay: a high-throughput qPCR approach combinable with next generation sequencing to study gut microbial diversity. *BMC Genomics,* 14**,** 1-14.

HERNÁNDEZ, M., DUMONT, M. G., YUAN, Q. & CONRAD, R. 2015. Different bacterial populations associated with the roots and rhizosphere of rice incorporate plant-derived carbon. *Appl. Environ. Microbiol.,* 81**,** 2244-2253.

HOU, Y., WANG, X.-L., SAHA, T. T., ROY, S., ZHAO, B., RAIKHEL, A. S., et al. 2015. Temporal coordination of carbohydrate metabolism during mosquito reproduction. *PLoS Genet.,* 11**,** e1005309-e1005309.

LUCAS, K. J., ZHAO, B., ROY, S., GERVAISE, A. L. & RAIKHEL, A. S. 2015. Mosquito-specific microRNA-1890 targets the juvenile hormone-regulated serine protease JHA15 in the female mosquito gut. *RNA Biol.,* 12**,** 1383-1390.

MALLOTT, E. K., BORRIES, C., KOENIG, A., AMATO, K. R. & LU, A. 2020. Reproductive hormones mediate changes in the gut microbiome during pregnancy and lactation in Phayre's leaf monkeys. *Sci. Rep.,* 10**,** 9961.

MEADOWS, K. E. 1968. A simple method of mosquito ovary dissection. *Fla. Entomol.***,** 31-35.

MEKURIAW, W., BALKEW, M., MESSENGER, L. A., YEWHALAW, D., WOYESSA, A. & MASSEBO, F. 2019. The effect of ivermectin® on fertility, fecundity and mortality of *Anopheles arabiensis* fed on treated men in Ethiopia. *Malar. J.,* 18**,** 357.

MITCHELL, S. N., KAKANI, E. G., SOUTH, A., HOWELL, P. I., WATERHOUSE, R. M. & CATTERUCCIA, F. 2015. Evolution of sexual traits influencing vectorial capacity in anopheline mosquitoes. *Science,* 347**,** 985-988.

OGUNRINADE, A. 1980. The measurement of blood meal size in *Aedes aegypti* (L.). *Afr. J. Med. Med. Sci.,* 9**,** 69-71.

OLIVEIRA, J. H. M., GONÇALVES, R. L., LARA, F. A., DIAS, F. A., GANDARA, A. C. P., MENNA-BARRETO, R. F., et al. 2011. Blood meal-derived heme decreases

ROS levels in the midgut of *Aedes aegypti* and allows proliferation of intestinal microbiota. *PLoS Pathog.,* 7.

PICHLER, M., COSKUN, Ö. K., ORTEGA-ARBULÚ, A.-S., CONCI, N., WÖRHEIDE, G., VARGAS, S., et al. 2018. A 16S rRNA gene sequencing and analysis protocol for the Illumina MiniSeq platform. *MicrobiologyOpen,* 7**,** e00611.

POLLOCK, J., GLENDINNING, L., WISEDCHANWET, T. & WATSON, M. 2018. The madness of microbiome: attempting to find consensus “best practice” for 16S microbiome studies. *Appl. Environ. Microbiol.,* 84**,** e02627-02617.

PONDEVILLE, E., MARIA, A., JACQUES, J.-C., BOURGOUIN, C. & DAUPHIN-VILLEMANT, C. 2008. *Anopheles gambiae* males produce and transfer the vitellogenic steroid hormone 20-hydroxyecdysone to females during mating. *Proc. Natl. Acad. Sci. U. S. A.,* 105**,** 19631-19636.

QUINCE, C., WALKER, A. W., SIMPSON, J. T., LOMAN, N. J. & SEGATA, N. 2017. Shotgun metagenomics, from sampling to analysis. *Nat. Biotechnol.,* 35**,** 833-844.

RAIKHEL, A. S., KOKOZA, V. A., ZHU, J., MARTIN, D., WANG, S.-F., LI, C., et al. 2002. Molecular biology of mosquito vitellogenesis: from basic studies to genetic engineering of antipathogen immunity. *Insect Biochem. Mol. Biol.,* 32**,** 1275-1286.

RODGERS, F. H., GENDRIN, M., WYER, C. A. & CHRISTOPHIDES, G. K. 2017. Microbiota-induced peritrophic matrix regulates midgut homeostasis and prevents systemic infection of malaria vector mosquitoes. *PLoS Pathog.,* 13**,** e1006391.

ROY, S., SAHA, T. T., JOHNSON, L., ZHAO, B., HA, J., WHITE, K. P., et al. 2015. Regulation of gene expression patterns in mosquito reproduction. *PLoS Genet.,* 11**,** e1005450-e1005450.

ROY, S., SAHA, T. T., ZOU, Z. & RAIKHEL, A. S. 2017. Regulatory Pathways Controlling Female Insect Reproduction. *Annu. Rev. Entomol.*

ROY, S., SMYKAL, V., JOHNSON, L., SAHA, T. T., ZOU, Z. & RAIKHEL, A. S. 2016. Regulation of reproductive processes in female mosquitoes. Elsevier.

SCARAFFIA, P. Y. 2016. Disruption of mosquito blood meal protein metabolism. Elsevier.

SHAW, W. R. & CATTERUCCIA, F. 2018. Vector biology meets disease control: Using basic research to fight vector-borne diseases. *Nat. Microbiol.*, 1-1.

SMITH, A., SHIMADA, T. & RASKIN, L. 2017. A comparative evaluation of community structure in full-scale digesters indicates that two-phase digesters exhibit greater microbial diversity than single-phase digesters. *Environ. Sci. (Camb.),* 3, 304-311.

SOTA, T. & MOGI, M. 1992. Interspecific variation in desiccation survival time of *Aedes* (Stegomyia) mosquito eggs is correlated with habitat and egg size. *Oecologia,* 90, 353-358.

STRAND, M. R. 2018. Composition and functional roles of the gut microbiota in mosquitoes. *Curr. Opin. Insect.,* 28, 59-65.

STRAUB, T. J., SHAW, W. R., MARCENAC, P., SAWADOGO, S. P., DABIRÉ, R. K., DIABATÉ, A., et al. 2020. The *Anopheles coluzzii* microbiome and its interaction with the intracellular parasite *Wolbachia*. *Sci. Rep.,* 10.

SULIS, G., DANIELS, B., KWAN, A., GANDRA, S., DAFTARY, A., DAS, J., et al. 2020. Antibiotic overuse in the primary health care setting: a secondary data analysis of standardised patient studies from India, China and Kenya. *BMJ Glob. Health,* 5, e003393.

WANG, X., HOU, Y., SAHA, T. T., PEI, G., RAIKHEL, A. S. & ZOU, Z. 2017. Hormone and receptor interplay in the regulation of mosquito lipid metabolism. *Proc. Natl. Acad. Sci. U. S. A.*, 201619326-201619326.

WANG, Y., GILBREATH III, T. M., KUKUTLA, P., YAN, G. & XU, J. 2011. Dynamic gut microbiome across life history of the malaria mosquito *Anopheles gambiae* in Kenya. *PLoS One,* 6.

WERLING, K., SHAW, W. R., ITOE, M. A., WESTERVELT, K. A., MARCENAC, P., PATON, D. G., et al. 2019. Steroid Hormone Function Controls Non-competitive *Plasmodium* Development in *Anopheles*. *Cell,* 177**,** 315-325.

WILKINSON, A., EBATA, A. & MACGREGOR, H. 2018. Interventions to Reduce Antibiotic Prescribing in LMICs: A Scoping Review of Evidence from Human and Animal Health Systems. *Antibiotics (Basel, Switzerland),* 8**,** 2.

XIAO, X., YANG, L., PANG, X., ZHANG, R., ZHU, Y., WANG, P., et al. 2017. A Mesh–Duox pathway regulates homeostasis in the insect gut. *Nat. Microbiol.,* 2**,** 17020.

ZHANG, X. & RAIKHEL, A. S. 2020. Hormonal regulation of microRNA expression dynamics in the gut of the yellow fever mosquito *Aedes aegypti*. *RNA Biol.***,** 1-10.

CHAPTER 4

The 20-hydroxyecdysone signaling pathway regulates *Anopheles arabiensis* gut bacterial microbiome homeostasis via the Imd pathway

4.1 Introduction

While blood-feeding on a vertebrate host, mosquitoes ingest several pathogens, including bacteria (Muturi et al., 2019, Muturi et al., 2021). Besides, several anopheline female tissues (e.g., the gut, salivary glands, and ovaries) are inhabited by commensal bacteria. These latter constitute the mosquito bacterial microbiome (Tchioffo et al., 2016). To prevent the uncontrolled proliferation of these bacteria to levels that compromise its survival, the mosquito deploys multiple innate immune responses which are either mediated by the Immune deficiency (Imd) pathway, the Toll pathway, or the Janus kinase-signal transducer and activator of transcription (Jak-STAT) pathway (Gabrieli et al., 2021, Kumar et al., 2018, Meister et al., 2005, Zakovic and Levashina, 2017). Of these, the Imd pathway plays an essential role in mosquitoes anti-bacterial immune responses (Barletta et al., 2017, Russell et al., 2021). The sequence of events that lead to the Imd pathway-mediated activation of mosquitoes immune defenses can be summarized into four phases (indicated as white numbers within green octagons, Figure 4.1).

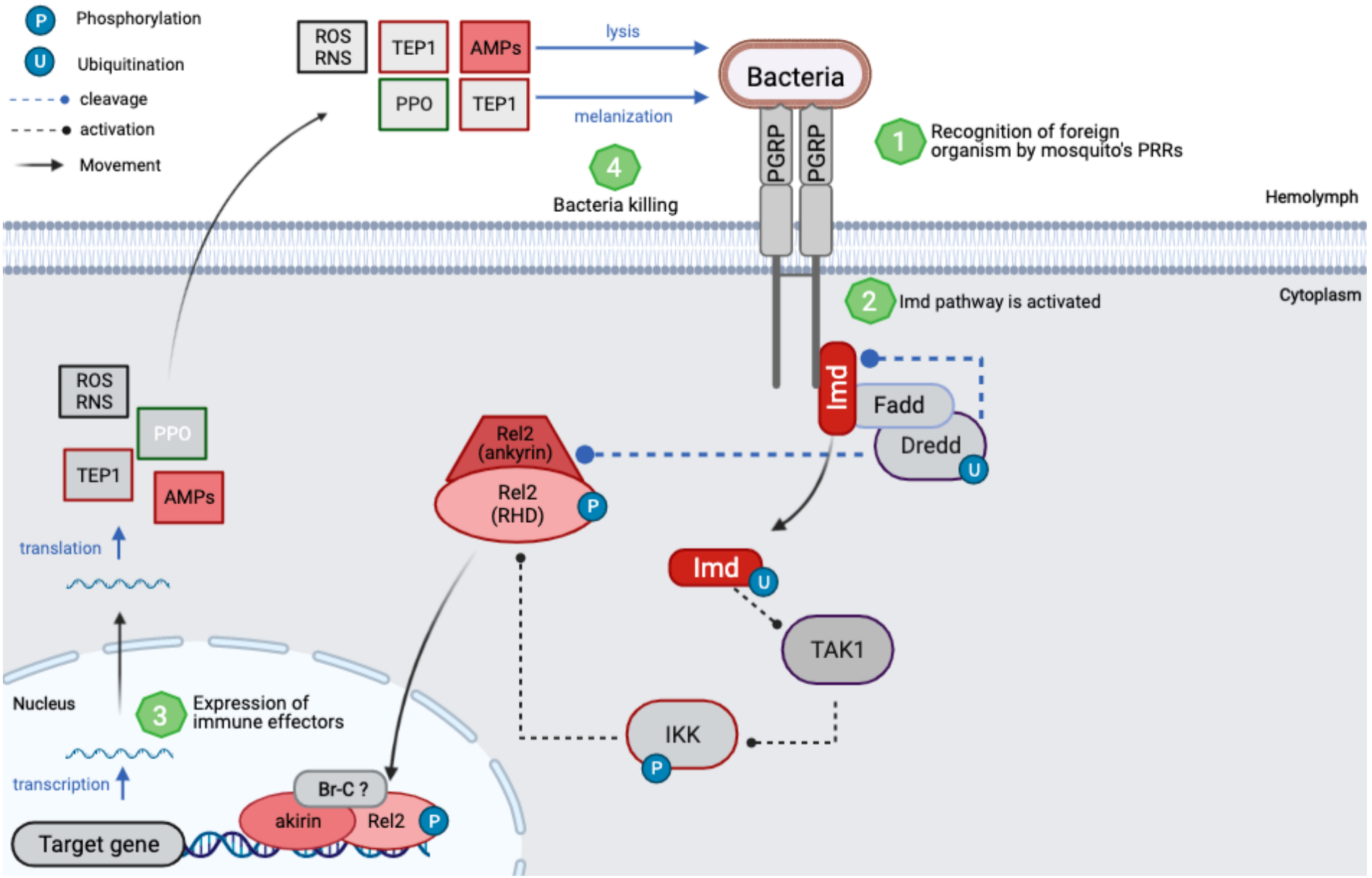
Phosphorylation
Ubiquitination
cleavage
activation
Movement
ROS
RNS
TEP1
AMPs
PPO
TEP1
lysis
melanization
Bacteria
4
Bacteria killing
PGRP
PGRP
1
Recognition of foreign organism by mosquito's PRRs
Hemolymph
Cytoplasm
2
Imd pathway is activated
Imd
Fadd
Dredd
U
Rel2 (ankyrin)
Rel2 (RHD)
P
Imd
U
TAK1
IKK
P
ROS
RNS
PPO
TEP1
AMPs
translation
Nucleus
3
Expression of immune effectors
transcription
Br-C ?
akirin
Rel2
P
Target gene

Figure 4.1: *Anopheles* females anti-bacterial immune responses mediated by the Immune deficiency (Imd) pathway [created with information from (Kumar et al., 2018, Rodgers et al., 2017, Russell et al., 2021, Wang et al., 2019, Zakovic and Levashina, 2017, Zhang et al., 2021)]. The proteins displayed in *shades of red* are relevant to this study. The question mark (?) next to Br-C indicated that this interaction has been hypothesized based on co-immunoprecipitation experiments in *Drosophila*, but not yet confirmed in mosquitoes. Details about each phase is provided in the text. Abbreviations: PGRP, peptidoglycan recognition protein; Imd, Immune deficiency; Fadd, Fas Associated Via Death Domain; Dredd, Death related ced-3/Nedd2-like caspase; TAK1 , Transforming growth factor ß-activated kinase 1; IKK, IκB kinase; Rel2, relish 2; RHD, Rel homology domain; AMP, antimicrobial peptide; TEP1, thioester-containing protein 1; PPO, prophenol oxidase; ROS, reactive oxygen species; RNS, reactive nitrogen species; Br-C, Broad Complex; PRR, Pattern recognition receptor.

In the first phase, mosquitoes need to recognize that foreign organisms have invaded their tissues. *Anopheles* pattern recognition receptors (PRRs) achieve this step by recognizing and binding to the pathogen-associated molecular patterns (PAMPs) on the foreign microbes (Kumar et al., 2018, Zakovic and Levashina, 2017, Zhang et al., 2021). Bacteria most characterized PAMP is their cell wall peptidoglycan polymer, which is recognized by a mosquito PRR family known as peptidoglycan recognition proteins or PGRPs (Das et al., 2009, Dong et al., 2009, Gendrin et al., 2017, Meister et al., 2009) (Figure 4.1).

The binding of bacteria peptidoglycan to mosquitoes PGRP initiates the second phase, which is the activation of two immune signaling pathways: the Toll and Immune deficiency (Imd) pathways (Kumar et al., 2018, Meister et al., 2005, Zakovic and Levashina, 2017). Since the Imd pathway is the focus of this chapter, it will be discussed further. Most of the knowledge on insects Imd pathway stems from studies in *D. melanogaster*. Nonetheless, orthologues of *Drosophila* Imd-related proteins have been identified in *An. gambiae* genome (Rodgers et al., 2017), suggesting that the Imd pathway is conserved between the two insects. After recognizing the bacterial invader, Imd binds to PGRP, and this complex recruits two more proteins, namely the

Fas Associated Via Death Domain (Fadd) and the Death related ced-3/Nedd2-like caspase (Dredd) (Figure 4.1). After being ubiquitinated, Dredd cleaves off Imd, and this latter can now also be ubiquitinated. This post-translational modification (ubiquitination) activates the Transforming growth factor ß-activated kinase 1 (TAK1) protein, which in turn activates the IκB kinase (IKK) protein by phosphorylation (Figure 4.1). IKK can now phosphorylate relish 2 (Rel2), a protein consisting of 2 domains: the ankyrin domain and the Rel homology domain (RHD). Rel2 phosphorylation acts as a signal for Dredd to cleave off its ankyrin domain (Figure 4.1).

Phase 3 is initiated after Rel2 remaining RHD domain translocates to the nucleus and binds to akirin (Figure 4.1). The Rel2/akirin complex acts as a transcription factor that induces the expression of immune effector proteins. Examples of such effector proteins include antimicrobial peptides (AMPs), reactive oxygen species (ROS), reactive nitrogen species (RNS), thioester-containing protein 1 (TEP1), and prophenol oxidases (PPOs). Finally, in phase 4, the immune effector molecules produced earlier (phase 3) kill the invading bacteria by lysis or melanization. Specifically, lysis is induced by TEP1, AMPs, and ROS/RNS, while PPO and TEP1 activate melanization (Figure 4.1). AMPs are discussed further below due to their relevance to the study.

AMPs are small (7-100 amino acids) cationic peptides secreted by the fat body or hemocytes (reviewed in Mylonakis et al., 2016, Torrent et al., 2012, Yi et al., 2014). In adult mosquitoes, at least 17 AMPs have been reported. Their expression has been detected in different tissues such as the midgut, fat body, salivary glands, and hemolymph (Contreras-Garduño et al., 2015, Tian et al., 2010, Vizioli et al., 2000, Xiao et al., 2014). Furthermore, AMPs are constitutively expressed in these tissues to maintain a basal level of immunity, but their expression increases upon pathogen challenge (Contreras-Garduño et al., 2015, Dong et al., 2009, Tian et al., 2010, Vizioli

et al., 2000, Vizioli et al., 2001a, Vizioli et al., 2001b, Xiao et al., 2014). Depending on the bacterial challenge, the Imd pathway induces at least five *An. gambiae* AMPs: *cecropin-1*, *cecropin-3*, *gambicin-1*, *defensin-1*, and *attacin-c* (Table 4.1).

Table 4.1: Anti-bacterial activities of five Imd-induced antimicrobial peptides in mosquitoes [compiled with information from (Bai et al., 2019, Eappen et al., 2013, Kaushal et al., 2016, Li et al., 2020, Magalhaes et al., 2010, Meister et al., 2005, Ramirez et al., 2019, Vizioli et al., 2000, Vizioli et al., 2001a, Vizioli et al., 2001b, Warr et al., 2008)].

	Gram-positive (Mosquito species)	**Gram-negative** (Mosquito species)	**Induced by Imd and/or Toll**
Defensin-1	***Bacillus* spp.** (*An. gambiae*)	***Asaia*** (*An. stephensi*, *An. gambiae*)	Imd (*Ae. aegypti*)
	***Enterococcus* spp.** (*An. gambiae*)	***Wolbachia*** (*Ae. aegypti*)	
	***Staphylococcus* spp.** (*An. gambiae*)	***E. coli*** (*An. gambiae, Ae. aegypti*)	
	M. luteus (*An. gambiae*)	***Se. marcescens*** (*An. sinensis*, *An. stephensi*)	
Cecropin-1[a]	***S aureus*** (*An. gambiae*)	***Asaia*** (*An. stephensi*, *An. gambiae*)	Imd (*Ae. aegypti*, *An. gambiae)*
		E. coli (*Ae. aegypti*, *Ae. albopictus*)	
		Se. marcescens (*An. sinensis*, *An. stephensi*)	
		F. novicida (*Ae. albopictus*)	
Cecropin-3[a]	***S aureus*** (*An. gambiae*)	***E. coli*** (*Ae. aegypti, An. gambiae*)	Imd (*An. gambiae)*
Gambicin-1	***M. luteus*, *B. subtilis*, and *S. aureus*** (*An. stephensi*)	***E. coli*** (*An. gambiae, Ae. aegypti, An. coluzzii*)	Imd and Toll (*Ae. aegypti, An. gambiae*)
		E. cloacae*, *Sa. typhimurium*, *Se. marcescens, Ps. Aeruginosa (*An. stephensi*)	
		Se. marcescens (*An. sinensis*)	
Attacin-c	n/d	n/d	Imd and Toll (*Ae. aegypti*)

n/d = not determined = no information found in mosquitoes literature
[a] Induced by 20E in mosquitoes

While the types of anti-bacterial activities of multiple AMPs has been investigated in mosquitoes (Table 4.1), their hormonal regulation —especially by 20E— is still poorly understood, despite the evidence that disturbing the 20E signaling regulates some of these AMPs (Table 4.2). In addition, the experiments conducted to investigate how the 20E signaling pathway regulates AMP production in mosquitoes revealed that several parameters could influence this regulation, including the anopheline species, the 20E pathway manipulation, the meal type —blood versus sugar, the 20E or dsEcR dose, the time at which AMP expression is measured, and the tissue in which AMP expression is measured (Table 4.2). In addition, studies in the fruitfly *Drosophila melanogaster* indicate that disturbing the 20E signaling pathway only affects AMPs expression if the manipulation was followed by a pathogen (e.g. bacteria or bacteria peptidoglycan) challenge (Table S7). Moreover, while the Imd pathway is known to regulate AMP production in mosquitoes (Figure 4.1), the experimental evidence that 20E signaling regulates the Imd pathway is still lacking.

Table 4.2: Manipulating the 20E signaling pathway affects AMPs expression in mosquitoes and fruitflies. Abbreviations: cec-1 = cecropin-1, cec-3 = cecropin-3, def-1 = defensin-1.

Mosquito species	*An. gambiae*	*An. gambiae*	*An. gambiae*	*An. coluzzii*	*D. melanogaster*
Blood feeding	Yes	No	No	No	N/A
20E pathway manipulation	**dsEcR** (690 ng per mosquito)	**20E** (500 ng per mosquito)	**20E** (500 ng per mosquito)	**20E** (2,500 ng per mosquito))	**20E** (1 µg/ml)
Immune challenge	No	No	No	No	No
Differentially expressed AMPs	None of the AMPs tested (*def-1*, *cec-1*)	*cec-1* *cec-3*	*cec-1* *cec-3*	No AMP	*cec-1, attacin-c, diptericin, drosocin*
Technique for gene expression	qPCR	RNA-seq	qPCR	RNA-seq	qPCR
Time at which gene expression was measured	48 hpi	24 hpi	24 hpi	24 hpi	13 time points (15 min to 6 hpi)
Tissue	Gut Fat body	Sua 4.0 cells	Whole mosquito	Gut	Malpighian tubules
References	Werling, 2020	Reynolds et al., 2020	Reynolds et al., 2020	Dahalan et al., 2019	Verma and Tapadia, 2015

In this chapter, the relationship between the 20E signaling pathway, the Imd pathway and AMP production was investigated. For this purpose, the 20E signaling pathway was disturbed (either by 20E injection or *EcR* depletion) and the effect on the expression of selected immune genes was assessed with qPCR. These included AMPs (*cecropin-1*, *cecropin-3*, *defensin-1*, *attacin-c*, and *gambicin-1*) and key genes of the Imd pathway (*Imd*, *Rel2*, and *akirin*). In addition, the expression of two extra immune genes —*mesh* and *duox*— was also measured to determine whether other non-Imd linked immune defenses, are also regulated by the Imd pathway. The mesh-duox pathway has previously been implicated in anti-bacterial immune defenses, since *mesh* depletion results in the proliferation of the microbiome (Xiao et al., 2017). In addition, *mesh* induces the expression of *duox*, and this latter activates the production of ROS and TEP1 in *An. gambiae* and *Ae. aegypti* (Kakani et al., 2019, Kumar et al., 2010). For the 10 genes selected, their expression was measured in the gut tissues, the carcass tissues, and the whole mosquito (after disturbing the 20E signaling pathway), since the tissue may influence how 20E regulates immune gene expression (Tables 4.2, S7). Moreover, in 20E injection experiments, the expression of the 10 selected immune genes was measured at different time points, based on the knowledge that the time elapsed since the manipulation of the 20E pathway may affect whether a change in immune gene expression is detected (Tables 4.2, S7). Finally, because the AMPs selected can target Gram-negative and/or Gram-positive bacteria, a decision was taken to determine if both bacterial types influence *EcR* expression. Therefore, *E. coli* (Gram-negative) and *S. aureus* (Gram-positive) bacteria were injected into mosquitoes, and *EcR* expression was measured at different time points thereafter.

4.2 Materials and Methods

4.2.1 Ethics statement, mosquito rearing, and bacterial cultures

The procedures used in this study were approved by the animal research ethics committee as mentioned earlier (section 2.2.1) and *An. arabiensis* mosquitoes were reared as described previously (section 2.2.2). *Escherichia coli* cultures were obtained from Dr Betty Maepa (Antiviral Gene Therapy Unit, University of the Witwatersrand). The *Staphylococcus aureus* culture was received from Dr Angela Botes (Department of Microbiology, University of the Witwatersrand, South Africa).

4.2.2 RNA purifications, cDNA synthesis, and qPCR

Total RNA was purified as described earlier (section 2.2.4), while gene expression analyses were carried out using the protocol outlined in section 2.2.8. The primers optimized in chapter 2 (Table 2.1) were also used here. *RpL19* and *RpS7* were used as reference genes. Additional primers targeting selected immune genes were designed (section 4.2.3).

4.2.3 Gene-specific primer design

Primers were designed to amplify ten immune genes according to the method described earlier (section 2.2.3). These included five AMP genes (*attacin-c*, *defensin-1*, *cecropin-1*, *cecropin-3,* and *gambicin-1*), three Imd pathway-related genes (*Imd*, *Rel2*, and *akirin*), and finally, two non-AMP genes (*mesh* and *duox*). The final primer sequences are outlined below (Tables 4.3, S1). All primers were validated by measuring their qPCR efficiencies (Table S2) and ensuring that a single amplicon of the correct size and sequence was obtained during amplification (Table S4, Figure S4).

Table 4.3: List of qPCR primers designed in this study.

	Forward (5'---> 3')	Reverse (5'---> 3')	Amplicon size (bp)
Cec-1	GTTAAGGCGCTCGGTTAG	CCTCTCTCTCTCTCTCTGC	98
Cec-3	GAACTTCACCAAGCTGTTCATC	CACATTACGTCCGAGCTTCT	124
Gamb-1	GGACAGACGACCATCAATAG	CAGAGCTCCACTCACAAG	98
Def-1	GCGGTGCCAATCTCAATA	CTTGGCCCGATAGTTCTC	80
Att	CTAGCTACACGCAGCATT	CAGTAACCGTGCGAGAAA	85
Imd	CCACACTGGCTGAGCAAATA	GTTCCACAACAACGTCACAAG	95
Rel2	CGATCAGAGTGCTGCCTATAC	TGCTGCTGCTGCTGATAA	96
Akirin	TGCTGAAAGAACGAGAGGATG	CGTCTCTGTATTTGGTCGTATGT	115
Mesh	GACGAGGGCAAGGATAAGAAG	TCATTGGATCTTCCCAGTTGTAG	100
Duox	TCGTTGGATGGTGAGGTTATG	CCTTGTCCTTGTCGACGATATT	130

Abbreviations: Cec-1 = Cecropin-1; Cec-3 = Cecropin-3; Gamb-1 = Gambicin-1; Def-1 = Defensin-1; Att = Attacin-c; Imd = Immune Deficiency-1, Rel2 = Relish 2.

4.2.4 Preparation and injection of 20E

A 20-hydroxyecdysone (20E) stock solution was prepared by dissolving 20E (cat no: H5142-25MG, Sigma-Aldrich) into 2 ml of 100% ethanol to obtain a concentration of 10 mg/ml. Before use, this stock solution was diluted 1:10 in 1x PBS to make 1 mg/ml (i.e., 1 ng/nl) working aliquots. For experiments, 3-days old cold-anesthetized females were injected intrathoracically with 69 nl of the working aliquots (i.e., 69 ng of 20E per mosquito) using the Nanoject II (Drummond). The negative control mosquitoes were injected with 69 nl of 100% ethanol diluted 1:10 in 1x PBS. All procedures were performed with sterile (autoclaved) 1x PBS. After injection, the surviving mosquitoes

were kept in the insectary under standard rearing conditions until RNA extraction at 1, 3, 9, 12, and 24 hours post-injection (hpi).

4.2.5 Immune challenge with heat-inactivated bacteria

Both *E. coli* and *S. aureus* were grown overnight in a shaking incubator in 5 ml Luria-Broth medium (cat no: L3397, Sigma-Aldrich) until reaching an optical density (OD_{600}) of 0.406 (*E. coli*) or 0.601 (*S. aureus*). At this point, the bacteria were heat-inactivated by incubation at 70˚C for 30 min (as in Kessel et al., 2020), then pelleted by centrifugation (10,000xg for 10 min). The bacterial pellet was washed twice in sterile 1x PBS (each 10,000xg for 10 min) and resuspended in 5 ml of sterile 1x PBS. The final bacterial concentrations were $2x10^8$ CFU/ml for either *E. coli* or *S. aureus*. Before injections, the bacteria were diluted 1:10 in sterile 1x PBS, and 69 nl of this dilution (i.e., 1,380 CFU) was injected into the thorax of cold-anesthetized virgin female mosquitoes (n=100) with the Nanoject II (Drummond). Negative control mosquitoes (n=100) were injected with 1x PBS. There was a typical 20%-40% mortality after injection in each group. After injection, a portion of the surviving mosquitoes (n=15 mosquitoes per biological replicate) were kept in the insectary until RNA extraction at 6, 12, 18, and 24 hpi.

4.2.6 Effect of *EcR* knockdown on tissue-specific immune gene expression

To investigate how *EcR* knockdown impacted immune genes expression in the gut and carcass (i.e., remaining tissues after removing the gut), we injected 3-day old mosquitoes with either dsEcR or dsGFP to induce RNAi (n=100 injected mosquitoes per group), as previously described (section 2.2.9). Two days later, a portion of the surviving mosquitoes (n=15 mosquitoes per biological replicate) were dissected in PBS to separate their guts from their carcass (see section 3.2.2 for protocol). All tissues

were kept in TRIzol™ reagent (cat no: 15596026, Thermo Scientific) at -80˚C until RNA purifications and cDNA synthesis. One microliter of either cDNAs samples (from gut or carcass tissues) was then used as a template in qPCR experiments to measure selected immune genes expression (sections 4.2.2-4.2.3).

4.2.7 Data analysis

qPCR data analysis

All the qPCR data were analysed as described in chapter 3 (section 3.2.5)

Statistical analysis

All experiments were performed in 2-3 independent biological replicates (see figure legends), and the means ± SEM are displayed. Statistical analyses were performed with GraphPad Prism v.9.1.0 (GraphPad Inc, USA) with details specified in figures legends. No test for data normalization was performed, and as such, Gaussian distribution was assumed in all cases unless indicated otherwise. For this reason, parametric statistical methods were selected. The choice for a specific statistical test was explained previously (section 3.2.5). Unless indicated otherwise, statistical significance was assessed by setting a *p*-value cutoff of 0.05 so that all values below this cutoff would be considered statistically significant.

4.3 Results

Notes:
(1) All the raw data are presented in Appendix 4
(2) Each time the term "expression" or "level" or "abundance" is used (when referring to a transcript/mRNA), it means the RNE values.

4.3.1 Effect of *EcR* depletion on tissue-specific immune gene expression

To investigate whether the 20E signaling pathway regulates the gut bacterial microbiome by modulating AMP expression via the Imd pathway, the expression of ten immune genes was measured in the gut and carcass (i.e., whole mosquito minus the gut) of dsEcR-injected mosquitoes. These immune genes included five AMPs, three Imd pathway-related genes, as well as two non-AMP genes (Table 4.3).

In the midgut, dsEcR injection depleted *EcR* levels, as indicated by its mRNA expression that was significantly reduced (unpaired *t*-test: $p = 0.0298$) by 63% (Figure 4.2). Following *EcR* depletion, only two of the selected genes were significantly differentially expressed. These included *cecropin-3* which was down-regulated by 51% (unpaired *t*-test: $p = 0.0189$), and *attacin-c* which was up-regulated by 21% (unpaired *t*-test: $p = 0.0020$) (Figure 4.2). In contrast, the expression of the remaining genes was unaffected, as indicated by the unpaired *t*-test *p*-values of 0.4754 (*cec-1*), 0.7498 (*gamb-1*), 0.0670 (*def-1*), 0.2669 (*duox*), 0.4629 (*mesh*), 0.7622 (*Imd*), 0.4319 (*rel2*), and 0.8458 (*akr*) (Figure 4.2).

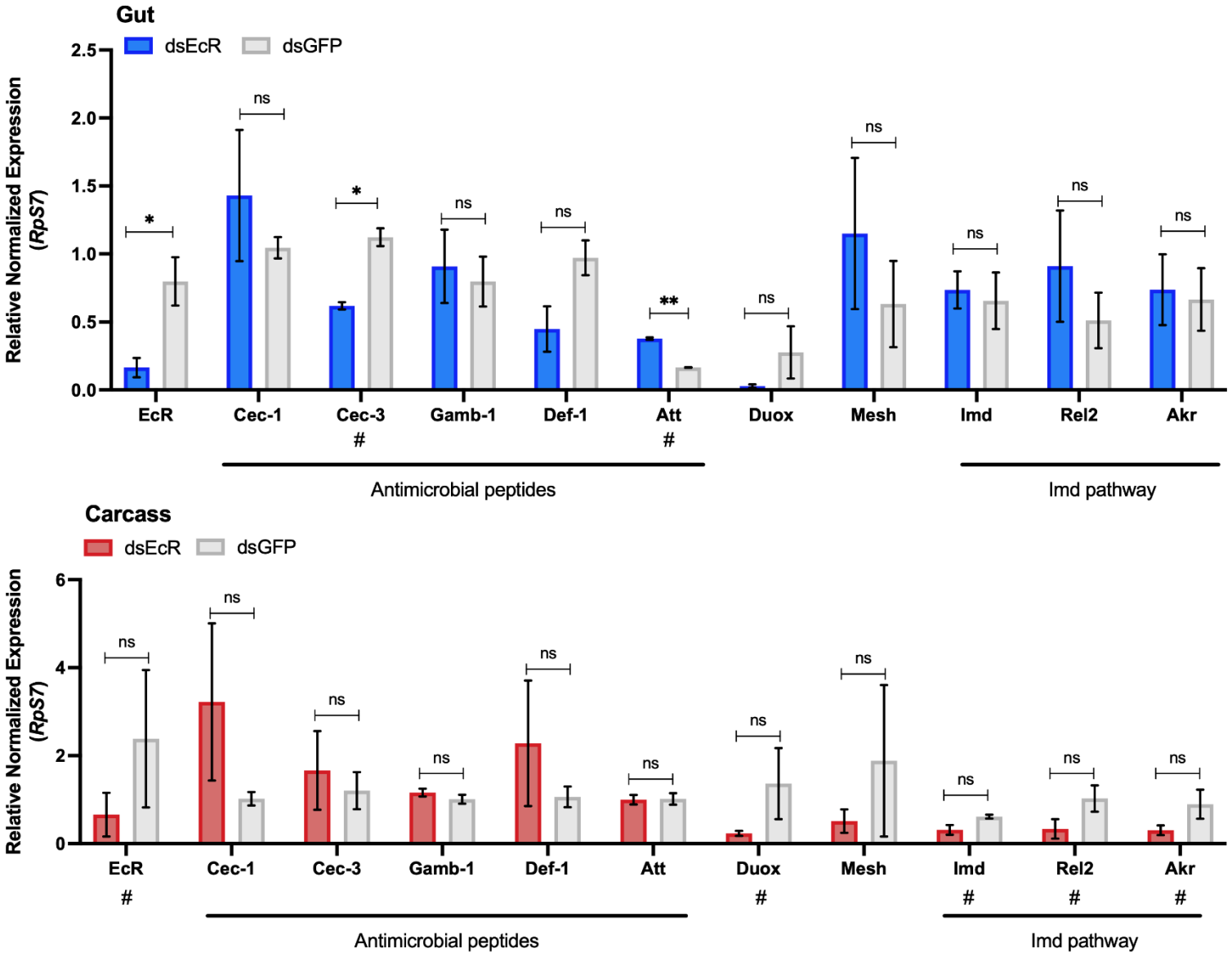
Gut
dsEcR
dsGFP
Relative Normalized Expression (RpS7)
2.5
2.0
1.5
1.0
0.5
0.0
*
ns
*
ns
ns
**
ns
ns
ns
ns
ns
EcR
Cec-1
Cec-3
#
Gamb-1
Def-1
Att
#
Duox
Mesh
Imd
Rel2
Akr
Antimicrobial peptides
Imd pathway
Carcass
dsEcR
dsGFP
Relative Normalized Expression (RpS7)
6
4
2
0
ns
ns
ns
ns
ns
ns
ns
ns
ns
ns
ns
EcR
#
Cec-1
Cec-3
Gamb-1
Def-1
Att
Duox
#
Mesh
Imd
#
Rel2
#
Akr
#
Antimicrobial peptides
Imd pathway

Figure 4.2: Tissue-specific mRNA expression of selected immune genes after *EcR* silencing. RNE values are plotted. Means ± SEM from 2-3 independent biological replicates is indicated. A total of 15 mosquitoes were used per biological replicate. Abbreviations: EcR = ecdysone receptor; cec-1 = cecropin-1; cec-3 = cecropin-3, gamb-1 = gambicin-1; def-1 = defensin-1; att = attacin-c; duox = dual oxidase; Imd = immune deficiency; rel2 = relish 2; akr = akirin. *p<0.05, **p<0.01, ^{ns} not significant.

In the carcass tissues on the other hand, dsEcR injection did not significantly affect the expression of any selected genes (Figure 4.2). Indeed, the unpaired *t*-test *p*-values corresponded to 0.4033 (*EcR*), 0.2868 (*cec-1*), 0.6663 (*cec-3*), 0.3254 (*gamb-1*), 0.4468 (*def-1*), 0.9225 (*att*), 0.2977 (*duox*), 0.5144 (*mesh*), 0.1292 (*Imd*), 0.2058 (*rel2*), and 0.2331 (*akr*). Overall, the results presented here suggested that the change immune gene expression that follows dsEcR injection is tissue specific. Also, even though AMP expression was affected in the gut, it appears that the direction of the change depends on the AMP.

4.3.2 Hormone (20E) injection alters anti-bacterial immune responses in a time-point dependent manner

To investigate whether the increase in 20E titers that follows the ingestion of a blood meal could induce the production of immune effectors that prevent an uncontrolled blood-induced microbiome proliferation the following approach was used. *Anopheles arabiensis* female mosquitoes were injected with 20E, and the expression of 10 immune genes (Table 4.3) was measured in the whole mosquito at five time points post injection. Although two factors (20E injection and time elapsed since injection) could affect the gene expression, a two-way ANOVA analysis could not be used to assess the difference in gene expression post-20E injection, since it was found that the time elapsed since injection also affected the immune genes RNE values in the

PBS-injected mosquito group (two-way ANOVA analysis, data not shown). Therefore, to circumvent this problem, an unpaired *t*-test was used at each time point to measure the effect of 20E injection on gene expression, while the RNE ratios (20E/PBS) were compared with the one-way ANOVA analysis (followed by Tukey *post hoc* analysis) to measure the contribution of time to gene expression (Figures 4.3-4.5).

Three out of the 5 AMPs tested were differentially expressed after 20E injection. *Cec-1* was significantly down-regulated in the 20E-injected mosquitoes (compared to the PBS-injected mosquitoes) at 1 hpi and 24 hpi, while it was unaffected at the remaining time points (Figure 4.3a). *Cec-3* RNE value decreased significantly in the 20E-injected mosquitoes at 24 hpi but was not affected at the earlier time points (Figure 4.3a). *Attacin* expression decreased significantly in the 20E-injected mosquitoes at 3 hpi only (Figure 4.3a). In contrast, 20E injected mosquitoes did not display any statistically significant difference in the expression of *attacin* or *gambicin-1* (Figure 4.3a).

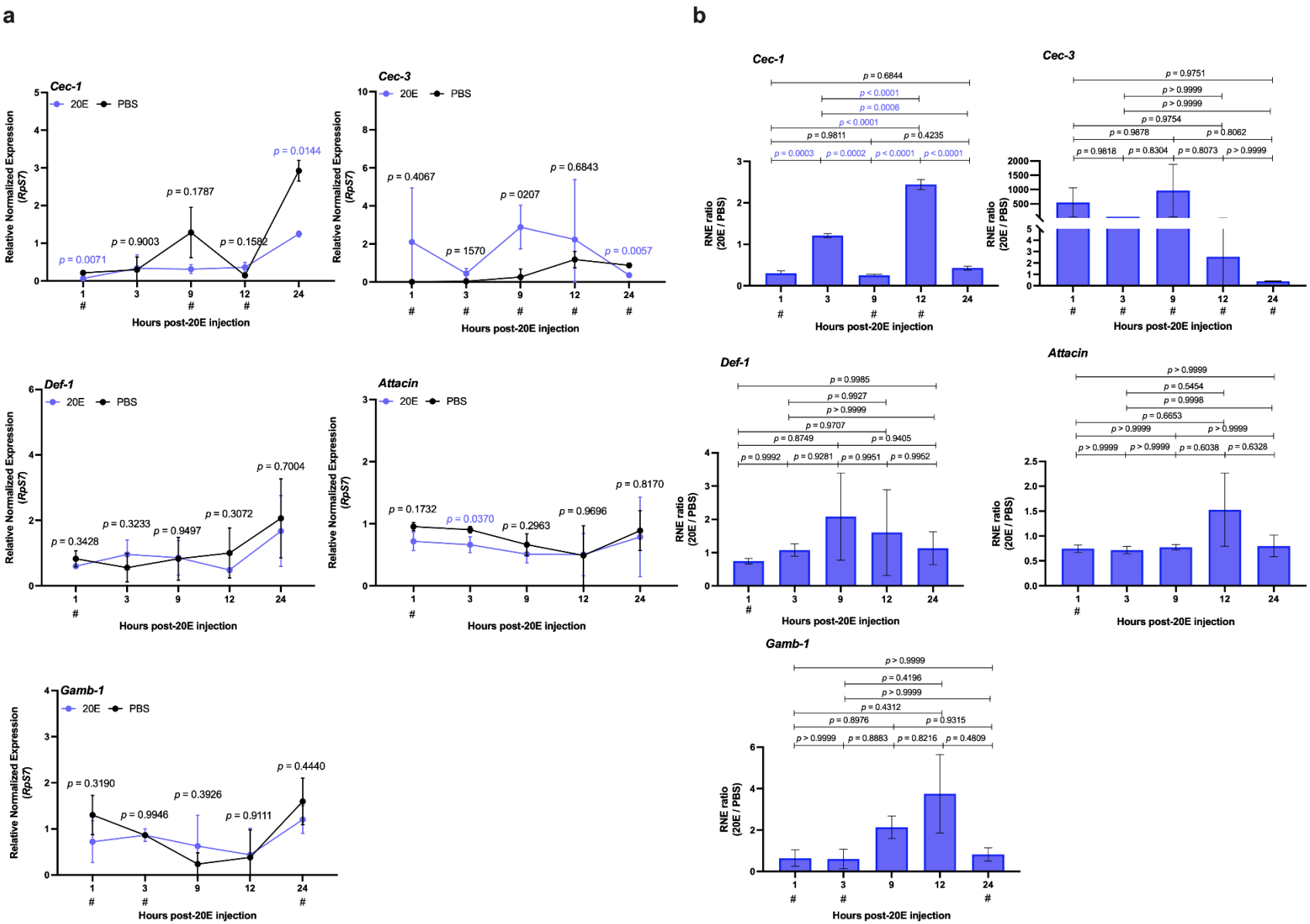
a
Cec-1
20E
PBS
Relative Normalized Expression (RpS7)
p = 0.0071
p = 0.9003
p = 0.1787
p = 0.1582
p = 0.0144
Hours post-20E injection
Cec-3
p = 0.4067
p = 1570
p = 0207
p = 0.6843
p = 0.0057
Def-1
p = 0.3428
p = 0.3233
p = 0.9497
p = 0.3072
p = 0.7004
Attacin
p = 0.1732
p = 0.0370
p = 0.2963
p = 0.9696
p = 0.8170
Gamb-1
p = 0.3190
p = 0.9946
p = 0.3926
p = 0.9111
p = 0.4440
b
Cec-1
RNE ratio (20E / PBS)
p = 0.6844
p < 0.0001
p = 0.0006
p < 0.0001
p = 0.9811
p = 0.4235
p = 0.0003
p = 0.0002
p < 0.0001
p < 0.0001
Hours post-20E injection
Cec-3
p = 0.9751
p > 0.9999
p > 0.9999
p = 0.9754
p = 0.9878
p = 0.8062
p = 0.9818
p = 0.8304
p = 0.8073
p > 0.9999
Def-1
p = 0.9985
p = 0.9927
p > 0.9999
p = 0.9707
p = 0.8749
p = 0.9405
p = 0.9992
p = 0.9281
p = 0.9951
p = 0.9952
Attacin
p > 0.9999
p = 0.5454
p = 0.9998
p = 0.6653
p > 0.9999
p > 0.9999
p > 0.9999
p > 0.9999
p = 0.6038
p = 0.6328
Gamb-1
p > 0.9999
p = 0.4196
p > 0.9999
p = 0.4312
p = 0.8976
p = 0.9315
p > 0.9999
p = 0.8883
p = 0.8216
p = 0.4809

Figure 4.3: Transcript abundance of AMPs after 20E injection. (**a**) Effect of 20E injection. RNE means ± SEM from 2-3 independent biological replicates is represented. A total of 12-15 mosquitoes were used per biological replicate per time point. # Only 2 biological replicates were used. Statistical significance at each time point was assessed with an unpaired *t*-test, and *p*-values for each comparison are indicated. (**b**) Effect of time on gene expression. Statistical significance was assessed with a one-way ANOVA analysis, followed by the Tukey *post hoc* test to correct for multiple comparisons. Shown are the *p*-values of the Tukey analysis. In both (**a,b**), the *p*-values indicated in blue indicate where the means compared are statistically significantly different.

From the time-point analysis, *cec-1* showed a cyclic expression (one-way ANOVA: F= 193.0, df = 4; $p < 0.0001$), increasing from 1 hpi to 3 hpi, then returning to the basal level at 9 hpi, increasing again at 12 hpi to return to its basal level at 24 hpi (Figure 4.3b). In contrast, the RNE ratios of the remaining AMPs did not fluctuate significantly over time, including *cec-3* (one-way ANOVA: F= 0.5005, df = 4; $p = 0.7380$), *def-1* (one-way ANOVA: F= 0.2967, df = 4; $p = 0.8729$), *attacin* (one-way ANOVA: F=0.8826, df = 4; $p = 0.5115$), and *gambicin-1* (one-way ANOVA: F= 1.376, df = 4; $p = 0.3336$). Thus, the Tukey *post hoc* analysis did not detect any statistically significant change between the expression of these genes (Figure 4.3b).

Since the Imd pathway is one of pathways that induce the production of AMPs (Figure 4.1), and 20E injection affected the expression of at least 3 AMPs (Figure 4.3), it was hypothesized that 20E injection could also alter the expression of the three selected Imd-related genes. Surprisingly, 20E injection did not affect the expression of *Imd*, *Rel 2*, or *akirin* (Figure 4.4a). Similarly, the time elapsed since injection did not affect the expression of *Imd* (one-way ANOVA: F= 1.456, df = 4; $p = 0.3012$), *Rel 2* (one-way ANOVA: F= 0.8210 df = 4; $p = 0.5510$), or *akirin* (one-way ANOVA: F= 0.8220, df = 4; $p = 0.5462$). As a result, the Tukey *post hoc* analysis did not detect any statistically significant change between the expression of these genes (Figure 4.4b).

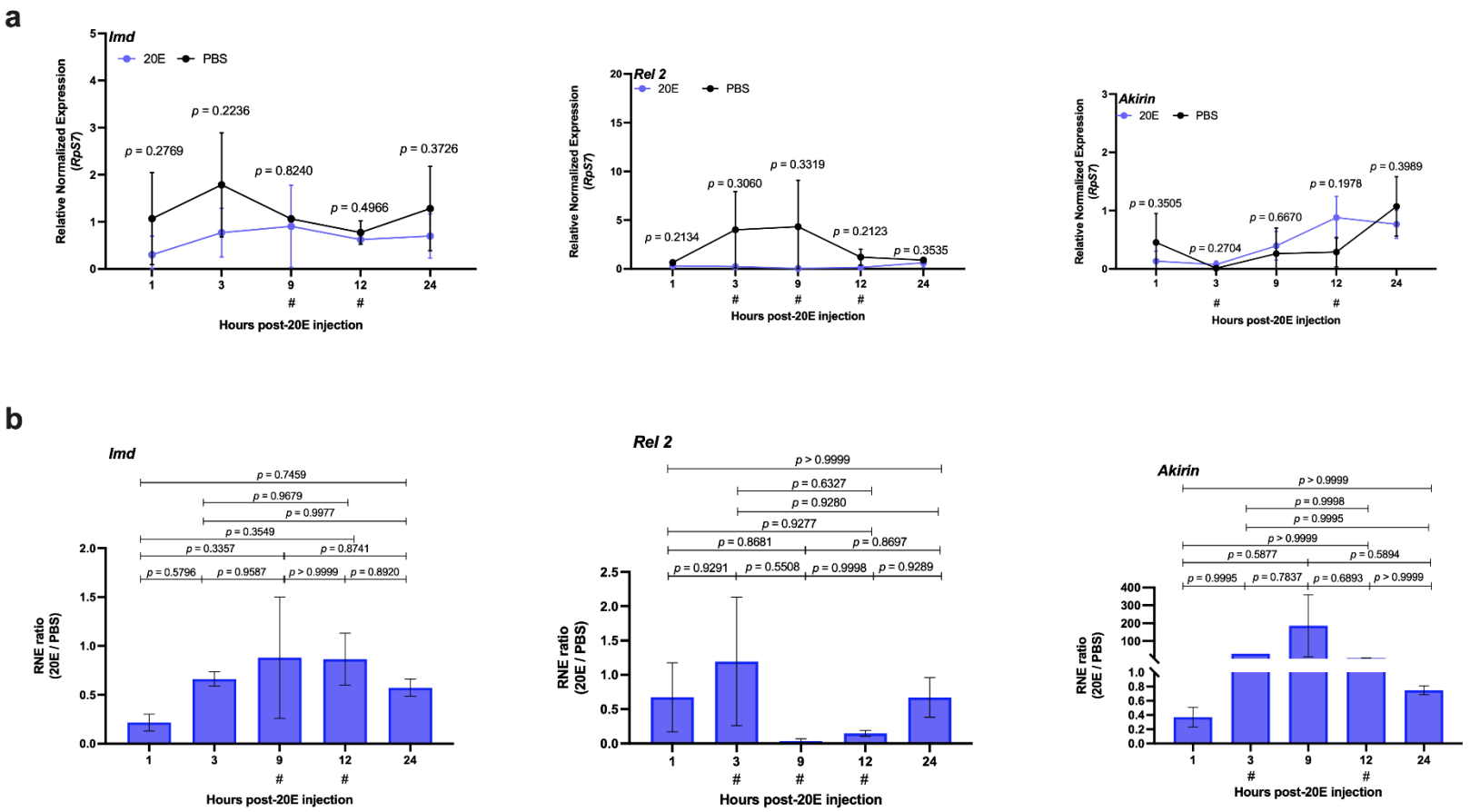

Figure 4.4: Transcript abundance of selected Imd-related genes at different time points post 20E injection. (**a**) Effect of 20E injection. RNE means ± SEM from 2-3 independent biological replicates is represented. A total of 12-15 mosquitoes were used per biological replicate per time point. # Only 2 biological replicates were used. Statistical significance at each time point was assessed with an unpaired *t*-test, and *p*-values for each comparison are indicated. (**b**) Effect of time on gene expression. Statistical significance was assessed with a one-way ANOVA analysis, followed by the Tukey *post hoc* test to correct for multiple comparisons. Shown are the *p*-values of the Tukey analysis.

To examine whether some non-AMP mediated responses were activated by 20E, the expression of *mesh* and *duox* were also measured. Mosquitoes injected with 20E did not display any statistically significant difference in *mesh* expression, but *duox* expression was significantly induced at 3 hpi (Figure 4.5a). Neither *mesh* (one-way ANOVA: F= 1.002, df = 4; p = 0.4849), nor *duox* (one-way ANOVA: F= 0.5039, df = 4; p = 0.7358) expression were affected by the time elapsed since injection. Hence, the Tukey *post hoc* analysis did not detect any statistically significant change between the expression of these genes (Figure 4.5b).

4.3.3 *EcR* transcript abundance decreased upon immune challenge with Gram-negative bacteria, but not Gram-positive bacteria

In chapter 3, a link was established between *EcR* transcript abundance and the abundance of gut commensal bacteria (Figure 3.3a,b). However, because the antibiotics used target both Gram-negative and Gram-positive bacteria, it was not possible to determine whether both types of bacteria influence *EcR* transcript levels. To address this question, *An. arabiensis* females were injected with either *E. coli* (Gram-negative) or *S. aureus* (Gram-positive), and *EcR* expression was measured at 6 hrs, 12 hrs, 18 hrs, and 24 hrs post-bacterial injection. The negative control mosquitoes were injected with PBS. In addition, the mRNA expression of *gambicin-1* was measured as a positive control since this AMP is reportedly induced by both bacteria (Table 4.1).

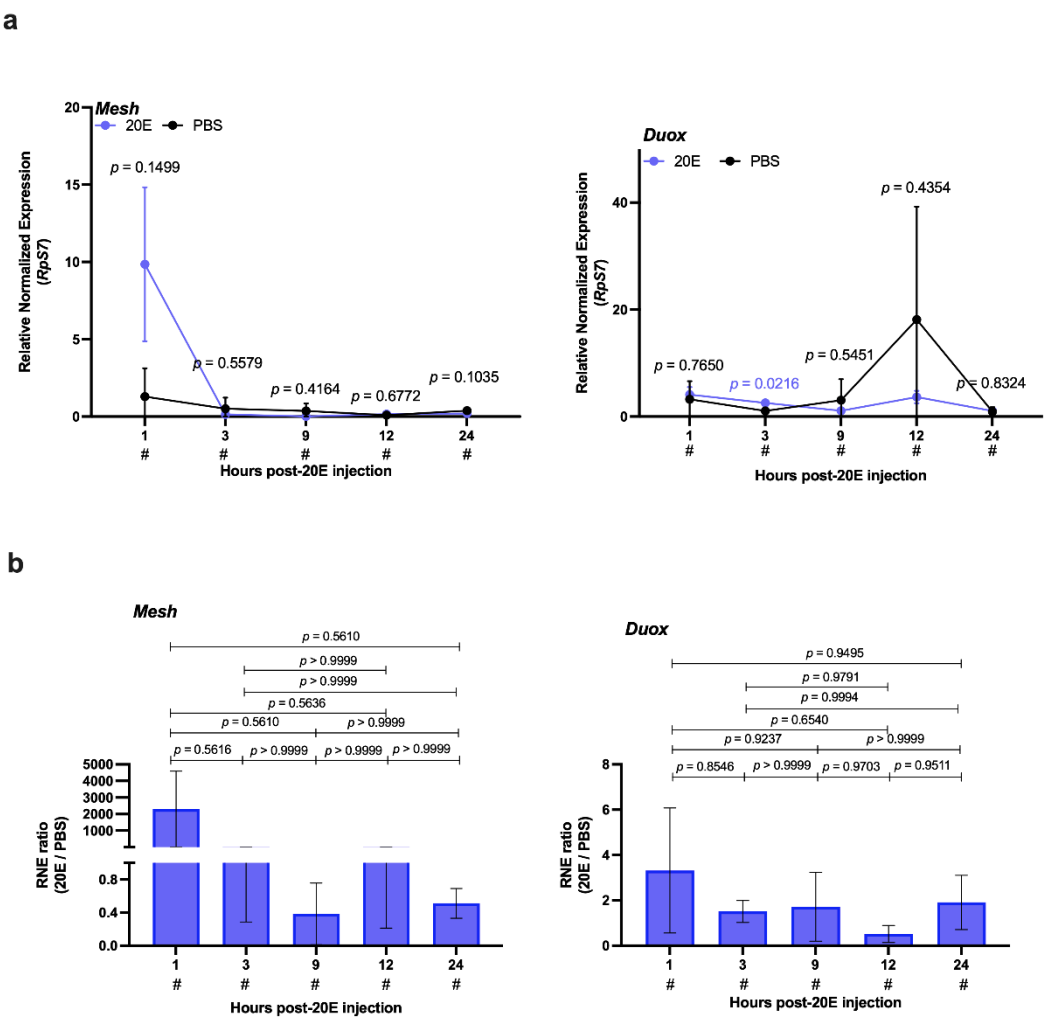

Figure 4.5: Transcript abundance of *mesh* and *duox* at different time points post 20E injection. (**a**) Effect of 20E injection. RNE means ± SEM from 2-3 independent biological replicates is represented. A total of 12-15 mosquitoes were used per biological replicate per time point. # Only 2 biological replicates were used. Statistical significance at each time point was assessed with an unpaired *t*-test, and *p*-values for each comparison are indicated. (**b**) Effect of time on gene expression. Statistical significance was assessed with a one-way ANOVA analysis, followed by the Tukey *post hoc* test to correct for multiple comparisons. Shown are the *p*-values of the Tukey analysis.

Injection with *E. coli* was first validated by showing that *gambicin-1* —the positive control— expression was induced in *E. coli*-injected mosquitoes relative to PBS-injected mosquitoes, albeit at 12 hpi only (Figure 4.6a). Indeed, at this time point, *gambicin-1* transcript abundance significantly increased from 0.89247 ± 0.34534 to 1.67951 ± 0.48986. In contrast, *gambicin-1* expression was not affected at the other time points. With respect to *EcR* expression, *E. coli* injection significantly reduced *EcR* abundance at 24 hpi from 1.0074 ± 0.1216 in PBS-injected mosquitoes to 0.2601 ± 0.1228 in *E. coli*-injected mosquitoes (Figure 4.6a). At the remaining time points, *EcR* expression was not affected. The time elapsed since bacterial injection only influenced *gambicin-1* expression (one-way ANOVA: F= 22.13, df = 3; p = 0.0059), but not *EcR* expression (one-way ANOVA: F= 0.3410, df = 3; p = 0.7983). These results were corroborated by the Tukey *post hoc* analysis (Figure 4.6a).

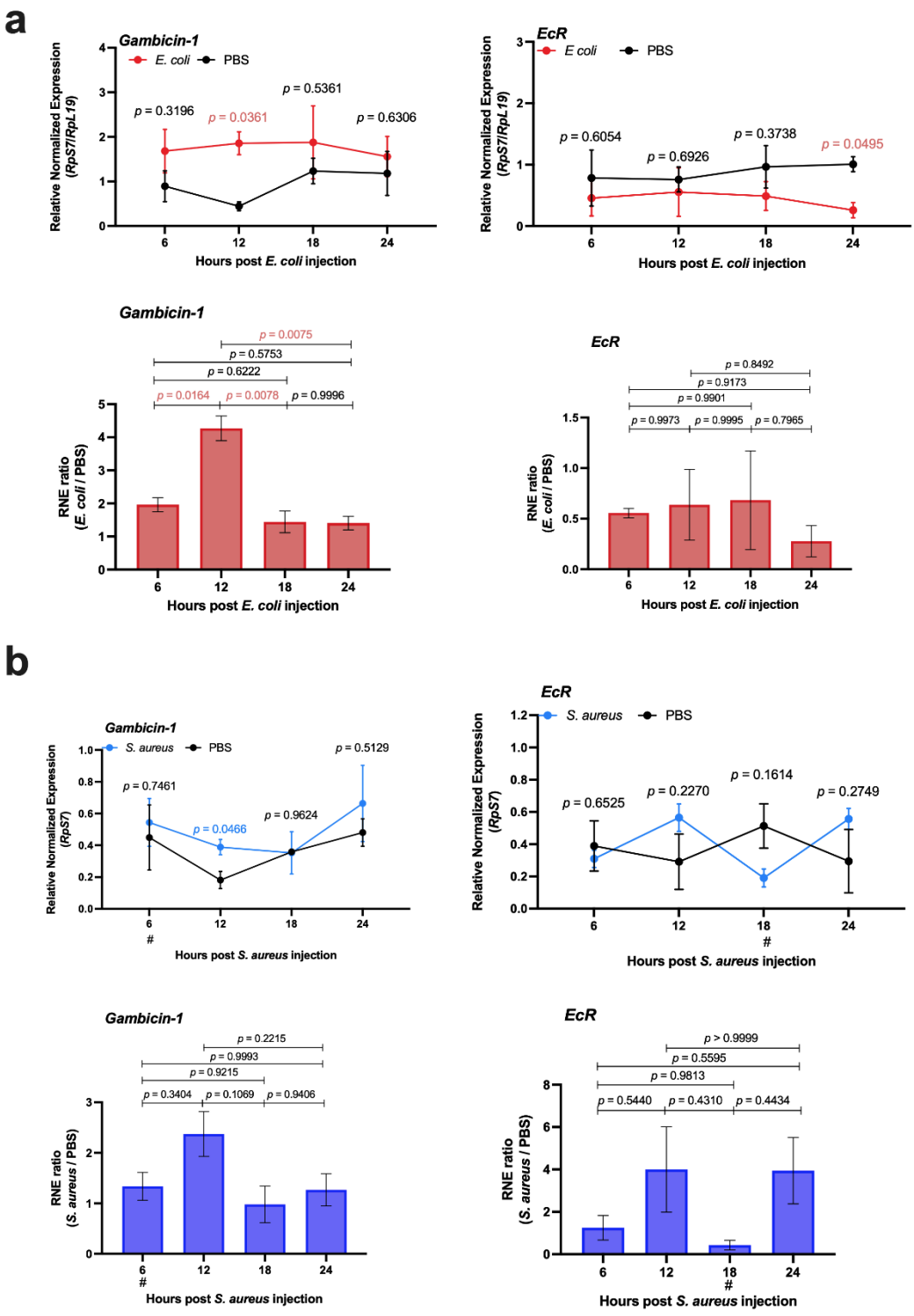

Figure 4.6: Expression of *EcR* and *Gambicin-1* at different time points post-bacterial injection. (**a**) *E. coli* challenge. RNE means ± SEM values from 2 independent biological replicates are shown to measure the effect of *E. coli* (line graphs), while RNE ratios are used to measure the effect of time (bar graphs). (**b**) *S. aureus* challenge. RNE means ± SEM values from 2-3 independent biological replicates are shown. A total of 15 mosquitoes were used per biological replicate.

Abbreviation: hpi = hours post injection. #Only 2 biological replicates were used. *P*-values indicated in color (blue or red) indicate statistical significance.

In the case of *S. aureus* injection, the experiment was also validated by showing that *gambicin-1* —the positive control— expression was induced in *S. aureus*-injected mosquitoes relative to PBS-injected mosquitoes, also at 12 hpi only (Figure 4.6b). At this time point, *gambicin-1* transcript abundance significantly increased from 0.1817 ± 0.0543 in PBS-injected mosquitoes to 0.3884 ± 0.0482 in the bacteria-injected mosquitoes. In contrast, *gambicin-1* expression was not affected at the other time points. Unlike the *E. coli* experiment, mosquitoes injected with *S. aureus* did not display any change in *EcR* expression, at any time point (Figure 4.6b). The time elapsed since bacterial injection did not influence *gambicin-1* expression (one-way ANOVA: F= 2.827, df = 3; p = 0.1163), or *EcR* expression (one-way ANOVA: F= 1.480, df = 3; p = 0.3006). These results were corroborated by the Tukey *post hoc* analysis (Figure 4.6b).

4.4 Discussion

Anopheles Imd pathway plays a key role in activating several anti-bacterial immune defenses, including the production of AMPs, ROS, RNS, TEP1, and PPO (Figure 4.1). These immune defenses not only protect the mosquito against the invasion of external bacteria, but they also prevent an uncontrolled proliferation of its commensal bacterial microbiome (Barletta et al., 2017). In *An. gambiae*, the 20E signaling pathway has been identified as a key regulator of the Imd pathway-mediated anti-bacterial responses, such as the expression of PPOs (Werling, 2020), and selected AMPs (*cec-1* and *cec-3*) (Reynolds et al., 2020). In addition, 20E priming before *E. coli* feeding

prevents the proliferation of these bacteria within *An. gambiae* (Reynolds et al., 2020). Despite these studies, several questions pertaining to the extent to which mosquitoes antibacterial innate immune responses are regulated by the 20E signaling pathway remain unanswered.

Firstly, Werling (2020) measured the expression of 34 immune genes in the midgut and abdominal carcass of females *An. gambiae* that had been dsEcR-injected and subsequently blood-fed. Among these genes, were two AMPs (*cec-1* and *def-1*), two PPOs (*PPO3* and *PPO9*), and three genes of the complement system (*TEP1*, *LRIM1*, and *APL1C*). While many of these genes are linked to the Imd pathway (Figure 4.1), no direct relationship between the Imd pathway and *EcR* expression was established. Furthermore, because the authors focused on the expression of these genes in two tissues (the midgut and abdominal carcass), any impact of *EcR* depletion on immune gene expression in the head or thorax was likely missed. In addition, because Barletta et al. (2017) demonstrated that blood-feeding also induces the Imd pathway through *Rel2* activation, both dsEcR and blood-feeding could have contributed to the expression of immune genes in Werling's study design (Werling, 2020).

In this chapter, the effect of RNAi-mediated *EcR* depletion on the expression of ten immune genes —of which eight were related to the Imd pathway— was measured in the gut and carcass (whole mosquito minus the gut). For this study, only non-blood fed mosquitoes were used to eliminate any contribution of blood-feeding to immune gene expression. Moreover, to allow for comparison with Werling's study, the same dose of dsEcR (i.e., 690 ng per mosquito) was used, and RNA abundance was also measured at 48 hours post-dsRNA injection.

Similar to the previous study that did not detect any change in *cec-1* and *def-1* expression in the gut after silencing *EcR* (Werling, 2020), the expression of these two

genes was not affected in the gut under our experimental settings (Figure 4.2). Nonetheless, *cec-3* and *attacin* were significantly down-regulated and up-regulated, respectively (Figure 4.2). These results suggest that the impact of *EcR* depletion on the gut-specific AMP gene expression is influenced by both the type of AMP, and whether the mosquitoes were blood-fed after dsRNA injection. Surprisingly, none of the Imd pathway genes tested (*Imd*, *rel2*, and *akirin*) were affected in the gut after *EcR* silencing, despite evidence that the Imd pathway regulates *cec-1* and *cec-3* expression in *An. gambiae* (Meister et al., 2005). It is possible that the high variance detected between biological replicates could have masked any change in RNE values. This high variance could be due to (1) pipetting errors, or (2) the circadian rhythm of mosquitoes which necessitates that all samples be collected at the same time. Alternatively, the regulation of AMP expression by 20E signaling in the gut could be mediated by the Toll immune pathway. This latter hypothesis agrees with Reynolds et al. (2020) who reported an increase in *Toll 7* expression in 20E-injected *An. gambiae* mosquitoes Sua 4.0 cells, as well as Zhang et al. (2017) who demonstrated that *gambicin-1* is regulated by the Toll pathway in *Ae. aegypti* mosquitoes Aag2 cells.

The last two genes whose expression was measured in the midgut included *mesh* and *duox*, and neither of these genes showed differential expression post *EcR* depletion, in agreement with Reynolds et al. (2020) who did not detect a change in the expression of these genes after disturbing the 20E signaling pathway (by injecting 20E). Furthermore, it was previously reported that *mesh* abundance correlates with the expression of *Imd* and *rel2* in *Ae. aegypti* (Xiao et al., 2017). Therefore, the absence of variation in both *mesh* and *duox* expression was coherent with the lack of change in *Imd*, *rel2* and *akirin* transcript abundance.

In the carcass however, none of the ten immune genes selected were affected by dsEcR injection (Figure 4.2). However, it is not possible to conclude whether *EcR*

depletion affects immune gene expression in the carcass, since *EcR* expression was not statistically significantly reduced (Figure 4.2). Nonetheless, it is also possible that any change in gene expression could have been masked by the mixture of tissues (head, hemolymph, thorax, malpighian tubules, fat body, ovaries) present in the carcass. For example, Verma et al. (2015) showed that in *Drosophila* malpighian tubules, the expression of AMPs in ecdysone mutants (flies that cannot produce 20E) is significantly reduced. Similarly, a separate study in *Ae. aegypti* mosquitoes revealed that the regulation of AMP production may be detected in the fat body where these AMPs are produced (Chang et al., 2021). Since AMPs are produced in the fat body and released into the hemolymph before entering their target tissues [reviewed in (Mylonakis et al., 2016, Torrent et al., 2012, Yi et al., 2014)], future studies investigating how dsEcR affect AMP gene expression in mosquitoes could perhaps focus on their expression in gut, fat body, and hemolymph tissues.

The above gut/carcass experiment illustrated how weakening the 20E signaling pathway —by depleting *EcR* levels— affects immune gene expression. In the second part of this study, whether strengthening 20E signaling influences immune gene expression was explored. To date, only two studies in mosquitoes, to my knowledge, have addressed this question in anopheline mosquitoes *in vivo* (Table 4.2). These two studies highlighted that in mosquitoes, the impact of 20E injection on the expression of immune genes is dose-dependent (Dahalan et al., 2019, Reynolds et al., 2020). Interestingly, Verma et al. (2015) reported in a separate study in *Drosophila* that the time elapsed since 20E injection could also influence how 20E regulates immune gene expression. To test if this finding is also true in anopheline mosquitoes, the expression of the 10 selected immune genes were measured at five time points post 20E injection.

Consistent with the findings in *D. melanogaster* (Verma and Tapadia, 2015), the expression of *cec-1* post-20E injection was cyclic. However, while Verma et al. (2015) found that 20E injection increases AMP expression in *Drosophila* (*attacin*, *cec-1*, and *cec-3*), this study showed that these 3 AMPs were down-regulated post 20E injection (Figure 4.3a). This discrepancy could result from the dose of 20E they used (1 µg/ml), the time points at which AMP expression was measured —13 time points spanning from 15 min to 6 hrs post-20E treatment in Verma's study, as opposed to 5 time points spanning from 1 hr to 24 hrs post-treatment in our study (Figures 4.3-4.5). In addition, the tissue in which AMP expression was measured (malpighian tubules in Verma's study versus whole body in our study) could have also contributed to the discrepancy observed. Finally, the type of insect (i.e., vector mosquito versus non-vector fruitfly) may also explain why the AMP response was different between the two studies.

When my findings were compared to those in *An. gambiae* at the common time point, i.e., 24 hpi (Reynolds et al., 2020), the following observations were made. First, in the *in vitro* RNA-seq study (Sua 4.0 cells), Reynolds et al. (2020) identified 2 AMPs genes that were differentially expressed post-20E injection: *cec-1* and *cec-3.* The similar 2 AMPs were also differentially expressed in this study, although they were down-regulated. The discrepancy could result from the dose of 20E used in both studies (500 ng versus 69 ng), or the tissue used (Sua 4.0 cells versus whole mosquito). Second, in both studies, no genes of the Imd pathway were identified as regulated by the 20E signaling pathway, suggesting that the 20E-mediated regulation of AMP expression may be mediated by the Toll pathway.

Surprisingly, although *cec-1* was differentially expressed in both Reynolds' study and this study, Dahalan et al. (2019) did not find any change in *cec-1* expression in the gut of *An. coluzzii* female mosquitoes injected with 2.5 µg of 20E. Not only is the dose of 20E used by Dahalan 36 times and 5 times higher than the one used in this

study and Reynolds' study, respectively, but also, Dahalan et al. (2019) measured immune gene expression in the gut, as opposed to the two other studies where immune gene expression was measured in the whole mosquito. Furthermore, because Dahalan et al. (2019) only used one time point post injection (24 hpi), it is difficult to conclude whether a high dose of 20E suppressed the induction —or repression— of *cec-1*. Therefore, further studies in *An. coluzzii* should investigate whether using lower doses of 20E could result in the activation/repression of immune genes, either in the gut tissues or the whole mosquito.

Consistent with findings in *An. gambiae* (Reynolds et al., 2020) and *An. coluzzii* (Dahalan et al., 2019), the expression of *defensin-1* and *gambicin-1* were not affected in *An. arabiensis* after 20E injection. Since these three studies only focus either on the whole mosquito or the gut, it is difficult to conclude whether other tissues (e.g., the malpighian tubules) or different time points could have detected a change in the expression of these two AMPs. In agreement with this idea, Verma et al. (2015) demonstrated that both *defensin-1* and *gambicin-1* expression is induced by 20E injection in *Drosophila* malpighian tubules.

At least two reasons may explain why not all AMPs responsed to manipulating the 20E signaling pathway. Firstly, t he effect of 20E on immune gene expression can be influenced by whether 20E injection is followed by a pathogen challenge (Table S7). Indeed, in *Drosophila*, AMPs are only induced post-20E injection when 20E injection is followed by exposure to peptidoglycan, a component of bacteria cell walls (Flatt et al., 2008). This finding was proven true regardless of the method used to disturb the 20E signaling pathway, including 20E injection, dsEcR injection or dsUSP injection (Flatt et al., 2008). Therefore, further studies should investigate if pathogen exposure is necessary for the 20E signaling pathway to induce the expression of innate immune genes in mosquitoes. Since the 5 AMPs tested respond to both Gram-

negative and Gram-positive bacteria (Table 4.1), this pathogen exposure could be conducted with either bacteria type. Secondly, it is possible that other pathways could have contributed to the selective differential expression of AMPs. In agreement with this hypothesis, *gamb-1* which was not differentially expressed in any manipulation of the 20E pathway is regulated by the Toll, Imd, and Jak-STAT pathways (Zhang et al., 2017). In contrast, the other AMPs investigated are primarily regulated by the Imd pathway (Zhang et al., 2017). Furthermore, Chang et al. (2021) showed that AMPs are repressed by the Juvenile Hormone (JH) in the fat body upon mosquito adult eclosion till 72 hrs post eclosion. Therefore, because the regulation of AMPs in mosquitoes involves different pathways, it is possible that disturbing one of them is compensated by the next pathway to maintain a basal level of immunity in mosquitoes. However, this hypothesis remains to be tested experimentally. Such experiments could include RNA-sequencing of the mosquito after manipulating the 20E signaling pathway to determine whether the genes in the toll, Jak-STAT, or Juvenile Hormone pathways are also differentially expressed.

Noteworthy, a high variation was detected between the biological replicates. This variation is likely due to the difference in tissues used. Indeed, post-20E injection, I measured the expression of genes in the whole mosquito, while Werling (2020), Reynolds (2020), and Verma (2015) measured it in the gut, cell line, and malpighian tubules, respectively. In addition the circadian rhythm of the mosquito —which necessitates that the time at which the samples were collected is the same between biological replicate— could also explain why a high variation was detected between biological replicates.

Overall, based on (i) the impact of 20E injection on AMP expression (specifically the downregulation of *cec-1*, *cec-3*, and *attacin*), and (ii) the observation that both the gut microbiome and 20E titers significantly increase after a blood meal (Araujo et al.,

2011, Xiao et al., 2017), the following model could be proposed to explain the tripartite relationship between the 20E signaling pathway, the gut microbiome, and immune gene expression after a blood meal. First, the anopheline female mosquito takes a blood meal. This blood meal increases 20E titers and EcR expression as previously reported (Araujo et al., 2011, Raikhel et al., 2002, Roy et al., 2015). Following this increased in 20E signaling, several immune defenses are reduced, as evidenced by the down-regulation of *cec-1*, *cec-3* and *attacin* expression post-20E injection (Figure 4.3). The decrease in the mosquito immune defenses thus favour the proliferation of the gut bacterial microbiome. However, to ensure that the gut bacteria do not expand to a level that will compromise the mosquito fitness, a basal level of immune gene expression (those genes that were not affected by disturbing 20E signaling) is maintained to preserve bacterial homeostasis. While this is only a model, future studies should investigate whether 20E signaling regulates the midgut bacterial homeostasis in mosquitoes.

Finally, although a link between bacteria abundance and *EcR* expression was established in chapter 3 (section 3.3.1), the type of bacteria (i.e., Gram-negative versus Gram-positive) that are correlated to *EcR* expression was not explored. In this chapter, only *E. coli* injection influenced *EcR* expression, but not *S. aureus* injection. It is difficult to conclude that Gram-positive bacteria do not affect *EcR* expression, especially because only one species of Gram-positive bacteria was tested. Besides, although delivering the bacteria by injection ensured that a precise number of bacteria was injected —as previously reported (Blandin et al., 2002, Dong et al., 2009, Schnitger et al., 2007)—, a study published in 2021 demonstrated that administering bacteria orally leads to more profound transcriptomic changes in the mosquito than when they are injected intrathoracically (San Dekmak et al., 2021). Therefore, the possibility that administering *S. aureus* orally could have affected *EcR* mRNA expression cannot be

excluded, and this needs to be investigated in future. In addition, using a higher dose of *S. aureus*, or injecting live-bacteria, or measuring *EcR* expression at later time points may also affect how *S. aureus* regulate *EcR* expression. Each of these parameters need to be investigated in further experiments before concluding that infecting mosquitoes with *S. aureus* does not affect the transcript abundance of *EcR*.

4.5 References

ARAUJO, R. V., MACIEL, C., HARTFELDER, K. & CAPURRO, M. L. 2011. Effects of *Plasmodium gallinaceum* on hemolymph physiology of *Aedes aegypti* during parasite development. *J. Insect Physiol.,* 57**,** 265-273.

BAI, L., WANG, L., VEGA-RODRÍGUEZ, J., WANG, G. & WANG, S. 2019. A Gut Symbiotic Bacterium *Serratia marcescens* Renders Mosquito Resistance to *Plasmodium* Infection Through Activation of Mosquito Immune Responses. *Front. Microbiol.,* 10**,** 1580.

BARLETTA, A. B. F., NASCIMENTO-SILVA, M. C. L., TALYULI, O. A. C., OLIVEIRA, J. H. M., PEREIRA, L. O. R., OLIVEIRA, P. L. & SORGINE, M. H. F. 2017. Microbiota activates IMD pathway and limits *Sindbis* infection in *Aedes aegypti*. *Parasit. Vectors,* 10**,** 1-9.

BLANDIN, S., MOITA, L. F., KÖCHER, T., WILM, M., KAFATOS, F. C. & LEVASHINA, E. A. 2002. Reverse genetics in the mosquito *Anopheles gambiae*: targeted disruption of the *Defensin* gene. *EMBO. Rep.,* 3**,** 852-856.

CHANG, M.-M., WANG, Y.-H., YANG, Q.-T., WANG, X.-L., WANG, M., RAIKHEL, A. S. & ZOU, Z. 2021. Regulation of antimicrobial peptides by juvenile hormone

and its receptor, Methoprene-tolerant, in the mosquito *Aedes aegypti*. *Insect Biochem. Mol. Biol.,* 128**,** 103509.

CONTRERAS-GARDUÑO, J., RODRÍGUEZ, M. C., HERNÁNDEZ-MARTÍNEZ, S., MARTÍNEZ-BARNETCHE, J., ALVARADO-DELGADO, A., IZQUIERDO, J., HERRERA-ORTIZ, A., MORENO-GARCÍA, M., VELAZQUEZ-MEZA, M. E. & VALVERDE, V. 2015. *Plasmodium berghei i*nduced priming in *Anopheles albimanus* independently of bacterial co-infection. *Dev. Comp. Immunol.,* 52**,** 172-181.

DAHALAN, F. A., CHURCHER, T. S., WINDBICHLER, N. & LAWNICZAK, M. K. N. 2019. The male mosquito contribution towards malaria transmission: Mating influences the *Anopheles* female midgut transcriptome and increases female susceptibility to human malaria parasites. *PLoS Pathog.,* 15**,** e1008063.

DAS, S., DONG, Y., GARVER, L. & DIMOPOULOS, G. 2009. *Specificity of the innate immune system: a closer look at the mosquito pattern-recognition receptor repertoire*, Oxford University Press: New York, NY, USA.

DONG, Y., MANFREDINI, F. & DIMOPOULOS, G. 2009. Implication of the mosquito midgut microbiota in the defense against malaria parasites. *PLoS Pathog.,* 5**,** e1000423-e1000423.

EAPPEN, A. G., SMITH, R. C. & JACOBS-LORENA, M. 2013. Enterobacter-Activated Mosquito Immune Responses to *Plasmodium* Involve Activation of SRPN6 in *Anopheles stephensi*. *PLoS One,* 8**,** e62937.

FLATT, T., HEYLAND, A., RUS, F., PORPIGLIA, E., SHERLOCK, C., YAMAMOTO, R., GARBUZOV, A., PALLI, S. R., TATAR, M. & SILVERMAN, N. 2008. Hormonal regulation of the humoral innate immune response in *Drosophila melanogaster*. *J. Exp. Biol.,* 211**,** 2712-2724.

GABRIELI, P., CACCIA, S., VAROTTO-BOCCAZZI, I., ARNOLDI, I., BARBIERI, G., COMANDATORE, F. & EPIS, S. 2021. Mosquito Trilogy: Microbiota, Immunity and Pathogens, and Their Implications for the Control of Disease Transmission. *Front. Microbiol.,* 12**,** 633.

GENDRIN, M., TURLURE, F., RODGERS, F. H., COHUET, A., MORLAIS, I. & CHRISTOPHIDES, G. K. 2017. The peptidoglycan recognition proteins PGRPLA and PGRPLB regulate *Anopheles* immunity to bacteria and affect infection by *Plasmodium*. *J. Innate Immun.,* 9**,** 333-342.

KAKANI, P., KAJLA, M., CHOUDHURY, T. P., GUPTA, L. & KUMAR, S. 2019. *Anopheles stephensi* Dual Oxidase silencing activates the Thioester-Containing Protein 1 pathway to suppress *Plasmodium* development. *J. Innate Immun.,* 11**,** 496-505.

KAUSHAL, A., GUPTA, K., SHAH, R. & VAN HOEK, M. L. 2016. Antimicrobial activity of mosquito cecropin peptides against Francisella. *Dev. Comp. Immunol.,* 63**,** 171-180.

KUMAR, A., SRIVASTAVA, P., SIRISENA, P., DUBEY, S. K., KUMAR, R., SHRINET, J. & SUNIL, S. 2018. Mosquito innate immunity. *Insects,* 9**,** 95.

KUMAR, S., MOLINA-CRUZ, A., GUPTA, L., RODRIGUES, J. & BARILLAS-MURY, C. 2010. A peroxidase/dual oxidase system modulates midgut epithelial immunity in *Anopheles gambiae*. *Science,* 327**,** 1644-1648.

LI, H.-H., CAI, Y., LI, J.-C., SU, M. P., LIU, W.-L., CHENG, L., CHOU, S.-J., YU, G.-Y., WANG, H.-D. & CHEN, C.-H. 2020. C-type lectins link immunological and reproductive processes in *Aedes aegypti*. *Iscience,* 23**,** 101486.

MAGALHAES, T., LEANDRO, D. C. & AYRES, C. F. J. 2010. Knock-down of REL2, but not defensin A, augments *Aedes aegypti* susceptibility to *Bacillus subtilis* and *Escherichia coli*. *Acta Tropica,* 113**,** 167-173.

MEISTER, S., AGIANIAN, B., TURLURE, F., RELÓGIO, A., MORLAIS, I., KAFATOS, F. C. & CHRISTOPHIDES, G. K. 2009. *Anopheles gambiae* PGRPLC-mediated defense against bacteria modulates infections with malaria parasites. *PLoS Pathog.,* 5**,** e1000542-e1000542.

MEISTER, S., KANZOK, S. M., ZHENG, X.-L., LUNA, C., LI, T.-R., HOA, N. T., CLAYTON, J. R., WHITE, K. P., KAFATOS, F. C. & CHRISTOPHIDES, G. K. 2005. Immune signaling pathways regulating bacterial and malaria parasite infection of the mosquito *Anopheles gambiae*. *Proc. Natl. Acad. Sci. U. S. A.,* 102**,** 11420-11425.

MUTURI, E. J., DUNLAP, C., RAMIREZ, J. L., ROONEY, A. P. & KIM, C.-H. 2019. Host blood-meal source has a strong impact on gut microbiota of *Aedes aegypti*. *FEMS Microbiol. Ecol.,* 95**,** fiy213.

MUTURI, E. J., NJOROGE, T. M., DUNLAP, C. & CÁCERES, C. E. 2021. Blood meal source and mixed blood-feeding influence gut bacterial community composition in *Aedes aegypti*. *Parasit. Vectors,* 14**,** 83.

MYLONAKIS, E., PODSIADLOWSKI, L., MUHAMMED, M. & VILCINSKAS, A. 2016. Diversity, evolution and medical applications of insect antimicrobial peptides. *Philos. Trans. R. Soc. Lond. B Biol. Sci.,* 371**,** 20150290-20150290.

RAIKHEL, A. S., KOKOZA, V. A., ZHU, J., MARTIN, D., WANG, S.-F., LI, C., SUN, G., AHMED, A., DITTMER, N. & ATTARDO, G. 2002. Molecular biology of mosquito vitellogenesis: from basic studies to genetic engineering of antipathogen immunity. *Insect Biochem. Mol. Biol.,* 32**,** 1275-1286.

RAMIREZ, J. L., MUTURI, E. J., BARLETTA, A. B. F. & ROONEY, A. P. 2019. The *Aedes aegypti* IMD pathway is a critical component of the mosquito antifungal immune response. *Dev. Comp. Immunol.,* 95**,** 1-9.

REYNOLDS, R. A., KWON, H. & SMITH, R. C. 2020. 20-hydroxyecdysone (20E) primes innate immune responses that limit bacteria and malaria parasite survival in *Anopheles gambiae*. *mSphere,* 5**,** e00983-00919.

RODGERS, F. H., GENDRIN, M. & CHRISTOPHIDES, G. K. 2017. The mosquito immune system and its interactions with the microbiota: Implications for disease transmission. *Arthropod Vector: Controller of Disease Transmission.*

ROY, S., SAHA, T. T., JOHNSON, L., ZHAO, B., HA, J., WHITE, K. P., GIRKE, T., ZOU, Z. & RAIKHEL, A. S. 2015. Regulation of gene expression patterns in mosquito reproduction. *PLoS Genet.,* 11**,** e1005450-e1005450.

RUSSELL, T. A., AYAZ, A., DAVIDSON, A. D., FERNANDEZ-SESMA, A. & MARINGER, K. 2021. Imd pathway-specific immune assays reveal NF-κB stimulation by viral RNA PAMPs in *Aedes aegypti* Aag2 cells. *PLoS Negl. Trop. Dis.,* 15**,** e0008524.

SAN DEKMAK, A., YANG, X., ZU DOHNA, H., BUCHON, N. & OSTA, M. A. 2021. The route of infection influences the contribution of key immunity genes to antibacterial defense in *Anopheles gambiae*. *J. Innate Immun.,* 13**,** 106-125.

SCHNITGER, A. K. D., KAFATOS, F. C. & OSTA, M. A. 2007. The melanization reaction is not required for survival of *Anopheles gambiae* mosquitoes after bacterial infections. *J. Biol. Chem.,* 282**,** 21884-21888.

TCHIOFFO, M. T., BOISSIÈRE, A., ABATE, L., NSANGO, S. E., BAYIBÉKI, A. N., AWONO-AMBÉNÉ, P. H., CHRISTEN, R., GIMONNEAU, G. & MORLAIS, I. 2016. Dynamics of Bacterial Community Composition in the Malaria Mosquito's Epithelia. *Front. Microbiol.,* 6**,** 1500.

TIAN, L., GUO, E., DIAO, Y., ZHOU, S., PENG, Q., CAO, Y., LING, E. & LI, S. 2010. Genome-wide regulation of innate immunity by juvenile hormone and 20-hydroxyecdysone in the *Bombyx* fat body. *BMC Genomics,* 11**,** 549-549.

TORRENT, M., PULIDO, D., RIVAS, L. & ANDREU, D. 2012. Antimicrobial peptide action on parasites. *Curr. Drug Targets,* 13**,** 1138-1147.

VERMA, P. & TAPADIA, M. G. 2015. Early gene Broad complex plays a key role in regulating the immune response triggered by ecdysone in the Malpighian tubules of *Drosophila melanogaster*. *Mol. Immunol.,* 66**,** 325-339.

VIZIOLI, J., BULET, P., CHARLET, M., LOWENBERGER, C., BLASS, C., MÜLLER, H. M., DIMOPOULOS, G., HOFFMANN, J., KAFATOS, F. & RICHMAN, A. 2000. Cloning and analysis of a cecropin gene from the malaria vector mosquito, *Anopheles gambiae*. *Insect Mol. Biol.,* 9**,** 75-84.

VIZIOLI, J., BULET, P., HOFFMANN, J. A., KAFATOS, F. C., MÜLLER, H.-M. & DIMOPOULOS, G. 2001a. Gambicin: a novel immune responsive antimicrobial peptide from the malaria vector *Anopheles gambiae*. *Proc. Natl. Acad. Sci. U. S. A.,* 98**,** 12630-12635.

VIZIOLI, J., RICHMAN, A. M., UTTENWEILER-JOSEPH, S., BLASS, C. & BULET, P. 2001b. The defensin peptide of the malaria vector mosquito *Anopheles gambiae*: antimicrobial activities and expression in adult mosquitoes. *Insect Biochem. Mol. Biol.,* 31**,** 241-248.

WANG, Q., REN, M., LIU, X., XIA, H. & CHEN, K. 2019. Peptidoglycan recognition proteins in insect immunity. *Mol. Immunol.,* 106**,** 69-76.

WARR, E., DAS, S., DONG, Y. & DIMOPOULOS, G. 2008. The Gram-Negative Bacteria-Binding Protein gene family: Its role in the innate immune system of *Anopheles gambiae* and in anti-*Plasmodium* defence. *Insect Mol. Biol.,* 17**,** 39-51.

WERLING, K. 2020. *The insect steroid hormone 20-hydroxyecdysone as a key regulator of the interplay between Anopheles gambiae and Plasmodium falciparum.* PhD, Harvard University.

XIAO, X., LIU, Y., ZHANG, X., WANG, J., LI, Z., PANG, X., WANG, P. & CHENG, G. 2014. Complement-related proteins control the flavivirus infection of *Aedes aegypti* by inducing antimicrobial peptides. *PLoS Pathog.,* 10**,** e1004027.

XIAO, X., YANG, L., PANG, X., ZHANG, R., ZHU, Y., WANG, P., GAO, G. & CHENG, G. 2017. A Mesh–Duox pathway regulates homeostasis in the insect gut. *Nat. Microbiol.,* 2**,** 17020.

YI, H.-Y., CHOWDHURY, M., HUANG, Y.-D. & YU, X.-Q. 2014. Insect antimicrobial peptides and their applications. *Appl. Microbiol. Biotechnol.,* 98**,** 5807-5822.

ZAKOVIC, S. & LEVASHINA, E. A. 2017. NF-κB-like signaling pathway REL2 in immune defenses of the Malaria vector *Anopheles gambiae*. *Front. Cell. Infect. Microbiol.,* 7**,** 258.

ZHANG, R., ZHU, Y., PANG, X., XIAO, X., ZHANG, R. & CHENG, G. 2017. Regulation of antimicrobial peptides in Aedes aegypti Aag2 cells. *Front. Cell. Infect. Microbiol.,* 7**,** 22.

ZHANG, W., TETTAMANTI, G., BASSA, T., HERYANTO, C., ELEFTHERIANOS, I. & MOHAMED, A. 2021. Regulators and signalling in insect antimicrobial innate immunity: Functional molecules and cellular pathways. *Cell. Signal.,* 83**,** 110003.

CHAPTER 5

Concluding summary

5.1 Re-statement of the problem

Two mosquito-related traits that favor malaria transmission in a region are the number of mosquitoes present, and their ability to sustain *Plasmodium* development (Shaw and Catteruccia, 2018). Hence, the molecular processes that regulate these traits are commonly targeted by mosquito control interventions (Cansado-Utrilla et al., 2021, Shaw and Catteruccia, 2018). One of these molecular processes is the 20E signaling pathway, which is activated when the steroid hormone 20E binds to its receptor, EcR (Ekoka et al., 2021). With respect to vector abundance, studies in *An. gambiae* and *Ae. aegypti* have revealed that the 20E signaling pathway regulates mosquitoes physiological processes such as mating, blood feeding, digestion, vitellogenesis, egg production and fertility —all of which ultimately affect reproduction and thus mosquitoes abundance (Table 1.2).

As described earlier (section 1.5.1), several questions remain unanswered regarding how the 20E signaling pathway regulates *Anopheles* mosquitoes abundance. For example, whether the 20E signaling pathway regulates *An. arabiensis* vitellogenesis, fecundity, fertility, and gut bacteria proliferation, has never been investigated. In this project, the above questions were addressed using a South African strain of *An. arabiensis*. Here, the principal findings are reviewed and their application to mosquito control discussed. Furthermore, outstanding questions that should be

addressed to better understand the tripartite relationship between *An. arabiensis* gut bacteria, 20E signaling pathway, and reproduction, are also outlined.

5.2 Key findings

5.2.1 *EcR* depletion compromises *An. arabiensis* reproductive output

To determine whether the 20E signaling pathway regulates *An. arabiensis* reproductive output, this pathway was blocked —by silencing *EcR*— and several phenotypes were assessed such as the expression of four yolk genes (as an indication of vitellogenesis), fecundity, and fertility. Consistent with previous reports in *Ae. aegypti* (Cho et al., 1995, Raikhel et al., 2002), *EcR* expression in *An. arabiensis* was induced during vitellogenesis, reaching a peak at 24 hPBM (Figure 2.2). As expected, not only did *EcR*-depleted mosquitoes contained fewer *EcR* transcripts at 24 hPBM, but they also showed a reduced expression of two yolk genes — *vitellogenin* and *VCP*— at the same time point (Figure 2.8). Likewise, previous studies reported a decrease in *vitellogenin* and *VCP* transcript levels in *EcR*-depleted *An. gambiae* or *Ae. aegypti* (Baldini et al., 2013, Roy et al., 2015, Werling et al., 2019). Unlike previous work, the expression of the remaining two yolk genes, *lipophorin* and *VCB*, was not significantly affected after *EcR* silencing. It is possible that the impact of *EcR* depletion on *lipophorin* expression was undetectable because it was measured in the whole mosquito instead of the fat body where they are synthesized (Sun et al., 2000, Werling et al., 2019). Likewise, studies that demonstrated a reduction in *VCB* expression post *EcR* silencing measured its expression in the fat body (Roy et al., 2015).

With respect to *An. arabiensis* reproductive output in the first gonotrophic cycle, *EcR* silencing neither affected the number of eggs laid, nor the percentage of females

that laid eggs (Figure 2.7). Similarly, Maharaj (2021) found that *EcR* depletion in *An. funestus* does not affect the number of eggs laid, but rather the total number of eggs developed (i.e., the sum of eggs retained in the ovaries and those laid) (Maharaj, 2021). While Werling et al. (2019) did not measure the number of eggs oviposited after *EcR* silencing, they reported that *EcR* silencing also reduces the number of eggs developed by *An. gambiae* females. Does it mean that *EcR* silencing has no effect on oviposition? According to a report in *Ae. aegypti*, silencing *EcR* only affects oviposition in the second gonotrophic cycle (Bryant and Raikhel, 2011). Therefore, *EcR* depletion may affect *An. arabiensis* oviposition in the second gonotrophic cycle, but it should be confirmed with further experiments. Such experiments could compare the number of eggs deposited (laid) between dsEcR- and dsGFP- injected mosquitoes in at least 3-5 gonotrophic cycles to see at which (and for how many) gonotrophic cycles oviposition is affected. Nonetheless, a reduction in fertility was observed in the first gonotrophic cycle (Figure 2.7), in agreement with studies in *An. funestus* (Maharaj et al., 2022) and *An. gambiae* (Gabrieli et al., 2014) showing that blocking the 20E signaling pathway in adult females reduce their eggs fertility.

How are the above-mentioned results applicable to *An. arabiensis* chemical control? Since manipulating *EcR* expression compromised *An. arabiensis* reproductive output (by reducing its fertility), one can expect that chemicals which target the 20E signaling pathway could be an asset for *An. arabiensis* control. These chemicals may include 20E agonists such as methoxyfenozide and halofenozide, which have already shown promising results in *An. gambiae* (section 1.4.1). These chemicals could be used (i) in rotation with current insecticides as part of IRS and ITNs programmes to form part of an insecticide resistance management plan, (ii) as part of attractive toxic sugar baits (ATSBs), or (iii) as larvicides.

5.2.2 In *An. arabiensis*, the 20E signaling pathway may regulate the gut microbiome homeostasis

Given a previous report that 20E injection compromises *E. coli* proliferation in *An. gambiae* (Reynolds et al., 2020), the relationship between *An. arabiensis* 20E signaling pathway and its commensal gut bacteria was investigated. *EcR* transcript abundance was reduced in antibiotic-fed *An. arabiensis* females (Figure 3.3b). Since the antibiotic cocktail used (penicillin, streptomycin, gentamicin) may target both Gram-positive and Gram-negative bacteria, a separate experiment was conducted to determine whether both bacterium types influence *EcR* expression. While injecting *An. arabiensis* with *E. coli* decreased their *EcR* expression, no effect was observed when the mosquitoes were injected with *S. aureus*, suggesting that only Gram-negative bacteria influence *EcR* expression (Figure 4.6). However, more experiments should be conducted with different species of Gram-positive bacteria (and different doses of bacteria) before concluding that these latter do not influence *EcR* expression. In addition, a different mode of bacterial administration (e.g. oral feeding) could be tested. This latter consists in supplementing the sugar meal of mosquitoes with the desired bacteria so that when they feed, they also ingest the bacteria. This mode of bacterial administration appears to have more profound effects on the mosquito transcriptome (San Dekmak et al., 2021).

To assess whether the 20E signaling pathway regulates bacterial proliferation by immune mechanisms, *An. arabiensis* females were injected with 20E and the expression of ten immune genes was measured at different time points post 20E injection. These included five AMPs (*cecropin-1*, *cecropin-3*, *defensin-1*, *gambicin-1*, *attacin-c*), three Imd pathway genes (*akirin*, *Imd* and *rel2*), as well as *mesh* and *duox*. From the results obtained (Figures 4.3-4.5), the following model was proposed (Figures 4.7). After taking a blood meal, mosquitoes 20E titers increase and this boost

in 20E signaling initially decreases the expression of three AMPs (*cec-1*, *cec-3*, and *attacin*). As a result, the gut bacteria proliferate rapidly. However, to ensure that this proliferation does not become detrimental to the mosquito fitness, the remaining AMPs (and perhaps other immune responses) are not down-regulated. Overall, this model suggests that *An. arabiensis* gut bacteria homeostasis is regulated by 20E signaling via the Imd pathway. Notably, it is important to mention that no genes from either the Toll or the Jak-STAT pathways were investigated here, so future experiments should also be conducted to identify whether a link exists between the 20E signaling pathway and these two immune pathways. These experiments could include silencing *EcR* (or injecting 20E) and measuring the expression of key players of the Toll pathway (e.g. *Relish-1*, *MyD88*) and the Jak-Stat pathway (e.g. *STAT, dome*).

From a biomedical research perspective, while the gut bacteria have been linked to mosquitoes susceptibility to *Plasmodium* infection (section 1.2.3), very little is known on the molecular mechanisms underlying this relationship. The findings presented in this section uncover that the gut bacteria could influence mosquitoes vector competence by modulating their 20E signaling pathway. Alternatively, the 20E signaling pathway could influence mosquitoes susceptibility to *Plasmodium* infection by modulating their gut microbiome. While this looks like a *"chicken or egg —which came first*" enigma, further research may allow us to better understand the tripartite relationship between 20E signaling, vector competence and the gut microbiome.

5.3 Future perspectives

This thesis provided evidence that disturbing the 20E signaling pathway in the malaria vector *An. arabiensis* compromises its reproductive output, by reducing the fertility of its eggs and reducing the expression of key yolk genes. For this reason, 20E agonists

may be effective against *An. arabiensis*. However, before the use of these chemicals can be formalized, several studies are needed to investigate their resistance mechanisms, cross-resistance with the insecticides currently in use, and the possibility to use these chemicals as part of attractive toxic sugar baits (ATSB) to target mosquitoes outdoors. Besides, while the phylogenetic results reported in chapter 2 suggest that EcR function is conserved in *Anopheles* mosquitoes, additional field trials should confirm that 20E agonists can target all these *Anopheles* species simultaneously. A recent study revealed that *E. coli* infected *An. arabiensis* mosquitoes were less susceptible to the pyrethroid deltamethrin (Barnard et al., 2019). Here, *E. coli*-injected *An. arabiensis* had fewer *EcR* transcripts (Chapter 4). Does it mean that the 20E signaling pathway regulates deltamethrin resistance in *An. arabiensis*? If so, this will be consistent with previous reports showing that reducing 20E titers in *Culex pipiens pallens* increases their susceptibility to deltamethrin (Sun et al., 2019, Ye et al., 2017). Besides, while a link between 20E signaling and the gut microbiome was established in this study, it would be interesting to investigate if 20E signaling also regulates the salivary glands and ovaries microbiomes, as these tissues are also important for mosquitoes vectorial capacity. Finally, the model proposed here to explain how the 20E signaling pathway regulates the gut bacterial homeostasis focused on the Imd pathway. However, the Toll pathway has also been implicated in mosquitoes anti-bacterial immunity. Therefore, the relationship between the Toll pathway and the 20E signaling pathway should also be investigated.

5.4 References

BALDINI, F., GABRIELI, P., SOUTH, A., VALIM, C., MANCINI, F. & CATTERUCCIA, F. 2013. The interaction between a sexually transferred steroid hormone and a female protein regulates oogenesis in the malaria mosquito *Anopheles gambiae*. *PLoS Biol.,* 11**,** e1001695-e1001695.

BARNARD, K., JEANRENAUD, A. C., BROOKE, B. D. & OLIVER, S. V. 2019. The contribution of gut bacteria to insecticide resistance and the life histories of the major malaria vector *Anopheles arabiensis* (Diptera: Culicidae). *Sci. Rep.,* 9**,** 1-11.

BRYANT, B. & RAIKHEL, A. S. 2011. Programmed autophagy in the fat body of *Aedes aegypti* is required to maintain egg maturation cycles. *PLoS One,* 6**,** e25502-e25502.

CANSADO-UTRILLA, C., ZHAO, S. Y., MCCALL, P. J., COON, K. L. & HUGHES, G. L. 2021. The microbiome and mosquito vectorial capacity: rich potential for discovery and translation. *Microbiome,* 9**,** 1-11.

CHO, W.-L., KAPITSKAYA, M. Z. & RAIKHEL, A. S. 1995. Mosquito ecdysteroid receptor: analysis of the cDNA and expression during vitellogenesis. *Insect Biochem. Mol. Biol.,* 25**,** 19-27.

EKOKA, E., MAHARAJ, S., NARDINI, L., DAHAN-MOSS, Y. & KOEKEMOER, L. L. 2021. 20-Hydroxyecdysone (20E) signaling as a promising target for the chemical control of malaria vectors. *Parasit. Vectors,* 14**,** 86.

GABRIELI, P., KAKANI, E. G., MITCHELL, S. N., MAMELI, E., WANT, E. J., ANTON, A. M., SERRAO, A., BALDINI, F. & CATTERUCCIA, F. 2014. Sexual transfer of the steroid hormone 20E induces the postmating switch in *Anopheles gambiae*. *Proc. Natl. Acad. Sci. U. S. A.,* 111**,** 16353-16358.

MAHARAJ, S. 2021. Impact of *Ecdysone receptor* knockdown on *Anopheles funestus* longevity, reproductive success and *Plasmodium falciparum* susceptibility (unpublished work). South Africa: University of the Witwatersrand.

MAHARAJ, S., EKOKA, E., ERLANK, E., NARDINI, L., READER, J., BIRKHOLTZ, L.-M. & KOEKEMOER, L. L. 2022. The ecdysone receptor regulates several key physiological factors in Anopheles funestus. *Malar. J.,* 21**,** 1-13.

RAIKHEL, A. S., KOKOZA, V. A., ZHU, J., MARTIN, D., WANG, S.-F., LI, C., SUN, G., AHMED, A., DITTMER, N. & ATTARDO, G. 2002. Molecular biology of mosquito vitellogenesis: from basic studies to genetic engineering of antipathogen immunity. *Insect Biochem. Mol. Biol.,* 32**,** 1275-1286.

REYNOLDS, R. A., KWON, H. & SMITH, R. C. 2020. 20-hydroxyecdysone (20E) primes innate immune responses that limit bacteria and malaria parasite survival in *Anopheles gambiae*. *mSphere,* 5**,** e00983-00919.

ROY, S., SAHA, T. T., JOHNSON, L., ZHAO, B., HA, J., WHITE, K. P., GIRKE, T., ZOU, Z. & RAIKHEL, A. S. 2015. Regulation of gene expression patterns in mosquito reproduction. *PLoS Genet.,* 11**,** e1005450-e1005450.

SAN DEKMAK, A., YANG, X., ZU DOHNA, H., BUCHON, N. & OSTA, M. A. 2021. The route of infection influences the contribution of key immunity genes to antibacterial defense in *Anopheles gambiae*. *J. Innate Immun.,* 13**,** 106-125.

SHAW, W. R. & CATTERUCCIA, F. 2018. Vector biology meets disease control: Using basic research to fight vector-borne diseases. *Nat. Microbiol.,* 4**,** 20-34.

SUN, J., HIRAOKA, T., DITTMER, N. T., CHO, K.-H. & RAIKHEL, A. S. 2000. Lipophorin as a yolk protein precursor in the mosquito, *Aedes aegypti*. *Insect Biochem. Mol. Biol.,* 30**,** 1161-1171.

SUN, X., XU, N., XU, Y., ZHOU, D., SUN, Y., WANG, W., MA, L., ZHU, C. & SHEN, B. 2019. A novel miRNA, miR-13664, targets CpCYP314A1 to regulate deltamethrin resistance in *Culex pipiens pallens*. *Parasitology,* 146**,** 197.

WERLING, K., SHAW, W. R., ITOE, M. A., WESTERVELT, K. A., MARCENAC, P., PATON, D. G., PENG, D., SINGH, N., SMIDLER, A. L., SOUTH, A., DEIK, A. A., MANCIO-SILVA, L., DEMAS, A. R., MARCH, S., CALVO, E., BHATIA, S. N., CLISH, C. B. & CATTERUCCIA, F. 2019. Steroid hormone function controls non-competitive *Plasmodium* development in *Anopheles*. *Cell,* 177**,** 315-325.

YE, W., LIU, X., GUO, J., SUN, X., SUN, Y., SHEN, B., ZHOU, D. & ZHU, C. 2017. piRNA-3878 targets P450 (CpCYP307B1) to regulate pyrethroid resistance in *Culex pipiens pallens*. *Parasitol. Res.,* 116**,** 2489-2497.

Supplementary Figures

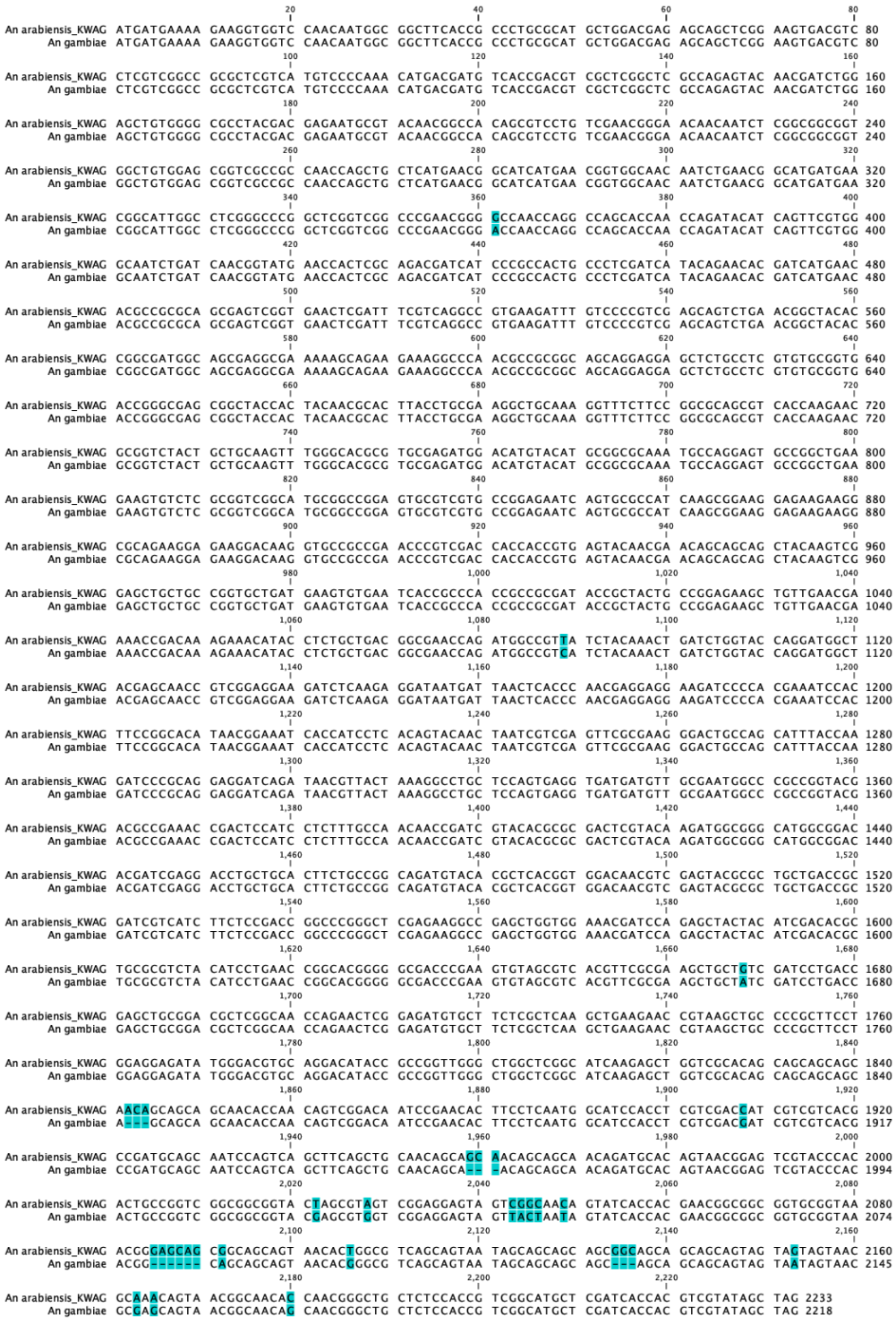

Figure S1: Nucleotide sequence alignment of *An. gambiae* and *An. arabiensis* *EcR* sequences (open-reading frame). The alignment was performed with CLC Genomics Workbench demo version 11.0.1 (CLC Bio, Qiagen), which uses a progressive algorithm to compute alignments. KWAG *EcR* sequence is the one obtained in this study, while *An. gambiae EcR* sequence was retrieved from VectorBase (Accession no: AGAP028634). The numbers on the top and side of the

sequences indicate the residue position. Non-identical residues are highlighted in blue. The alignment shows that both sequences are 98.6% similar, with 32 mismatches (blue residues) out of 2,233 residues.

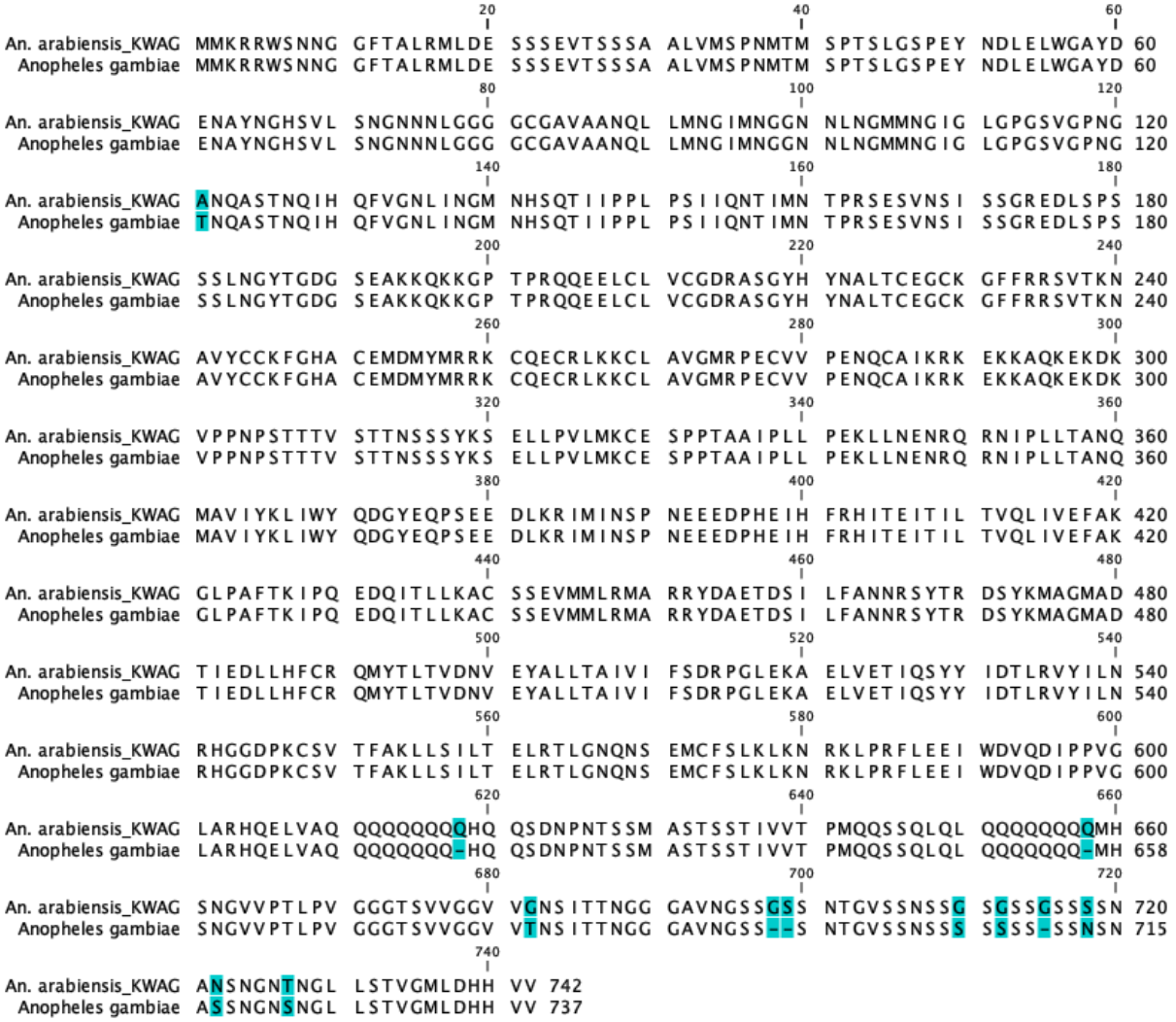

Figure S2: Amino acid sequence alignment of *An. gambiae* and *An. arabiensis EcR* sequences. The alignment was performed with CLC Genomics Workbench demo version 11.0.1 (CLC Bio, Qiagen), which uses a progressive algorithm to compute alignments. KWAG *EcR* sequence is the one obtained in this study, while *An. gambiae EcR* sequence was retrieved from VectorBase (Accession no: AGAP028634). The numbers on the top and side of the sequences indicate the residue position. Non-identical residues are highlighted in blue. The alignment shows that both sequences are 98.4% similar, with only 12 mismatches (blue residues) out of 742 residues

A

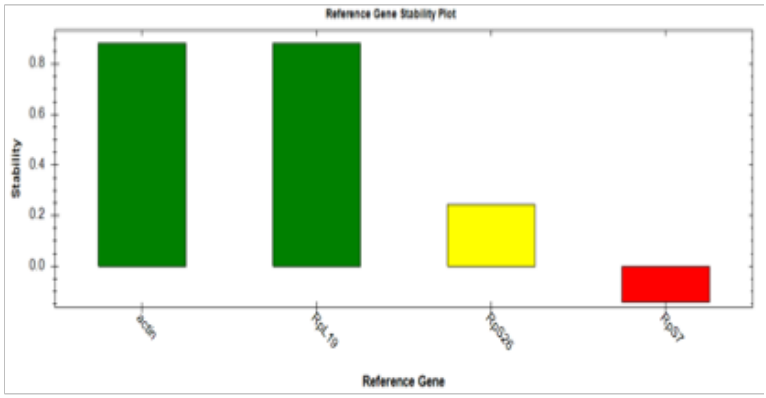

B

Order	Gene Name	Evaluation	Avg M Value	Stability (Ln(1/AvgM))	# Samples
1	actin	Ideal	0.414	0.883	4
2	RpL19	Ideal	0.414	0.883	4
3	RpS26	Acceptable	0.783	0.244	4
4	RpS7	Unstable	1.154	-0.143	4

Figure S3: Evaluation of four candidate reference genes for the vitellogenesis time point experiment (Section 2.3.2). Four genes were tested for their stable expression at the different time points selected post blood meal. After performing a qPCR experiment with cDNA from these different time points, we used the geNorm algorithm (incorporated in the CFX maestro software) to determine the stability coefficient of each of the test reference genes. A stable reference should have an M-value below 0.5 (Taylor et al., 2010). (A) the stability plot shows that both Actin and RpL19 have the highest stability and they are equally stable. (B) This is confirmed by their M-value, which is below 0.5, as expected for housekeeping genes in eukaryotes. Therefore, for the time-point experiment, gene expression was normalized to *RpL19* using the $2^{-\Delta\Delta Cq}$ method.

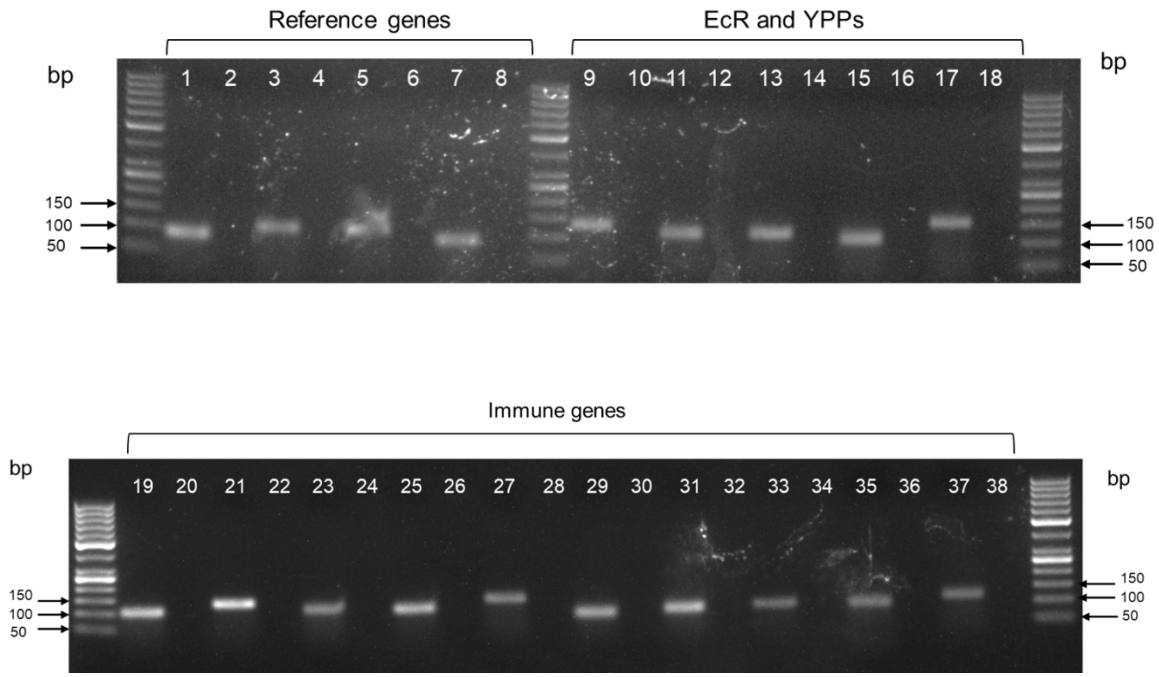

Lane	Amplicon	Expected size (bp)	Lane	Amplicon	Expected size (bp)	Lane	Amplicon	Expected size (bp)	Lane	Amplicon	Expected size (bp)
1	RpL19	85	11	VCP	108	21	Cec-3	124	31	Att	85
2	NTC		12	NTC		22	NTC		32	NTC	
3	RpS7	109	13	Lp	114	23	Mesh	100	33	Imd	95
4	NTC		14	NTC		24	NTC		34	NTC	
5	RpS26	108	15	VCB	102	25	Gamb-1	98	35	Rel-2	96
6	NTC		16	NTC		26	NTC		36	NTC	
7	Actin	85	17	Vg	149	27	Duox	130	37	Akr	115
8	NTC		18	NTC		28	NTC		38	NTC	
9	EcR	117	19	Cec-1	98	29	Def-1	80			
10	NTC		20	NTC		30	NTC				

Figure S4: Analysis of all qPCR products on a 1% (w/v) agarose/TAE gel. For size determination, a 50 bp DNA ladder was used. NTC, no-template control. No contamination was detected.

Highlighted in yellow. Primers for amplification of entire EcR coding sequence (target region: 2,218 bp); start and stop codon are indicated in bold italics.
Blue- dsRNA target region (492 bp). Underlined are primer binding sites
Red – qPCR target region (117 bp). Underlined are primer binding sites

CGCAAG***ATG***ATGAAAAGAAGGTGGTCCAACAATGGCGGCTTCACCGCCCTGCGCATGCTGGACG
AGAGCAGCTCGGAAGTGACGTCCTCGTCGGCCGCGCTCGTCATGTCCCCAAACATGACGATGTC
ACCGACGTCGCTCGGCTCGCCAGAGTACAACGATCTGGAGCTGTGGGGCGCCTACGACGAGAA
TGCGTACAACGGCCACAGCGTCCTGTCGAACGGGAACAACAATCTCGGCGGCGGTGGCTGTGG
AGCGGTCGCCGCCAACCAGCTGCTCATGAACGGCATCATGAACGGTGGCAACAATCTGAACGGC
ATGATGAACGGCATTGGCCTCGGGCCCGGCTCGGTCGGCCCGAACGGCGCCAACCAGGCCAGC
ACCAACCAGATACATCAGTTCGTGGGCAATCTGATCAACGGTATGAACCACTCGCAGACGATCAT
CCCGCCACTGCCCTCGATCATACAGAACACGATCATGAACACGCCGCGCAGCGAGTCGGTGAAC
TCGATTTCGTCAGGCCGTGAAGATTTGTCCCCGTCGAGCAGTCTGAACGGCTACACCGGCGATG
GCAGCGAGGCGAAAAAGCAGAAGAAAGGCCCAACGCCGCGGCAGCAGGAGGAGCTCTGCCTC
GTGTGCGGTGACCGGGCGAGCGGCTACCACTACAACGCACTTACCTGCGAAGGCTGCAAAGGT
TTCTTCCGGCGCAGCGTCACCAAGAACGCGGTCTACTGCTGCAAGTTTGGGCACGCGTGCGAGA
TGGACATGTACATGCGGCGCAAATGCCAGGAGTGCCGGCTGAAGAAGTGTCTCGCGGTCGGCA
TGCGGCCGGAGTGCGTCGTGCCGGAGAATCAGTGCGCCATCAAGCGGAAGGAGAAGAAGGCGC
AGAAGGAGAAGGACAAGGTGCCGCCGAACCCGTCGACCACCACCGTGAGTACAACGAACAGCA
GCAGCTACAAGTCGGAGCTGCTGCCGGTGCTGATGAAGTGTGAATCACCGCCCACCGCCGCGA
TACCGCTACTGCCGGAGAAGCTGTTGAACGAAAACCGACAAAGAAACATACCTCTGCTGACGGC
GAACCAGATGGCCGTTATCTACAAACTGATCTGGTACCAGGATGGCTACGAGCAACCGTCGGAG
GAAGATCTCAAGAGGATAATGATTAACTCACCCAACGAGGAGGAAGATCCCCACGAAATCCACTT
CCGGCACATAACGGAAATCACCATCCTCACAGTACAACTAATCGTCGAGTTCGCGAAGGGACTG
CCAGCATTTACCAAGATCCCGCAGGAGGATCAGATAACGTTACTAAAGGCCTGCTCCAGTGAGGT
GATGATGTTGCGAATGGCCCGCCGGTACGACGCCGAAACCGACTCCATCCTCTTTGCCAACAAC
CGATCGTACACGCGCGACTCGTACAAGATGGCGGGCATGGCGGACACGATCGAGGACCTGCTG
CACTTCTGCCGGCAGATGTACACGCTCACGGTGGACAACGTCGAGTACGCGCTGCTGACCGCGA
TCGTCATCTTCTCCGACCGGCCCGGGCTCGAGAAGGCCGAGCTGGTGGAAACGATCCAGAGCT
ACTACATCGACACGCTGCGCGTCTACATCCTGAACCGGCACGGGGGCGACCCGAAGTGTAGCG
TCACGTTCGCGAAGCTGCTGTCGATCCTGACCGAGCTGCGGACGCTCGGCAACCAGAACTCGGA
GATGTGCTTCTCGCTCAAGCTGAAGAACCGTAAGCTGCCCCGCTTCCTGGAGGAGATATGGGAC
GTGCAGGACATACCGCCGGTTGGGCTGGCTCGGCATCAAGAGCTGGTCGCACAGCAGCAGCAG
CAACACCAACAGTCGGACAATCCGAACACTTCCTCAATGGCATCCACCTCGTCGACCATCGTCGT
CACGCCGATGCAGCAATCCAGTCAGCTTCAGCTGCAACAGCAGCAACAGATGCACAGTAACGGA
GTCGTACCCACACTGCCGGTCGGCGGCGGTACTAGCGTAGTCGGAGGAGTAGTCGGCAACAGT
ATCACCACGAACGGTGCGGTAAACGGCAGCAGCGGCAGCAGTAACACTGGCGTCAGCAGTAATA
GCAGCAGCAGCAGCAGCAGCAGTAGTAGTAGTAACGCAAACAGTAACGGCAACACCAACGGGCT
GCTCTCCACCGTCAGCATGCTCGATCACCACGTCGTA***TAG***CTAGCGTAGGGCA

Figure S5: *EcR* primer binding location. *Anopheles arabiensis* full *EcR* coding sequence (downloaded from VectorBase) that served as template for primers design. The qPCR target region was selected outside of the dsRNA target region, to ensure that during qPCR, I would not measure dsRNA, but only *An. arabiensis EcR*.

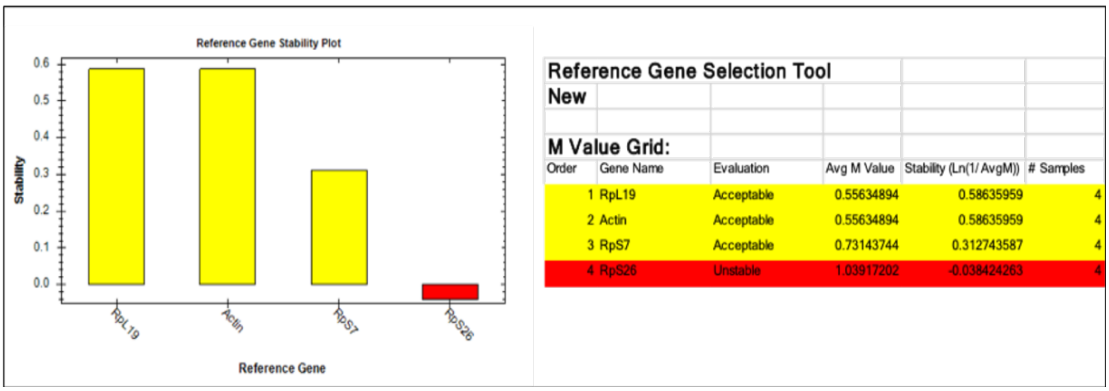

Reference Gene Selection Tool

New

M Value Grid:

Order	Gene Name	Evaluation	Avg M Value	Stability (Ln(1/ AvgM))	# Samples
1	RpL19	Acceptable	0.55634894	0.58635959	4
2	Actin	Acceptable	0.55634894	0.58635959	4
3	RpS7	Acceptable	0.73143744	0.312743587	4
4	RpS26	Unstable	1.03917202	-0.038424263	4

Figure S6: Selection of reference genes for RNAi experiments. The expression of the same four candidate reference genes (actin, RpL19, RpS26, and RpS7) was evaluated for stability during RNAi experiments using a method similar as above for the time-point experiments. The only difference here is that the expression of the four candidate reference genes was analyzed in dsEcR- and dsGFP-injected mosquitoes, at two days post-injection (dpi) since previous studies measured EcR knockdown at 2 dpi (Werling et al., 2019). Based on the geNorm analysis, *RpL19*, *Actin*, and *RpS7* were stably expressed between the dsEcR- and dsGFP- injected mosquitoes. RpS7 and RpL19 were used in all the RNAi experiments to normalize the expression values.

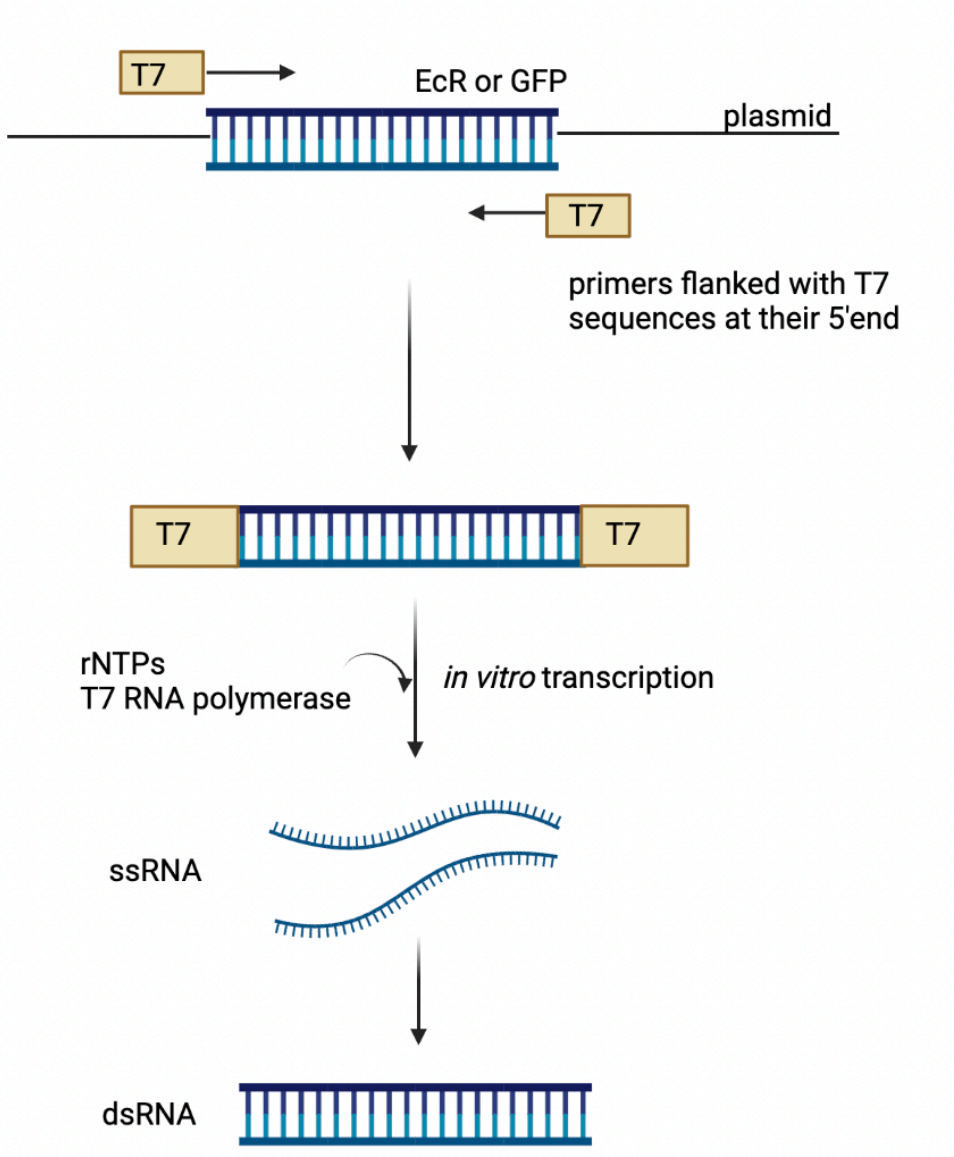

Figure S7: Process of *in vitro* transcription. Plasmids containing the EcR or GFP target sequence (~500 bp) are used as templates in a PCR reaction with primers flanked with the T7 promoter sequence at their 5' ends. The resulting dsDNA PCR product is then used as template for *in vitro* transcription with the RNA polymerase. The produced two single-stranded RNA (ssRNAs) strands then annealed to produce double-stranded RNA (dsRNA).

Supplementary Tables

Table S1
Accession numbers for all the mosquito primers used in this thesis.

	Gene name	VectorBase ID*
RpL19	Ribosomal Protein L19	AARA005369
RpS7	Ribosomal Protein S7	AARA000046
EcR	Ecdysone Receptor	AARA015604
RpS26	Ribosomal protein S26	AARA003197
Actin	ß-actin	AARA002780
Lp	Lipophorin	AARA007073
Vg	Vitellogenin	AARA011601
VCB	Cathepsin b-like protease	AARA006453
VCP	Vitellogenin carboxypeptidase	AARA008075
Mesh	Mesh	AARA010496
Duox	Dual oxidase	AARA003798
Cec-1	Cecropin-1	AARA015680
Cec-3	Cecropin-3	AARA010362
Gamb-1	Gambicin-1	AARA010954
Def-1	Defensin-1	AARA006271
Att-C	Attacin-C	AARA005779
Imd	Immune deficiency	AARA003561
Rel2	Relish 2	AARA009084
akirin	akirin	AARA009142

*The IDs were retrieved from VectorBase website in July 2020.

Table S2
Efficiency and annealing temperature of all mosquito qPCR primer pairs mentioned in this thesis.

	qPCR efficiency (%)	R^2-value (standard curve)	Annealing temperature (°C)
RpL19	100.5	0.989	55
RpS7	97.0	0.992	55
EcR	108.9	0.975	54
RpS26	96.9	0.997	55
Actin	99.1	0.985	54
Lp	90.0	0.979	55
Vg	101.8	0.987	47
VCB	97.4	0.987	55
VCP	99.8	0.980	55
Mesh	109.1	0.984	54
Duox	95.3	0.980	54
Cec-1	100.5	0.996	54
Cec-3	93.2	0.994	54
Gamb-1	105.9	0.991	54
Def-1	95.6	0.980	54
Att	106.9	0.980	54
Imd	94.7	0.981	54
Rel2	94.8	0.982	54
Akirin	96.8	0.987	54
Flavo 16S	N/A	N/A	54
Entero 16S	N/A	N/A	60
Aceto 16S	N/A	N/A	54

Table S3

Output results (MEGA v.10.2.4) from computing the most appropriate substitution model to account for multiple comparisons at the same residue. Models with the lowest Bayesian Information Criterion (BIC) are considered the most suitable. The analysis was made from 12 amino acid sequences.

Model	BIC		Model	BIC
JTT+G	16371,60404		cpREV+G+F	16782,12282
JTT+G+I	16380,54237		cpREV+G+I	16793,44402
JTT+G+F	16408,51759		rtREV+I+F	16820,72307
JTT+G+I+F	16417,45549		JTT	16828,38369
Dayhoff+G+F	16446,50403		cpREV+G+I+F	16832,63877
Dayhoff+G	16449,57458		LG+I	16848,79271
Dayhoff+G+I+F	16455,44192		cpREV+G	16857,92442
Dayhoff+G+I	16458,51246		JTT+F	16871,46566
LG+G+F	16474,9964		rtREV+I	16888,35843
WAG+G	16483,25412		Dayhoff	16903,33472
LG+G+I+F	16483,93417		Dayhoff+F	16919,55564
WAG+G+I	16492,19226		WAG	16930,71622
WAG+G+F	16502,07104		WAG+F	16966,22006
WAG+G+I+F	16511,00873		mtREV24+I+F	16983,59265
rtREV+G+F	16522,3074		LG+F	16986,09948
rtREV+G+I+F	16531,24512		rtREV+F	17041,43668
LG+G	16559,18936		mtREV24+G	17060,7483
LG+G+I	16568,12728		mtREV24+G+I	17069,68634
rtREV+G	16594,55601		LG	17071,18686
rtREV+G+I	16603,49384		rtREV	17120,48062
mtREV24+G+F	16619,57097		cpREV+I+F	17204,40597
mtREV24+G+I+I	16628,50895		cpREV+I	17222,55097
JTT+I	16647,78731		mtREV24+F	17237,85498
JTT+I+F	16691,72442		cpREV+F	17302,83276
Dayhoff+I	16720,02234		cpREV	17318,41311
Dayhoff+I+F	16725,22382		mtREV24+I	17459,2687
WAG+I	16745,64383		mtREV24	17756,764
WAG+I+F	16773,49712			
LG+I+F	16773,9708			

Abbreviations: TR = General Time Reversible; JTT = Jones-Taylor-Thornton; rtREV = General reverse transcriptase; cpREV = General reversible chloroplast; mtREV24 = General reversible mitochondria

Table S4
Sequencing results of all qPCR products.

			BLASTn results (against *An. arabiensis* transcriptome database on VectorBase)		
Putative qPCR product	**Expected amplicon size (bp)**	**Number of bases sequenced**	**Alignment length**	**% identity**	**Target name and ID (as of 25.08.20)**
RpL19	85	86	86/86	100	RpL19 AARA005369-RA
RpS7	109	109	109/109	100	RpS7 AARA000046-RA
EcR	117	128	128/128	92.2	Ecdysone receptor AARA015604-RA
RpS26	108	110	108/110	100	RpS26 AARA003197-RA
Actin	85	87	87/87	93.1	Actin AARA002780-RA
Lp	114	115	115/115	100	Lp AARA007073-RA
Vg	149	150	149/150	99.3	Vg AARA011601-RA
VCB	102	104	104/104	98.1	VCB AARA006453-RA
VCP	108	110	109/110	100	VCP AARA008075-RA
Mesh	100	101	101/101	98	Mesh AARA010496-RA
Duox	130	133	132/133	100	Duox AARA003798-RA
Cec-1	98	100	100/100	97	Cec-1 AARA015680-RA
Cec-3	124	126	125/126	99.2	Cec-3 AARA010362-RA
Gamb-1	98	95	95/95	98.9	Gamb-1 AARA010954-RA
Def-1	80	192	192/192	98.4	Def-1 AARA006271-RA
Att	85	83	83/83	98.8	Att AARA005779-RA
Imd	95	84	84/84	98.8	Imd AARA003561-RA
Rel-2	96	103	95/103	96.9	Rel2 AARA009084-RA
Akirin	115	117	115/117	100	Akirin AARA009142-RA

Table S5

Pilot study to determine whether 3 or 4 days are required by *An. arabiensis* (KWAG strain) to achieve 100% mating success. For this experiment 20 females and 20 males were placed in cages (10 females + 10 males per cage) from the day of emergence and fed on 10% sugar water *ad libitum*. In cage 1, the mosquitoes mated for 3 days. In cage 2, the mosquitoes mated for 4 days. After the specified time, the spermatheca of females was dissected to determine whether it contained sperm. The experiment was performed in 2 biological replicates. The percentage mating is calculated as the number of females mated relative to the total number of females in that group.

	Mating time (3 days)	**Mating time (4 days)**
	Mated? (Yes/No)	**Mated? (Yes/No)**
1	Yes	Yes
2	Yes	Yes
3	Yes	Yes
4	No	Yes
5	No	Yes
6	Yes	Yes
7	Yes	Yes
8	Yes	Yes
9	Yes	Yes
10	Yes	Yes
11	No	Yes
12	Yes	Yes
13	Yes	Yes
14	Yes	Yes
15	Yes	Yes
16	No	Yes
17	Yes	Yes
18	Yes	Yes
19	Yes	Yes
20	No	Yes
Mating success rate (%)	**75**	**100**

Table S6

Unpaired *t*-test results associated with Figure 2.9

Abbreviation: dpi = day post dsEcR injection.

		Unpaired t-test: Gene expression in dsEcR-injected mosquitoes versus dsGFP-injected mosquitoes
	dpi	***p*-values**
Acetobacteriaceae	1	0.377361
	2	0.400018
	3	0.538561
Flavobacteriaceae	1	0.379165
	2	0.467374
	3	0.943064
Enterobacteriaceae	1	0.373022
	2	0.466994
	3	0.233972
Eubacteria	1	0.170412
	2	0.589296
	3	0.136411

Table S7

In the fruitfly *Drosophila melanogaster*, the 20E-mediated regulation of AMPs may necessitate a pathogen challenge. Abbreviations: PGN = peptidoglycan, a component of bacteria cell walls.

	D. melanogaster	***D. melanogaster***	***D. melanogaster***	***D. melanogaster***	***D. melanogaster***	***D. melanogaster***	***D. melanogaster***
20E manipulation	-	-	20E	20E	dsEcR	dsUSP	20E
Immune challenge	-	+ (PGN)	-	+ (PGN)	+ (PGN)	+ (PGN)	-
Number of differentially expressed AMPs	0 out of 3 AMPs	0 out of 3 AMPs	0 out of 3 AMPs	All 3 AMPs	0 out of 1	0 out of 1	All AMPs tested
Technique for gene expression	Northern Blot	Northern Blot	Northern Blot	Northern Blot	Northern Blot	Northern Blot	qPCR
Tissue where gene expression is measured	**S2 cells**	**S2 cells**	**S2 cells**	**S2 cells**	**S2 cells**	**S2 cells**	**Malpighian tubules**
Time at which gene expression is measured	24 hpi	24 hpi	24 hpi	8 time points (from 12 hpi to 60 hpi) Effect only detected at 18 hpi or above	24 hpi	24 hpi	13 time points (15 min to 6 hpi)
References	Flatt et al., 2008	Flatt et al., 2008	Flatt et al., 2008	Flatt et al., 2008	Flatt et al., 2008	Flatt et al., 2008	Verma et al., 2015

Appendix-1

Ethics waiver letter

ANIMAL RESEARCH ETHICS COMMITTEE
Registration number: AREC-101210-002

July 23, 2018

To whom it may concern,
Reference : Waiver Etouman Koekemoer 20180723O
Re: Waiver from the Animal Research Ethics Committee of the University of the Witwatersrand

Student : Elodie Ekoka Etouman
Student number : 2069764
Degree : PhD Candidate
Study Title : "Infection of the mosquito Anopheles arabiensis with the protozan parasite Plasmodium falciparum in order to study the interaction between these two organisms".

Department: Maureen Coetzee Insectary, Wits Research Institute for Malaria;
Theresa Coetzer's laboratory (Wits Research Institute for Malaria),

Supervisor: Prof Lizette Koekemoer ; Email: Lizette.Koekemoerwits.ac.za
Wits Research Institute for Malaria, Sandringham; Tel: + 0117172424;

Full clearance certificate from the AREC of the University of the Witwatersrand is NOT required.

Reason: This study uses mosquitoes (invertebrates).

Comment/Notes : Full ethics application was made – waiver issued.

Please contact me should you require further information.

Yours sincerely

GP Candy

Geoffrey Candy
Chair : Animal Ethics Research Committee, University of the Witwatersrand

Geoffrey P Candy PhD
Professor, Department of Surgery, Faculty of Health Sciences, University of the Witwatersrand, *7 York Road Parktown 2193, Johannesburg; Tel: 27-11-717-2574; Email: geoffrey.candy@wits.ac.za*

Appendix-2

Raw data

Appendix 2.1: Raw data table associated with Figure 2.8

			Quantification cycle (Cq)			Relative Normalized Expression against RpL19 and RpS7				
Gene	dsRNA	Treatment	Biol Rep 1	Biol Rep 2	Biol Rep 3	Biol Rep 1	Biol Rep 2	Biol Rep 3	Mean NRE	SEM
RpL19	EcR	Sugar	17.42	16.85	17.37	Not Applicable (Reference gene)				
	GFP	Sugar	16.27	15.23	15.58					
RpS7	EcR	Sugar	18.08	17.40	17.44	Not Applicable (Reference gene)				
	GFP	Sugar	17.01	15.96	16.30					
VCB	EcR	Sugar	17.99	17.37	17.16	1.11583	1.09602	1.52916	1.247	0.141
	GFP	Sugar	17.25	15.88	16.31	0.86996	1.08387	1.0255	0.993	0.064
VCP	EcR	Sugar	20.79	19.96	20.42	0.64711	0.73279	0.64772	0.676	0.028
	GFP	Sugar	19.11	18.05	18.62	0.96572	0.97388	0.83894	0.926	0.044
Lp	EcR	Sugar	20.24	19.12	19.29	0.56372	0.78701	0.84444	0.732	0.086
	GFP	Sugar	18.79	17.32	17.16	0.72217	0.96583	1.38199	1.023	0.193
Vg	EcR	Sugar	33.16	28.20	24.70	0.00011	0.00211	0.02865	0.010	0.009
	GFP	Sugar	22.19	18.06	17.68	0.09876	0.83837	1.38281	0.773	0.372
EcR	EcR	Sugar	26.72	25.78	26.00	0.32433	0.39916	0.41434	0.379	0.028
	GFP	Sugar	24.24	23.28	22.83	0.84693	0.79419	1.38281	1.008	0.188

Appendix 2.2: Raw data table associated with Figure 2.9

			Quantification cycle (Cq)			Relative Normalized Expression (RNE) against RpS7			Mean	SEM
Gene	dpi	dsRNA	Biol Rep 1	Biol Rep 2	Biol Rep 3	Biol Rep 1	Biol Rep 2	Biol Rep 3		
RpS7	1	dsEcR	21.63	31.45	19.71	Not applicable				
		dsGFP	19.86	26.18	25.65					
	2	dsEcR	22.61	24.54	18.34					
		dsGFP	21.69	29.07	20.38					
	3	dsEcR		34.87	18.91					
		dsGFP		36.49	27.04					
EcR	1	dsEcR	25.03	24.58	31.68	0.56024	60.81001	0.02038	20.46354333	20.1738353
		dsGFP	23.42	23.11	29.65	5.8208	6540.061	0.30774	2182.06318	2178.999491
	2	dsEcR	23.77	23.52	29.81	4.78101	73.78476	0.01876	26.19484333	23.83463784
		dsGFP	22.82	22.67	28.4	17.38538	942.24074	0.02915	319.88509	311.2181582
	3	dsEcR		23.55	34.85		51317.62276	0.0145	25658.81863	25658.80413
		dsGFP		23.13	29.35		211161.411	0.08937	105580.7502	105580.6608

			Quantification cycle (Cq)			Relative Normalized Expression (RNE) against RpS7			Mean	SEM
Gene	**dpi**	**dsRNA**	**Biol Rep 1**	**Biol Rep 2**	**Biol Rep 3**	**Biol Rep 1**	**Biol Rep 2**	**Biol Rep 3**		
RpS7	1	dsEcR	24.02	24.24	28.45	Not applicable				
		dsGFP	24.15	22.97	27.2					
	2	dsEcR	24.61	22.52	27.8					
		dsGFP	24.39	24.16	28.11					
	3	dsEcR		21.63	28.19					
		dsGFP		23.37	27.57					
Aceto	1	dsEcR	29.09	27.76	30.98	0.0452	0.13201	15.56685	5.24802	5.159475859
		dsGFP	28.71	23.88	29.37	0.06413	0.80886	112.8529	37.90863	37.4727517
	2	dsEcR	30.71	24.3	23.65	0.02207	0.44271	12.01267	4.15915	3.928637032
		dsGFP	27.61	22.76	22.57	0.16316	3.99626	31.45491	11.87144333	9.854056507
	3	dsEcR		24.3	23		0.79399	24.7901	12.792045	11.998055
		dsGFP		22.23	21.06		1	61.38741	31.193705	30.193705
Flavo	1	dsEcR	21.93	22.16	23.35	0.28286	0.96738	4.16005	1.80343	1.194764311
		dsGFP	19.62	21.22	19.83	1.52653	1.21267	112.8529	38.5307	37.16121045
	2	dsEcR	24.9	21.55	15.13	0.05435	0.56371	26.03531	8.884456667	8.57668719
		dsGFP	17.71	20.09	13.35	6.79612	4.80291	72.19599	27.93167333	22.13963654
	3	dsEcR		20.99	16.07		0.80239	14.37871	7.59055	6.78816
		dsGFP		20.15	15.36		1.49667	15.24262	8.369645	6.872975
Entero	1	dsEcR	32.24	35.37	30.64	0.22311	0.00858	2.95833	1.06334	0.949516738
		dsGFP	28.99	34.76	26.48	2.31172	0.03174	22.40171	8.24839	7.107201218
	2	dsEcR	34.53	32.51	26.96	0.06858	0.1101	24.35344	8.177373333	8.088042214
		dsGFP	27.68	31.24	25.39	6.79612	0.14219	89.57726	32.17185667	28.76690196
	3	dsEcR		34.07	32.18		0.02796	0.85249	0.440225	0.412265
		dsGFP		27.17	30.6		1	1.65219	1.326095	0.326095
Eubacteria	1	dsEcR	29.46	31.82	28.43	0.10907	0.02481	1.63609	0.58999	0.523615267
		dsGFP	23.87	28.92	25.35	5.73478	0.07683	5.87132	3.89431	1.909146926
	2	dsEcR	34.31	28.36	23.43	0.00572	0.00625	33.66526	11.22574333	11.21975833
		dsGFP	29.91	27.3	22.33	0.10364	0.04053	89.57726	29.90714333	29.8350639
	3	dsEcR		29.54	32.42		0.00497	0.08655	0.04576	0.04079
		dsGFP		20.15	27.04		1	2.33762	1.66881	0.66881

Appendix 2.3: Raw data associated with Figure 3.3

Figure 3.3a

		Quantification cycle (Cq)			Relative Normalized Expression (RNE) against RpS7			Mean	SEM	%change
Gene	**Group**	**Biol Rep 1**	**Biol Rep 2**	**Biol Rep 3**	**Biol Rep 1**	**Biol Rep 2**	**Biol Rep 3**			
RpS7	aseptic	21.34	22.97	21.8	**Not applicable**					
	septic	25.21	25.15	23						
Entero	aseptic	27.25	32.37	27.75	1.03884	0.00048	0.01263			
	septic	27.65	29.58	25.13	11.55013	0.00249	0.17798			
Total	aseptic	26.57	30.42	29	0.00778	0.00167	0.00198	0.00488	0.00290	15.50
	septic	26.21	19.51	23.76	0.14666	14.6271	0.17303	0.15985	0.01319	

Figure 3.3b

		Quantification cycle (Cq)			Relative Normalized Expression (RNE) against RpS7 and RpL19			Mean	SEM	%cahnge
Gene	**Group**	**Biol Rep 1**	**Biol Rep 2**	**Biol Rep 3**	**Biol Rep 1**	**Biol Rep 2**	**Biol Rep 3**			
RpS7	aseptic	18.01	19.02	15.59	**Not applicable**					
	septic	17.54	24.16	15.5						
RpL19	aseptic	17.99	19.08	15.2						
	septic	17.32	23.32	14.73						
EcR	aseptic	30.42	31.84	24.16	0.0578	0.04458	0.72933	0.05119	0.00661	8.33
	septic	28.73	34.84	23.43	0.12519	0.14374	1	0.134465	0.009275	

Appendix 2.4: Raw data table associated with Figure 3.7 and 3.8b

			Quantification cycle (Cq)			Relative Normalized Expression against RpL19 and RpS7					
Gene	dsRNA	Treatment	Biol Rep 1	Biol Rep 2	Biol Rep 3	Biol Rep 1	Biol Rep 2	Biol Rep 3	Mean NRE	SEM	% change
RpL19	EcR	antibiotics	16.97	16.38	16.80	Not Applicable (Reference gene)					
	GFP	antibiotics	16.49	15.03	15.95						
	EcR	Sugar	17.40	16.82	17.29						
	GFP	Sugar	16.27	15.23	15.58						
RpS7	EcR	antibiotics	17.41	17.12	17.19	Not Applicable (Reference gene)					
	GFP	antibiotics	17.02	15.92	16.61						
	EcR	Sugar	18.08	17.38	17.44						
	GFP	Sugar	17.01	15.96	16.30						
VCB	EcR	antibiotics	17.71	16.82	17.05	0.9238	1.25797	1.27686	1.153	0.115	34.72
	GFP	antibiotics	17.54	16.16	17.00	0.76853	0.82445	0.82398	0.806	0.019	
	EcR	Sugar	17.99	17.37	17.16	1.11583	1.09602	1.52916	1.247	0.141	
	GFP	Sugar	17.25	15.88	16.31	0.86996	1.08387	1.0255	0.993	0.064	
VCP	EcR	antibiotics	19.78	20.15	19.91	0.88787	0.50431	0.70806	0.700	0.111	29.96
	GFP	antibiotics	19.41	17.90	18.53	0.84915	1	1.14986	1.000	0.087	
	EcR	Sugar	20.79	19.96	20.42	0.64711	0.73279	0.64772	0.676	0.028	25.03
	GFP	Sugar	19.11	18.05	18.62	0.96572	0.97388	0.83894	0.926	0.044	
Lp	EcR	antibiotics	19.56	19.35	18.93	0.62079	0.5271	0.83421	0.661	0.091	
	GFP	antibiotics	18.91	17.83	17.15	0.71856	0.62616	1.78354	1.043	0.371	
	EcR	Sugar	20.24	19.12	19.29	0.56372	0.78701	0.84444	0.732	0.086	
	GFP	Sugar	18.79	17.32	17.16	0.72217	0.96583	1.38199	1.023	0.193	
Vg	EcR	antibiotics	27.93	29.32	37.00	0.00272	0.00076	0.0000000	0.001	0.001	
	GFP	antibiotics	21.85	19.11	19.34	0.13584	0.2239	0.5683	0.309	0.132	
	EcR	Sugar	33.16	28.20	24.70	0.00011	0.00211	0.02865	0.010	0.009	76.30
	GFP	Sugar	22.19	18.06	17.68	0.09876	0.83837	1.38281	0.773	0.372	
EcR	EcR	antibiotics	25.34	26.03	26.01	0.57747	0.264	0.31759	0.386	0.097	49.65
	GFP	antibiotics	24.50	23.35	23.42	0.76456	0.69612	1.18799	0.883	0.154	
	EcR	Sugar	26.72	25.78	26.00	0.32433	0.39916	0.41434	0.379	0.028	62.87
	GFP	Sugar	24.24	23.28	22.83	0.84693	0.79419	1.38281	1.008	0.188	

Appendix 2.5: Raw data table associated with Figure 3.8a

		Quantification cycle (Cq)			Relative Normalized Expression (RNE) against RpS7			Ratio RNE antibiotics / RNE control			Mean Ratio	SEM	% change
Gene	**Treatment**	**Biol Rep 1**	**Biol Rep 2**	**Biol Rep 3**	**Biol Rep 1**	**Biol Rep 2**	**Biol Rep 3**	**Biol Rep 1**	**Biol Rep 2**	**Biol Rep 3**			
RpS7	antibiotics	27.61	28.39	27.72					N/A				
	control	28.93	29.05	28.16									
Enterobacteria	antibiotics	26.15	26.93	26.85	0.00403	0.00402	0.0027	0.00071768	0.149664929	0.149664929	0.100015846	0.049649	89.99841544
	Sugar	17.02	24.85	20.39	5.61533	0.02686	0.3202						
Total (Eubacteria)	antibiotics	35.39	21.96	23.54	0.00009	2.81813	0.06873	3.4997E-05	0.377884454	0.222477584	0.200132345	0.109646	79.98676548
	control	21.97	19.9	22.38	2.57162	7.45765	0.30893						

Appendix 2.6: Raw data table associated with Figure 4.2 (gut)

		Quantification cycle (Cq)			Relative Normalized Expression (RNE) against RpS7			Mean	SEM
Gene	Treatment	Biol Rep 1	Biol Rep 2	Biol Rep 3	Biol Rep 1	Biol Rep 2	Biol Rep 3		
RpS7	dsEcR	17.3	16.79	16.81					
	dsGFP	16.18	15.71	15.95					
EcR	dsEcR	30.82	29.57	28.25	0.0642	0.12532	0.30264	0.1641	0.07150
	dsGFP	26.96	25.32	25.66	0.44335	1	0.95117	0.7982	0.17797
Cec-1	dsEcR	17.23	15.81	17.29	1.08578	2.38345	0.82147	1.4302	0.48268
	dsGFP	16.27	15.9	15.82	1.00114	0.93835	1.19707	1.0455	0.07791
Cec-3	dsEcR	16.06	14.87	15.85	0.64526	1.21129	0.59167	0.8161	0.19821
	dsGFP	14.28	13.89	13.92	1.05836	1	1.18843	1.0823	0.05569
Gamb-1	dsEcR	16.82	15.04	15.82	0.50559	1.42082	0.80017	0.9089	0.26974
	dsGFP	15.98	14.29	14.62	0.43087	1	0.96115	0.7973	0.18358
Def-1	dsEcR	18.66	16.5	17.51	0.20892	0.7677	0.3676	0.4481	0.16625
	dsGFP	15.71	14.96	14.87	0.76973	0.93691	1.20775	0.9715	0.12762
Att	dsEcR	26.57	26.28	26.3	0.38659	0.3873	0.36865	0.3808	0.00610
	dsGFP	26.7	25.38	26.55	0.16822	0.30325	0.16261	0.2114	0.04597
duox	dsEcR	33.82	31.96	34.12	0.01824	0.05422	0.0117	0.0281	0.01322
	dsGFP	31.91	27.11	29.6	0.03268	0.65598	0.14078	0.2765	0.19230
Mesh	dsEcR	29.14	24.92	24.37	0.09101	1.38909	1.97182	1.1506	0.55588
	dsGFP	27.74	24.95	24.14	0.11445	0.57294	1.20775	0.6317	0.31697
Imd	dsEcR	25.92	24.67	25.01	0.49781	0.9706	0.73922	0.7359	0.13649
	dsGFP	25.68	23.38	24.19	0.28032	0.99787	0.68787	0.6554	0.20778
Rel2	dsEcR	29.51	26.11	25.61	0.12726	1.09819	1.50559	0.9103	0.40882
	dsGFP	28.66	25.62	25.63	0.10861	0.64814	0.7768	0.5112	0.20468
Akr	dsEcR	24.92	22.94	22.41	0.25199	0.81759	1.14256	0.7374	0.26019
	dsGFP	24.03	21.39	22.04	0.22289	1	0.77281	0.6652	0.23069

Appendix 2.7: Raw data table associated with Figure 4.2 (carcass)

		Quantification cycle (Cq)			Relative Normalized Expression (RNE) against RpS7			Mean	SEM
Gene	Treatmer	Biol Rep 1	Biol Rep 2	Biol Rep 3	Biol Rep 1	Biol Rep 2	Biol Rep 3		
RpS7	dsEcR	28.41	20.81	20.75					
	dsGFP	23.36	20.43	22.07					
EcR	dsEcR	33.11	30.21	32.97	30.180	1.157	0.164	10.5002	9.84396
	dsGFP	32.34	28.06	31.96	1.554	3.946	0.822	2.1070	0.94341
Cec-1	dsEcR	23.5	18.03	18.2	6.790	1.551	1.323	3.2211	1.78548
	dsGFP	21.37	18.53	19.52	0.897	0.843	1.323	1.0208	0.15167
Cec-3	dsEcR	37.13	21.72	22.36	0.014	3.081	1.896	1.6637	0.89302
	dsGFP	27.25	22.11	24.1	0.390	1.807	1.417	1.2049	0.42241
Gamb-1	dsEcR	28.46	21.21	21.08	1.335	1.047	1.099	1.1605	0.08846
	dsGFP	23.88	21.11	22.27	0.964	0.863	1.203	1.0098	0.10095
Def-1	dsEcR	32.48	19.35	20.78	0.108	4.970	1.769	2.2825	1.42699
	dsGFP	24.96	20.84	22.62	0.596	1.360	1.234	1.0632	0.23643
Att	dsEcR	31.02	23.72	23.9	1.200	0.975	0.825	1.0002	0.10892
	dsGFP	25.93	23.66	24.89	1.234	0.781	1.038	1.0175	0.13116
duox	dsEcR	31.64	29.79	30.45	15.562	0.289	0.176	5.3424	5.11014
	dsGFP	30.82	26.5	30.11	0.829	2.173	0.555	1.1859	0.50012
Mesh	dsEcR	36.59	33.88	35.47	23.103	0.779	0.248	8.0434	7.53128
	dsGFP	35.28	31.29	37.42	1.729	3.605	0.160	1.8315	0.99568
Imd	dsEcR	25.5	24.17	25.17	32.900	0.426	0.204	11.1768	10.86160
	dsGFP	24.08	23.37	24.8	2.657	0.570	0.660	1.2958	0.68126
Rel2	dsEcR	28.05	26.62	28.88	40.132	0.557	0.112	13.6002	13.26633
	dsGFP	28.27	24.99	27.5	1.040	1.326	0.725	1.0303	0.17336
Akr	dsEcR	25.84	23.61	24.64	17.188	0.416	0.195	5.9330	5.62790
	dsGFP	24.36	21.67	24.43	1.447	1.225	0.564	1.0789	0.26535

Appendix 2.8: Raw data table associated with Figures 4.3-4.5

									Line graphs				
			Quantification cycle (Cq)			Relative Normalized Expression (RNE) against RpS7			Mean RNE	RNE SEM	RNE ratio 20E/PBS		
	hpi	Treatment	Biol Rep 1	Biol Rep 2	Biol Rep 3	Biol Rep 1	Biol Rep 2	Biol Rep 3			BR 1	BR 2	BR 3
Imd	1	20E	32.55	35.94	29.01	1.22402	0.03707	0.21129	0.49079	0.370046916	0.34	0.052698918	0.257419591
		PBS	29.19	26.88	25.01	3.55394	0.70343	0.8208	1.69272	0.931224917			
	3	20E	28.23	33.74	26.31	2.21425	0.08397	0.75188	1.01670	0.629052315	0.77	0.523340605	0.692542922
		PBS	29.38	31.09	25.66	2.87871	0.16045	1.08568	1.37495	0.797912017			
	9	20E	25.31	28.42	27.94	2.46348	23.92569	0.45989	8.94969	7.510306254	1.50	17.76602981	0.260007011
		PBS	29.5	26.59	25.08	1.6456	1.34671	1.76876	1.58702	0.125306252			
	12	20E	31.17	37.48	26.79	1.08774	0.02029	0.90888	0.67230	0.330070076	1.13	0.123298493	0.599501339
		PBS	32.08	35.62	28.29	0.96541	0.16456	1.51606	0.88201	0.392366637			
	24	20E	25.85	27.07	27.1	1.97047	0.81895	0.5051	1.09817	0.44545915	0.53	0.742461605	0.44386836
		PBS	24.73	26.03	26.32	3.74248	1.10302	1.13795	1.99448	0.874056498			
RpS7	1	20E	25.43	23.77	19.35								
		PBS	23.6	18.95	17.31								
	3	20E	21.96	22.75	18.48								
		PBS	23.49	21.03	18.36								
	9	20E	19.19	25.58	19.4								
		PBS	22.8	19.6	18.48								
	12	20E	23.87	24.44	19.23								
		PBS	24.61	25.59	21.47								
	24	20E	19.41	19.36	18.7								
		PBS	19.21	18.76	19.09								

			Quantification cycle (Cq)			Relative Normalized Expression (RNE) against RpS7			Mean	SEM	RNE ratio 20E/PBS		
	hpi	Treatment	Biol Rep 1	Biol Rep 2	Biol Rep 3	Biol Rep 1	Biol Rep 2	Biol Rep 3			BR1	BR2	BR3
Rel2	1	20E	32.35	33.01	28.7	0.65664	0.13137	0.12174	0.30325	0.176716867	1.678913861	0.206148197	0.134808318
		PBS	31.27	25.92	23.77	0.39111	0.63726	0.90306	0.64381	0.147823518			
	3	20E	31.08	24.26	26.44	0.14272	28.06721	0.31964	9.50986	9.278817224	2.133193032	2.133193032	0.258080143
		PBS	27.04	23.63	24.37	6.77537	13.15737	1.23853	7.05709	3.443554915			
	9	20E	31.17	26.54	29.69	0.01982	41.1233	0.06346	13.73553	13.69389246	0.002575524	18.05173655	0.066719936
		PBS	26.17	24.73	24.87	7.69552	2.27808	0.95114	3.64158	2.062847109			
	12	20E	32.61	25.88	28.61	0.18659	29.25585	0.11937	9.85394	9.700976074	0.104390102	0.371378074	0.191086779
		PBS	30.09	25.61	28.47	1.78743	78.77646	0.62469	27.06286	25.85897852			
	24	20E	25.64	26.32	27.74	1.06226	0.63917	0.15159	0.61767	0.263107419	1.187108166	0.635749667	0.189217865
		PBS	25.69	25.07	25.72	0.89483	1.00538	0.80114	0.90045	0.059025934			
Akirin	1	20E	34.53	31.19	24.12	0.01636	0.05235	0.32929	0.13267	0.098859111	0.627541235	0.156436768	0.32929
		PBS	32.04	23.7	20.48	0.02607	0.33464	1	0.45357	0.287369199			
	3	20E	28.22	30.84	22.35	0.11705	0.0331	0.61721	0.25579	0.182329391	28.7826087	28.7826087	0.627635018
		PBS	32.34	33.97	21.56	0.0194	0.00115	0.98339	0.33465	0.324414447			
	9	20E	24.55	29.32	24.36	0.21953	0.67762	0.28939	0.39551	0.142487699	22.49282787	533.5590551	0.37603628
		PBS	32.65	32.4	22.03	0.00976	0.00127	0.76958	0.26020	0.254700125			
	12	20E	32.39	33.82	24.01	1.135504429	0.62560907	15.1719365	5.64435	4.766066747	2.428389769	5.696200782	0.77916458
		PBS	34.41	37.48	25.89	0.467595624	0.109829182	19.47205622	6.68316	6.39528192			
	24	20E	24.82	24.65	23.32	0.601512518	0.653684624	1.040059934	0.76509	0.138309565	0.835087919	0.77916458	0.628506687
		PBS	24.36	23.69	23.04	0.720298431	0.838955775	1.654811245	1.07136	0.293732107			

			Quantification cycle (Cq)			Relative Normalized Expression (RNE) against RpS7			Mean	SEM	RNE ratio 20E/PBS		
	hpi	Treatment	Biol Rep 1	Biol Rep 2	Biol Rep 3	Biol Rep 1	Biol Rep 2	Biol Rep 3			BR1	BR2	BR3
Cec-1	1	20E	24.15	25.54	21.54	0.60776	0.07356	0.05503	0.24545	0.181233958	0.126155149	0.357729903	0.24666069
		PBS	19.34	19.24	17.48	4.81756	0.20563	0.2231	1.74876	1.534406621			
	3	20E	20.44	22.6	23.59	0.71725	0.2787	0.0073	0.33442	0.206829649	1.257728237	1.257728237	1.117917305
		PBS	22.09	21.21	23.63	0.66197	0.22159	0.00653	0.29670	0.192899937			
	9	20E	18.54	25.73	17.47	0.39421	0.2273	0.95572	0.52574	0.220321498	0.224636442	0.279420261	3.603906633
		PBS	20	17.91	18.4	1.75488	0.81347	0.26519	0.94451	0.434999364			
	12	20E	23.03	24.35	16.71	0.45095	0.26719	1.44059	0.71958	0.364388577	2.561924781	2.319558989	4.659841501
		PBS	25.12	26.72	21.17	0.17602	0.11519	0.30915	0.20012	0.057273402			
	24	20E	17.17	16.99	18	1.19309	1.29827	0.40733	0.96623	0.281094655	0.382338143	0.476001393	0.272279412
		PBS	15.58	15.32	16.52	3.12051	2.72745	1.496	2.44799	0.489330495			
Cec-3	1	20E	29.84	27.84	17.88	0.07005	0.08829	4.11221	1.42352	1.344356978	0.832639962	37.41101695	1065.339378
		PBS	27.75	28.25	25.9	0.08413	0.00236	0.00386	0.03012	0.027010138			
	3	20E	23.2	25.26	29.21	0.62759	0.26222	0.00088	0.29690	0.181744518	46.99283154	46.99283154	3.826086957
		PBS	28.03	29.09	31.01	0.06405	0.00558	0.00023	0.02329	0.020440096			
	9	20E	18.41	24.11	19.03	2.56378	4.15367	1.92317	2.88021	0.663042718	83.02396373	2806.533784	2.560573582
		PBS	28.39	29.58	19.47	0.03088	0.00148	0.75107	0.26114	0.245110311			
	12	20E	26.37	35.78	19.53	4.458834546	0.009730075	20.48742363	8.31866	6.218458778	5.098242509	0.006569503	26.53822547
		PBS	29.46	29.68	26.5	0.87458267	1.481097552	0.771996743	1.04256	0.221260045			
	24	20E	18.96	21.49	20.72	2.0404	0.34127	0.36778	0.91648	0.562010439	135.8455393	0.37368738	0.438569504
		PBS	25.85	19.46	19.92	0.01502	0.91325	0.83859	0.58895	0.287774873			

			Quantification cycle (Cq)			Relative Normalized Expression (RNE) against RpS7			Mean	SEM	RNE ratio 20E/PBS		
	hpi	Treatment	Biol Rep 1	Biol Rep 2	Biol Rep 3	Biol Rep 1	Biol Rep 2	Biol Rep 3			BR1	BR2	BR3
Attacin	1	20E	31.52	28.36	23.52	0.21578	0.61146	0.82156	0.54960	0.177587863	0.131037037	0.672651068	0.82156
		PBS	26.77	22.97	21.19	1.64671	0.90903	1	1.18525	0.232221296			
	3	20E	26.19	27.21	23.28	0.78375	0.66987	0.53145	0.66169	0.072947485	0.793177351	0.793177351	0.569327348
		PBS	27.46	25.15	22.35	0.93512	0.84454	0.93347	0.90438	0.029922125			
	9	20E	24.4	30.57	23.87	0.39909	0.46524	0.66439	0.50957	0.079728928	0.841962025	0.664980061	0.812034027
		PBS	27.76	24	22.65	0.474	0.69963	0.81818	0.66394	0.10094632			
	12	20E	30.34	28.56	24.12	0.16737	0.84658	0.49648	0.50348	0.196102245	1.166829336	2.940534908	0.478373561
		PBS	31.29	31.27	25.3	0.14344	0.2879	1.03785	0.48973	0.277214612			
	24	20E	24.93	22.64	23.52	0.32308	1.51708	0.52257	0.78758	0.36926973	0.46904081	1.206271965	0.723640845
		PBS	23.63	22.31	23.44	0.68881	1.25766	0.72214	0.88954	0.184312971			
Def-1	1	20E	21.38	24	19.29	10.49748	0.54033	0.66223	3.90001	3.298921021	31810.54545	0.825675036	0.66223
		PBS	34.52	18.91	16.66	0.00033	0.65441	1	0.55158	0.293124282			
	3	20E	21	21.84	18.98	1.23606	1.19421	0.44932	0.95986	0.255557382	1.265455123	1.265455123	0.701613029
		PBS	26.4	20.46	18.35	0.08441	0.9437	0.64041	0.55617	0.251605967			
	9	20E	19.23	24.38	19.77	0.62165	1.46361	0.49222	0.85916	0.304525797	4.67722519	1.02099029	0.538917173
		PBS	25.06	18.43	17.96	0.13291	1.43352	0.91335	0.82659	0.377951334			
	12	20E	24.11	24.75	19.89	0.54064	0.5139	0.40451	0.48635	0.04164171	4.178698408	0.335875767	0.299685875
		PBS	26.91	24.33	20.39	0.12938	1.53003	1.34978	1.00306	0.439929707			
	24	20E	18.17	17.21	18.6	1.51052	2.82855	0.68363	1.67423	0.624572385	1.88815	1.299646205	0.213092986
		PBS	18.88	16.98	16.76	0.8	2.1764	3.20813	2.06151	0.697536692			

			Quantification cycle (Cq)			Relative Normalized Expression (RNE) against RpS7			Mean	SEM	RNE ratio 20E/PBS		
	hpi	Treatment	Biol Rep 1	Biol Rep 2	Biol Rep 3	Biol Rep 1	Biol Rep 2	Biol Rep 3			BR1	BR2	BR3
Gamb-1	1	20E	26.98	36.88	19.53	0.40359	0.00013	1.04329	0.48234	0.303697478	0.251509656	0.002844017	1.04329
		PBS	23.17	23.65	17.55	1.60467	0.04571	1	0.88346	0.45378969			
	3	20E	22.58	30.65	18.78	0.76813	0.00497	0.96061	0.57790	0.291805638	0.13414305	0.13414305	1.074664101
		PBS	23.99	26.03	18.77	0.83641	0.03705	0.89387	0.58911	0.276527934			
	9	20E	20.35	31.54	19.23	0.53289	0.01909	1.33536	0.62911	0.383008214	2.689326268	1.042599672	2.673821633
		PBS	25.38	25.62	19.73	0.19815	0.01831	0.49942	0.23863	0.140351319			
	12	20E	26.38	30.6	19.34	0.20809	0.01648	1.09448	0.43968	0.332037952	2.825774036	7.390134529	1.020598849
		PBS	28.62	34.65	21.62	0.07364	0.00223	1.07239	0.38275	0.345433976			
	24	20E	19.67	22.55	18.44	0.99119	0.13011	1.41772	0.84634	0.378691176	0.507685531	9.300214439	1.142300038
		PBS	18.49	25.16	19.02	1.95237	0.01399	1.24111	1.06916	0.56612873			
Mesh	1	20E	30.04	27.3	32.17	6.33675	13.37369	0.02152	6.57732	3.856315874	4591.847826	5.15980169	0.0257327
		PBS	40.39	24.86	24.85	0.00138	2.5919	0.83629	1.14319	0.763400108			
	3	20E	39.24	24.59	27.54	0.00097	43.40149	0.29158	14.56468	14.41864906	4.29751337	4.29751337	0.286570743
		PBS	37.8	24.97	25.62	0.00761	10.09921	1.01748	3.70810	3.208825051			
	9	20E	32.79	28.09	33.45	0.01256	27.40157	0.00917	9.14110	9.130235052	0.75708258	8.219838072	0.012901501
		PBS	35.99	25.15	26.25	0.01659	3.33359	0.71077	1.35365	1.010048393			
	12	20E	32.97	26.74	31.37	0.28357	31.55167	0.03441	10.62322	10.46447386	16.29712644	0.325351389	0.212814645
		PBS	37.73	26.27	31.38	0.0174	96.97721	0.16169	32.38543	32.29591519			
	24	20E	26.22	28.57	28.92	1.38657	0.26276	0.13033	0.59322	0.398512899	26.44107551	0.690982723	0.331072499
		PBS	30.75	27.43	27.71	0.05244	0.38027	0.39366	0.27546	0.111575308			

			Quantification cycle (Cq)			Relative Normalized Expression (RNE) against RpS7			Mean	SEM	RNE ratio 20E/PBS		
	hpi	Treatment	Biol Rep 1	Biol Rep 2	Biol Rep 3	Biol Rep 1	Biol Rep 2	Biol Rep 3			BR1	BR2	BR3
duox	1	20E	30.34	27.97	26.25	3.12677	5.10011	0.78622	3.00437	1.246815766	0.556420213	6.07814418	0.78622
		PBS	27.67	25.76	23.87	5.61944	0.83909	1	2.48618	1.567320149			
	3	20E	27.14	27.97	26.22	2.57964	2.53028	0.44166	1.85053	0.70457743	1.99330387	1.99330387	0.539933251
		PBS	30.33	27.24	25.21	0.82077	1.26939	0.81799	0.96938	0.15000548			
	9	20E	25.54	28.6	25.96	1.15497	11.65456	0.99537	4.60163	3.526764285	0.197643954	22.44931137	3.238133967
		PBS	26.81	27.1	26.74	5.84369	0.51915	0.30739	2.22341	1.811171907			
	12	20E	28.25	28.83	24.29	4.53147	4.47844	2.82864	3.94618	0.558981327	#DIV/0!	0.135407646	0.887538986
		PBS		27.1	26.36		33.07376	3.18706	18.13041	12.20119418			
	24	20E	26.59	25.83	25.15	0.65006	1.05898	1.07447	0.92784	0.138960297	1.083668128	3.104420732	0.711079786
		PBS	26.51	26.86	25.05	0.59987	0.34112	1.51104	0.81734	0.354800033			

Appendix 2.9: Raw data table associated with Figure 4.6

			Cq		RNE		Mean	SEM	RNE ratio *E. coli* / PBS	
	hpi	Treatment	Biol Rep 1	Biol Rep 2	Biol Rep 1	Biol Rep 2			BR1	BR2
RpL19	6	E coli	18.35	18.4						
		PBS	18.48	17.48						
	12	E coli	18.88	19.06						
		PBS	16.99	16.31						
	18	E coli	18.09	18.49						
		PBS	18.23	16.22						
	24	E coli	19.29	17.09						
		PBS	16.64	15.64						
RpS7	6	E coli	18.86	19.25						
		PBS	18.89	18.55						
	12	E coli	19.5	20.02						
		PBS	17.75	17.24						
	18	E coli	18.53	19.53						
		PBS	18.55	17.41						
	24	E coli	19.55	18						
		PBS	17.18	16.7						
Gambicin	6	E coli	18.47	19.56	2.16937	1.18965	1.67951	0.48986	1.752587231	2.174346133
		PBS	19.36	19.87	1.23781	0.54713	0.89247	0.34534		
	12	E coli	19.1	19.85	2.11364	1.59838	1.85601	0.25763	3.899345079	4.642809423
		PBS	19.24	19.3	0.54205	0.34427	0.44316	0.09889		
	18	E coli	17.87	19.92	2.69292	1.05613	1.874525	0.818395	1.77361821	1.115708853
		PBS	18.77	17.88	1.51832	0.9466	1.23246	0.28586		
	24	E coli	19.4	18.39	2.00876	1.10286	1.55581	0.45295	1.200564195	1.610672976
		PBS	17.15	17.7	1.67318	0.68472	1.17895	0.49423		
EcR	6	E coli	28.71	31.09	0.74444	0.16602	0.45523	0.28921	0.600514653	0.507768534
		PBS	28.05	29.3	1.23967	0.32696	0.783315	0.456355		
	12	E coli	28.94	31.87	0.95114	0.15875	0.554945	0.396195	0.986946416	0.286671362
		PBS	27.09	27.3	0.96372	0.55377	0.758745	0.204975		
	18	E coli	28.45	30.66	0.7252	0.25433	0.489765	0.235435	1.171264294	0.194097625
		PBS	28.75	26.1	0.61916	1.31032	0.96474	0.34558		
	24	E coli	30.25	30.18	0.382889499	0.137261602	0.260076	0.122814	0.432268615	0.121581869
		PBS	26.67	25.84	0.885767519	1.128964405	1.007366	0.121598		

			Cq			RNE			Mean	SEM	RNE ratio 20E/PBS		
	hpi	Treatment	Biol Rep 1	Biol Rep 2	Biol Rep 3	Biol Rep 1	Biol Rep 2	Biol Rep 3			BR1	BR2	BR3
RpS7	6	aureus	16.74	18.98	17.35								
		PBS	19.87	16.5	18.44								
	12	aureus	15.98	17.94	16.17								
		PBS	16.71	15.97	18.26								
	18	aureus	15.66	17.27	16.77								
		PBS	16.44	16.07	19.24								
	24	aureus	15.48	16.76	16.36								
		PBS	17.31	16.9	15.58								
EcR	6	aureus	27.98	29.43	27.72	0.2032	0.35246	0.37145			2.408153591	0.725659344	0.622454964
		PBS	32.38	26.48	28.12	0.08438	0.48571	0.59675					
	12	aureus	25.38	28.07	26.02	0.72592	0.43644	0.53107			7.647703329	0.689086775	3.666091399
		PBS	29.04	25.57	29.98	0.09492	0.63336	0.14486					
	18	aureus	24.42	29.1	27.72	1.13726	0.13417	0.2468			4.54467711	0.206443969	0.656540129
		PBS	27.38	25.63	29.59	0.25024	0.64991	0.37591					
	24	aureus	25.02	26.9	26.09	0.65572	0.43361	0.57931			5.902070207	5.084545028	0.842902456
		PBS	29.41	29.39	25.06	0.1111	0.08528	0.68728					
Gambicin	6	aureus	16.71	17.58	18.14	0.69398	1.79116	0.39346			1.060515297	19.85764967	1.610033554
		PBS	19.93	19.41	19.91	0.65438	0.0902	0.24438					
	12	aureus	16.47	18.86	17.24	0.48282	0.35855	0.32392			1.671988087	3.192218661	2.251477028
		PBS	17.94	18.57	20.5	0.28877	0.11232	0.14387					
	18	aureus	15.8	19.07	18.24	0.61669	0.19505	0.24496			1.695460919	0.520660936	0.723812901
		PBS	17.34	16.93	20.24	0.36373	0.37462	0.33843					
	24	aureus	14.92	18.53	16.14	1	0.19842	0.79182			1.701316819	0.641741324	1.455150234
		PBS	17.51	18.04	15.9	0.58778	0.30919	0.54415					